

INVESTIGATIONS OF HIGHLY CONJUGATED MACROCYCLES AND  
POLYMERS FOR AGGREGATION AND CHEMICAL SENSING

by

BRITTA NICOLE BODEN

H. B. Sc., University of Toronto, 2000

M. Sc., Queen's University, 2002

A THESIS SUBMITTED IN PARTIAL FULFILLMENT OF THE REQUIREMENTS  
FOR THE DEGREE OF

DOCTOR OF PHILOSOPHY

in

THE FACULTY OF GRADUATE STUDIES

(Chemistry)

THE UNIVERSITY OF BRITISH COLUMBIA

October 2007

© Britta Nicole Boden, 2007

## Abstract

With the goal of developing Schiff base macrocycles with conjugation extended over multiple aromatic rings, new phenanthrene and triphenylene-containing bis(salicylates) were synthesized. A convenient route to 3,6,9,10-tetraalkoxy-2,7-diiodophenanthrene was developed. This compound has been found to be a useful precursor for Pd-catalyzed cross-coupling reactions.

Macrocycles were synthesized by Schiff base condensation of the phenanthrene and triphenylene precursors. Reaction of smaller phenanthrene and triphenylene bis(salicylates) with 1,2-dialkoxy-4,5-phenylenediamine afforded macrocycles in poor yield and purity, but formation of the macrocycle was confirmed by mass spectrometry. Condensation of larger phenanthrene ethynylene bis(salicylates) with phenylenediamines formed [3+3] Schiff base macrocycles in good yield and could be purified through recrystallization. These two large macrocycles were weakly luminescent, and showed decrease in intensity of emission in solution over time. Addition of nitroaromatic compounds to solutions of the macrocycles caused quenching of luminescence, but Stern-Volmer constants could not be determined. One of the macrocycles aggregates in solution and shows some order in the solid state. Association constants for self-assembly of this macrocycle in chloroform were determined, and aggregation was found to be enthalpically driven and entropically disfavoured. Both large macrocycles can complex metals, but low solubility prevents thorough characterization of the metal complexes.

Phenanthrene-containing poly(phenyleneethynylene)s (PPEs) and poly(phenylenevinylene)s (PPVs) were synthesized via the Sonogashira and Heck couplings, respectively. The PPEs had high molecular weight and both polymers were

extremely luminescent with  $\Phi_F = 70\%$  for the PPE and  $\Phi_F = 59\%$  for the PPV. These polymers show potential for use in solar cells and nitroaromatic sensors.

Dithienylsalphen monomers were made using 4-(2-thienyl)salicylaldehyde and 5-(2-thienyl)salicylaldehyde. These monomers were coordinated to Ni(II), Cu(II) and vanadyl, and tested for electropolymerization. Conjugated dithienylsalphen monomers polymerize poorly, while non-conjugated dithienylsalphen monomers form good films through electropolymerization. Ultraviolet-visible spectroscopy confirmed extended conjugation in *N,N'*-phenylenebis(4-(2-thienyl)salicylideneimine).

## Table of Contents

Abstract.....	ii
Table of Contents .....	iv
List of Tables .....	vii
List of Figures.....	viii
List of Figures.....	viii
List of Symbols and Abbreviations .....	xvi
Acknowledgements .....	xxiii
Statement of Co-Authorship.....	xxiv
Chapter 1 .....	1
Introduction.....	1
1.1    Supramolecular Chemistry.....	1
1.1.1    Background .....	1
1.1.2    Macrocycles .....	3
1.1.3    Shape-Persistent Macrocycles.....	8
1.2    Schiff Base Chemistry.....	14
1.2.1    Salen and Salphen.....	14
1.2.2    Schiff Base Macrocycles .....	17
1.3    Phenanthrene and Triphenylene.....	23
1.3.1    Polycyclic Aromatic Hydrocarbons.....	23
1.3.2    Macrocycles containing PAHs .....	24
1.3.3    PAHs in Materials Chemistry.....	30
1.4    Conjugated Molecules as Sensors for Nitroaromatic Compounds .....	33
1.5    Research Goals .....	37
1.6    References.....	41
Chapter 2 .....	47
Synthesis of Phenanthrene and Triphenylene Precursors .....	47
2.1    Introduction.....	47
2.1.1    Phenanthrene.....	47
2.1.2    Triphenylene.....	50
2.1.3    Further Functionalization toward Macrocycle Precursors .....	51
2.2    Discussion.....	52
2.2.1    Synthesis of Precursor 70a.....	52
2.2.2    Attempted Synthesis of Precursor 70b.....	55

2.2.3	Synthesis of Precursor 71 .....	68
2.2.4	Synthesis of Precursor 72 .....	70
2.2.5	Synthesis of Precursor 73 .....	74
2.2.6	Conclusions .....	76
2.3	Experimental .....	77
2.3.1	General Methods and Materials .....	77
2.3.2	Synthetic Procedures .....	78
2.4	References .....	108
<b>Chapter 3 .....</b>		<b>110</b>
<b>Synthesis of Phenanthrene and Triphenylene Macrocycles.....</b>		<b>110</b>
3.1	Introduction.....	110
3.1.1	Synthesis of [3+3] Macrocycles.....	110
3.2	Discussion.....	112
3.2.1	Attempted Synthesis of Macrocycle 68 .....	112
3.2.2	Synthesis of Macrocycle 69 .....	116
3.2.3	Synthesis of Macrocycle 74 and Macrocycle 75 .....	122
3.2.4	Conclusions.....	128
3.3	Experimental .....	129
3.3.1	General Methods and Materials .....	129
3.3.2	Synthetic Procedures .....	129
3.4	References .....	136
<b>Chapter 4 .....</b>		<b>137</b>
<b>Self-Assembly, Metal Complexation and Sensing Studies of Phenanthrene Ethyne Macrocycles .....</b>		<b>137</b>
4.1	Introduction.....	137
4.1.1	Aggregation of Macrocycles.....	137
4.1.2	Metallation of Macrocycles .....	139
4.1.3	Macrocycle Sensors.....	141
4.1.4	Properties of Macrocycles 74 and 75.....	142
4.2	Discussion.....	143
4.2.1	Aggregation of Macrocycles 74 and 75 .....	143
4.2.2	Metal Complexation of Macrocycles 74 and 75 .....	152
4.2.3	Optical Properties of Macrocycles 74 and 75 .....	158
4.2.4	Sensing of Nitroaromatics .....	164
4.2.5	Conclusions.....	166
4.3	Experimental .....	166
4.3.1	General Methods and Materials .....	166
4.3.2	Synthetic Procedures .....	168
4.4	References .....	170

<b>Chapter 5 .....</b>	<b>172</b>
<b>Synthesis and Characterization of Phenanthrene-containing Conjugated Polymers.....</b>	<b>172</b>
<b>5.1 Introduction.....</b>	<b>172</b>
<b>5.1.1 Conjugated Polymers.....</b>	<b>172</b>
<b>5.2 Discussion.....</b>	<b>175</b>
<b>5.2.1 Synthesis of Phenanthrene-containing PPEs.....</b>	<b>175</b>
<b>5.2.2 Synthesis of Phenanthrene-containing PPVs.....</b>	<b>178</b>
<b>5.2.3 Applications of 77.....</b>	<b>181</b>
<b>5.2.4 Conclusions.....</b>	<b>181</b>
<b>5.3 Experimental.....</b>	<b>182</b>
<b>5.3.1 General Methods and Materials.....</b>	<b>182</b>
<b>5.3.2 Synthetic Procedures.....</b>	<b>182</b>
<b>5.4 References.....</b>	<b>188</b>
<b>Chapter 6 .....</b>	<b>190</b>
<b>Synthesis and Characterization of Thienyl-Schiff Base Monomers.....</b>	<b>190</b>
<b>6.1 Introduction.....</b>	<b>190</b>
<b>6.1.1 Schiff Base Polymers.....</b>	<b>190</b>
<b>6.2 Discussion.....</b>	<b>194</b>
<b>6.2.1 Synthesis of 5-thienyl Salphen Monomers.....</b>	<b>194</b>
<b>6.2.2 Synthesis of 4-thienyl Salphen Monomers.....</b>	<b>196</b>
<b>6.2.3 Absorption of Salphen Monomers.....</b>	<b>199</b>
<b>6.2.4 Conclusions.....</b>	<b>201</b>
<b>6.3 Experimental.....</b>	<b>201</b>
<b>6.3.1 General Methods and Materials.....</b>	<b>201</b>
<b>6.3.2 Synthetic Procedures.....</b>	<b>201</b>
<b>6.4 References.....</b>	<b>212</b>
<b>Chapter 7 .....</b>	<b>213</b>
<b>Conclusions and Future Directions .....</b>	<b>213</b>
<b>7.1 Overview.....</b>	<b>213</b>
<b>7.2 Future Directions.....</b>	<b>214</b>
<b>7.2.1 Schiff Base Macrocycles.....</b>	<b>214</b>
<b>7.2.2 Self-Assembly.....</b>	<b>217</b>
<b>7.2.3 Phenanthrene-Containing Polymers.....</b>	<b>217</b>
<b>7.2.4 Sensing.....</b>	<b>218</b>
<b>7.3 References.....</b>	<b>219</b>

## List of Tables

<b>Table 1.1</b>	Selected Stern-Volmer constants for nitroaromatics.....	36
<b>Table 3.1</b>	Synthetic conditions for the formation of macrocycle <b>69</b> .....	119
<b>Table 4.1</b>	Association constants $K_E$ for dimerization of <b>75</b> in $CDCl_3$ . ....	147
<b>Table 4.2</b>	Thermodynamic data for dimerization of <b>75</b> in $CDCl_3$ . ....	149

## List of Figures

<b>Figure 1.1</b> Examples of a) hydrogen bonding, b) $\pi$ - $\pi$ stacking, c) ion-dipole electrostatic interactions.....	1
<b>Figure 1.2</b> a) Sensing by release of a fluorophore, b) Sensing of an analyte by fluorescence quenching (purple indicates luminescence, while blue indicates quenching).....	2
<b>Figure 1.3</b> Structures of 18-crown-6 ( <b>1</b> ), cryptand [2.2.2] ( <b>2</b> ), and spherand <b>3</b> .....	3
<b>Figure 1.4</b> a) Cone, b) partial cone, c) 1,3 alternate and d) 1,2 alternate conformations of <i>p</i> - <i>tert</i> -butylcalix[4]arene <b>4</b> , R = H, <sup><i>i</i></sup> Pr, e) complexation of sodium and f) a bridged calixarene.....	4
<b>Figure 1.5</b> $\alpha$ -Cyclodextrin, <b>5</b> .....	5
<b>Figure 1.6</b> a) Peptide-based macrocycle <b>6</b> and b) hydrogen bonding induced stacking of macrocycle <b>6</b> .....	6
<b>Figure 1.7</b> An example of a) a rotaxane <b>7</b> and b) a catenane <b>8</b> .....	7
<b>Figure 1.8</b> Some macrocyclic sensors; a) binding of Na <sup>+</sup> to a monoaza-18-crown-6 sensor, <b>9</b> ; b) pyrene modified $\beta$ -cyclodextrin with inclusion of a guest, <b>10</b> .....	8
<b>Figure 1.9</b> Porphyrin ( <b>11</b> ) and one of Sanders' porphyrin dendrimers, <b>12</b> .....	9
<b>Figure 1.10</b> Macrocycles <b>14</b> and <b>15</b> .....	11
<b>Figure 1.11</b> Macrocycle <b>16</b> , where M = Mg(II) or Zn(II), was synthesized using template <b>16-T</b> (left). <sup>37</sup> .....	12
<b>Figure 1.12</b> Shape-persistent macrocycles <b>17-19</b> with potential metal binding sites, showing coordination of metals to <b>17</b> at top right.....	13
<b>Figure 1.13</b> Various salen and salphen complexes.....	16
<b>Figure 1.14</b> Early Schiff base macrocycles.....	17
<b>Figure 1.15</b> Robson macrocycle, <b>27</b> .....	18
<b>Figure 1.16</b> Texaphyrin <b>28</b> and Schiff base expanded porphyrin <b>29</b> .....	19
<b>Figure 1.17</b> Early examples of [3+3] macrocycles, <b>30-32</b> .....	19
<b>Figure 1.18</b> a) A [3+3] Schiff base macrocycle, <b>33</b> . b) Heptazinc complex of <b>33</b> , <sup>68</sup> c) A postulated structure of ion-induced tubular assembly of <b>33</b> . <sup>67</sup> .....	21
<b>Figure 1.19</b> Schiff base macrocycles <b>34</b> and <b>35</b> .....	22

<b>Figure 1.20</b> The structures of anthracene (36), phenanthrene (37), triphenylene (38), chrysene (39), pyrene (40) and tetracene (41). .....	23
<b>Figure 1.21</b> Helicenes 42 and 43, R = <sup>n</sup> C <sub>12</sub> H <sub>25</sub> . .....	25
<b>Figure 1.22</b> Optimized structure of cyclo[12]phenacene 44 and a partially deoxygenated molecular belt, 45.....	26
<b>Figure 1.23</b> Phenanthrenophane 48 and triphenanthro[24]annulene 49. ....	28
<b>Figure 1.24</b> Macrocycles containing triphenylene. A representation of tritopic receptor complexation (top left), <sup>88</sup> with tritopic receptor 50 and dibenzylammonium guest (top right). Expanded Zn-phthalocyanine 51, (bottom). ....	29
<b>Figure 1.25</b> Phenanthrene-containing PPP-type polymers 52-54 (R = <sup>n</sup> C <sub>10</sub> H <sub>21</sub> , <i>p</i> -(C <sub>6</sub> H <sub>4</sub> )- <sup>n</sup> C <sub>10</sub> H <sub>21</sub> for polymers 53 and 54).....	30
<b>Figure 1.26</b> Triphenylene-containing PPE, R = 2-ethylhexyl.....	31
<b>Figure 1.27</b> Helicene Schiff base polymers 56 and 57 (top). The bottom figure shows three dimensional representations of the polymer. <sup>98</sup> .....	32
<b>Figure 1.28</b> A typical hexasubstituted triphenylene 58 with liquid crystalline properties and a pentaalkoxy triphenylene 59 with different R groups (R = Br, Ac, CN, CCSi(Me) <sub>3</sub> ). .....	33
<b>Figure 1.29</b> Di- and trinitrotoluene and di- and trinitrophenol. ....	34
<b>Figure 1.30</b> Polymers 62-66 for nitroaromatic sensing.....	35
<b>Figure 1.31</b> Macrocycle 67 for sensing nitroaromatics.....	36
<b>Figure 1.32</b> Phenanthrene and triphenylene macrocycles.....	37
<b>Figure 1.33</b> Phenanthrene and triphenylene-based salicylates 70-73. ....	38
<b>Figure 1.34</b> Macrocycles 74 and 75.....	39
<b>Figure 1.35</b> Comparison of salphen and phenanthrene (top). Poly(salphenyleneethynylene) 76 and a phenanthrene analogue 77.....	40
<b>Figure 2.1</b> Numbering of the carbon atoms of phenanthrene. ....	48
<b>Figure 2.2</b> Numbering of the carbon atoms of triphenylene.....	50
<b>Figure 2.3</b> Structures of phenanthrene and triphenylene-containing precursors 70-73. ..	52
<b>Figure 2.4</b> <sup>1</sup> H NMR spectrum (300 MHz, DMSO- <i>d</i> <sub>6</sub> ) of 70a (* = DMSO- <i>d</i> <sub>6</sub> ).....	55

<b>Figure 2.5</b> Precursor <b>70b</b> .....	55
<b>Figure 2.6</b> Aromatic and formyl region of the $^1\text{H}$ NMR (300 MHz) of a mixture of <b>92a</b> ( $\bullet$ ) and <b>92b</b> ( $*$ ) in $\text{DCM-}d_2$ .....	59
<b>Figure 2.7</b> $^1\text{H}$ NMR (300 MHz, $\text{DMSO-}d_6$ ) of <b>100/101</b> (top) and <b>101</b> (bottom).....	64
<b>Figure 2.8</b> ORTEP representation of the crystal structure of <b>101</b> ·2 DMSO. DMSO molecules are omitted from the extended structure for clarity. ....	65
<b>Figure 2.9</b> Hypothetical structures for <b>100</b> . ....	66
<b>Figure 2.10</b> Precursor <b>71</b> , where $\text{R} = {}^n\text{C}_6\text{H}_{13}$ . ....	68
<b>Figure 2.11</b> $^1\text{H}$ NMR (400 MHz, $\text{CDCl}_3$ ) spectrum of <b>71</b> ( $*$ = $\text{CDCl}_3$ ).....	70
<b>Figure 2.12</b> $^1\text{H}$ NMR (300 MHz, $\text{CDCl}_3$ ) spectrum of diol <b>72</b> ( $*$ = $\text{CDCl}_3$ ).....	73
<b>Figure 2.13</b> $^1\text{H}$ NMR (400 MHz, $\text{CDCl}_3$ ) spectrum of diol <b>73b</b> ( $*$ = $\text{CDCl}_3$ ). ....	76
<b>Figure 3.1</b> IR spectra of <b>70a</b> (left) and <b>117</b> (right) as KBr discs. ....	113
<b>Figure 3.2</b> $^1\text{H}$ NMR spectra (400 MHz, $\text{CDCl}_3$ ) of filtrate (top) and solid (bottom) of <b>68b</b> synthesis ( $*$ = $\text{CDCl}_3$ ). ....	115
<b>Figure 3.3</b> MALDI-TOF spectrum of macrocycle <b>68b</b> . The insets show a simulation of the simulated isotope distribution for the $[\text{68b} + \text{H}]^+$ ion (bottom) and the expanded experimental data for this peak (top). ....	116
<b>Figure 3.4</b> $^1\text{H}$ NMR spectrum (300 MHz, $\text{CDCl}_3$ ) of reaction products from attempted synthesis of <b>69</b> ( $*$ = $\text{CDCl}_3$ ).....	118
<b>Figure 3.5</b> MALDI-TOF mass spectrum of <b>69</b> . Simulations of isotope distribution for macrocycle <b>69</b> (top, left) and monoreduced macrocycle <b>119</b> (top, right).....	120
<b>Figure 3.6</b> MALDI-TOF mass spectrum of Ni(II)-templated product, with magnification inset. ....	121
<b>Figure 3.7</b> $^1\text{H}$ NMR spectrum (300 MHz) of <b>74</b> in $\text{CDCl}_3$ ( $*$ = $\text{CDCl}_3$ ).....	124
<b>Figure 3.8</b> MALDI-TOF mass spectrum of <b>74</b> . ....	125
<b>Figure 3.9</b> $^1\text{H}$ NMR spectrum (400 MHz) of <b>75</b> in $\text{CDCl}_3$ ( $*$ = $\text{CDCl}_3$ ).....	127
<b>Figure 3.10</b> MALDI-TOF mass spectrum of <b>75</b> . ....	128
<b>Figure 4.1</b> Representation of macrocycle aggregation.....	138
<b>Figure 4.2</b> Macrocycles <b>27</b> , <b>33-35</b> . ....	140

<b>Figure 4.3</b> Macrocyclic sensors <b>19</b> and <b>67</b> .....	141
<b>Figure 4.4</b> Macrocycles <b>74</b> and <b>75</b> .....	142
<b>Figure 4.5</b> Stacked <sup>1</sup> H NMR spectra (400 MHz, CDCl <sub>3</sub> , 1.5 mM) of <b>74</b> at various temperatures (* = CDCl <sub>3</sub> ). .....	144
<b>Figure 4.6</b> Stacked <sup>1</sup> H NMR spectra (400 MHz, CDCl <sub>3</sub> , RT) of <b>74</b> at two concentrations (* = CDCl <sub>3</sub> ). .....	144
<b>Figure 4.7</b> Stacked <sup>1</sup> H NMR spectra (400 MHz, CDCl <sub>3</sub> , 1.4 mM) of <b>75</b> at various temperatures (* = CDCl <sub>3</sub> ). .....	145
<b>Figure 4.8</b> Stacked <sup>1</sup> H NMR spectra (400 MHz, CDCl <sub>3</sub> , RT) of <b>75</b> at two concentrations (* = CDCl <sub>3</sub> ). .....	145
<b>Figure 4.9</b> Plots of chemical shift vs. concentration of <b>75</b> for a) OH, b) CH=N, c) phenylenediimine proton, and d) phenylenediimine OCH <sub>2</sub> at different temperatures (● = 5 °C, ○ = 15 °C, ▼ = 25 °C, Δ = 35 °C, ■ = 45 °C, □ = 55 °C) in CDCl <sub>3</sub> . The curves in b) and c) represent the best fit of these data to the dimer model, equation 4.1.....	146
<b>Figure 4.10</b> van't Hoff plots for the dimerization of <b>75</b> a) imine K <sub>E</sub> and b) phenylenediimine K <sub>E</sub> . .....	148
<b>Figure 4.11</b> Structures of hypothetical dimers of <b>74</b> (top) and <b>75</b> (bottom), with ChemDraw representations on the left and Spartan models on the right.....	151
<b>Figure 4.12</b> Powder X-Ray diffraction pattern of <b>75</b> .....	152
<b>Figure 4.13</b> MALDI-TOF mass spectrum of <b>122</b> . .....	154
<b>Figure 4.14</b> MALDI-TOF mass spectrum of <b>123</b> . .....	156
<b>Figure 4.15</b> MALDI-TOF mass spectrum of <b>124</b> , and mono- and dimetallated <b>75</b> . ....	158
<b>Figure 4.16</b> Normalized absorption (dashed) and emission (solid) of <b>72</b> (black, 7.6 x 10 <sup>-6</sup> M) and <b>74</b> (red, 4.2 x 10 <sup>-6</sup> M) in DCM. ....	159
<b>Figure 4.17</b> Normalized absorption (dashed) and emission (solid) of <b>73b</b> (black, 7.6 x 10 <sup>-6</sup> M) and <b>75</b> (red, 2.9 x 10 <sup>-6</sup> M) in DCM.....	159
<b>Figure 4.18</b> Normalized absorption (dashed) and emission (solid) of <b>74</b> (black, 4.2 x 10 <sup>-6</sup> M) and <b>75</b> (red, 2.9 x 10 <sup>-6</sup> M) in DCM. ....	160
<b>Figure 4.19</b> Emission spectra of <b>74</b> (4.2 x 10 <sup>-7</sup> M, left) and <b>75</b> (4.2 x 10 <sup>-7</sup> M, right) in DCM over time where black is t = 0 min and blue is t ≈ 300 min.....	161

<b>Figure 4.20</b> Emission spectra of <b>74</b> (left) and <b>75</b> (right) in toluene ( $7.8 \times 10^{-7}$ M for both solutions) over time where black is $t = 0$ min and blue is $t \approx 420$ min. ....	162
<b>Figure 4.21</b> Emission spectra of <b>74</b> ( $1.6 \times 10^{-6}$ M, dashed) and <b>75</b> ( $1.4 \times 10^{-6}$ M, solid) in toluene before (black) and after (red) addition of <i>p</i> -TsOH. ....	163
<b>Figure 4.22</b> Emission spectra of <b>74</b> (dashed) and <b>75</b> (solid) in DCM ( $5.0 \times 10^{-6}$ M) before (black) and after (red) the addition of DNT. ....	165
<b>Figure 5.1</b> Examples of poly(fluorene) and poly(carbazole). ....	173
<b>Figure 5.2</b> Conjugated polymers <b>52-55</b> and <b>76</b> . ....	174
<b>Figure 5.3</b> $^1\text{H}$ NMR spectrum (300 MHz, $\text{CDCl}_3$ ) of <b>77</b> (* = $\text{CDCl}_3$ ). ....	177
<b>Figure 5.4</b> GPC of polymer <b>77</b> in THF (ca. 1 mg/mL) measured relative to polystyrene standards. ....	177
<b>Figure 5.5</b> Absorption (dashed line) and emission (solid line) spectra of model compound <b>109</b> (black, $3.5 \times 10^{-6}$ M) and polymer <b>77</b> in DCM (blue, 2.6 mg/L) and in the solid state (red). ....	178
<b>Figure 5.6</b> Optical spectroscopy of <b>126</b> (black) and <b>128</b> (red) in DCM. Absorption spectra (dashed line, $4.0 \times 10^{-6}$ M) and emission spectra (solid line, 2.0 mg/L). ..	179
<b>Figure 5.7</b> Emission spectrum of <b>77</b> (black, 1.4 mg/L) and <b>77</b> after the addition of DNT (red). ....	181
<b>Figure 6.1</b> Early examples of Schiff base polymers. ....	191
<b>Figure 6.2</b> Schiff base PPEs <b>76</b> and <b>135</b> . ....	192
<b>Figure 6.3</b> Thiophene-containing Schiff base monomers <b>136-138</b> . ....	193
<b>Figure 6.4</b> $^1\text{H}$ NMR (300 MHz, $\text{CDCl}_3$ ) spectrum of <b>140a</b> (* = $\text{CDCl}_3$ ). ....	195
<b>Figure 6.5</b> Monomer <b>140</b> , with breaks in conjugation shown in red. Conjugated monomer <b>147</b> , with the path of conjugation in blue. ....	196
<b>Figure 6.6</b> $^1\text{H}$ NMR (300 MHz, $\text{CDCl}_3$ ) spectrum of <b>147a</b> (* = $\text{CDCl}_3$ ). ....	198
<b>Figure 6.7</b> Formation of the radical cations for <b>140</b> and <b>147</b> , showing one resonance structure for each monomer. ....	199
<b>Figure 6.8</b> Normalized absorption spectra of dithienylsalphen monomers in DCM (concentration $4.0 - 5.0 \times 10^{-6}$ M), where a) <b>140a</b> (black), <b>147a</b> (red) b) <b>141a</b> (black), <b>148a</b> (red) c) <b>142a</b> (black), <b>149a</b> (red), d) <b>143a</b> (black), <b>150a</b> (red). ....	200

## List of Schemes

<b>Scheme 1.1</b> Selected syntheses of phenyleneethynylene macrocycle <b>13</b> .....	10
<b>Scheme 1.2</b> The Schiff base condensation. ....	14
<b>Scheme 1.3</b> Schiff base condensation to form salen (top) and salphen (bottom).....	15
<b>Scheme 1.4</b> Photocyclization of stilbene and <i>ortho</i> -terphenyl to phenanthrene, <b>37</b> , and triphenylene, <b>38</b> , respectively. ....	24
<b>Scheme 1.5</b> Synthesis of phenanthrene-containing coordination macrocycles <b>46</b> and <b>47</b> . ....	27
<b>Scheme 2.1</b> Stilbene syntheses: a) Perkin reaction followed by decarboxylation and b) Meerwein reaction, followed by photocyclization to phenanthrene. ....	48
<b>Scheme 2.2</b> Novel phenanthrene syntheses: a) three component coupling and b) Ullman and McMurry couplings.....	49
<b>Scheme 2.3</b> Nitration and acylation of phenanthrenequinone.....	50
<b>Scheme 2.4</b> Select methods of triphenylene synthesis. ....	51
<b>Scheme 2.5</b> Synthesis of <b>80 - 82</b> . ....	53
<b>Scheme 2.6</b> Synthesis of <b>83</b> .....	54
<b>Scheme 2.7</b> Deprotection of <b>83</b> to form <b>70a</b> . ....	54
<b>Scheme 2.8</b> Synthesis of <b>85 – 87a</b> .....	56
<b>Scheme 2.9</b> Synthesis of <b>88a</b> and <b>89</b> . ....	57
<b>Scheme 2.10</b> Synthesis of <b>90</b> and <b>91</b> , and attempted formylation of <b>91</b> . ....	58
<b>Scheme 2.11</b> Synthesis of <b>93 - 95</b> . ....	60
<b>Scheme 2.12</b> Synthesis of <b>86b</b> , <b>87b</b> and <b>89</b> .....	61
<b>Scheme 2.13</b> Synthesis of <b>96</b> .....	61
<b>Scheme 2.14</b> Synthesis and protection of <b>97</b> .....	62
<b>Scheme 2.15</b> Synthesis of <b>99-101</b> , <b>88b</b> . ....	63
<b>Scheme 2.16</b> Attempted routes to <b>70b</b> . ....	67

<b>Scheme 2.17</b> Synthesis of <b>103 – 106</b> and <b>71</b> .....	69
<b>Scheme 2.18</b> Attempted iodination of <b>87b</b> .....	71
<b>Scheme 2.19</b> Synthesis of <b>108</b> and <b>107</b> .....	71
<b>Scheme 2.20</b> Synthesis of model compound <b>109</b> .....	72
<b>Scheme 2.21</b> Synthesis of diol <b>72</b> .....	72
<b>Scheme 2.22</b> Initial synthesis of <b>73a</b> .....	74
<b>Scheme 2.23</b> Synthesis of <b>113, 114</b> and <b>73b</b> .....	75
<b>Scheme 3.1</b> General representation of the synthesis of a [3+3] Schiff base macrocycle (top) and synthesis of <b>33</b> .....	111
<b>Scheme 3.2</b> Attempted synthesis of <b>68a</b> .....	113
<b>Scheme 3.3</b> Synthesis of <b>68b</b> .....	114
<b>Scheme 3.4</b> Synthesis of <b>69</b> and monoreduced macrocycle <b>119</b> .....	117
<b>Scheme 3.5</b> Synthesis of model compounds <b>120</b> and <b>121</b> .....	122
<b>Scheme 3.6</b> Synthesis of macrocycle <b>74</b> .....	123
<b>Scheme 3.7</b> Synthesis of <b>75</b> . Breaks in the conjugation are denoted in red. ....	126
<b>Scheme 4.1</b> Synthesis of macrocycle <b>122</b> .....	153
<b>Scheme 4.2</b> Synthesis of macrocycle <b>123</b> .....	155
<b>Scheme 4.3</b> Synthesis of macrocycle <b>124</b> .....	157
<b>Scheme 4.4</b> Proposed mechanism of macrocycle decomposition, resulting in formation of a benzimidazole byproduct. Adapted from reference 27.....	164
<b>Scheme 5.1</b> Synthesis of polymer <b>77</b> .....	176
<b>Scheme 5.2</b> Synthesis of <b>126</b> and <b>128</b> .....	179
<b>Scheme 5.3</b> Synthesis of compound <b>129</b> and attempted polymerization.....	180
<b>Scheme 6.1</b> Synthesis of condensation polymers <b>133</b> and <b>134</b> .....	192
<b>Scheme 6.2</b> Synthesis of compounds <b>140-144</b> .....	195
<b>Scheme 6.3</b> Synthesis of compounds <b>146-150</b> .....	197

<b>Scheme 7.1</b> Proposed synthesis of <b>151</b> and <b>152</b> .....	215
<b>Scheme 7.2</b> Proposed incorporation of phenanthroline into [3+3] Schiff base macrocycles.....	216
<b>Scheme 7.3</b> Proposed syntheses of helical PPEs <b>154</b> and <b>155</b> .....	218

## List of Symbols and Abbreviations

Abbreviation	Description
°	degrees
A	analyte
Å	Ångstrom
Ac	acetyl
acac	acetylacetonate
aq.	aqueous
Ar	aromatic ring
Bn	benzyl
<sup>t</sup> Boc	<i>tert</i> -butyloxycarbonyl
br	broad
Bu	butyl
<sup>n</sup> Bu	<i>normal</i> -butyl
<sup>t</sup> Bu	<i>tert</i> -butyl
BuOct	2-butyloctyl
C	concentration (in association models)
°C	degrees Celsius
ca.	circa
cal	calories
Calc'd	calculated
CAN	cerium ammonium nitrate
CD	circular dichroism

$\text{cm}^{-1}$	wavenumber
d	doublet, lattice spacing
$\Delta$	reflux, change in
$\Delta H$	change in enthalpy
$\Delta S$	change in entropy
$\delta$	chemical shift (ppm)
Da	Daltons
DABCO	1,4-diazabicyclo[2.2.2]octane
dba	dibenzylideneacetone
DCM	dichloromethane
dd	doublet of doublets
dec.	decomposed
DMF	dimethylformamide
DMSO	dimethylsulfoxide
DNA	deoxyribonucleic acid
DNT	dinitrotoluene
DSC	differential scanning calorimetry
$\epsilon$	molar extinction coefficient ( $\text{L cm}^{-1} \text{mol}^{-1}$ )
$e^-$	electron
EI	electron impact
equiv.	equivalents
eqn.	equation
ESI	electrospray ionization

Et	ethyl
EtHex	2-ethylhexyl
g	gram
GPC	gel permeation chromatography
h	hours
$\theta$	angle in degrees
hv	light
HPLC	high performance liquid chromatography
Hz	hertz
I	intensity
$I_0$	initial intensity
IR	infrared
J	coupling constant (NMR)
K	Kelvin
kcal	kilocalories
$K_E$	association constant
$k_q$	rate of quenching
$K_{SV}$	Stern-Volmer constant
L	litre
$\lambda$	wavelength
$\lambda_{em}$	wavelength of maximum emission
$\lambda_{exc}$	wavelength of excitation
$\lambda_{max}$	wavelength of maximum absorption

LED	light emitting diode
M	concentration in Molar (mol/L)
M <sup>+</sup>	molecular ion
m	multiplet
<i>m</i>	meta
MALDI	matrix assisted laser desorption ionization
Me	methyl
MEH-PPV	poly[2-methoxy-5-(2-ethylhexyloxy)-1,4-phenylenevinylene]
MHz	megahertz
mg	milligrams
min	minutes
μL	microlitre
mL	millilitre
mM	millimolar
mmol	millimoles
M <sub>n</sub>	number average molecular weight
mol	moles
Mp.	melting point
MRI	magnetic resonance imaging
MS	mass spectrometry
mV	millivolts
M <sub>w</sub>	weight average molecular weight

$m/z$	mass to charge ratio
$\nu$	frequency
NBS	N-bromosuccinimide
NLO	non-linear optics
nm	nanometers
NMR	nuclear magnetic resonance
<i>o</i>	<i>ortho</i>
<i>o</i> -tol	<i>o</i> -tolyl
OLED	organic light emitting diode
P	chemical shift (in association models)
<i>p</i>	<i>para</i>
$P_a$	chemical shift of aggregate (in association models)
PAH	polycyclic aromatic hydrocarbon
$P_d$	chemical shift of dimer (in association models)
PDI	polydispersity index
Ph	phenyl
$P_m$	chemical shift of monomer (in association models)
ppb	parts per billion
PPE	poly(phenyleneethynylene)
ppm	parts per million
PPP	poly( <i>para</i> -phenylene)
PPV	poly(phenylenevinylene)
<sup><i>i</i></sup> Pr	<i>iso</i> -propyl

py	pyridine
q	quartet
R	substituents as defined, gas constant
Res.	resolution
RT	room temperature
s	singlet
salen	<i>N,N'</i> -ethylenebis(salicylideneimine)
salphen	<i>N,N'</i> -phenylenebis(salicylideneimine)
T	temperature
t	triplet
$\tau$	fluorescent lifetime
Tf	triflate
$T_g$	glass transition
THF	tetrahydrofuran
TLC	thin layer chromatography
TMA	trimethylacetyl
TMS	trimethylsilyl
TNT	trinitrotoluene
TOF	time of flight
TsOH	<i>p</i> -toluenesulfonic acid
$\Phi_F$	quantum yield of fluorescence
UV	ultraviolet
VC	variable concentration

Vis

visible

vs.

versus

VT

variable temperature

## Acknowledgements

Many people helped me during my Ph. D. studies. Dr. Mark MacLachlan gave me the opportunity to join his lab group and learn new research techniques, and helped me become a better scientist. The rest of the MacLachlan group members, both past and present gave me advice, made starting materials for me to use and helped keep me in good spirits when things weren't working. Specifically, I would like to thank Joseph for obtaining MALDI-TOF mass spectra, Alfred, Dave, Amanda, Joseph, Marc and Ago for letting me use their chemicals and everyone else for doing their lab jobs and keeping the place running. Kate Jardine was a summer student who worked with me on all the PPE research. I collaborated with Dr. Mike Wolf, Dr. Bryan Sih and Agostino Pietrangelo on the "Space Project". I would like to thank them for their part in the research and for a fun trip to Ottawa so I could become "enlightened". I would like to thank the Canadian Space Agency for funding to this project. I got a lot of help from all the members of the UBC Chemistry Department. All the mass spectroscopy and elemental analysis was done by the staff of the UBC Mass Spectrometry Centre. The NMR staff, led by Dr. Nick Burlinson, gave me great advice on various NMR experiments. Single crystal X-ray diffraction was performed by Dr. Brian Patrick and powder X-ray diffraction was obtained with the assistance of Anita Lam. GPC data was obtained by Mandy Yam and Bronwyn Gillon from the Gates Group. Lastly I would like to thank all my friends, my family and my kickboxing school for helping me to have fun and stay balanced.

## Statement of Co-Authorship

Chapter 1 – I wrote this chapter myself.

Chapter 2 – I performed the syntheses in this chapter myself, with the exception of compounds **107b**, **107c** and **109**, which were synthesized by Kate J. Jardine under my supervision, and compound **72**, which was initially synthesized by Joseph Hui. Characterization of **86b**, **87b**, **89**, **108**, **107b**, **107c** and **109** were done by Kate J. Jardine. Some starting materials were synthesized by other group members as follows: **80** from Mark J. MacLachlan, **102** by Amanda J. Gallant and David R. Edwards. The crystal structure of compound **101** was solved by Brian O. Patrick. The published/submitted sections of the chapters were co-written by Dr. Mark J. MacLachlan.

Chapter 3 – I performed the syntheses and characterizations in this chapter myself. Compounds **115a-d** were synthesized by other members of the MacLachlan group and BOC-protected phenylenediamine was made by Dr. Marc Sauer. The published/submitted sections of the chapters were co-written by Dr. Mark J. MacLachlan.

Chapter 4 – I performed the syntheses and characterizations, and wrote this chapter myself.

Chapter 5 - I performed the syntheses and characterization in this chapter myself, with the exception of compounds **125**, **127** and **128**, which were synthesized and characterized by Alfred C. W. Leung, and **77**, **129**, and **130** which were synthesized and characterized

by Kate J. Jardine, under my supervision. The published sections of the chapters were co-written by Dr. Mark J. MacLachlan.

Chapter 6 – I performed the synthesis and characterization in this chapter myself, and wrote this chapter myself. Electropolymerizations were performed by Dr. Bryan C. Sih. Material in this chapter was submitted for publication in a paper with several co-authors, but only the part that I wrote was included in the thesis.

Chapter 7 – I wrote this chapter myself

# Chapter 1

## Introduction

### 1.1 Supramolecular Chemistry

#### 1.1.1 Background

The term supramolecular chemistry, which was coined by Jean-Marie Lehn,<sup>1</sup> means “chemistry beyond the molecule”.<sup>2</sup> While individual molecules consist of atoms joined by covalent bonds, supramolecular chemistry makes use of intermolecular interactions, including hydrogen bonding,  $\pi$ -stacking and electrostatic forces (Figure 1.1), bringing molecules together to form larger species.<sup>3</sup> Hydrogen bonding enables compounds containing electronegative functional groups to interact with protons to form extended arrays. Molecules with aromatic rings can stack together by virtue of  $\pi$ - $\pi$  interactions. Electrostatic interactions include ion-ion, ion-dipole and dipole-dipole interactions, where positively and negatively charged species associate.

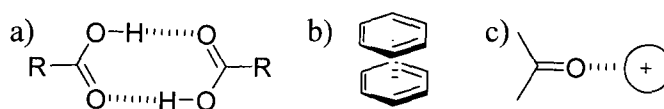


**Figure 1.1** Examples of a) hydrogen bonding, b)  $\pi$ - $\pi$  stacking, c) ion-dipole electrostatic interactions.

As supramolecular chemistry focuses on how molecules interact with one another, there is an emphasis on complementarity and preorganization.<sup>4</sup> Complementarity is the matching of a host molecule to the electronic and geometric needs of a guest. This

is best exemplified by DNA base pairs, which selectively hydrogen bond to each other.<sup>5</sup> Preorganization occurs when a host molecule has a defined conformation that undergoes minimal change upon guest complexation. Taking these concepts into account, one can design supramolecular complexes that can behave as molecular machines,<sup>6</sup> such as shuttles, switches, and sensors.

Chemical sensors exhibit a reversible change in physical properties when exposed to a stimulus.<sup>7, 8</sup> The change in properties may be electrochemical, such as alteration of redox potential, or optical, such as a change in colour. Chemosensors require both a mechanism for the sensor to interact with the analyte, as well as a means for signaling the presence of the analyte. Luminescence is a convenient signal for a chemosensor and it can either be “turned on” or “turned off” in the presence of an analyte (Figure 1.2). For example, a fluorescent indicator may coordinate to a host until competitive binding of an analyte releases the fluorophore to restore luminescence. On the other hand, the presence of an analyte can quench luminescence via photoinduced electron transfer or another electronic mechanism. Supramolecular complexes are often modified with appropriate fluorophores to form sensors for anions, cations and neutral species.

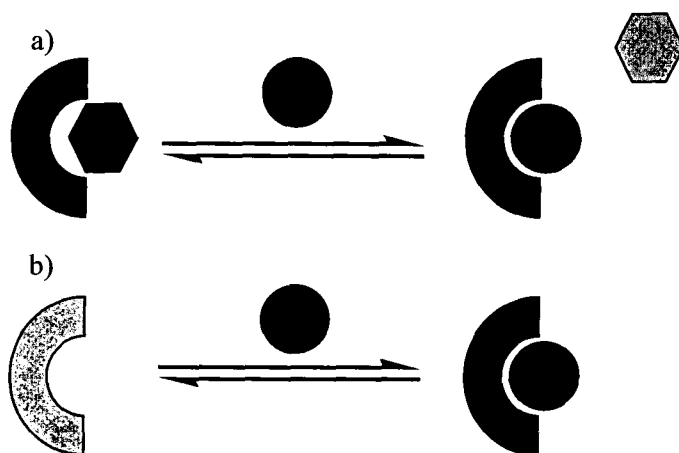


**Figure 1.2** a) Sensing by release of a fluorophore, b) Sensing of an analyte by fluorescence quenching (purple indicates luminescence, while blue indicates quenching).

### 1.1.2 Macrocycles

Macrocycles play an important role in supramolecular chemistry. A macrocycle is a large cyclic molecule, often containing heteroatoms or functional groups that allow for the participation in intermolecular interactions. Early examples of macrocycles, shown in Figure 1.3, include crown ethers, such as **1**, discovered by Charles Pedersen. The oxygen atoms in the ring enable the macrocycle to coordinate alkali metal cations.<sup>9</sup> By replacing two of the oxygen atoms with nitrogen atoms, another strand can be added to the macrocycle to form cryptands, **2**, developed by Jean-Marie Lehn.<sup>2</sup> Macropolycyclic compounds like **2** bind alkali metals even more strongly than crown ethers. Although unmetallated crown ethers and cryptands show a collapsed ring structure in the solid state, spherands, **3**, are more rigid, preorganized macrocycles that maintain their structure in the absence of metals.<sup>10</sup> Donald Cram devised these molecules so that they do not need to rearrange in solution to accommodate coordination. Pedersen, Lehn and Cram earned the Nobel Prize in Chemistry in 1987 for their pioneering work.

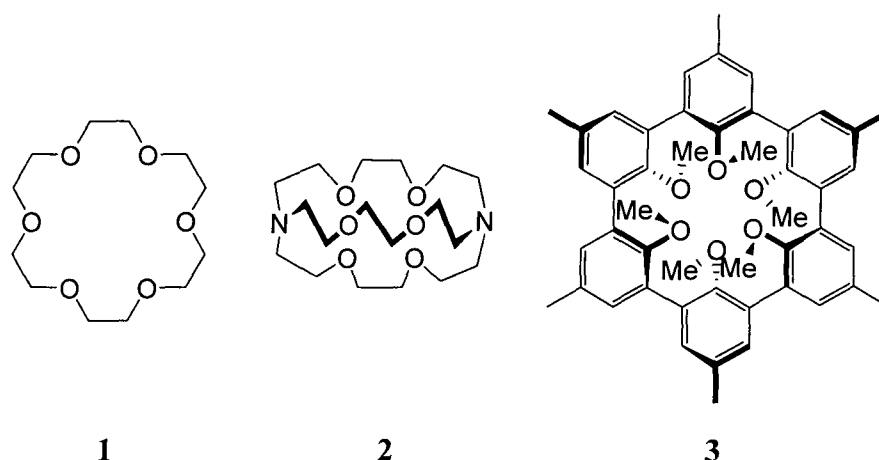


**Figure 1.3** Structures of 18-crown-6 (**1**), cryptand [2.2.2] (**2**), and spherand **3**.

Calixarenes (**4**, Figure 1.4) are similar to spherands, with the insertion of a methylene group between the aromatic rings.<sup>11</sup> Expansion of the backbone endows greater flexibility to the macrocycle, and the conformation of **4** can be tuned depending on the substituents on the individual aromatic rings. If all substituents are on the same rim of the macrocycle, it is referred to as a “cone” conformation. There are also “partial cone”, “1,2-alternate” and “1,3-alternate” conformations. Calixarene **4** is stable as a cone when R = H as a result of hydrogen bonding between hydroxyl groups, but it is mobile enough to rotate into different conformations.<sup>12</sup> When R = *i*Pr, the rotation of **4** is inhibited and a mixture of the four conformers results.<sup>11</sup> Coordination of alkali metals to ester groups or the aromatic rings can fix the configuration of the calixarene into the cone position.<sup>13</sup> Changing R to alkyl or silyl groups, or forming bridges on the ring, as in Figure 1.4f, can immobilize the conformation of the ring as well.<sup>14</sup>

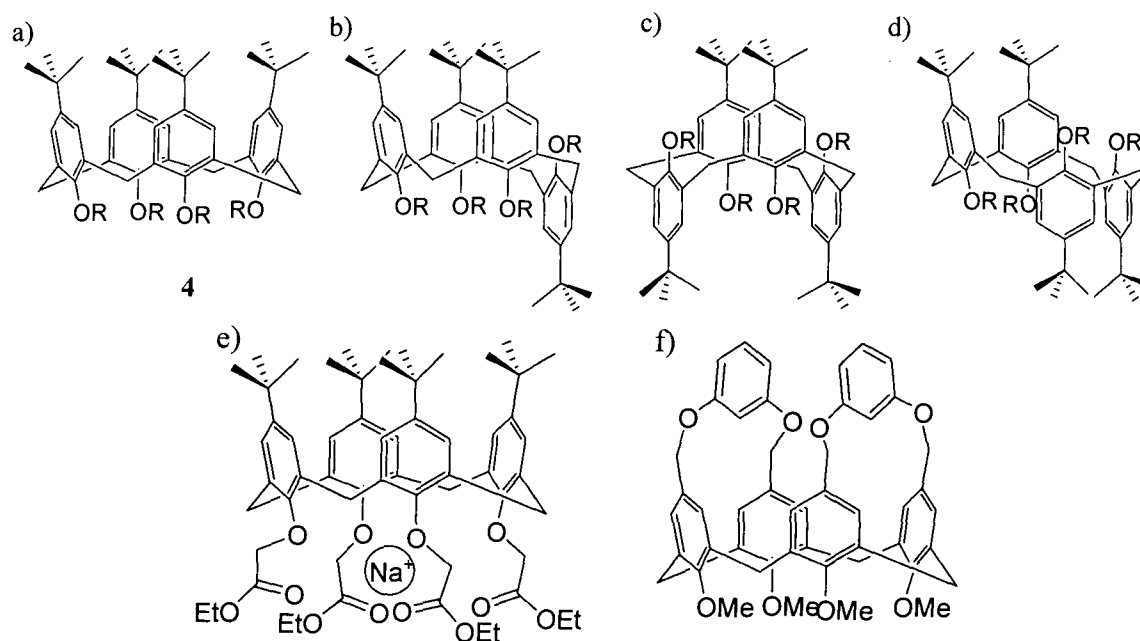


**Figure 1.4** a) Cone, b) partial cone, c) 1,3 alternate and d) 1,2 alternate conformations of *p*-tert-butylcalix[4]arene **4**, R = H, *i*Pr, e) complexation of sodium and f) a bridged calixarene.

Cyclodextrin is a macrocycle composed of glycopyranose units (**5**, Figure 1.5). This cyclic molecule has been studied for over a century, and can be produced naturally by enzyme conversion.<sup>15</sup> It usually contains six, seven or eight sugar units, called  $\alpha$ -,  $\beta$ -, or  $\gamma$ -cyclodextrin, respectively. Cyclodextrin is of interest to supramolecular chemists because it is a versatile host. In aqueous media, hydrophobic interactions between the cyclodextrin and the guest (examples include benzoic acids, steroids and terpenes)<sup>16, 17</sup> drive the formation of an inclusion complex.

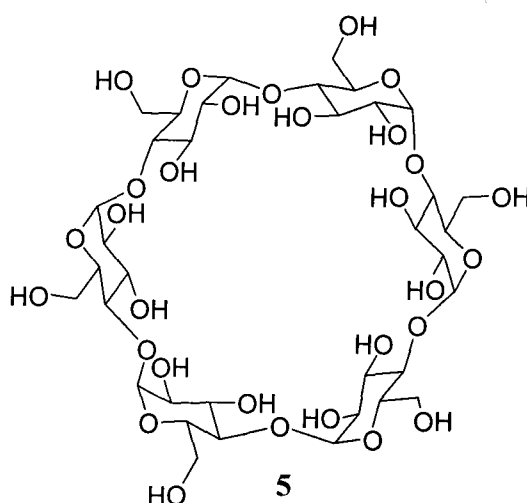


**Figure 1.5**  $\alpha$ -Cyclodextrin, **5**.

Hydrogen bonding is essential in the stacking of Ghadiri's peptide-based macrocycles (**6**, Figure 1.6).<sup>18, 19</sup> Early examples contain eight and twelve amino acids, which aggregate into nanotubes via hydrogen bonds between the amide protons and the carbonyl groups in adjacent rings. In this structure, the side chains of the peptides remain on the outside, enabling the inside of the macrocycle to remain hollow. The size of the pore can be tuned by increasing the number of amino acids in the peptide ring. These tubes can be grown to hundreds of nanometers in length with internal diameters of 7 and

13 Å, respectively and the larger macrocycles assemble into a closely packed hexagonal array.

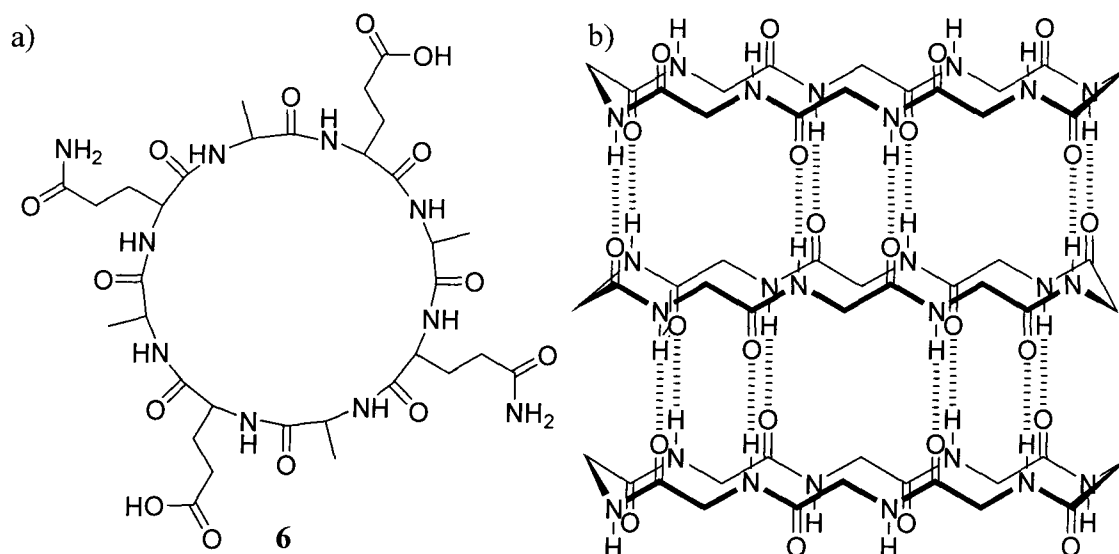


**Figure 1.6** a) Peptide-based macrocycle **6** and b) hydrogen bonding induced stacking of macrocycle **6**.

Both rotaxanes and catenanes are supramolecular structures with a macrocyclic component. Rotaxanes, such as **7**<sup>20</sup> (Figure 1.7), involve “threading” a molecule through a macrocycle and capping the ends to prevent “unthreading”. If the ends are left uncapped, the product is known as a pseudorotaxane. A catenane, for example **8**<sup>21</sup> (Figure 1.7), is obtained when two macrocycles are linked to one another.<sup>22</sup> More complicated rotaxanes and catenanes with multiple rings, coordination sites, or functional groups can potentially form molecular machines.

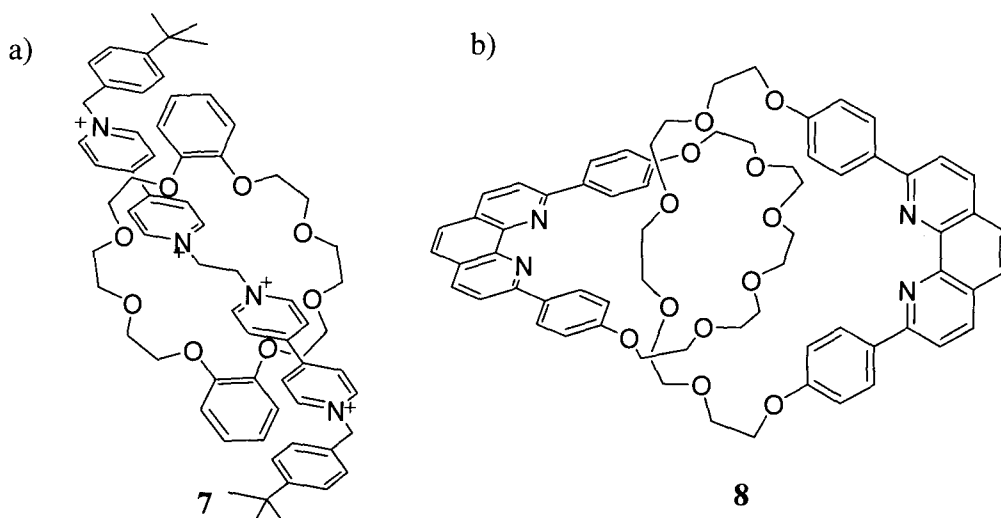


**Figure 1.7** An example of a) a rotaxane **7** and b) a catenane **8**.

The aforementioned supramolecular structures have the potential to become sensors if a signaling component that is sensitive to the changes in the molecule is added to the system. For example, addition of sodium or potassium ions to crown ethers with anthracene bound to the ring turns on emission<sup>23</sup> (**9**, Figure 1.8). Luminescence from the anthracene moiety is quenched in the unbound ether by electron transfer from the lone pair on the nitrogen atom of the crown ether. When a metal ion is bound, luminescence is recovered and an increase in quantum yield of fluorescence is observed. Also,  $\beta$ -cyclodextrin modified with fluorophores such as pyrene, **10**, becomes luminescent upon inclusion of a guest.<sup>24</sup> The guest displaces pyrene from the inside of the cyclodextrin cavity and restores luminescence.

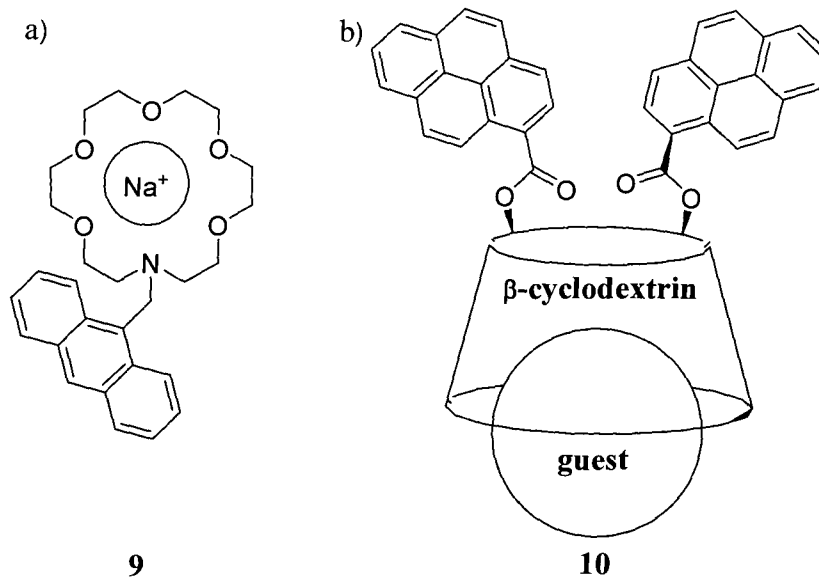


**Figure 1.8** Some macrocyclic sensors; a) binding of  $\text{Na}^+$  to a monoaza-18-crown-6 sensor, **9**; b) pyrene modified  $\beta$ -cyclodextrin with inclusion of a guest, **10**.

### 1.1.3 Shape-Persistent Macrocycles

Shape-persistent macrocycles are rigid cyclic molecules that hold their shape and often have large molecular surfaces and internal voids.<sup>25, 26</sup> Aromatic rings and alkynyl groups are often incorporated into the macrocycle to achieve rigidity. Functional groups can be placed in defined positions to tune the properties and purpose of the macrocycle.

One of the smallest shape-persistent macrocycles is porphyrin (**11**, Figure 1.9). This small macrocycle consists of four pyrrole rings joined by methine groups, and it is conjugated. Porphyrin is ubiquitous in nature in hemoglobin, and a similar macrocycle, chlorin, is present in chlorophyll. Porphyrin is of interest in materials chemistry because of its potential for light harvesting; it has been the focus of many studies that vary the metal center and the substituents on the outside of the ring. Among the examples of porphyrin arrays are the porphyrin dendrimers, **12**, from the group of Jeremy Sanders.<sup>27</sup> By linking individual porphyrins with flexible ethers and esters, porphyrin pentamers or

dendrimers can be formed that have the ability to inter- and intramolecularly coordinate DABCO between two metallated porphyrins.

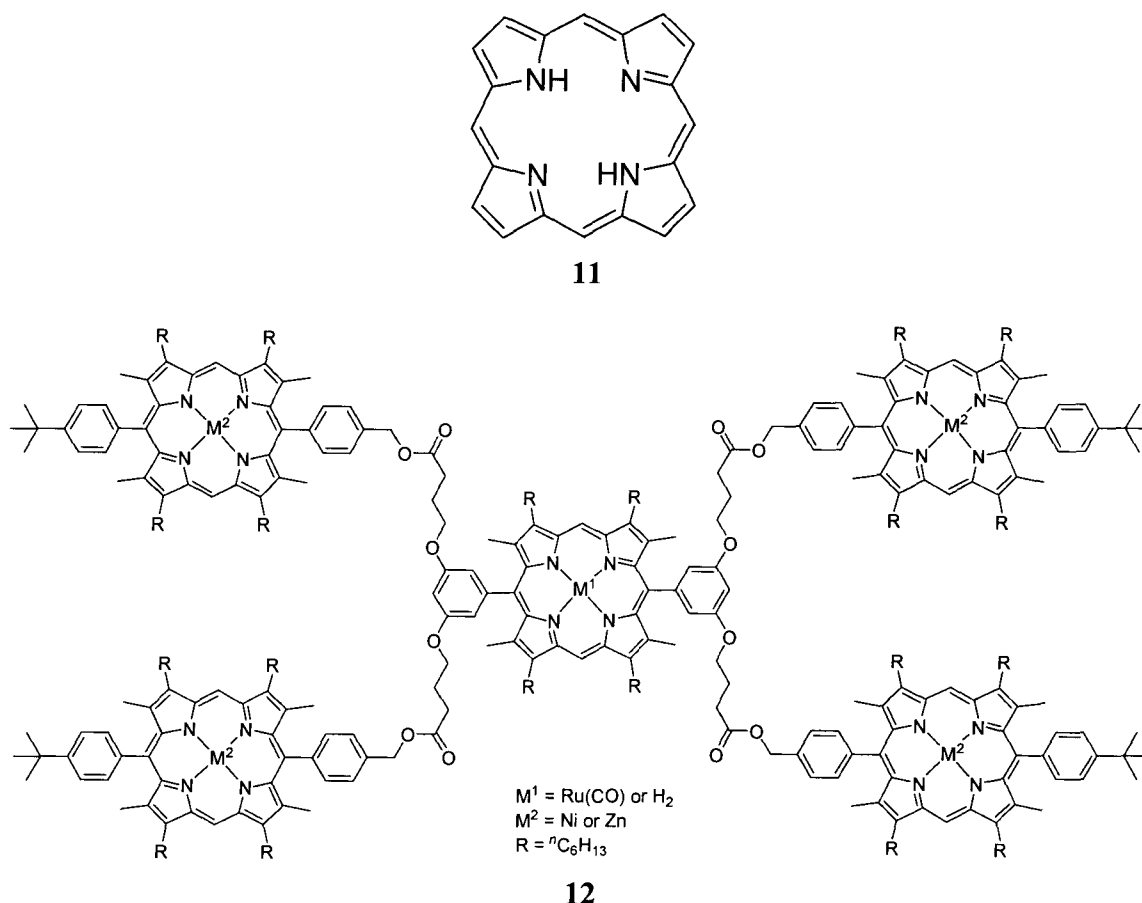
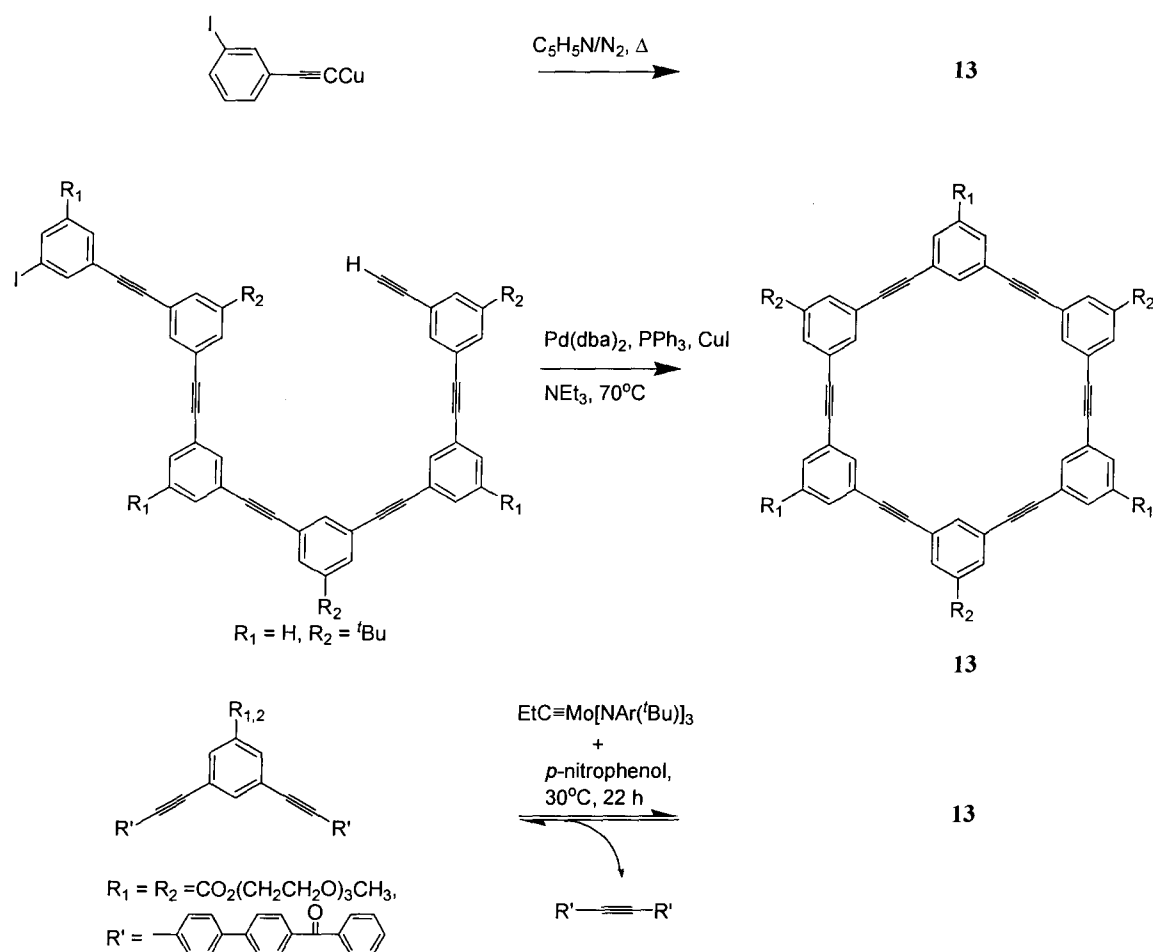


**Figure 1.9** Porphyrin (**11**) and one of Sanders' porphyrin dendrimers, **12**.

Since the discovery by Jeffrey Moore in 1992 that a hexa(phenyleneethynylene) macrocycle, **13**, can aggregate in solution,<sup>28</sup> interest in new conjugated macrocycles has increased. Macrocycle **13** was initially prepared in a one-pot synthesis by Staab and Neunhoffer in 1974 in 4.6% yield (Scheme 1.1).<sup>29</sup> Greater yields of **13** were obtained by using Pd-catalyzed coupling, followed by an intramolecular ring closing to make the same ring.<sup>30</sup> Recently, **13** was successfully synthesized via precipitation-driven alkyne metathesis.<sup>31</sup> The aromatic protons of **13** ( $R_1 = R_2 = \text{CO}_2^t\text{Bu}$ ) in  $\text{CDCl}_3$  exhibited upfield

shifts in  $^1\text{H}$  NMR spectra of increasing concentration. In aromatic NMR solvents, no resonance shift was observed, supporting the theory that  $\pi$ - $\pi$  stacking is responsible for the aggregation.

**Scheme 1.1** Selected syntheses of phenyleneethynylene macrocycle **13**.



A large variety of other macrocycles has been synthesized using high-dilution cross-coupling reactions.<sup>32-34</sup> Suzuki, Sonogashira and Glaser couplings can be employed to make oligo(arylene) macrocycles, arylene ethynylene macrocycles and bis(ethynylene) macrocycles. Schlüter synthesized **14** using a stepwise approach,<sup>35</sup> but the best yields for **14** are achieved via intramolecular ring closing, (the same products can be obtained by

bimolecular coupling). Whereas **14** is prepared via Suzuki couplings, synthesis of **15** proceeds via Sonogashira coupling followed by a bimolecular ring closing by the Glaser reaction.<sup>36</sup> Höger et al. have studied **15** modified with extra- and intraannular functional groups to make liquid crystalline phenyleneethynylene macrocycles. The outside chains promoted the formation of the mesogen, while the inner chains provided stability to the thermotropic mesophase.

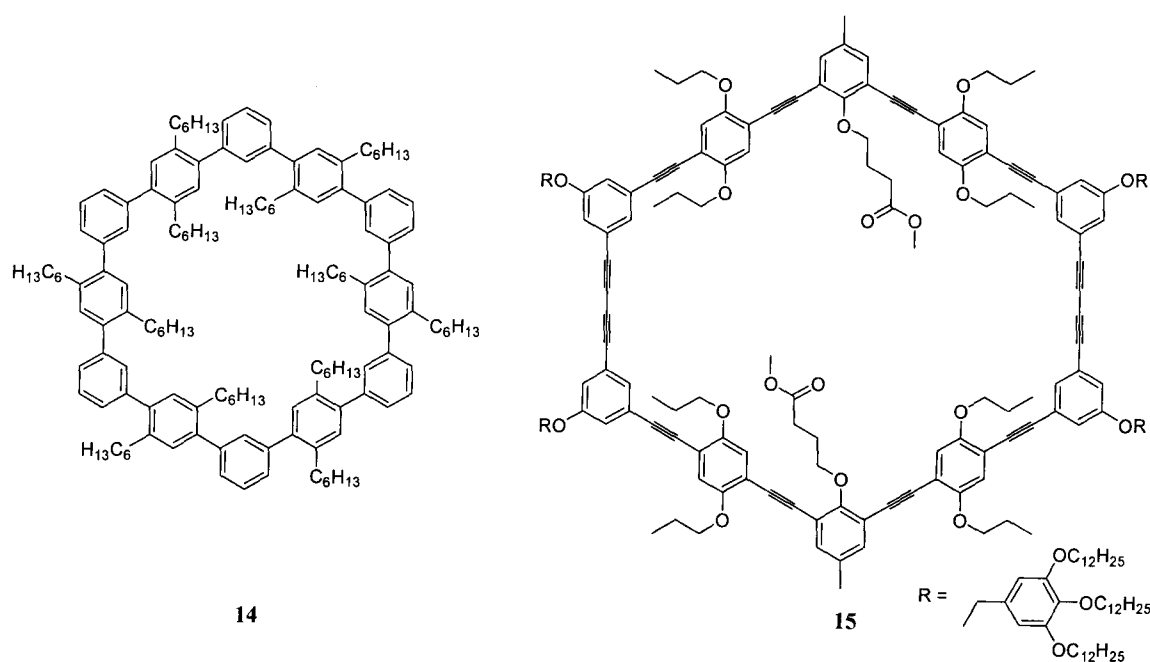


**Figure 1.10** Macrocycles **14** and **15**.

Templation is another technique applied to the synthesis of shape-persistent macrocycles. A supramolecular approach was used to construct a 35 Å hexaporphyrin macrocycle (**16**, Figure 1.11) with phenyleneethynylene linkers.<sup>37</sup> A template with pyridine groups, **16-T**, coordinates to the metal sites in the porphyrin, holding them in place for the Sonogashira coupling reaction.

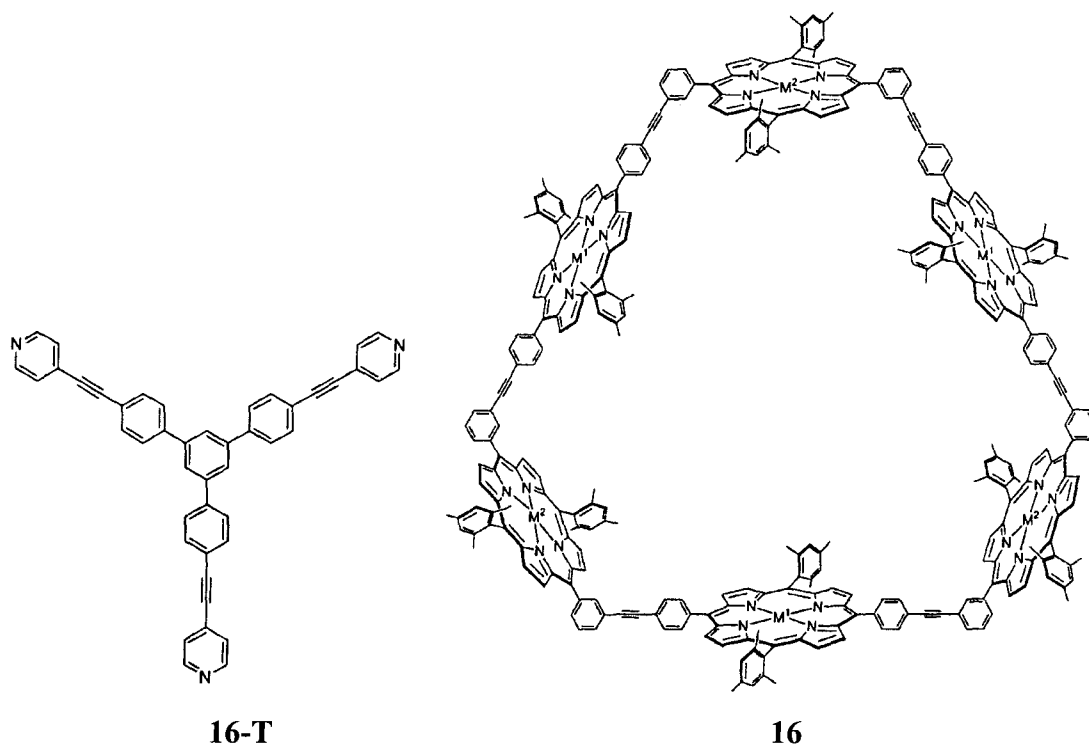


**Figure 1.11** Macrocycle **16**, where  $M = \text{Mg(II)}$  or  $\text{Zn(II)}$ , was synthesized using template **16-T** (left).<sup>37</sup>

By incorporating heteroatoms into shape-persistent macrocycles, metals can be coordinated to the macrocycle. Metal-free macrocycle **17** (Figure 1.12) is highly luminescent, but upon coordination to  $\text{Ru(II)}$  or  $\text{Os(II)}$ , luminescence is quenched (except for emission typical of polypyridine complexes).<sup>38</sup> “Twistophanes” such as **18** and **19** (Figure 1.12) are conjugated phenyleneethynylene macrocycles forced to twist and become non-planar due to geometric constraints. When bipyridyl moieties are incorporated into the backbone, they are able to sense particular metals. Compound **18** acts as a  $\text{Zn(II)}$  sensor, whereas the emission of **19** is quenched in the presence of both  $\text{Ag(I)}$  and  $\text{Cu(II)}$ .<sup>39, 40</sup>

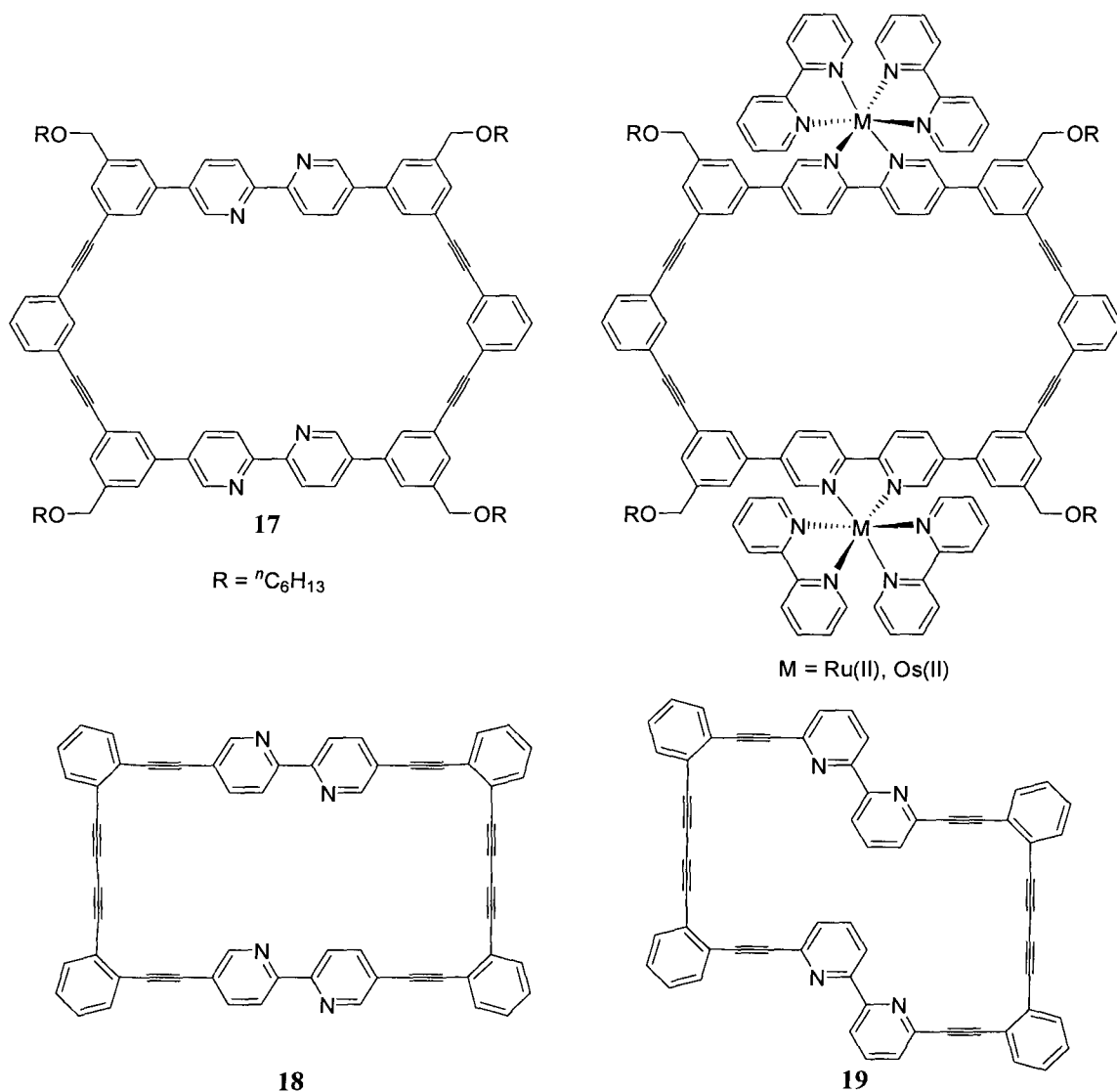


**Figure 1.12** Shape-persistent macrocycles **17-19** with potential metal binding sites, showing coordination of metals to **17** at top right.

Although **13** – **19** are interesting materials, many protection, deprotection and coupling reactions are often needed to synthesize the unclosed ring, which are tedious and decreases overall yield.<sup>41</sup> In order to obtain a high yield in the ring closing step, the reaction must be carried out in high dilution to prevent oligomer formation. It is ideal to synthesize macrocycles in fewer steps with high yields upon ring closing.

## 1.2 Schiff Base Chemistry

### 1.2.1 Salen and Salphen

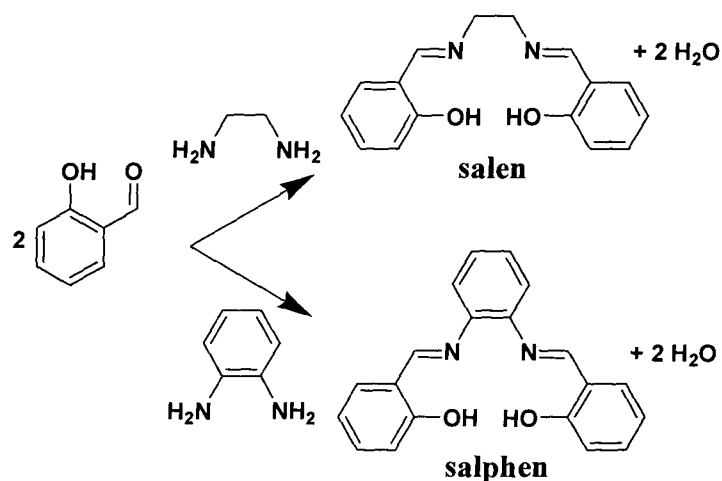
The Schiff base condensation (Scheme 1.2), discovered in 1864 by Hugo Schiff,<sup>42</sup> is the reaction of an amine with an aldehyde or a ketone to form an imine and a molecule of water. This reaction can be catalyzed with acid and is reversible, which commonly enables the formation of the desired (thermodynamic) product in good yield.

**Scheme 1.2** The Schiff base condensation.



If salicylaldehyde is condensed with ethylenediamine, the product is a proligand called *N,N'*-ethylenebis(salicylideneimine) or salen, that contains an  $\text{N}_2\text{O}_2$  coordination pocket when deprotonated (Scheme 1.3). A related conjugated molecule, *N,N'*-phenylenebis(salicylideneimine) or salphen, can be obtained through condensation of *o*-phenylenediamine with salicylaldehyde. Schiff base ligands are desirable because they are easy to synthesize, coordinate a large variety of metals and give complexes with useful properties. Some examples of these complexes are given in Figure 1.13.

**Scheme 1.3** Schiff base condensation to form salen (top) and salphen (bottom).



In a recent paper by Gürol and Ahsen, it is shown through polarized optical microscopy that salphen complexes (**20**) can behave as liquid crystals, similarly to triphenylene.<sup>43</sup> Substitution of long alkoxy chains (C<sub>8</sub>H<sub>17</sub>, C<sub>10</sub>H<sub>23</sub>, and C<sub>12</sub>H<sub>25</sub>) onto both the salicylaldehyde and the phenylenediimine of the salphen results in compounds that exhibit columnar mesophases. Shorter octyloxy chains cause an increase in the temperature of the change from the mesophase to the clearing point.

Chiral manganese salen catalysts (**21**) developed by Jacobsen are used for enantioselective epoxidation of olefins. Similar chiral chromium or cobalt salens catalyze ring opening of epoxides with nucleophiles such as azides with good conversion and enantiomeric excess.<sup>44, 45</sup>

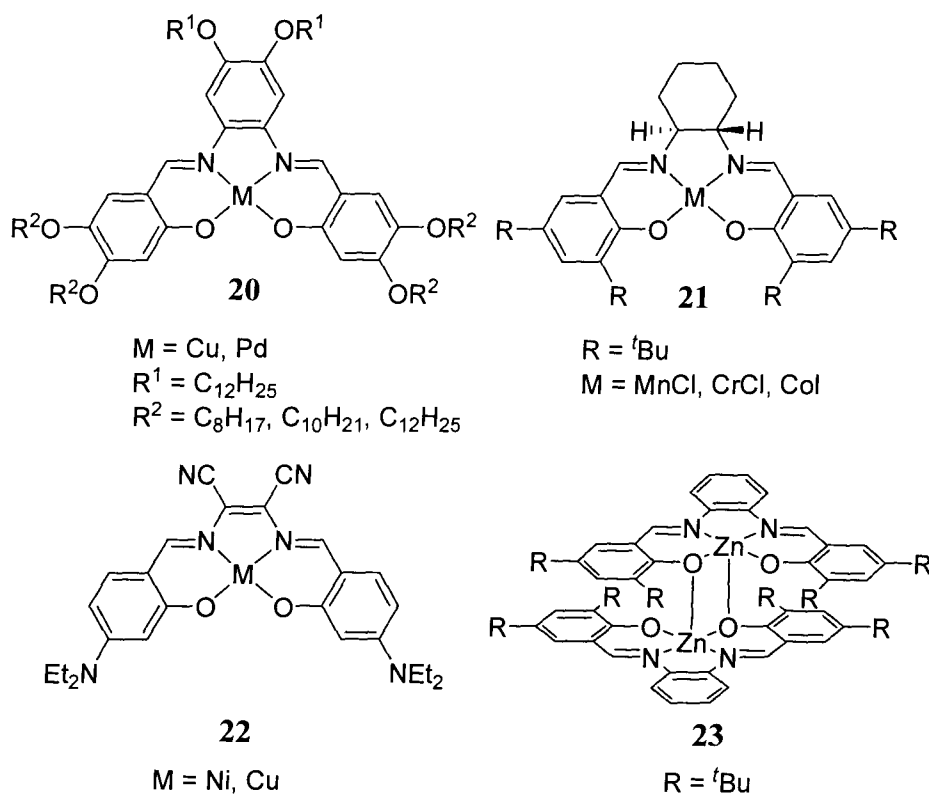


**Figure 1.13** Various salen and salphen complexes.

Salen and salphen ligands have also been found to “switch on” non-linear optical properties upon coordination of metals.<sup>46</sup> In particular, complexes with cyano and diethylamine groups that produce a donor-acceptor relationship in the ligand (**22**), show large second-order effects.

It has been previously found that Zn-salen complexes exhibit luminescence.<sup>47</sup> Recently it was reported that Zn-salphen dimers (**23**) show dynamic fluorescent quenching in the presence of various organic nitro compounds.<sup>48</sup> Most remarkably, 2,3-dimethyl-2,3-dinitrobutane, a compound found in explosives to facilitate detection by canines<sup>49</sup> and not easily detected by conventional fluorescent sensors, induces some quenching of luminescence.

## 1.2.2 Schiff Base Macrocycles

The ease and reversibility of the Schiff base condensation make it a practical tool in the ring closing step in a macrocyclization. The condensation forms a double bond, making it useful for synthesis of conjugated macrocycles. In addition, the incorporation of heteroatoms helps provide coordination sites to increase the functionality of the macrocycle. These factors have been considered by many researchers and it is apparent by the large assortment of Schiff base macrocycles found in the literature.<sup>50-52</sup> Generally, diformyl compounds are combined with equimolar quantities of diamine to form the macrocycle. The product of the condensation may consist of different amounts of the two components to form the macrocycle, such as [1+1] (diformyl to diamine), [2+2] and [3+3]. Some early Schiff base macrocycles that were synthesized in the 1960s are shown in Figure 1.14.<sup>53-55</sup>

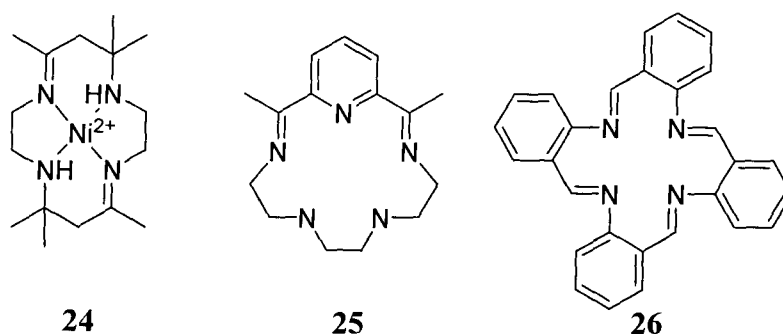


**Figure 1.14** Early Schiff base macrocycles.

One of the most famous examples of a Schiff base macrocycle is the Robson macrocycle, **27**, shown in Figure 1.15, first reported in 1970.<sup>56</sup> Generally, this [2+2] macrocycle is formed using metal templation. Recently, it was reported that the unmetallated Robson macrocycle can be synthesized using templation with protons to

form a salt, and can subsequently be complexed.<sup>57, 58</sup> Complex **27** incorporates two metals in very close proximity, which introduces the opportunity for metal-metal interactions.

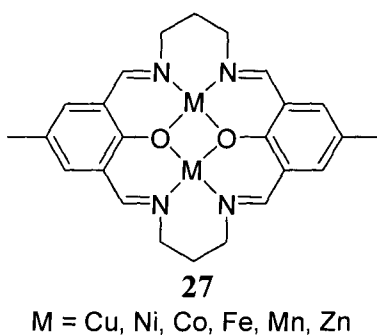


**Figure 1.15** Robson macrocycle, **27**.

Schiff base condensations have been used by Sessler and coworkers not only to incorporate salphen-type moieties into porphyrin, but also to synthesize expanded porphyrins that coordinate multiple metals. His group discovered Texaphyrin (**28**) in 1987,<sup>59</sup> (Figure 1.16) in which two imines replace one pyrrole unit of porphyrin. Cd(II) complexes of **28** and derivatives have been used as photodynamic therapy photosensitizers and Gd(III) complexes of **28** have potential as MRI contrast agents.<sup>60</sup> A hexaaza expanded porphyrin (**29**), a [2+2] Schiff base macrocycle, can coordinate two metals and it even binds methanol to form a neutral substrate complex.<sup>61, 62</sup>

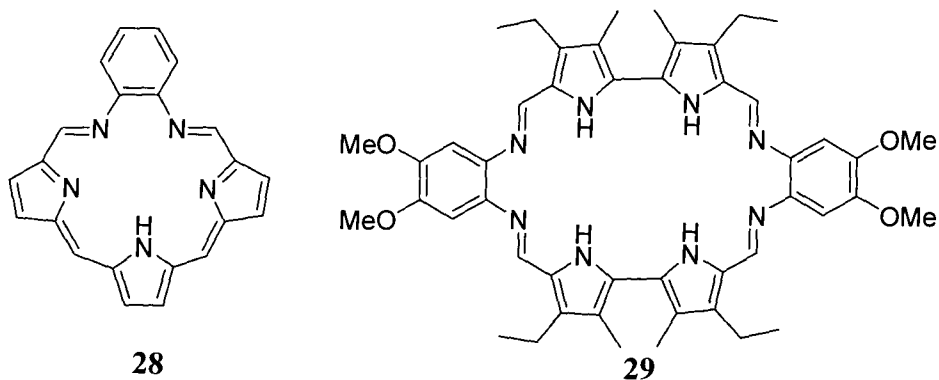


**Figure 1.16** Texaphyrin **28** and Schiff base expanded porphyrin **29**.

Reinhoudt and coworkers were the first to synthesize shape-persistent [3+3] Schiff base macrocycles using  $\text{Ba}^{2+}$  as a template metal. Unfortunately, the metal could not be removed to obtain a metal-free macrocycle (**30**, Figure 1.17).<sup>63</sup> Similar macrocycles, **31** and **32**, have been synthesized from chiral diamines, but are not fully conjugated and do not have hydroxyl groups to form salen pockets.<sup>64, 65</sup> It was shown that, unlike **27** and **30**, both **31** and **32** form selectively in good yield without a template and in the absence of detectable oligomers.

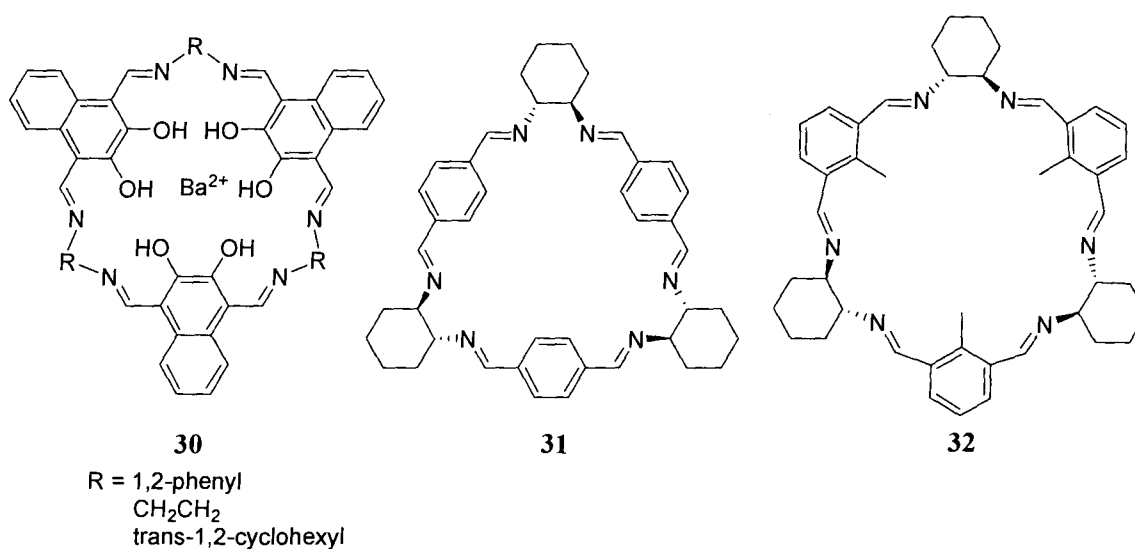


**Figure 1.17** Early examples of [3+3] macrocycles, **30-32**.

Initially it was thought that templation was necessary to form Schiff base macrocycles and prevent polymerization. Nabeshima and coworkers were successful in synthesizing a [3+3] macrocycle (**33**, R = H) without metal templation; however, the condensation reaction took two weeks (Figure 1.18).<sup>66</sup> Our group synthesized **33** with alkoxy chains pendant from the diamine to increase solubility.<sup>67</sup> It is believed the hydrogen bonding between the imine and hydroxyl promotes the formation of **33** without metal templation. Macrocycle **33** can template the formation of transition metal clusters. When heated in the presence of excess Zn(OAc)<sub>2</sub>, three metals coordinate to the N<sub>2</sub>O<sub>2</sub> pockets, and four additional Zn(II) are bridged by acetate groups to form a tetrahedral cluster on top of the macrocycle<sup>68</sup> (Figure 1.18b). Hexanickel or hexamanganese clusters also form from **33**.<sup>69</sup> In addition, the six hydroxyl groups coordinate to alkali metals, similar to 18-crown-6.<sup>67</sup> Stoichiometric addition of NaBPh<sub>4</sub> to a solution of **33** (R = OC<sub>6</sub>H<sub>13</sub>) induces aggregation, as evidenced by upfield resonance shifts of the imine and aromatic peaks in the <sup>1</sup>H NMR spectrum, and peaks assigned to sodium adducts in the electrospray mass spectrum.

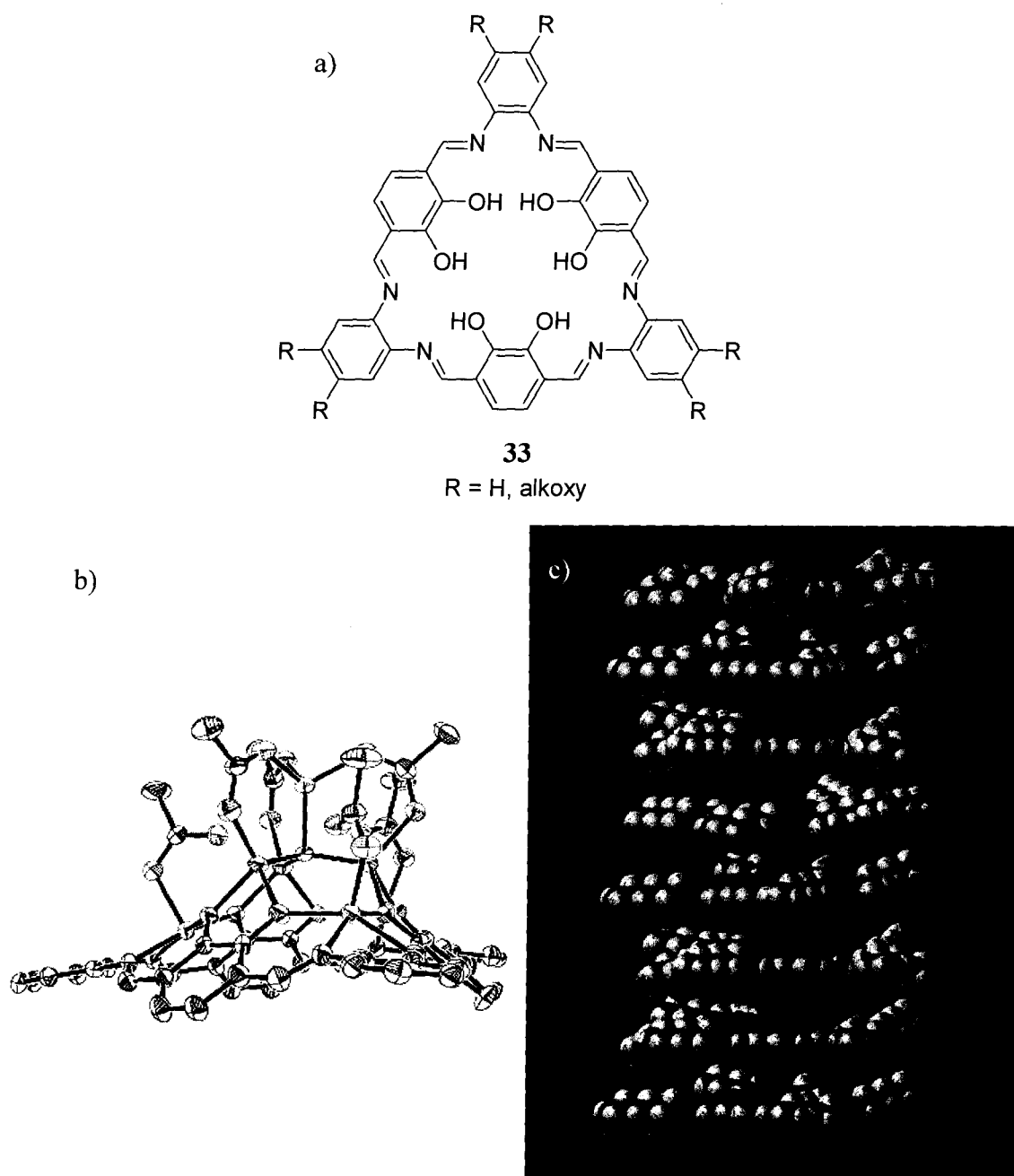


**Figure 1.18** a) A [3+3] Schiff base macrocycle, **33**. b) Heptazine complex of **33**,<sup>68</sup> c) A postulated structure of ion-induced tubular assembly of **33**.<sup>67</sup>

Larger [3+3] macrocycles, **34**, have been synthesized with phenyleneethynylene diols (Figure 1.19).<sup>70</sup> The Zn(II) complex of **34** is luminescent and aggregates in noncoordinating solvents such as dichloromethane (DCM). Deaggregation of this complex occurs upon addition of coordinating solvents such as tetrahydrofuran (THF) or

pyridine. This is apparent as peaks in the UV-Vis spectrum become sharper upon increasing the ratio of THF to DCM in the solution. Coordination of Ni(II) or Cu(II) to **34** quenches fluorescence, and these complexes do not aggregate, as UV-Vis absorption spectra appear sharp in both coordinating and non-coordinating solvents.

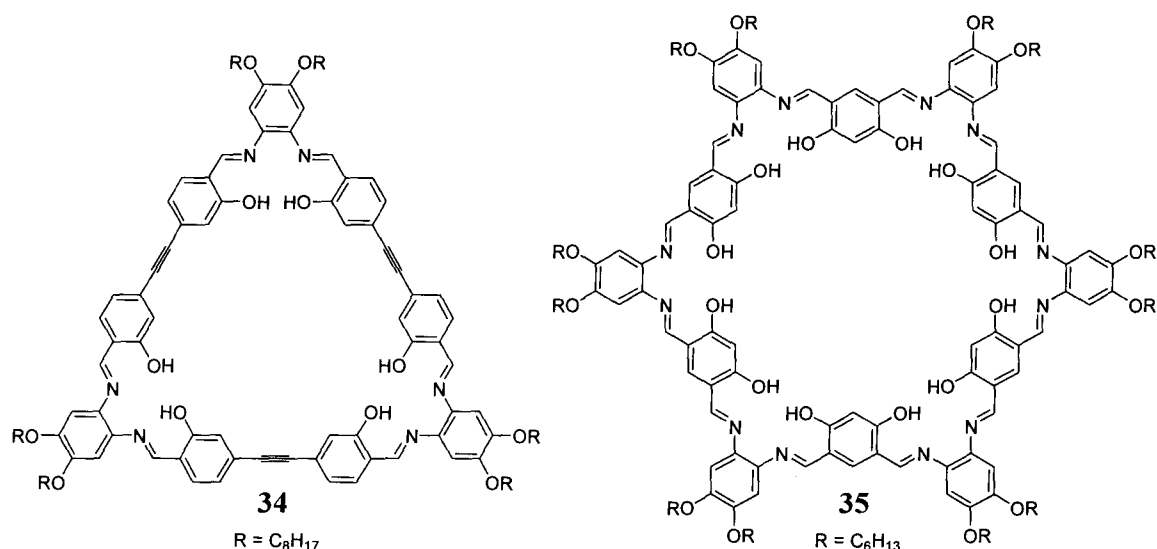


**Figure 1.19** Schiff base macrocycles **34** and **35**.

Recently, our group developed a [6+6] Schiff base macrocycle, **35**.<sup>71</sup> Macrocycle **35** is synthesized in two steps, whereby a 2:1 diamine:diol fragment is initially formed, followed by the addition of more diol to obtain **35**. There are six N<sub>2</sub>O<sub>2</sub> pockets in **35** that can coordinate vanadyl groups.

Compared to the stepwise routes to make phenyleneethynylene-based macrocycles, synthesis of Schiff base macrocycles is generally more straightforward and usually requires only one step, resulting in increased overall yield. In addition, the size and shape of the macrocycle can be tuned by changing the geometry of the starting materials, as evidenced by the formation of different [2+2], [3+3] and [6+6] rings.

### 1.3 Phenanthrene and Triphenylene

#### 1.3.1 Polycyclic Aromatic Hydrocarbons

Polycyclic aromatic hydrocarbons (PAHs) have been often used in materials chemistry to expand conjugation as well as to tune the size and shape of different compounds. PAHs, which consist of 6-membered aromatic rings as building blocks, range in size from as small as naphthalene to as large as graphite.<sup>72</sup> Both naphthalene and graphite are found in nature, where a naphthalene group is incorporated into the macrocyclic backbone of rifamycin derivatives, which are antibiotics used in the treatment of tuberculosis and leprosy.<sup>73</sup> PAHs are planar and may stack as a result of  $\pi$ - $\pi$  interactions between the aromatic rings.

There is a wide range of other polycyclic aromatic compounds. By increasing the number of aromatic rings to three, there are two isomers, anthracene (**36**) and phenanthrene (**37**), shown in Figure 1.20. Compounds with four aromatic rings include triphenylene (**38**), chrysene (**39**), pyrene (**40**), and tetracene (**41**). Increasing the number of aromatic rings rapidly increases the number of isomers available. These compounds and larger PAHs have been thoroughly studied as building blocks in organic synthesis and for useful optical and electronic properties.

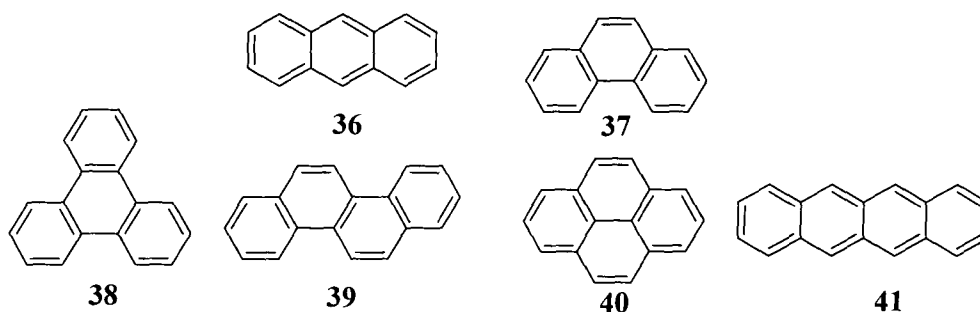
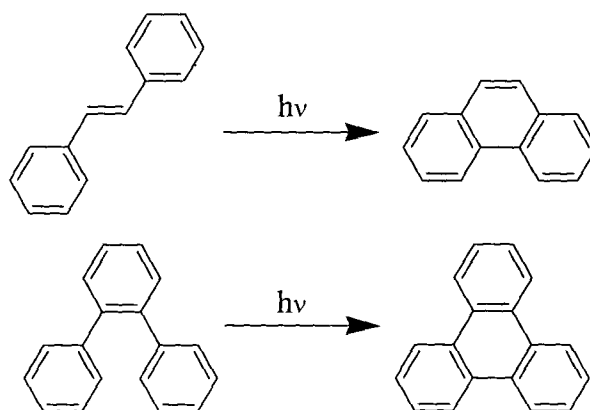


**Figure 1.20** The structures of anthracene (**36**), phenanthrene (**37**), triphenylene (**38**), chrysene (**39**), pyrene (**40**) and tetracene (**41**).

In addition to the notable ability to stack, many PAHs have interesting photophysical properties. Whereas the smaller PAHs are colourless, larger examples, such as tetracene, are intensely coloured. Many small PAHs are strongly luminescent, and some, for example pyrene, can behave as excimers in solution when concentrated.<sup>74</sup>

Phenanthrene, **37** can be synthesized by photocyclization of stilbene, as seen in Scheme 1.4. If the double bond of *cis*-stilbene is replaced by an aromatic ring, an *ortho*-terphenyl is obtained that photocyclizes to triphenylene, **38**. Compounds **37** and **38** have long been of interest to supramolecular and materials researchers because of their unique structure and stacking ability. Selected examples of PAH macrocycles and materials are discussed in the following sections.

**Scheme 1.4** Photocyclization of stilbene and *ortho*-terphenyl to phenanthrene, **37**, and triphenylene, **38**, respectively.



### 1.3.2 Macrocycles containing PAHs

Stilbene, phenanthrene and triphenylene can be used in the synthesis of a variety of unique structures, including helicenes, molecular belts and macrocycles. Helicenes are *ortho*-fused aromatic rings that form a corkscrew and are thus chiral. Some examples are

shown in Figure 1.21. Photocyclization is one method to make helicenes and has been used to make carbohelicenes that incorporate up to fourteen aromatic rings.<sup>75, 76</sup> However, photocyclization does not allow for regiocontrol and can produce side products, such as dimers. A number of other methods, such as the Diels-Alder reaction<sup>77</sup> and the Wittig reaction combined with homolytic aromatic substitution<sup>78</sup> have also been employed in helicene synthesis. Helicenes have been used as liquid crystals, sensors, and asymmetric catalysts. For example, dihydroxy-[6]helicene, **42**, can discriminate between chiral amines.<sup>79</sup> In addition, varying the number of alkoxy chains on [6]helicenes, for example **43**, alters its liquid crystalline properties.<sup>80</sup>

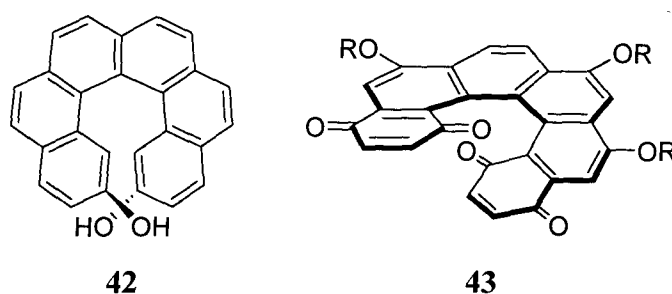


**Figure 1.21** Helicenes **42** and **43**, R = <sup>n</sup>C<sub>12</sub>H<sub>25</sub>.

Molecular belts are macrocycles that cannot be restricted to two dimensions and come in many well-known forms, including cyclodextrins, cucurbiturils and cavitands. Cyclacenes and cyclophenacenes are two belt-like molecules composed entirely of aromatic rings.<sup>81</sup> Compounds such as these are a challenge to synthesize and occasionally use phenanthrene as a precursor. Scott et al. attempted to use pyrolysis to make cyclo[12]phenacene (**44**, Figure 1.22) from a phenanthrene-containing macrocycle, but were unsuccessful. Stoddart and coworkers used phenanthrene and triphenylene as dienophiles to make belt and cage compounds. This attempt yielded a macrocycle, but

attempts to deoxygenate and make the fully conjugated ring were unsuccessful, resulting in compound **45**.<sup>82</sup>

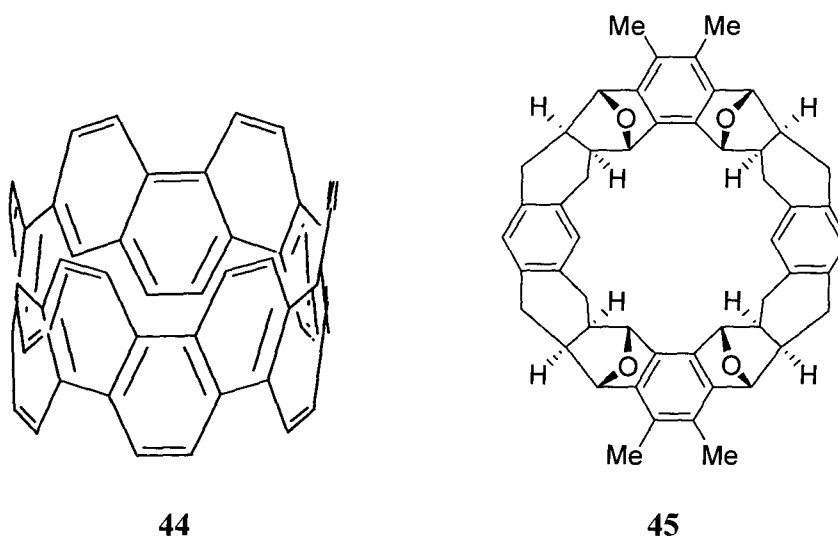
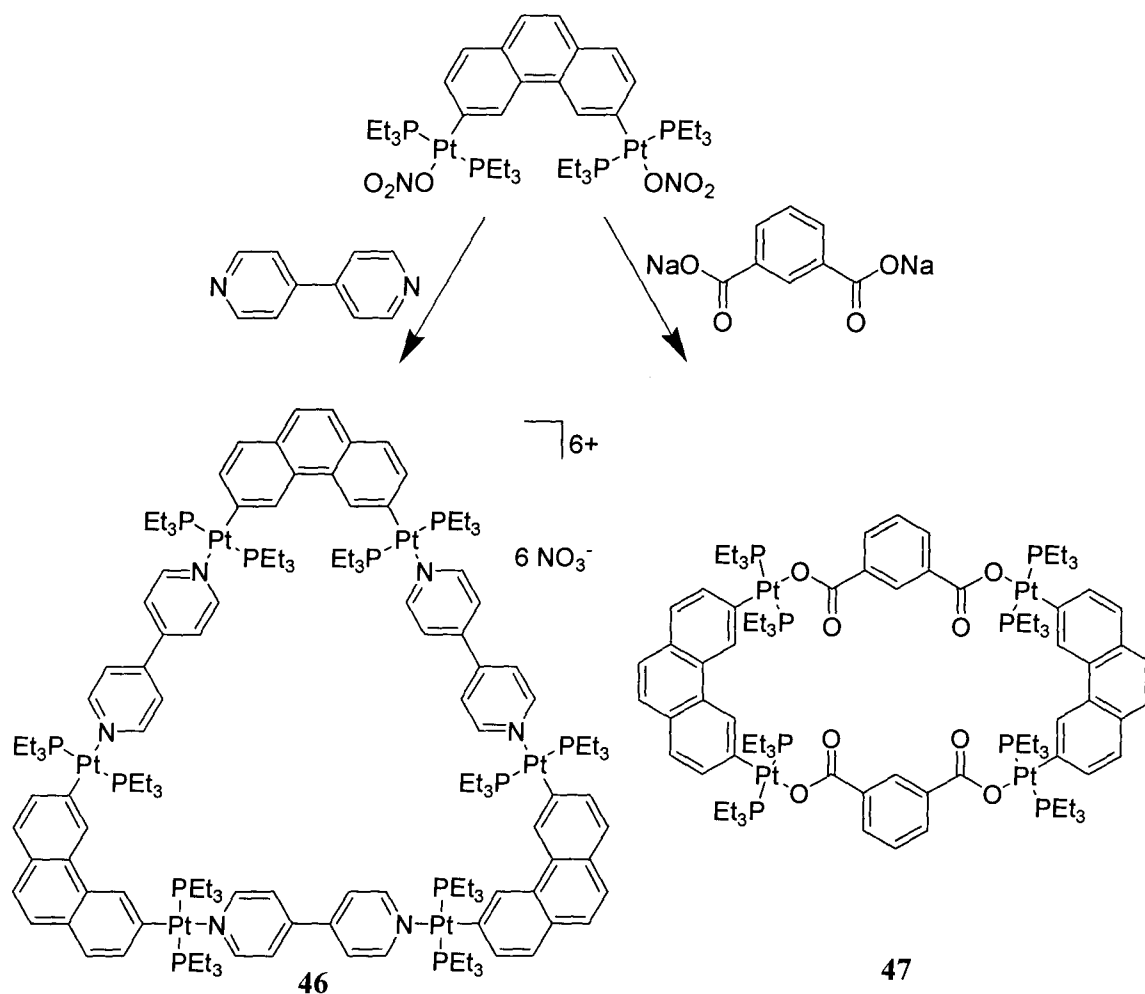


**Figure 1.22** Optimized structure of cyclo[12]phenacene **44** and a partially deoxygenated molecular belt, **45**.

Few entirely organic shape-persistent macrocycles incorporate phenanthrene into the backbone; however, there are several phenanthrene-containing coordination macrocycles that use metal ions as linkers of organic units to form a ring. Stang's group used phenanthrene to direct formation of coordination macrocycles **46** and **47** (Scheme 1.5). Pt(II) is bound to phenanthrene through oxidative addition to form a 60° building block. The metal initially binds labile nitrate ligands that can be displaced with bipyridyl or dicarboxylate ligands. The only products are the predesigned macrocycles.<sup>83, 84</sup>

**Scheme 1.5** Synthesis of phenanthrene-containing coordination macrocycles **46** and **47**.



Phenanthrenophanes **48** (Figure 1.23) have been studied to determine whether phenanthrenes forced into close proximity form intramolecular excimers.<sup>85</sup> After [2+2] photocycloaddition of divinyl phenanthrenes, only one isomer out of five exhibited fluorescent emission that was bathochromically shifted, indicative of excimer formation. No excimers were observed for the other compounds synthesized.

Macrocycle **49** is an annulene with phenanthrene incorporated into the backbone. Reported by Meier and coworkers, it is the only example of a fully conjugated phenanthrene-containing macrocycle.<sup>86</sup> Based on fluorescence and differential scanning

calorimetry (DSC) measurements, they claim **49** aggregates in solution and exhibits thermotropic liquid crystalline behaviour when endowed with peripheral alkoxy chains. Concentration dependence shown by broadening of aromatic and alkoxy resonances in  $^1\text{H}$  NMR spectra of **49** is also indicative of aggregation.<sup>87</sup>

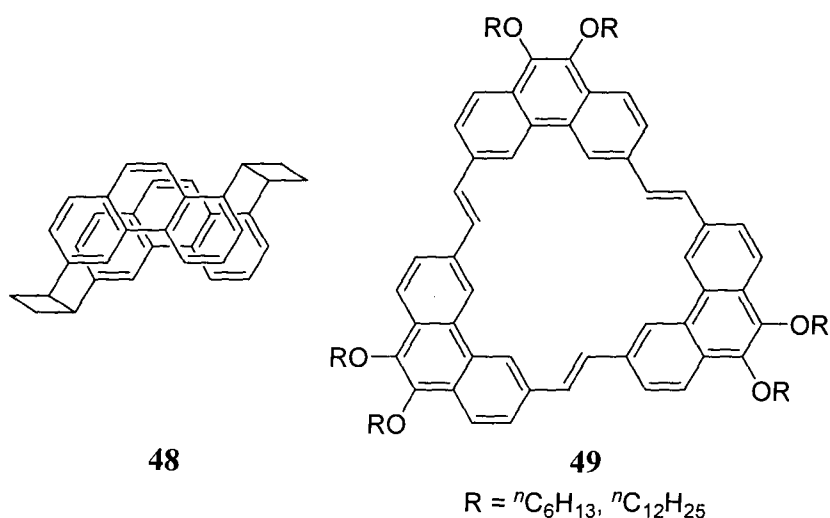


**Figure 1.23** Phenanthrenophane **48** and triphenanthro[24]annulene **49**.

Similar to phenanthrene, triphenylene has rarely been incorporated into macrocycles. For example, macrocycle **50** (Figure 1.24) contains triphenylene to link benzo-crown ethers. This forms a tritopic cation receptor for linked dibenzylammonium guests that can bind reversibly in the center of each crown ether to form a supramolecular bundle (a representation of the bundle is in Figure 1.24, top left).<sup>88</sup> Hydrogen bonding between the crown ether and ammonium, as well as  $\pi$ -stacking between the aromatic rings strongly encourage complexation in solution. In another macrocycle, **51**, triphenylene expands the size of phthalocyanine. The persistence of planarity, increased conjugation and the presence of alkoxy chains in different positions encourage

mesogenic properties.<sup>89</sup> In both of these examples, triphenylene only provides one bond in the macrocycle and does not contribute any extended conjugation to the ring.

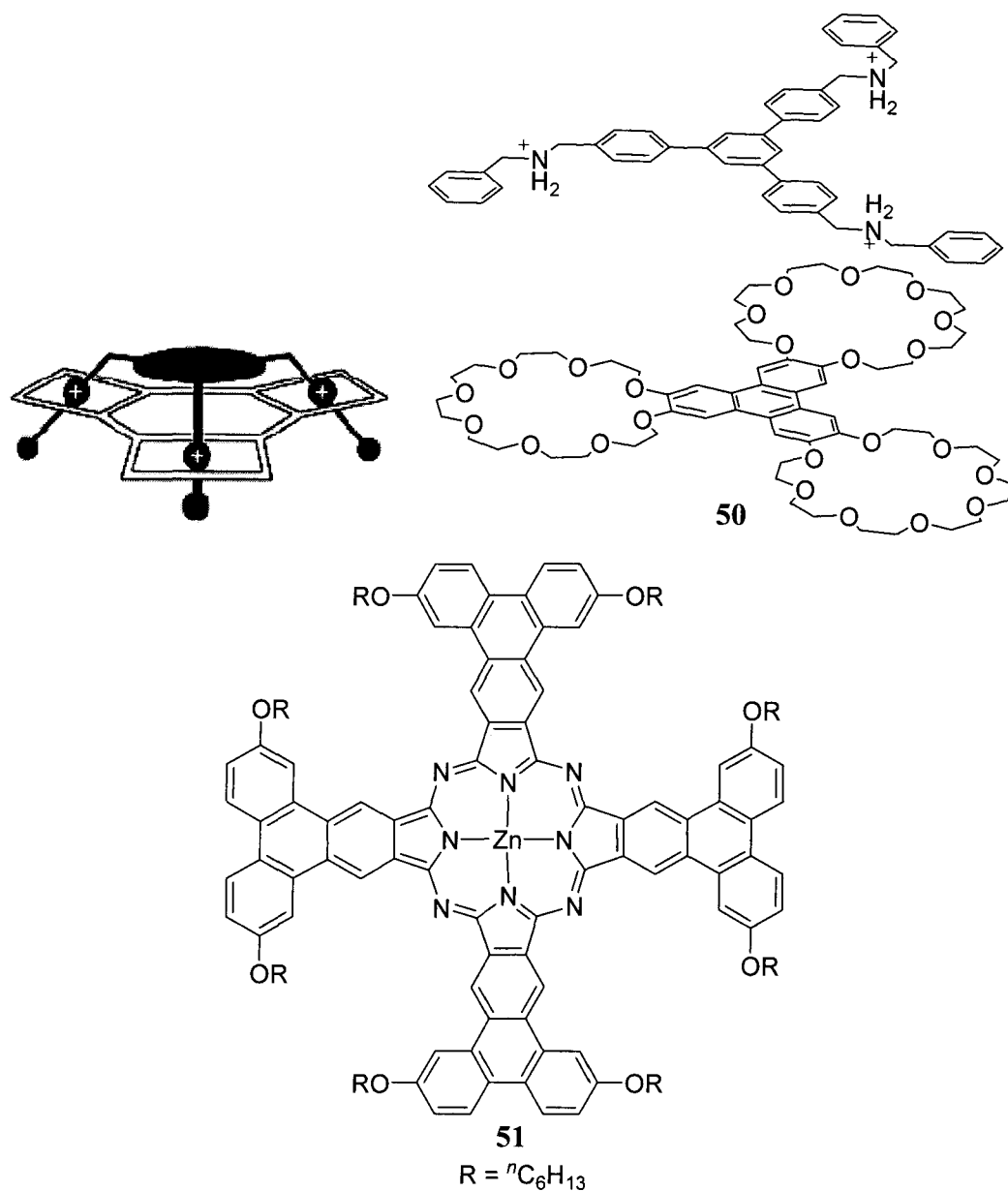


**Figure 1.24** Macrocycles containing triphenylene. A representation of tritopic receptor complexation (top left),<sup>88</sup> with tritopic receptor **50** and dibenzylammonium guest (top right). Expanded Zn-phthalocyanine **51**, (bottom).

### 1.3.3 PAHs in Materials Chemistry

Although there are not many examples of PAH-containing macrocycles, PAHs have been used extensively in materials chemistry. Phenanthrene has been incorporated into some polymers and triphenylene is known to form liquid crystals.

After it was discovered that conjugated polymers conduct when appropriately doped, many polymers with aromatic components in the backbone were developed.<sup>90, 91</sup> Phenanthrene extends the conjugation of the backbone by maintaining planarity of the polymer, unlike poly(*p*-phenylene) (PPP), which has benzene rings that are twisted relative to one another. Fluorene and carbazoles have been incorporated into many conjugated polymers;<sup>92, 93</sup> however, only two phenanthrene-based PPP type polymers have been synthesized (Figure 1.25). Suh and coworkers have synthesized poly(ethylhexyl-cyclopenta[*def*]phenanthrene), **52**.<sup>94, 95</sup> Polymer **52** had a molecular weight ( $M_n$ ) of 15000 g/mol and exhibits emission at 410 nm. This polymer was tested as an organic light emitting diode (OLED), and was found to be stable after both annealing the device and operating the OLED for 40 minutes. Mullen's group synthesized poly(2,7-phenanthrylene) **53** and poly(3,6-phenanthrylene) **54**, with  $M_n$  ranging from 3200 for **54**, to 47000 for **53**.<sup>96</sup> OLEDs made from films of **53** and **54** are less stable, as they exhibit decreased luminescence after running the device in air for 10 minutes.

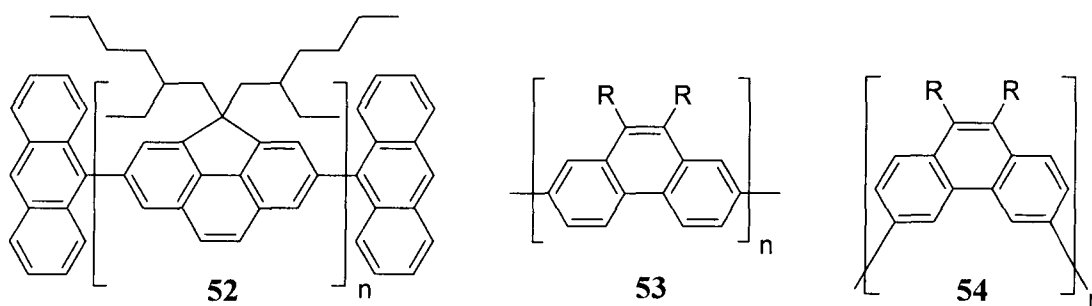


**Figure 1.25** Phenanthrene-containing PPP-type polymers **52-54** ( $R = {}^n\text{C}_{10}\text{H}_{21}$ , *p*-( $\text{C}_6\text{H}_4$ )- ${}^n\text{C}_{10}\text{H}_{21}$  for polymers **53** and **54**).

One example of a polymer with triphenylene in the backbone, **55**, comes from the Swager group; however, only a single benzene ring from the triphenylene is incorporated into the polymer chain (Figure 1.26).<sup>97</sup> Triphenylene was added to change the lifetime of the excited state of the polymer compared to analogous poly(phenyleneethynylene)s (PPE). All derivatives showed both the expected increase in lifetime and a decrease in quantum yield.

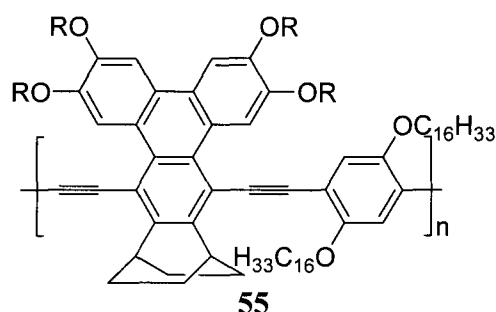


**Figure 1.26** Triphenylene-containing PPE, R = 2-ethylhexyl.

Examples of conjugated Schiff base helicene polymers (**56** and **57**) can be seen in Figure 1.27 (top).<sup>98, 99</sup> Isomeric diols were made with salicylate moieties on different carbon atoms of the helicene. The polymerizations proceeded via a Ni(II)-templated condensation reaction. Molecular weights were determined by MALDI-TOF mass spectrometry and gel permeation chromatography (GPC), and molecules with as many as ten repeating units were identified. The polymers were made with pure enantiomers of the helicenes to obtain an enantiopure product. The circular dichroism (CD) spectra of the polymers confirm the chirality of the molecules. As shown in Figure 1.27 (bottom), polymer **57** winds only in one direction, while the salphen and helicene wind in opposite directions in polymer **56**.

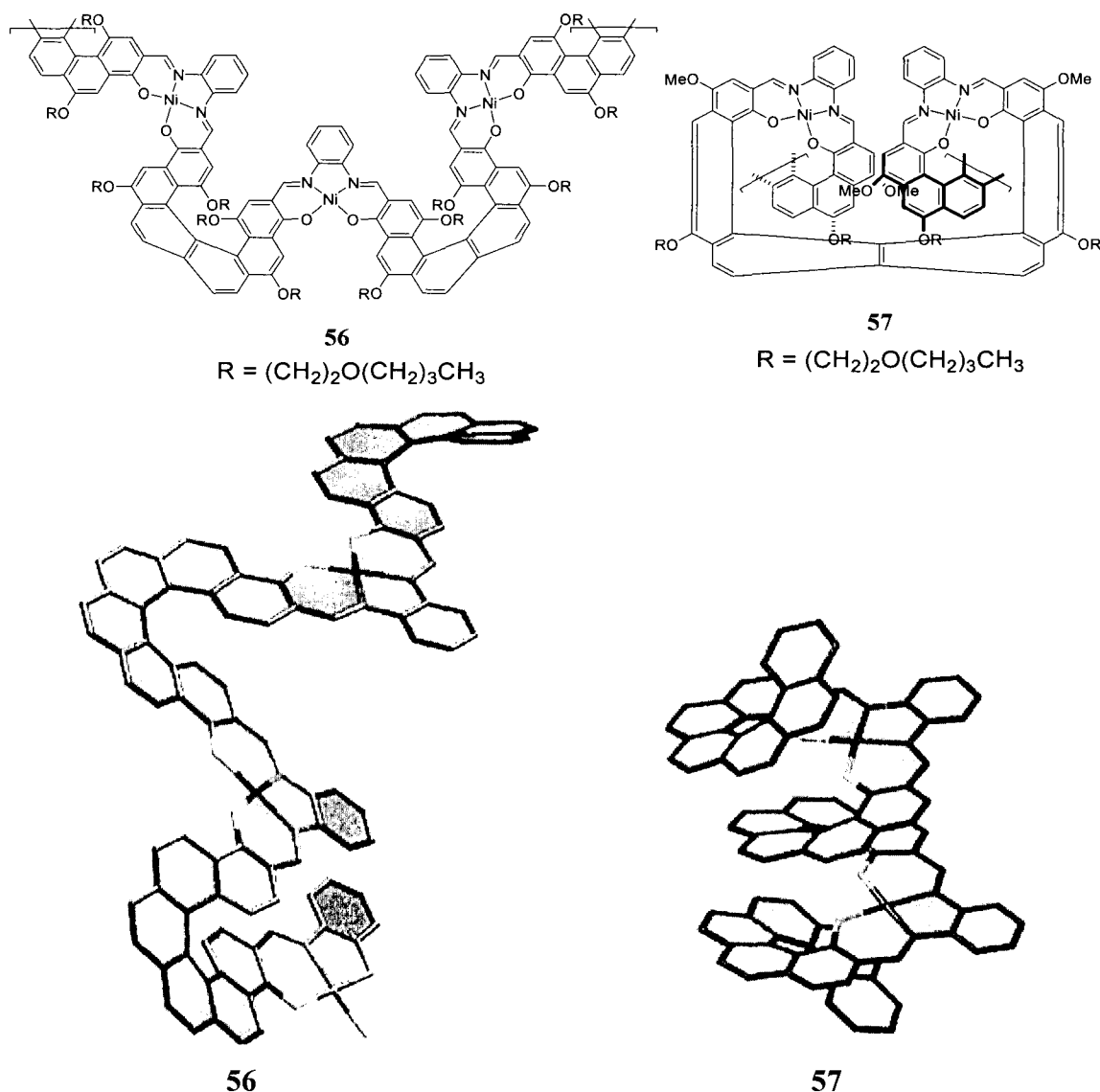


**Figure 1.27** Helicene Schiff base polymers **56** and **57** (top). The bottom figure shows three dimensional representations of the polymer.<sup>98</sup>

One of the most prominent uses of PAHs in materials chemistry is derived from substituted triphenylenes. They have the ability to stack in a columnar structure by virtue of  $\pi$ - $\pi$  interactions, and this property has aroused the interest of researchers in the field of discotic liquid crystals.<sup>100, 101</sup> Distance between individual molecules in the column is approximately 3.5-4.5 Å, while the distance between columns ranges from 20-40 Å, depending on the substituents on the ring.<sup>102, 103</sup> One dimensional conductive pathways

form, which allow liquid crystals to have a variety of uses including photovoltaic cells and electroluminescent devices. Symmetric hexasubstituted triphenylenes have been synthesized with an enormous variety of substituents and their liquid crystalline properties have been discussed in several reviews.<sup>100, 101, 103, 104</sup> One study of triphenylene-based liquid crystals compares compound **58**, a hexa-substituted triphenylene, shown in Figure 1.28, and **59**, a penta(alkoxy)triphenylene. This example demonstrates that changing one substituent on **59** to an electron-withdrawing group can alter mesogenic properties, optical absorption and emission.<sup>105</sup> For example, the wavelength of emission for **59** with R = Ac, is 100 nm bathochromically shifted from **58** and has a larger temperature range for the mesophase.

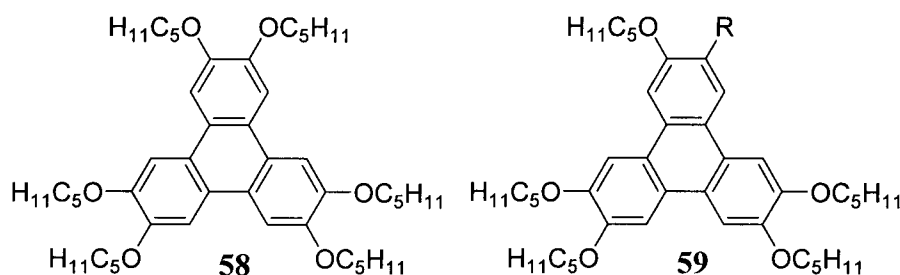


**Figure 1.28** A typical hexasubstituted triphenylene **58** with liquid crystalline properties and a pentaalkoxy triphenylene **59** with different R groups (R = Br, Ac, CN, CCSi(Me)<sub>3</sub>).

#### 1.4 Conjugated Molecules as Sensors for Nitroaromatic Compounds

Nitroaromatic compounds, such as di- and trinitrotoluene (**60a**, **61a**), and di- and trinitrophenol (picric acid) (**60b**, **61b**) (Figure 1.29) are components of a variety of explosives. While nitroaromatic compounds do not have high vapour pressures, they are nonetheless valuable targets for explosives detection. Compounds that produce an optical change when exposed to the vapour of nitroaromatics would provide convenient tools for

explosives detection, rather than using metal detectors (for sensing explosives encased in metal), canines or spectrometry.<sup>106</sup>

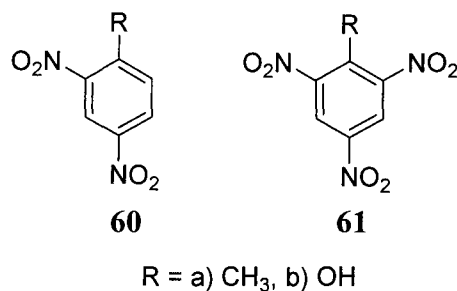


**Figure 1.29** Di- and trinitrotoluene and di- and trinitrophenol.

Conjugated polymer films (some examples include **62-64**) are able to detect nitroaromatics because the polymers donate electrons in the excited state to the analyte. Upon accepting photoexcited electrons, dinitrotoluene (DNT) and trinitrotoluene (TNT) undergo radiationless decay from the excited state, thus quenching the fluorescence. An example of this is seen in films of polymers **62** and **63** in Figure 1.30, which exhibit decreased luminescence in the presence of DNT and TNT vapour. Polymer films in the excited state also have greater electron delocalization, increasing the frequency of interaction with the analyte. However, the extent of quenching is highly dependent on film thickness.<sup>107</sup> Less of the nitroaromatic vapour diffuses into thick films, causing decreased quenching of luminescence. Swager's pentiptycene PPE, **64**, was designed to pack less efficiently, thus creating greater porosity in the polymer film.<sup>108</sup> Films of **64** showed 90% quenching upon exposure to TNT vapour for five minutes. Comparison of 25 Å films and 200 Å films show greater quenching in the thinner film despite the increased porosity, although this effect is less pronounced with dinitro- and mononitroaromatics. It is suggested that slower diffusion of TNT results from stronger interaction of the vapour with the films.

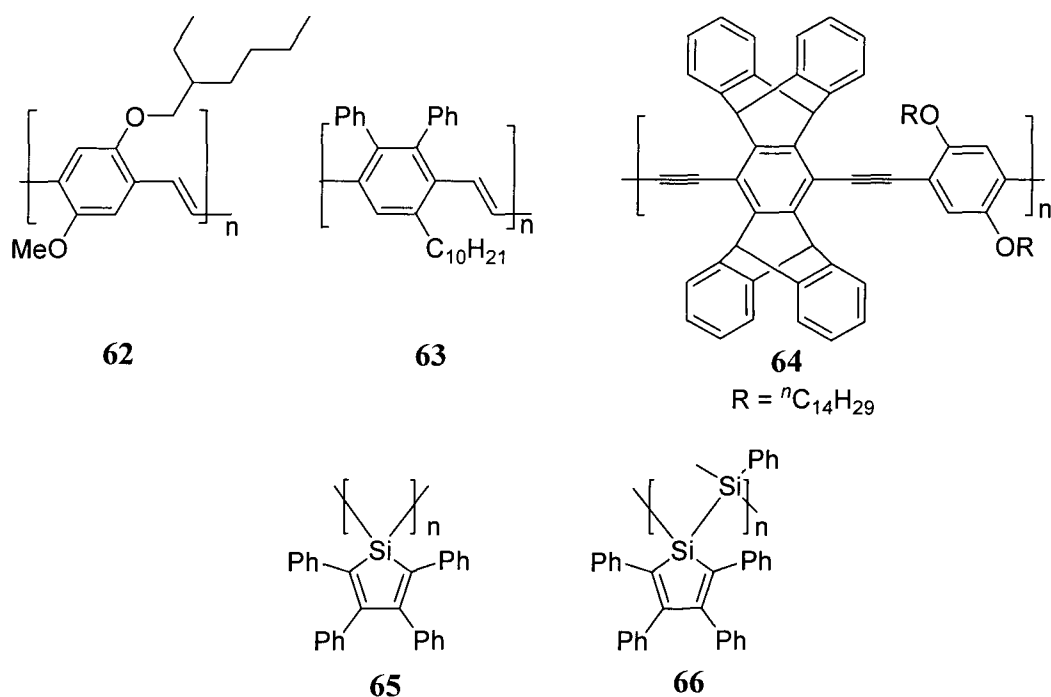


**Figure 1.30** Polymers **62-66** for nitroaromatic sensing.

Poly(metalloles) from Trogler's group (**65** and **66**, Figure 1.30) have been shown to exhibit quenched luminescence of both films and in solution in the presence of nitroaromatics. Films of polysilole **65** show decreased emission after exposure to TNT at 50 ppb in sea water for 60 seconds.<sup>109</sup> Solutions of polymer **66** were titrated with various nitroaromatics and it was determined that the greatest quenching was obtained from picric acid and TNT.<sup>110</sup>

The Stern-Volmer constant ( $K_{SV}$ ), a measure of the quenching efficiency, is specific for an analyte. This quantity is determined by comparing the ratio of luminescence intensity (where  $I_0$  is the initial intensity and  $I$  is the intensity after exposure to the analyte) versus concentration of the analyte  $A$ , according to the Stern-Volmer equation (1.1).<sup>111</sup>

$$I_0/I = 1 + K_{SV}[A] \quad (1.1)$$

Also,  $K_{SV}$  is the product of the fluorescent lifetime ( $\tau$ ) and the rate of quenching ( $k_q$ ), and larger values are indicative of greater sensitivity to the analyte. Selected  $K_{SV}$  values found for sensors of DNT, TNT and nitrobenzene (NB) are found in Table 1.1.

**Table 1.1** Selected Stern-Volmer constants for nitroaromatics.

Sensor	$K_{SV}$ (DNT)	$K_{SV}$ (TNT)	$K_{SV}$ (NB)
<b>65</b>	2420	4340	1200
<b>66</b>	2380	3940	1230
<b>23</b>	—	—	6.9

Only one macrocycle has been reported as a useful sensor of nitroaromatics. Luminescence of films of macrocycle **67** (Figure 1.31) decreases after exposure to the vapour of DNT or TNT.<sup>112</sup> As a result of the porosity of the nanofibril films, fluorescence quenching was as efficient for 90 nm thick films as for 15 nm thick films. Additionally, the luminescence quenching can be reversed by exposure to air or hydrazine and the films can be reused without a loss of sensitivity.

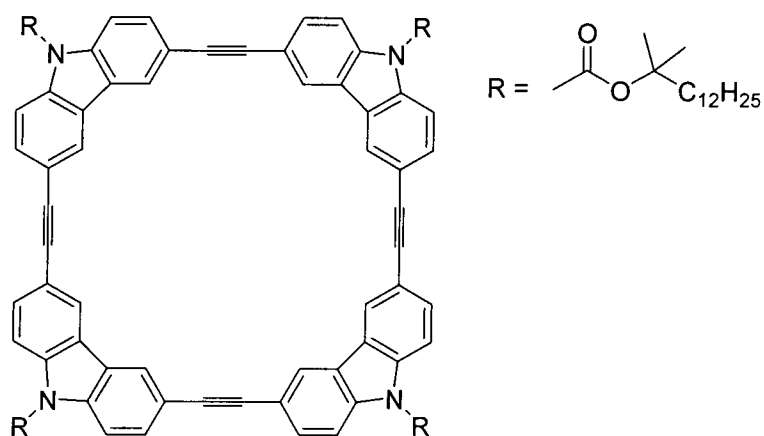


**Figure 1.31** Macrocycle **67** for sensing nitroaromatics.

## 1.5 Research Goals

The goals of this project were threefold: to synthesize and characterize new conjugated macrocycles that incorporate Schiff base moieties with PAH components, such as phenanthrene and triphenylene; to synthesize phenanthrene-containing PPEs; and to examine macrocycle aggregation and sensing of nitroaromatics by these compounds. A side project had the goal of synthesizing new thienyl-containing salphen monomers for electropolymerization.

Both **33** and **34** were previously synthesized by members of the MacLachlan group. By incorporating phenanthrene into the macrocycle as a spacer, we hoped to synthesize a macrocycle (**68**, Figure 1.32) with a pore size between those of **33** and **34**. As an intermediate sized macrocycle, we are interested in whether its behaviour with metals would be more like **33**, which templates the formation of metal clusters, or like **34**, which aggregates into tubes upon metal complexation. Also, with alkylated triphenylene as a spacer rather than phenanthrene, **69** can be formed. These macrocycles may exhibit liquid crystalline properties.

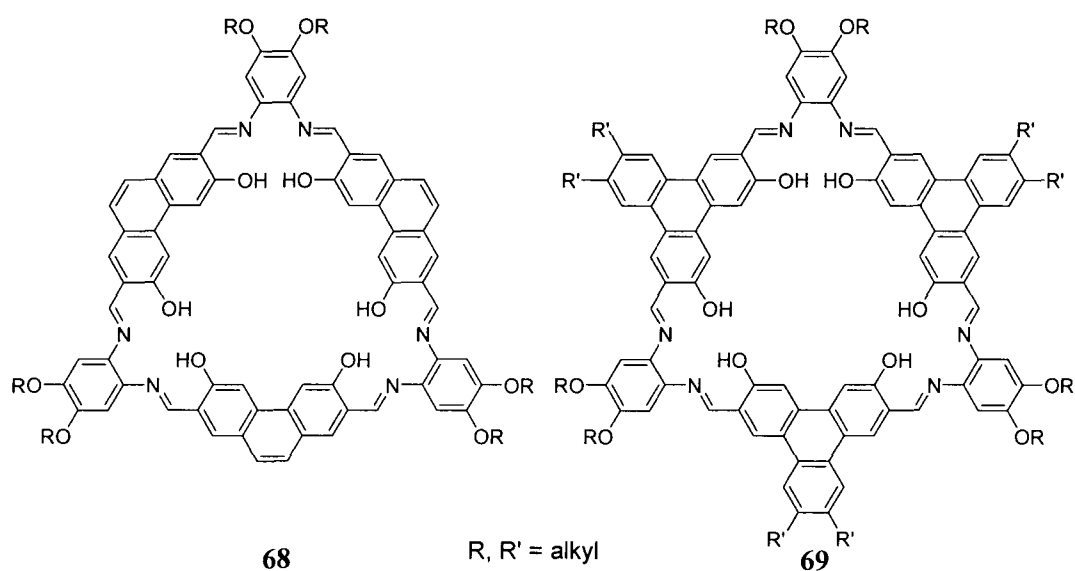


**Figure 1.32** Phenanthrene and triphenylene macrocycles.

To synthesize intermediate-sized macrocycles, phenanthrene and triphenylene diols must first be synthesized (shown in Figure 1.33). The geometry of the macrocycle is dictated by the angle of the formyl groups on the spacer. For example, in order for [3+3] macrocycles to form, the bonds from the spacer to the formyl groups must be parallel and for the [6+6] macrocycle, the formyl groups must be 120° apart. If the bonds are in the same line, a macrocycle with  $D_{3h}$  symmetry is formed and this will occur in the case of phenanthrene, as formyl groups can be placed across from each other on the 2,7 carbons.

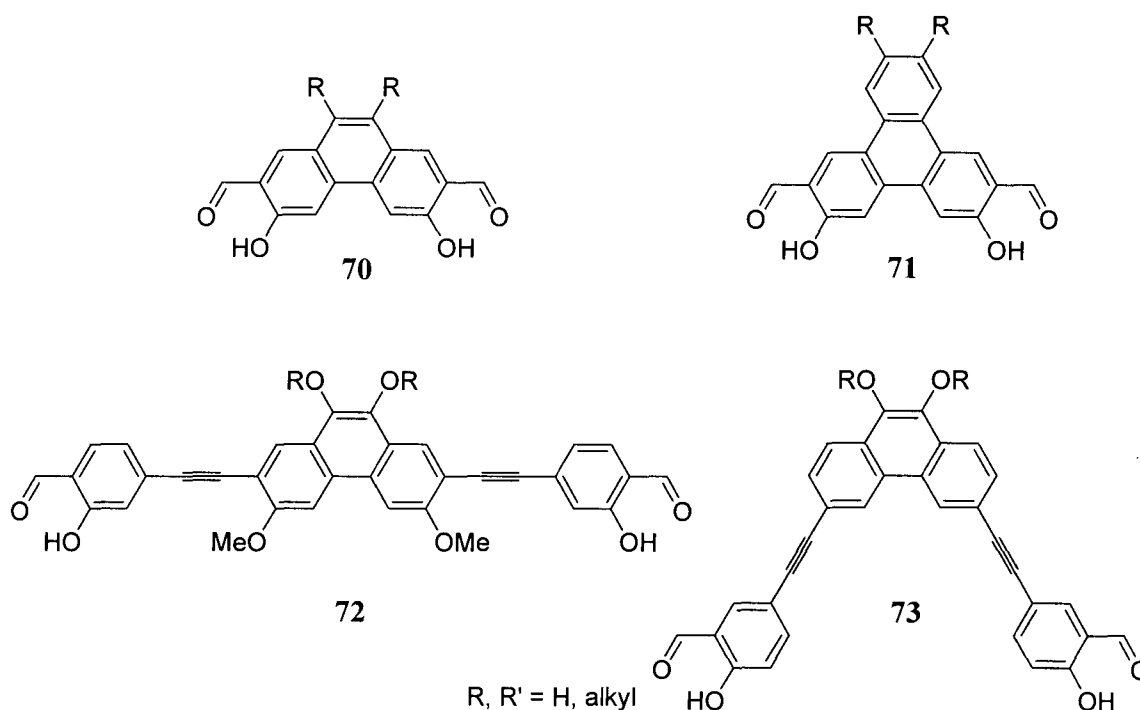


**Figure 1.33** Phenanthrene and triphenylene-based salicylates **70-73**.

Chapter 2 describes the synthesis of the diol precursors **70-71** as well as phenanthrene diols where conjugation is extended with ethynyl groups, **72-73**. Chapter 3 discusses the synthesis of Schiff base macrocycles from these precursors. The behaviour and applications of the largest macrocycles, **74** and **75** (Figure 1.34), are described in

Chapter 4, including aggregation studies and quenching of luminescence in the presence of nitroaromatics.

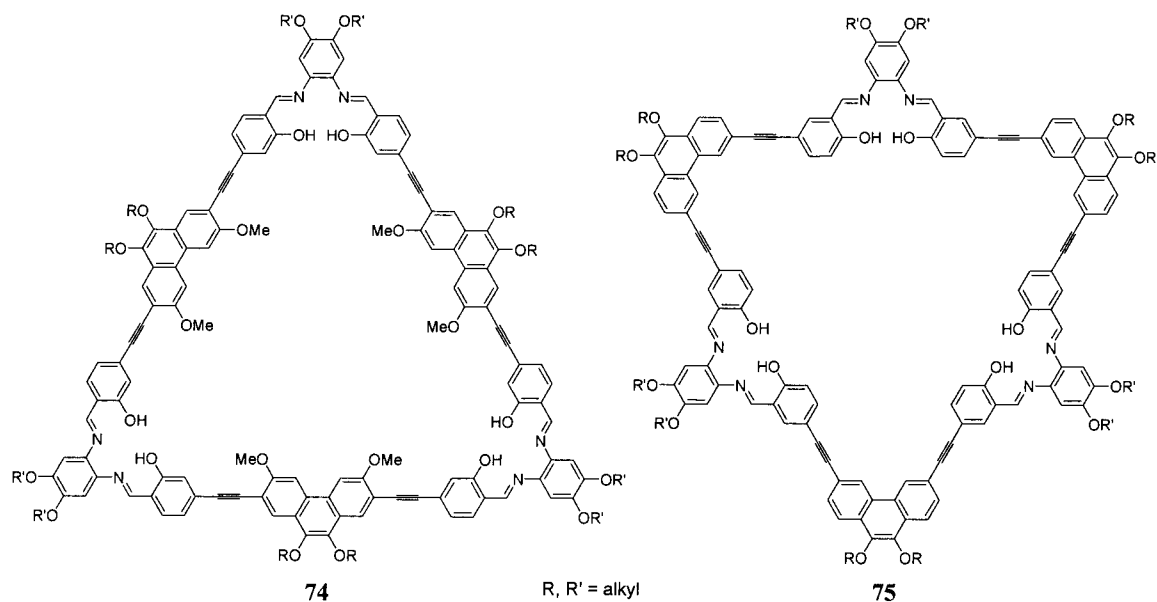


**Figure 1.34** Macrocycles **74** and **75**.

Triphenylene and phenanthrene have geometries that resemble organic salen or salphen. This comparison motivated us to create organic versions (**77**) of our group's poly(salphenyleneethynylene)s, **76** (Figure 1.35).<sup>113</sup> For these polymers to be made, sufficiently soluble co-monomers must be synthesized and tested for the ability to react under suitable conditions. The details of this study are contained in Chapter 5.

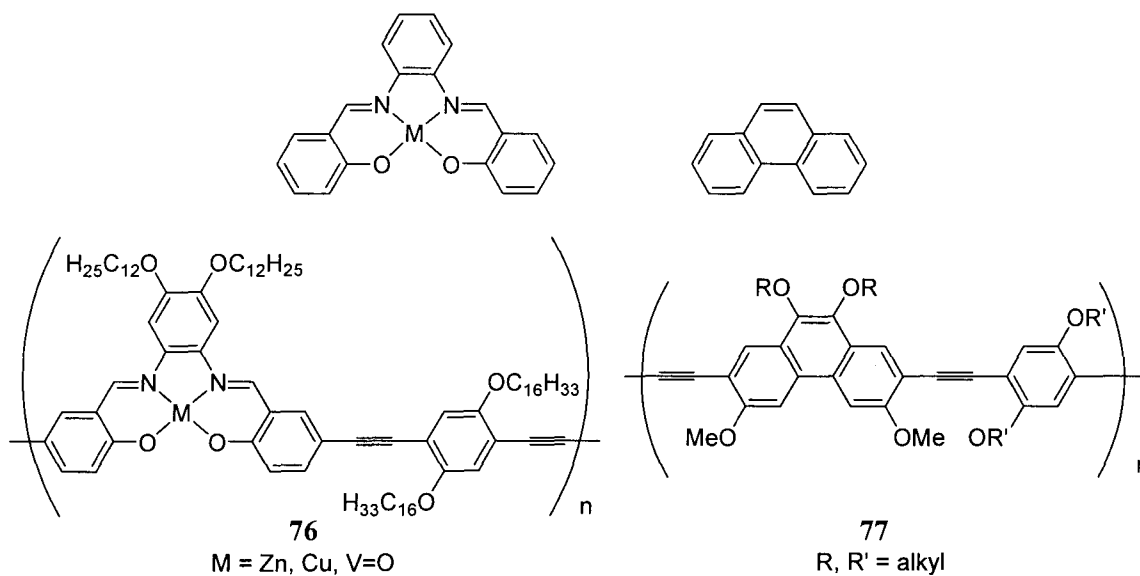


**Figure 1.35** Comparison of salphen and phenanthrene (top). Poly(salphenyleneethynylene) **76** and a phenanthrene analogue **77**.

Although thienyl-containing salen monomers have been synthesized previously, there are numerous aspects of these polymers that have not been studied. In a collaborative project with the Wolf group, we are interested in the change in properties when the monomers are polymerized under microgravity, especially the non-linear optical (NLO) aspects. My goal in this collaboration was to synthesize new monomers for electropolymerization and the results of this study are discussed in Chapter 6. Chapter 7 summarizes the thesis and discusses future work.

## 1.6 References

- (1) Lehn, J. -M. *Acc. Chem. Rev.* **1978**, *11*, 49-57.
- (2) Lehn, J. -M. *Angew. Chem.* **1988**, *100*, 91-116.
- (3) Gale, P. A. *Phil. Trans. R. Soc. Lond. A* **2000**, *358*, 431-453.
- (4) Steed, J. W.; Atwood, J. L. In *Supramolecular Chemistry*; John Wiley & Sons, Ltd: Toronto, 2000; pp 13-14.
- (5) Hannon, M. J. *Chem. Soc. Rev.* **2007**, *36*, 280-295.
- (6) Balzani, V.; Credi, A.; Raymo, F. M.; Stoddart, J. F. *Angew. Chem. Int. Ed.* **2000**, *39*, 3348-3391.
- (7) Wiskur, S. L.; Ait-Haddou, H.; Lavigne, J. J.; Anslyn, E. V. *Acc. Chem. Rev.* **2001**, *34*, 963-972.
- (8) Bell, T. W.; Hext, N. M. *Chem. Soc. Rev.* **2004**, 589-598.
- (9) Pedersen, C. J. *Angew. Chem.* **1988**, *100*, 1053-1059.
- (10) Cram, D. J. *Angew. Chem.* **1988**, *100*, 1041-1052.
- (11) Ikeda, A.; Shinkai, S. *Chem. Rev.* **1997**, *97*, 1713-1734.
- (12) Gutsche, C. D.; Levine, J. A. *J. Am. Chem. Soc.* **1982**, *104*, 2653-2655.
- (13) Arnaud-Neu, F.; Collins, E. M.; Deasy, M.; Ferguson, G.; Harris, S. J.; Kaitner, B.; Lough, A. J.; McKervey, M. A.; Marques, E.; Ruhl, B. L.; Schwing-Weill, M. J.; Seward, E. M. *J. Am. Chem. Soc.* **1989**, *111*, 8681-8691.
- (14) Ikeda, A.; Shinkai, S. *J. Chem. Soc. Perkin Trans. I* **1993**, 2671-2673.
- (15) Szejtli, J. *Chem. Rev.* **1998**, *98*, 1743-1753.
- (16) Aoyagi, T.; Nakamura, A.; Ikeda, H.; Ikeda, T.; Mihara, H.; Ueno, A. *Anal. Chem.* **1997**, *69*, 659-663.
- (17) Ueno, A.; Suzuki, I.; Osa, T. *Chem. Lett.* **1989**, 1059-1062.
- (18) Ghadiri, M. R.; Granja, J. R.; Milligan, R. A.; McRee, D. E.; Khazanovich, N. *Nature* **1993**, *366*, 324-327.
- (19) Khazanovich, N.; Granja, J. R.; McRee, D. E.; Milligan, R. A.; Ghadiri, M. R. *J. Am. Chem. Soc.* **1994**, *116*, 6011-6012.

- (20) Loeb, S. J.; Wisner, J. A. *Chem. Commun.* **1998**, 2757-2758.
- (21) Cesario, M.; Dietrich-Buchecker, C. O.; Guilhem, J.; Pascard, C.; Sauvage, J. -P. *J. Chem. Soc., Chem. Commun.* **1985**, 244-247.
- (22) Dietrich-Buchecker, C. O.; Sauvage, J. -P. *Chem. Rev.* **1987**, 87, 795-810.
- (23) de Silva, A. P.; de Silva, S. A. *J. Chem. Soc., Chem. Commun.* **1986**, 1709-1710.
- (24) Ueno, A. *Supramolecular Science* **1996**, 3, 31-36.
- (25) Höger, S. *Chem. Eur. J.* **2004**, 10, 1320-1329.
- (26) Zhang, W.; Moore, J. S. *Angew. Chem. Int. Ed.* **2006**, 45, 4416-4439.
- (27) Mak, C. C.; Bampos, N.; Darling, S. L.; Montalti, M.; Prodi, L.; Sanders, J. K. M. *J. Org. Chem.* **2001**, 66, 4476-4486.
- (28) Zhang, J.; Moore, J. S. *J. Am. Chem. Soc.* **1992**, 114, 9701-9702.
- (29) Staab, H. A.; Neunhoeffler, K. *Synthesis* **1974**, 424.
- (30) Moore, J. S.; Zhang, J. *Angew. Chem. Int. Ed.* **1992**, 31, 922-924.
- (31) Zhang, W.; Moore, J. S. *J. Am. Chem. Soc.* **2004**, 126, 12796.
- (32) Zhao, D.; Moore, J. S. *Chem. Commun.* **2003**, 807-818.
- (33) Grave, C.; Schlüter, A. D. *Eur. J. Org. Chem.* **2002**, 3075-3098.
- (34) Höger, S. *J. Polym. Sci. Part A: Polym. Chem.* **1999**, 37, 2685-2698.
- (35) Hensel, V.; Schlüter, A. D. *Chem. Eur. J.* **1999**, 5, 421-429.
- (36) Fischer, M.; Lieser, G.; Rapp, A.; Schnell, I.; Mamdouh, W.; De Feyter, S.; De Schryver, F. C.; Höger, S. *J. Am. Chem. Soc.* **2004**, 126, 214-222.
- (37) Li, J.; Ambroise, A.; Yang, S. I.; Diers, J. R.; Seth, J.; Wack, C. R.; Bocian, D. F.; Holten, D.; Lindsey, J. S. *J. Am. Chem. Soc.* **1999**, 121, 8927-8940.
- (38) Venturi, M.; Marchioni, F.; Balzani, V.; Opris, D. M.; Henze, O.; Schlüter, A. D. *Eur. J. Org. Chem.* **2003**, 4227-4233.
- (39) Baxter, P. N. W. *Chem. Eur. J.* **2002**, 8, 5250-5264.
- (40) Baxter, P. N. W. *J. Org. Chem.* **2001**, 66, 4170-4179.
- (41) Höger, S. *Angew. Chem. Int. Ed.* **2005**, 44, 3806-3808.

- (42) Schiff, H. *Annalen* **1864**, *131*, 118-119.
- (43) Gürol, İ; Ahsen, V. *Mol. Cryst. Liq. Cryst.* **2005**, *442*, 103-118.
- (44) Zhang, W.; Loebach, J. L.; Wilson, S. R.; Jacobsen, E. N. *J. Am. Chem. Soc.* **1990**, *112*, 2801-2803.
- (45) Jacobsen, E. N. *Acc. Chem. Rev.* **2000**, *33*, 421-431.
- (46) Di Bella, S.; Frangalà, I. *Synth. Met.* **2000**, *115*, 191-196.
- (47) Sano, T.; Nishio, Y.; Hamada, Y.; Takahashi, H.; Usuki, T.; Shibata, K. *J. Mater. Chem.* **2000**, *10*, 157-161.
- (48) Germain, M. E.; Vargo, T. R.; Khalifah, P. G.; Knapp, M. J. *Inorg. Chem.* **2007**, *46*, 4422-4429.
- (49) Thomas, S. W.; Amara, J. P. Bjork, R. E.; Swager, T. M. *Chem. Commun.* **2005**, 4572-4574.
- (50) Collinson, S. R.; Fenton, D. E. *Coord. Chem. Rev.* **1996**, *148*, 19-40.
- (51) Borisova, N. E.; Reshetova, M. D.; Ustynyuk, Y. A. *Chem. Rev.* **2007**, *107*, 46-79.
- (52) Radecka-Paryzek, W.; Patroniak, V.; Lisowski, J. *Coord. Chem. Rev.* **2005**, *249*, 2156-2175.
- (53) Curry, J. D.; Busch, D. H. *J. Am. Chem. Soc.* **1964**, *86*, 592-594.
- (54) Melson, G. A.; Busch, D. H. *J. Am. Chem. Soc.* **1964**, *86*, 4834-4837.
- (55) Curtis, N. F. *Chem. Commun.* **1966**, *23*, 881-883.
- (56) Pilkington, N. H.; Robson, R. *Aust. J. Chem.* **1970**, *23*, 2225-2236.
- (57) Tian, Y.; Tong, J.; Frenzen, G.; Sun, J. -Y. *J. Org. Chem.* **1999**, *64*, 1442-1446.
- (58) Atkins, A. J.; Black, D.; Blake, A. J.; Marin-Becerra, A.; Parsons, S.; Ruiz-Ramirez, L.; Schröder, M. *Chem. Commun.* **1996**, 457-464.
- (59) Sessler, J. L.; Johnson, R. M.; Lynch, V. *J. Org. Chem.* **1987**, *52*, 4394-4397.
- (60) Sessler, J. L.; Hemmi, G.; Mody, T. D.; Murai, T.; Burrell, A.; Young, S. W. *Acc. Chem. Rev.* **1994**, *27*, 43-50.
- (61) Sessler, J. L.; Tomat, E.; Mody, T. D.; Lynch, V. M.; Veauthier, J. M.; Mirsaidov, U.; Markert, J. T. *Inorg. Chem.* **2005**, *44*, 2125-2127.
- (62) Sessler, J. L.; Mody, T. D.; Lynch, V. *J. Am. Chem. Soc.* **1993**, *115*, 3346-3347.

- (63) Huck, W. T. S.; van Veggel, F. C. J. M.; Reinhoudt, D. N. *Recl. Trav. Chim. Pays-Bas* **1995**, *114*, 273-276.
- (64) Kuhnert, N.; Lopez-Periago, A. M. *Tetrahedron Lett.* **2002**, 3329-3332.
- (65) Gawroński, J.; Kolbon, H.; Kwit, M.; Katrusiak, J. *J. Org. Chem.* **2000**, *65*, 5768-5773.
- (66) Akine, S.; Taniguchi, T.; Nabeshima, T. *Tetrahedron Lett.* **2001**, *42*, 8861-8864.
- (67) Gallant, A. J.; MacLachlan, M. J. *Angew. Chem. Int. Ed.* **2003**, *42*, 5307-5310.
- (68) Gallant, A. J.; Chong, J. H.; MacLachlan, M. J. *Inorg. Chem.* **2006**, *45*, 5248-5250.
- (69) Nabeshima, T.; Miyazaki, H.; Iwasaki, A.; Akine, S.; Saiki, T.; Ikeda, C. *Tetrahedron* **2007**, *63*, 3328-3333.
- (70) Ma, C.; Lo, A.; Abdolmaleki, A.; MacLachlan, M. J. *Org. Lett.* **2004**, *6*, 3841-3844.
- (71) Hui, J. K. -H.; MacLachlan, M. J. *Chem. Commun.* **2006**, 2480-2482.
- (72) Watson, M. D.; Fechtenkötter, A.; Müllen, K. *Chem. Rev.* **2001**, *101*, 1267-1300.
- (73) Floss, H. G.; Yu, T. -W. *Chem. Rev.* **2005**, *105*, 621-632.
- (74) Azumi, T.; McGlynn, S. P. *J. Chem. Phys.* **1964**, *41*, 3131-3138.
- (75) Flammang-Barbieux, M.; Nasielski, J.; Martin, R. H. *Tetrahedron Lett.* **1967**, 743-744.
- (76) Laarhoven, W. H.; Prinsen, W. J. C. *Top. Curr. Chem.* **1984**, *125*, 63-130.
- (77) Fox, J. M.; Goldberg, N. R.; Katz, T. J. *J. Org. Chem.* **1998**, *63*, 7456-7462.
- (78) Harrowven, D. C.; Guy, I. L.; Nanson, L. *Angew. Chem. Int. Ed.* **2006**, *45*, 2242-2245.
- (79) Reetz, M. T.; Sostmann, S. *Tetrahedron* **2001**, *57*, 2515-2520.
- (80) Vyklický, L.; Eichhorn, S. H.; Katz, T. J. *Chem. Mater.* **2003**, *15*, 3594-3601.
- (81) Tahara, K.; Tobe, Y. *Chem. Rev.* **2006**, *106*, 5274-5290.
- (82) Ashton, P. R.; Girreser, U.; Giuffrida, D.; Kohnke, F. J.; Mathias, J. P.; Raymo, F. M.; Slawin, A. M. Z.; Stoddart, J. F.; Williams, D. J. *J. Am. Chem. Soc.* **1993**, *115*, 5422-5429.
- (83) Kryshenko, Y. K.; Seidel, S. R.; Arif, A. M.; Stang, P. J. *J. Am. Chem. Soc.* **2003**, *125*, 5193-5198.

- (84) Mukherjee, P. S.; Das, N.; Kryschenko, Y. K.; Arif, A. M.; Stang, P. J. *J. Am. Chem. Soc.* **2004**, *126*, 2464-2473.
- (85) Nakamura, Y.; Tsuihiji, T.; Mita, T.; Minowa, T.; Tobita, S.; Shizuka, H.; Nishimura, J. *J. Am. Chem. Soc.* **1996**, *118*, 1006-1012.
- (86) Meier, H.; Fetten, M.; Schnorpfeil, C. *Eur. J. Org. Chem.* **2001**, 779-786.
- (87) Schnorpfeil, C.; Meier, H.; Irie, M. *Helvetica Chim. Acta* **2001**, *84*, 2467-2475.
- (88) Fyfe, M. C. T.; Lowe, J. N.; Stoddart, J. F.; Williams, D. J. *Org. Lett.* **2000**, *2*, 1221-1224.
- (89) Cammidge, A. N.; Gopee, H. *Chem. Commun.* **2002**, 966-967.
- (90) Heeger, A. J. *Angew. Chem. Int. Ed.* **2001**, *40*, 2591-2611.
- (91) Kraft, A.; Grimsdale, A. C.; Holmes, A. B. *Angew. Chem. Int. Ed.* **1998**, *37*, 402-428.
- (92) Grazulevicius, J. V.; Strohmriegl, P.; Pielichowski, J.; Pielichowski, K. *Prog. Polym. Sci.* **2003**, *28*, 1297-1353.
- (93) Scherf, U.; List, E. J. W. *Adv. Mater.* **2002**, *14*, 477-487.
- (94) Suh, H.; Jin, Y.; Park, S. H.; Kim, D.; Kim, J.; Kim, C.; Kim, J. Y.; Lee, K. *Macromolecules* **2005**, *38*, 6285-6289.
- (95) Park, S. H.; Kim, J. Y.; Kim, S. H.; Jin, Y.; Kim, J.; Suh, H.; Lee, K. *Proc. of SPIE* **2005**, *5937*, 593710/1-593710/6.
- (96) Yang, C.; Scheiber, H.; List, E. J. W.; Jacob, J.; Müllen, K. *Macromolecules* **2006**, *39*, 5213-5221.
- (97) Rose, A.; Lugmair, C. G.; Swager, T. M. *J. Am. Chem. Soc.* **2001**, *123*, 11298-11299.
- (98) Dai, Y.; Katz, T. J. *J. Org. Chem.* **1997**, *62*, 1274-1285.
- (99) Dai, Y.; Katz, T. J.; Nichols, D. A. *Angew. Chem. Int. Ed.* **1996**, *35*, 2109-2111.
- (100) Kumar, S. *Liquid Crystals* **2005**, *32*, 1089-1113.
- (101) Kumar, S. *Liquid Crystals* **2004**, *31*, 1037-1059.
- (102) Markovitsi, D.; Germain, A.; Millié, P.; Lécuyer, P.; Gallos, L. K.; Argyrakis, P.; Bengs, H.; Ringsdorf, H. *J. Phys. Chem.* **1995**, *99*, 1005-1017.
- (103) van de Craats, A. M.; Warman, J. M. *Adv. Mater.* **2001**, *13*, 130-133.

- (104) Boden, N.; Bushby, R. J.; Lozman, O. R. *Mol. Cryst. Liq. Cryst.* **2003**, *400*, 105-113.
- (105) Rego, J. A.; Kumar, S.; Ringsdorf, H. *Chem. Mater.* **1996**, *8*, 1402-1409.
- (106) Toal, S. J.; Trogler, W. C. *J. Mater. Chem.* **2006**, *16*, 2871-2883.
- (107) Chang, C. -P.; Chao, C. -Y.; Huang, J. H.; Li, A. -K.; Hsu, C. -S.; Lin, M. -S.; Hsieh, B. R.; Su, A. C. *Synth. Met.* **2004**, *144*, 297-301.
- (108) Yang, J. -S.; Swager, T. M. *J. Am. Chem. Soc.* **1998**, *120*, 11864-11873.
- (109) Sohn, H.; Calhoun, R. M.; Sailor, M. J.; Trogler, W. C. *Angew. Chem. Int. Ed.* **2001**, *40*, 2104-2105.
- (110) Sohn, H.; Sailor, M. J.; Magde, D.; Trogler, W. C. *J. Am. Chem. Soc.* **2003**, *125*, 3821-3830.
- (111) Turro, N. J. In *Modern Molecular Photochemistry*; The Benjamin/Cummings Publishing Company, Inc.: Don Mills, Ontario, 1978; pp 246-248.
- (112) Naddo, T.; Che, Y.; Zhang, W.; Balakrishnan, K.; Yang, X.; Yen, M.; Zhao, J.; Moore, J. S.; Zang, L. *J. Am. Chem. Soc.* **2007**, *129*, 6978-6979.
- (113) Leung, A. C. W.; Chong, J. H.; Patrick, B. O.; MacLachlan, M. J. *Macromolecules* **2003**, *36*, 5051-5054.

## Chapter 2

### Synthesis of Phenanthrene and Triphenylene Precursors<sup>§</sup>

#### 2.1 Introduction

One of the goals of this project is to synthesize macrocycles containing aromatic groups to extend conjugation of the macrocyclic backbone. Precursors with salicylate groups of the necessary geometry have not been reported in the literature. However, polycyclic aromatic compounds such as phenanthrene and triphenylene have been studied extensively for use in materials chemistry, so there is a large body of research pertaining to the various syntheses and functionalization of these compounds.

##### 2.1.1 Phenanthrene

The photocyclization of stilbene to phenanthrene has previously been thoroughly explored.<sup>1-3</sup> Stilbenes can be synthesized using many methods, including the Perkin reaction and the Meerwein reaction to form both symmetric and unsymmetrical stilbenes (Scheme 2.1).<sup>2, 4</sup> This allows for diverse phenanthrenes to be synthesized with a large

---

<sup>§</sup> A version of this chapter has been published/accepted for publication/will be submitted for publication: (a) Boden, B.N.; Abdolmaleki, A.; Ma, C. T.-Z.; MacLachlan, M. J. "New Diformyldihydroxyaromatic Precursors for Luminescent Schiff base Macrocycles: Synthesis, Characterization, and Condensation Studies" *Can. J. Chem.* (b) Boden, B. N.; MacLachlan, M. J. "Aggregation of Giant Luminescent Schiff Base Macrocycles" (c) Boden, B.N.; Jardine, K.J.; Leung, A.C.W.; MacLachlan, M.J. "Tetraalkoxyphenanthrene: A New Precursor for Luminescent Conjugated Polymers" *Org. Lett.* **2006**, *8*, 1855-1858.

variety of substituents, such as alkyl, alkoxy or phenyl groups, on carbons 1-8. The numbering of the carbon atoms of phenanthrene is shown in Figure 2.1.

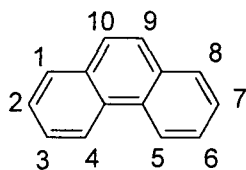
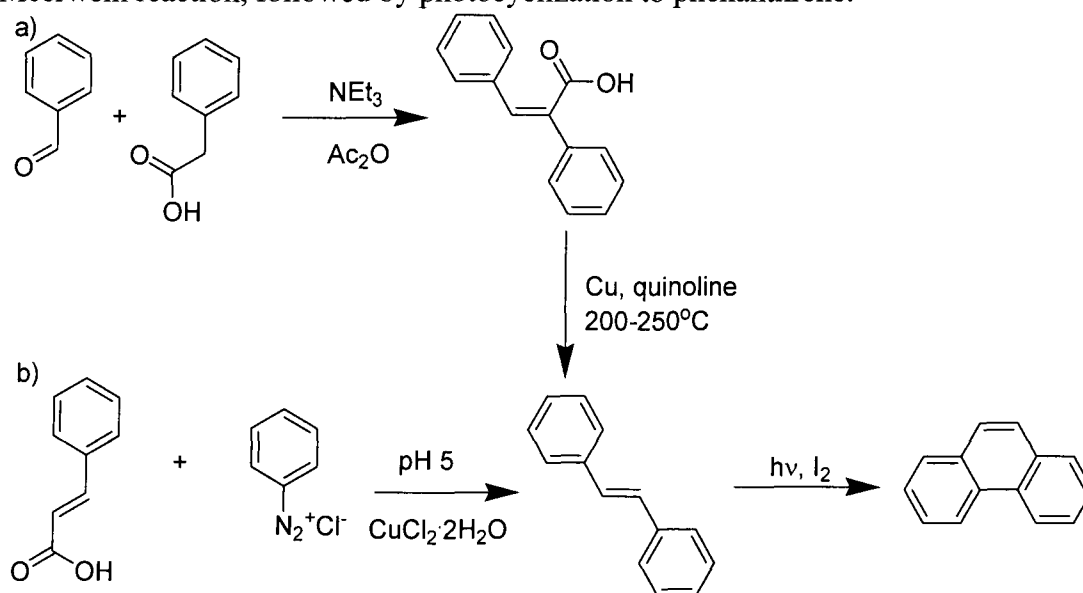


**Figure 2.1** Numbering of the carbon atoms of phenanthrene.

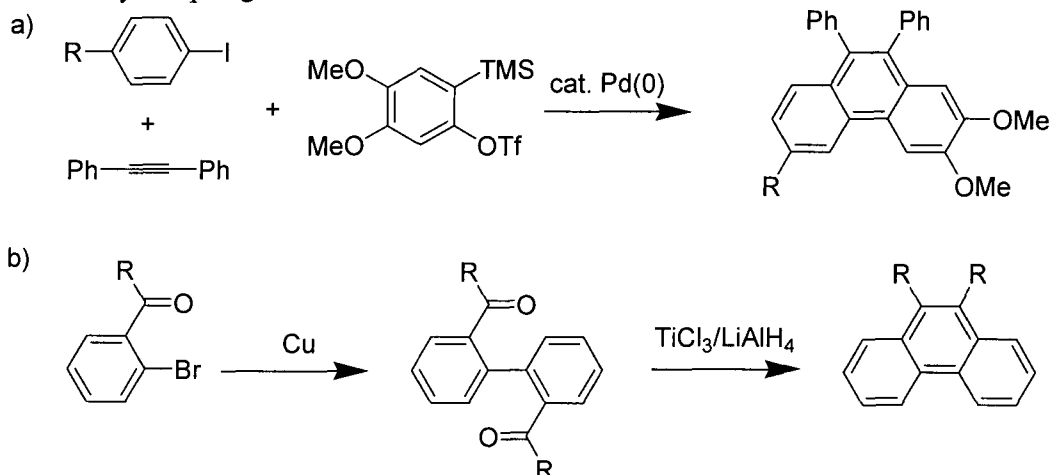
Heteroatoms can be incorporated into the rings of stilbenes to produce styrylpyridines or other heterocyclic analogues. These compounds can undergo photocyclization to produce varieties of benzoquinoline, phenanthrolines, phenanthrofurans, and phenanthrothiophenes.<sup>5</sup> While the photocyclization of functionalized stilbenes is reliable, dimerization of stilbene can occur if the solutions used are too concentrated.

**Scheme 2.1** Stilbene syntheses: a) Perkin reaction followed by decarboxylation and b) Meerwein reaction, followed by photocyclization to phenanthrene.



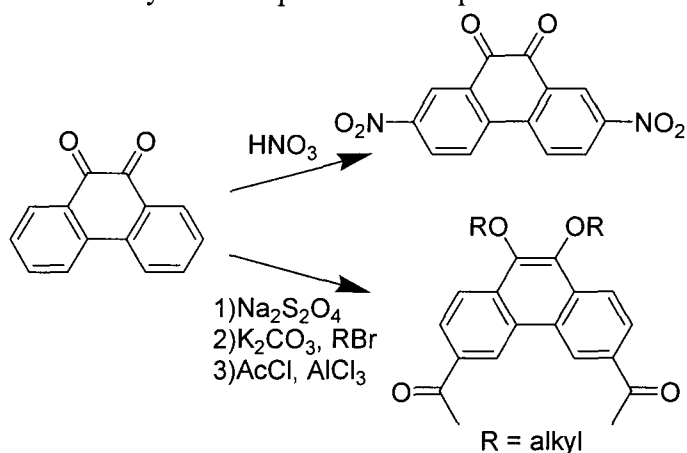
Some chemical routes have been found to obtain phenanthrene with substituents on the 9,10 positions. Pd-catalyzed coupling of aryl halides, alkynes and arynes gives unsymmetrically substituted phenanthrenes (Scheme 2.2).<sup>6</sup> This reaction can be used to prepare phenanthrene with a variety of substituents. Coupling of bromo or iodo benzophenones through the Ullman reaction followed by subsequent McMurry coupling gives phenanthrene substituted with alkyl groups in the 9,10 position.<sup>7</sup>

**Scheme 2.2** Novel phenanthrene syntheses: a) three component coupling and b) Ullman and McMurry couplings.



Synthesis of 9,10-phenanthrenequinone can be performed in several ways, by the addition of iodic acid to phenanthrene or oxidation of phenanthrene by potassium dichromate.<sup>8, 9</sup> The quinone generally directs electrophilic substitution, for example nitration, towards the 2,4,5 and 7 positions (Scheme 2.3).<sup>10</sup> However, other reactions, such as bromination, are selectively directed to the 3,6 positions. After reduction of the quinone, Friedel-Crafts acylations also occur at the 3,6 carbons.<sup>11, 12</sup> This creates versatility in synthesis of phenanthrene derivatives.

**Scheme 2.3** Nitration and acylation of phenanthrenequinone.



### 2.1.2 Triphenylene

Schultz first isolated triphenylene in 1880. Later, the first synthesis of triphenylene was developed by Mannich in 1907.<sup>13</sup> The carbon atoms of triphenylene are numbered as shown in Figure 2.2. The 1,4,5,8,9, and 12 carbons are referred to as the  $\alpha$  carbons and the 2,3,6,7,10 and 11 carbons are referred to the  $\beta$  carbons.

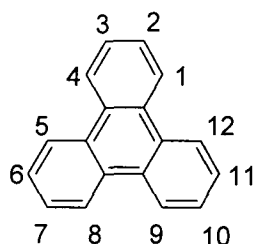
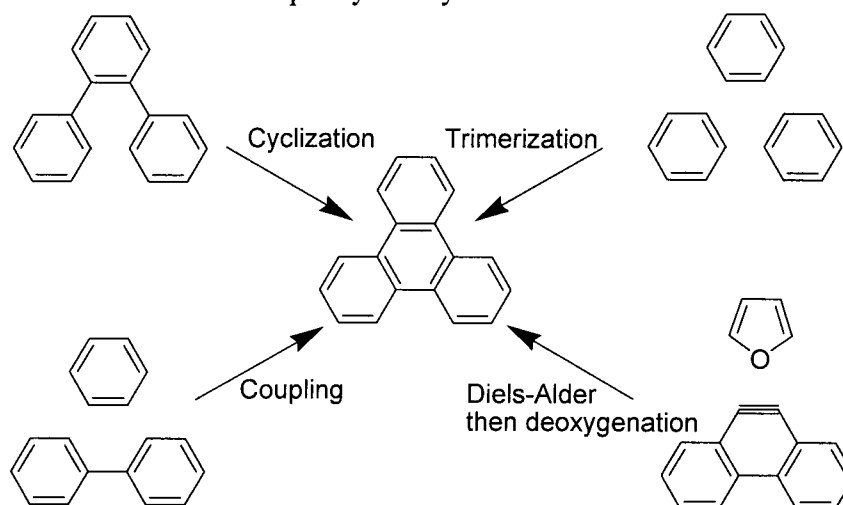


**Figure 2.2** Numbering of the carbon atoms of triphenylene.

Currently, triphenylene is synthesized using several different methods (Scheme 2.4).<sup>14</sup> Triphenylene with hexasymmetric substituents on the outer rings, such as those used in liquid crystals can be formed by the oxidative trimerization of 1,2-dialkoxybenzenes.<sup>15</sup> Other methods to make substituted triphenylenes include oxidative cyclizations, Diels-Alder cycloadditions, organometallic couplings, or photocyclizations.

These reactions use materials such as biphenyl, terphenyl<sup>16</sup> or phenanthrene to obtain unsymmetrically substituted triphenylenes. Aza-analogs of triphenylene have also been investigated. These compounds are often synthesized via condensation reactions of either hexaaminobenzene or hexaketocyclohexane.

**Scheme 2.4** Select methods of triphenylene synthesis.



Unsymmetric triphenylenes can undergo further functionalization. Triphenylene can be brominated<sup>17, 18</sup> or nitrated<sup>19, 20</sup> and the position of functionalization often depends on the existing substituents. It has also been established that it is often best to cyclize the triphenylene after most of the required groups are in place on the aromatic starting materials.

### 2.1.3 Further Functionalization toward Macrocycle Precursors

Halogenation has been determined to be the most useful method of substitution for functionalizing phenanthrene and triphenylene for our purposes. These groups can easily be converted into alkoxy, hydroxyl and formyl moieties, or can be used to form

carbon-carbon bonds by various coupling reactions. The most important structural feature that needs to be synthesized for our starting materials is the salicylate functionality, which features adjacent formyl and hydroxyl groups. This chapter discusses the development of the polycyclic aromatic precursors **70-73** used in macrocycle syntheses (Figure 2.3).

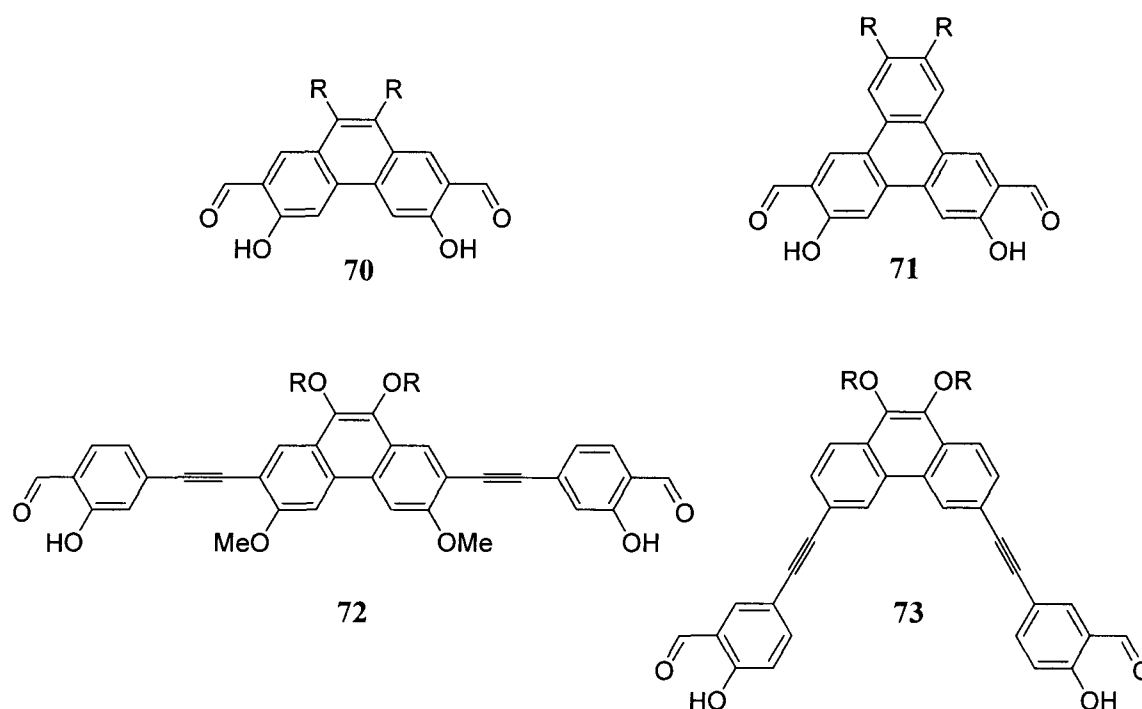


**Figure 2.3** Structures of phenanthrene and triphenylene-containing precursors **70-73**.

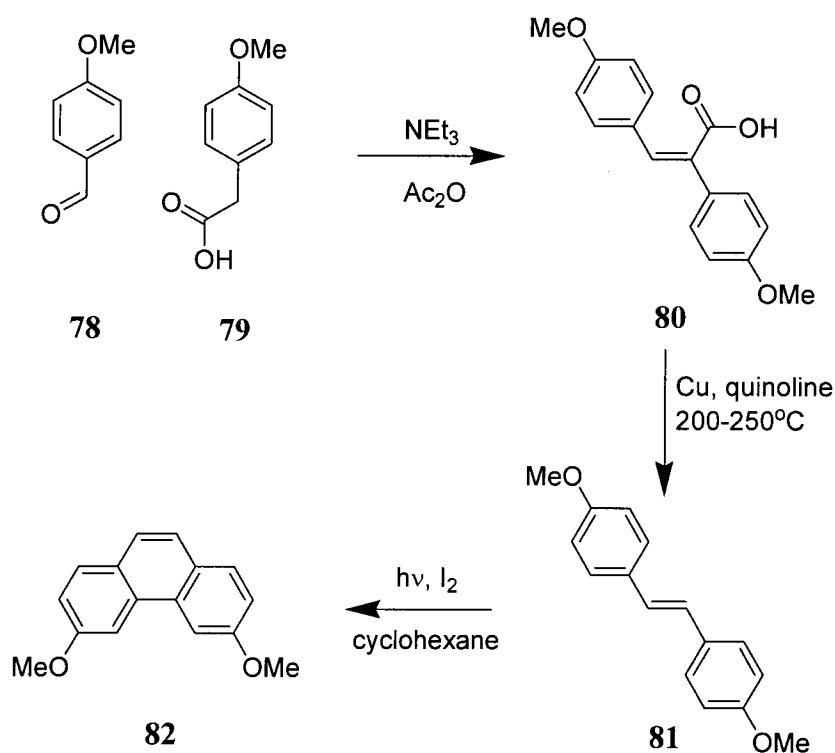
## 2.2 Discussion

### 2.2.1 Synthesis of Precursor **70a**

In order to synthesize a phenanthrene-containing macrocycle, it was first necessary to affix formyl groups in the 2,7 positions with adjacent hydroxyl moieties at the 3,6 positions. Phenanthrene can be made with a variety of substituents using a Perkin

coupling of the appropriate acid (**78**) and aldehyde (**79**), which is followed by decarboxylation of the product (**80**) to give a stilbene (Scheme 2.5). *Para*-methoxy trans-stilbene, **81**, isomerizes and photocyclizes in the presence of iodine and ultraviolet light.<sup>21</sup>

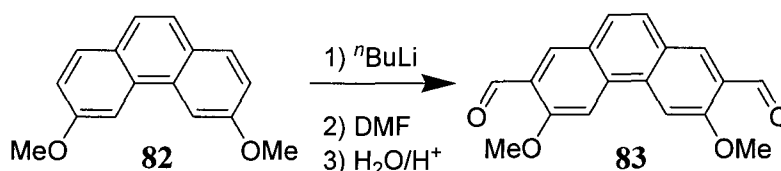
**Scheme 2.5** Synthesis of **80** - **82**.



Once isolated, 3,6-dimethoxyphenanthrene, **82**, was lithiated using  $n\text{BuLi}$  in hexanes<sup>22</sup> and quenched with anhydrous dimethylformamide (DMF) to form **83** (Scheme 2.6). Unfortunately, this reaction has a very low yield, with the highest recorded as 17%. This product can be recrystallized only after chromatography on silica using methylene chloride as solvent. Other products from this reaction were not identified, but likely by-

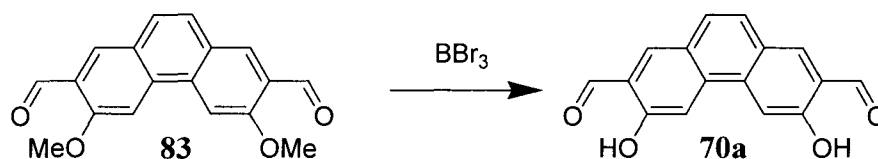
products include monoformylated dimethoxyphenanthrene and dimethoxyphenanthrene diformylated in the 2,5 positions.

**Scheme 2.6** Synthesis of **83**.



Compound **83** was deprotected with  $\text{BBr}_3$  to obtain the phenanthrene diol **70a** (Scheme 2.7). This compound was purified by passing it through silica with methylene chloride, although limited solubility makes this purification tedious and only possible in small batches. Compound **70a** can be recrystallized in DCM or THF. The  $^1\text{H}$  NMR spectrum of **70a** in dimethylsulfoxide- $d_6$  ( $\text{DMSO}-d_6$ ), shown in Figure 2.4, supports the anticipated structure by the appearance of an hydroxyl resonance at 10.96 ppm and the disappearance of the methoxy peak at 4.17 ppm.

**Scheme 2.7** Deprotection of **83** to form **70a**.



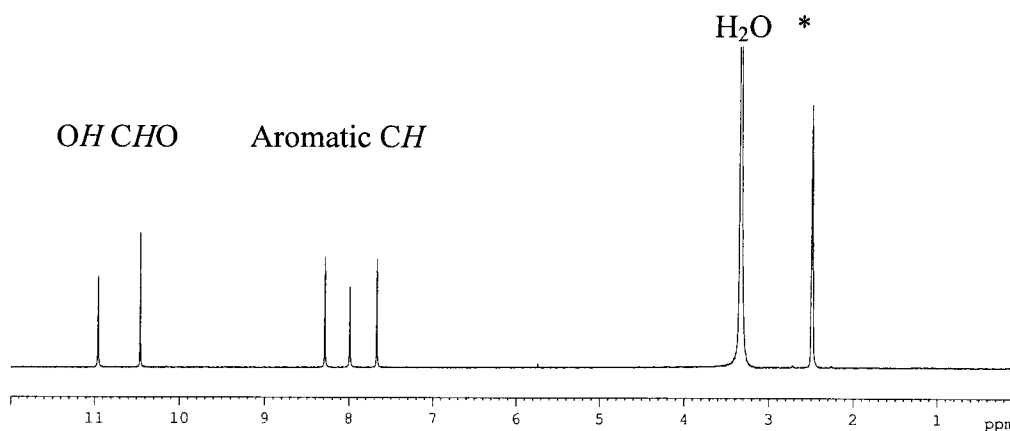


**Figure 2.4**  $^1\text{H}$  NMR spectrum (300 MHz,  $\text{DMSO-}d_6$ ) of **70a** (\* =  $\text{DMSO-}d_6$ ).

### 2.2.2 Attempted Synthesis of Precursor **70b**

As a result of the poor yields and low solubilities in the synthesis of **83** and **70a**, it was determined that an alternative diol was needed. 9,10-Phenanthrenequinone (**84**) can easily be reduced, and converted to alkoxy substituents. If salicylaldehyde moieties can be formed on the sides of the phenanthrenequinone as well as the new alkoxy chains, we can make a more soluble precursor, **70b**.

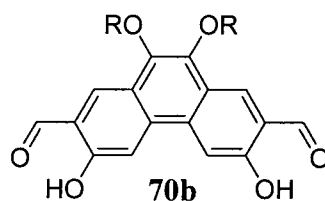
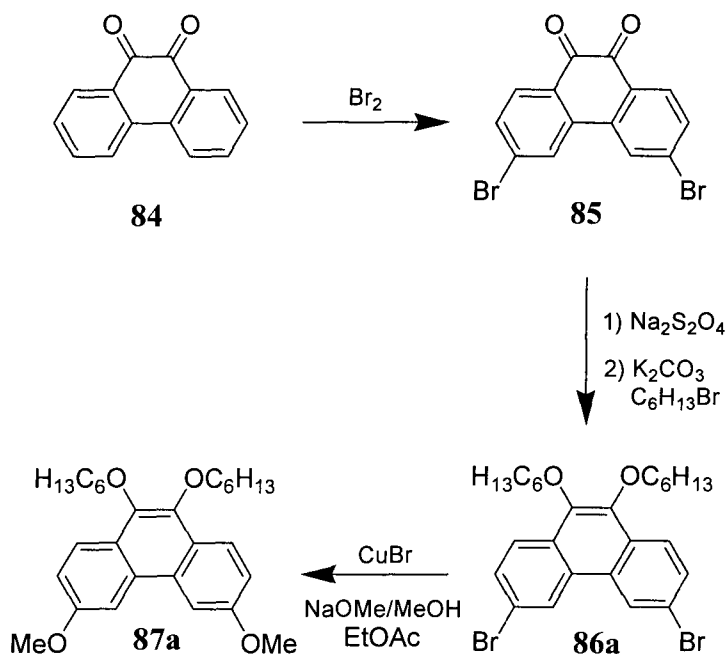


**Figure 2.5** Precursor **70b**.

It has previously been shown that phenanthrenequinone, **84**, selectively brominates in the 3,6 position to make **85** (Scheme 2.8). Next, reduction and alkylation of the quinone forms phenanthrene **86a** with the alkoxy chains needed to increase solubility. This reaction must be done in one pot as 9,10-dihydroxyphenanthrene easily reoxidizes to the quinone. Substitution of bromine with methoxy groups to make **87a** proceeded in

moderate yield using sodium methoxide and CuBr as a catalyst.<sup>23</sup> Although this reaction proceeds favourably, attempts to scale up the reaction beyond one or two grams of starting material resulted in decreased yields.

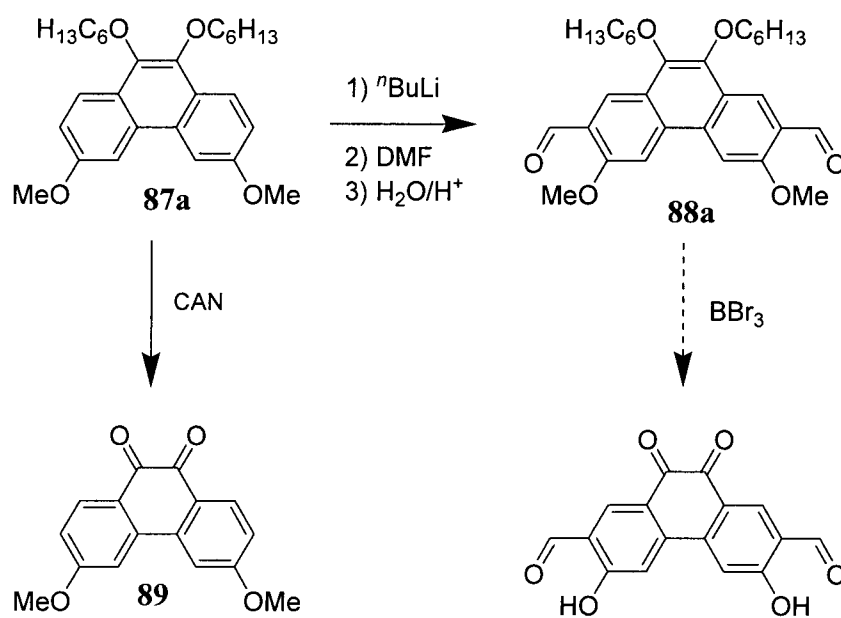
**Scheme 2.8** Synthesis of **85** – **87a**.



Unfortunately, lithiation and formylation of **87a**, similar to the synthesis of the unsubstituted phenanthrene, gave only a 6% yield of **88a** (Scheme 2.9). Additional products recovered included monoformylated phenanthrene and **87a**. Furthermore, it was feared that reaction of **88a** with  $\text{BBr}_3$  would also cleave the hexyl chains. It is well known that oxidative demethylation can occur using cerium ammonium nitrate (CAN).<sup>24</sup> To see whether this reaction was selective for either the 9,10 or 3,6 alkoxy groups, **87a** was stirred with CAN. Results of this reaction showed that the hexyl chains in the 9,10 positions were cleaved rather than the 3,6 methoxy groups and the quinone, **89**, was

obtained. It was theorized that substitution of a different protecting group in the 3,6 position would remedy this problem.

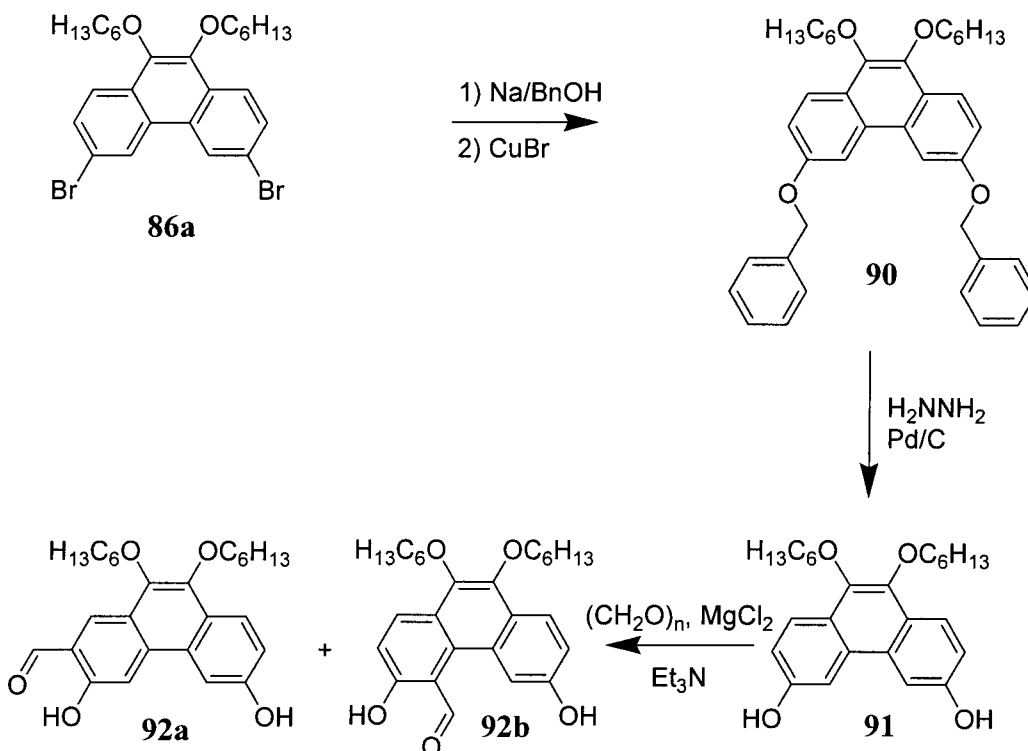
**Scheme 2.9** Synthesis of **88a** and **89**.



Sodium benzyloxide was made in situ and reacted with **86a** in the presence of CuBr to give **90**, with benzyl protected hydroxyl groups in the 3,6 positions (Scheme 2.10). Benzyl protecting groups are well-known to only cleave using hydrogenation conditions. In this case, hydrazine and Pd/C were used to afford a light brown product, **91**; however both of these reactions were found to be irreproducible. Once debenzylated, the dihydroxyl product was subjected to formylation using  $\text{SnCl}_4$  or  $\text{MgCl}_2$  and paraformaldehyde. In the presence of  $\text{MgCl}_2$ , only a small amount of monoformylated phenanthrene in either the 2 or 4 positions was observed, in addition to recovered starting material. Heating the reaction at progressively higher temperatures did not change the

yield or the products of the reactions. No formation of the desired dialdehyde was observed using  $\text{SnCl}_4$ .

**Scheme 2.10** Synthesis of **90** and **91**, and attempted formylation of **91**.



The starting material was separated from the monoformylated product using column chromatography, but the two monoformylated isomers, **92a** and **92b**, could not be separated. In the  $^1\text{H}$  NMR spectrum, two sets of formyl and hydroxyl peaks were identified (Figure 2.6). In addition, the aromatic peaks can be assigned to either **92a** or **92b** through integration. Compound **92b** has aromatic protons that are side by side, which exhibit *ortho* coupling resulting in doublets, while **92a** has protons that are opposite to each other, appearing as singlets in the spectrum. Because the more intense set of aromatic resonances consists of peaks that are all multiplets, it is clear that **92b** is

the dominant species produced. The second hydroxyl resonances appear in the  $^1\text{H}$  NMR spectrum at 5.30 ppm, underneath the solvent peak.

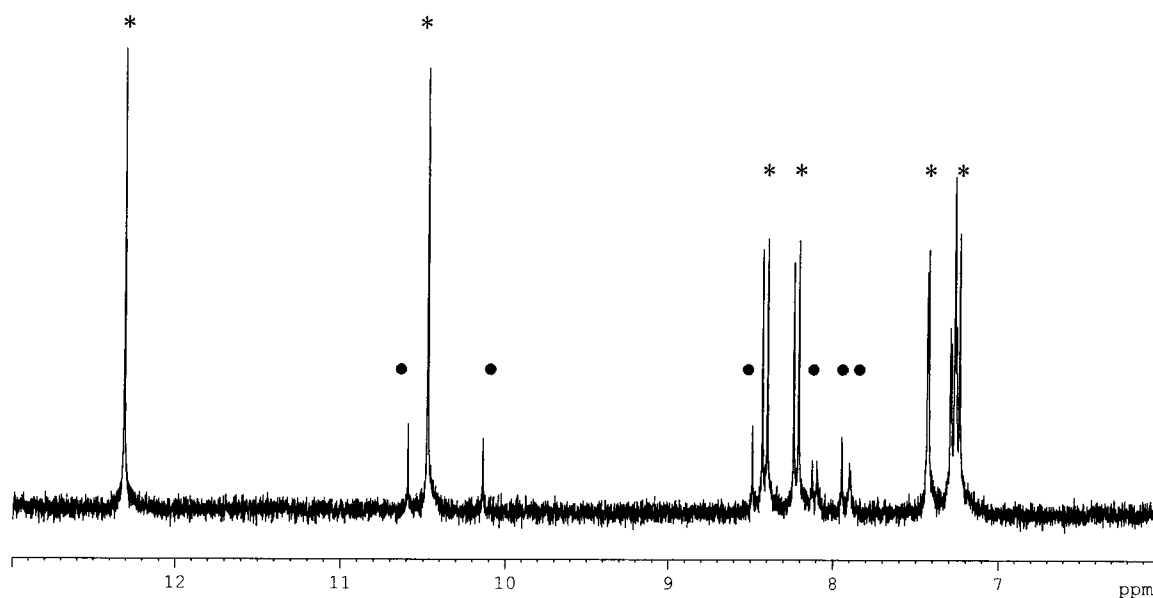


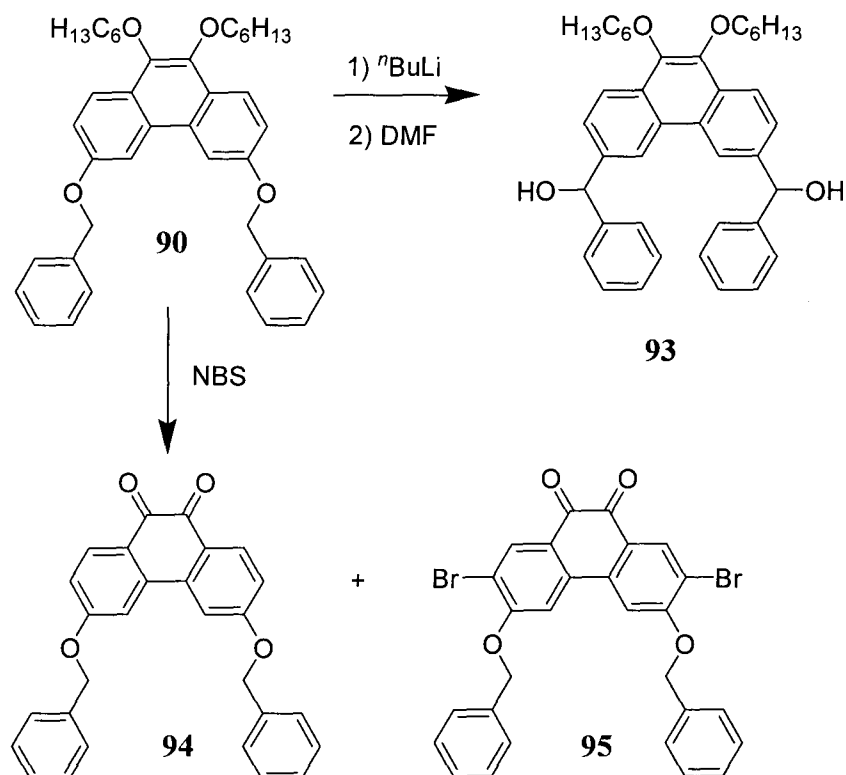
**Figure 2.6** Aromatic and formyl region of the  $^1\text{H}$  NMR (300 MHz) of a mixture of **92a** (•) and **92b** (\*) in  $\text{DCM-}d_2$ .

Lithiation of the dibenzyl-protected phenanthrene, followed by addition of DMF, resulted in a [1,2] Wittig rearrangement to form an alcohol, **93** (Scheme 2.11), rather than the desired formyl product. Reactions of this type were first observed in 1942 and have been discussed in work by Garst and more recently, by Barluenga.<sup>25,26</sup> It should be noted that although the Wittig rearrangement is known, there is literature confirming that the aldehyde can be formed using these conditions.<sup>27</sup>

As a result of the difficulties in formylation, we found it necessary to attempt bromination of the phenanthrene in the 2,7 positions. Initial experiments with NBS on benzyl-protected phenanthrene precursors, resulted cleavage of the 9,10 alkoxy chains, **94**, and is accompanied by bromination in low yield to afford **95**. Further bromination

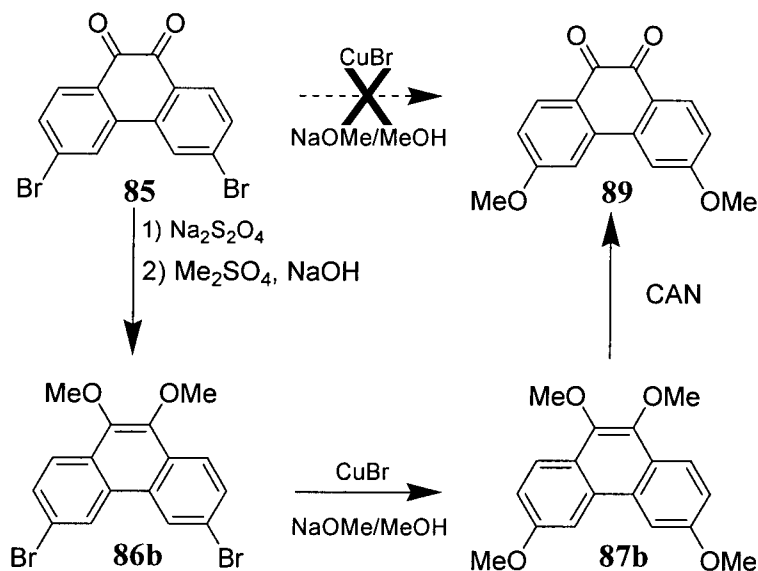
experiments were continued with the 3,6-methoxy protected phenanthrene due to the unreliability of the benzyl protection.

**Scheme 2.11** Synthesis of **93** - **95**.



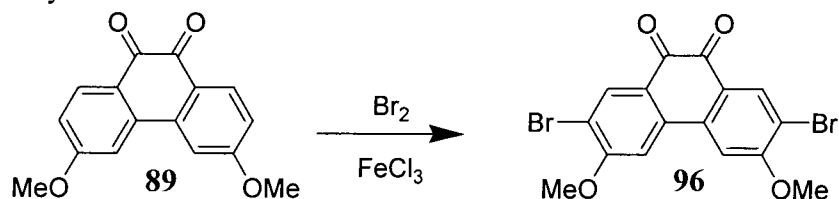
Because the 9,10 alkoxy chains are removed during bromination, we attempted to directly substitute the 3,6 bromines of **85** for methoxy groups using CuBr and NaOMe without protecting the quinone, but this reaction does not proceed (Scheme 2.12). As it appears that protection of the quinone is necessary for substitution, methoxy substituents were placed in the 9,10 position as protecting groups to make **86b**, which was then reacted with CuBr and NaOMe. Because we previously found the 9,10 alkoxy groups could easily be cleaved and oxidized using CAN, this deprotection was performed before bromination of the 2,7 carbons.

**Scheme 2.12** Synthesis of **86b**, **87b** and **89**.



The 2,7 positions of **89** could be brominated to afford **96**. It was discovered that optimal yields of **96** require reflux of **89** with both  $\text{Br}_2$  and  $\text{FeCl}_3$  in a solution of acetonitrile ( $\text{MeCN}$ ) and  $\text{DCM}$  (Scheme 2.13). This reaction does not always proceed to completion and sometimes requires the addition of more reagents. Any starting material and monobrominated quinone can be separated easily through column chromatography using  $\text{DCM}$  as the solvent.

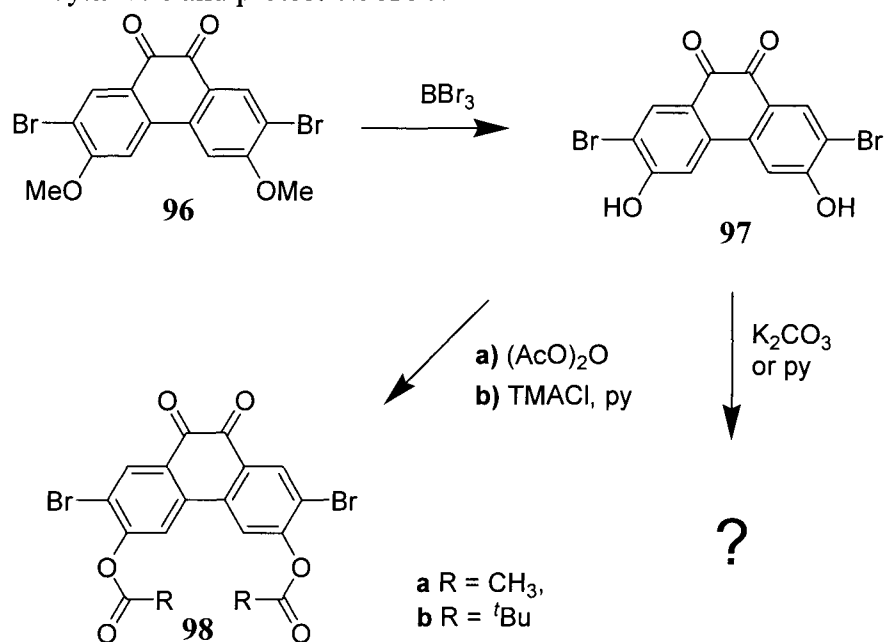
**Scheme 2.13** Synthesis of **96**.



The methoxy groups in **96** were deprotected to form **97** (Scheme 2.14), an orange solid that is not soluble in most solvents with the exception of  $\text{DMSO}$  and  $\text{THF}$ . At this

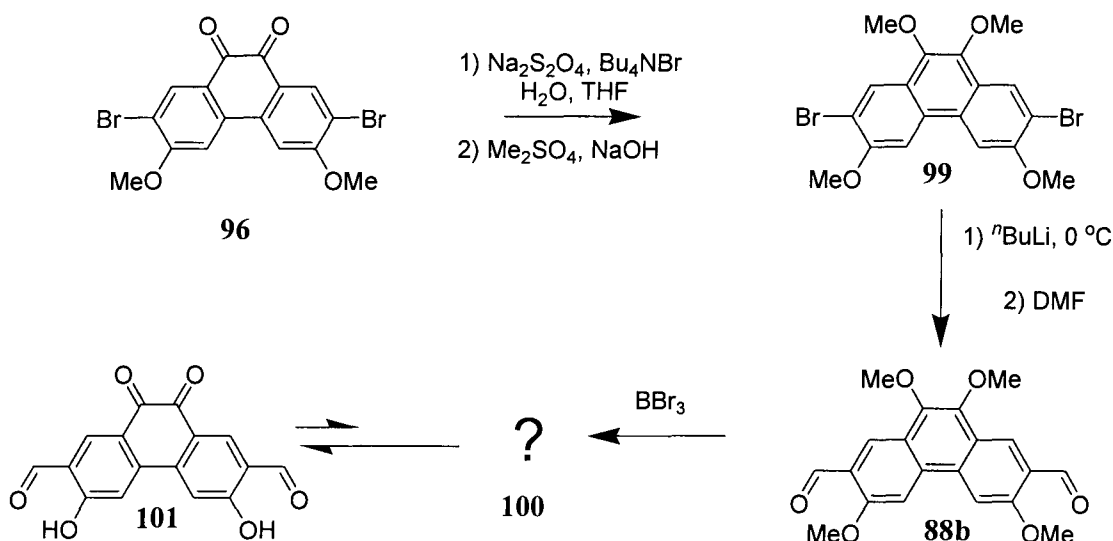
point, the synthetic plan involved protection of the hydroxyl, and reduction of the quinone for substitution of 9,10 alkoxy chains, which would be followed by lithiation, formylation and final deprotection. Unfortunately, attempts to protect **97** were hampered by a side reaction with base. Using  $K_2CO_3$  in DMF or pyridine in THF caused the solution to darken. None of the anticipated product had formed upon quenching. In addition, dissolution of **97** in  $Et_3N$  formed a blue solution, which gave a mixture of products after addition of acetic anhydride. Nonetheless, **97** could be protected with acetyl groups upon heating in pure acetic anhydride to give **98a**. Deprotection of the acetyl-protected hydroxyls is accomplished with the addition of base. Unfortunately, ether synthesis requires the addition of base, so this protecting group was useless, as the acetyl groups would cleave and a tetraalkoxy product would result. Trimethylacetyl protecting groups are slower to deprotect with base, but upon reduction and alkylation of **98b**, cleavage of these groups still occurred.

**Scheme 2.14** Synthesis and protection of **97**.



As an alternative route, the formylation of **96** before deprotecting the hydroxyl moieties was attempted. Prior to formylation of the phenanthrene, it was necessary to reduce the quinone to **99** to prevent addition of butyl chains to the 9,10 carbons (Scheme 2.15). Lithiation of **99** followed by addition of DMF gives a yellow solid, **88b**. Similarly to previous formylated phenanthrene derivatives, this compound was purified through chromatography and recrystallization. All methoxy groups can be cleaved using  $\text{BBr}_3$  to acquire **101**. This reaction initially gave a purple product, **100**, found to be insoluble in most solvents, except THF, DMSO, pyridine and DMF. Once in solution, the colour changed from purple to yellow. After removal of the solvent, a brown solid, **101**, was obtained.

**Scheme 2.15** Synthesis of **99-101**, **88b**.



$^1\text{H}$  NMR spectrum of the purple product shows two formyl resonances, three hydroxyl peaks and four peaks corresponding to the aromatic region (Figure 2.7). Alternatively, the  $^1\text{H}$  NMR spectrum of the brown solid supports the structure of **101**

with two aromatic peaks, one formyl peak and a hydroxyl resonance. After allowing the purple solid to stand for several weeks, the peaks at 10.67, 10.46, 8.45 and 7.92 ppm decrease in intensity, while the peaks for **101** increase, indicating that this solid is a mixture of **100/101** and slowly isomerizes into **101**.

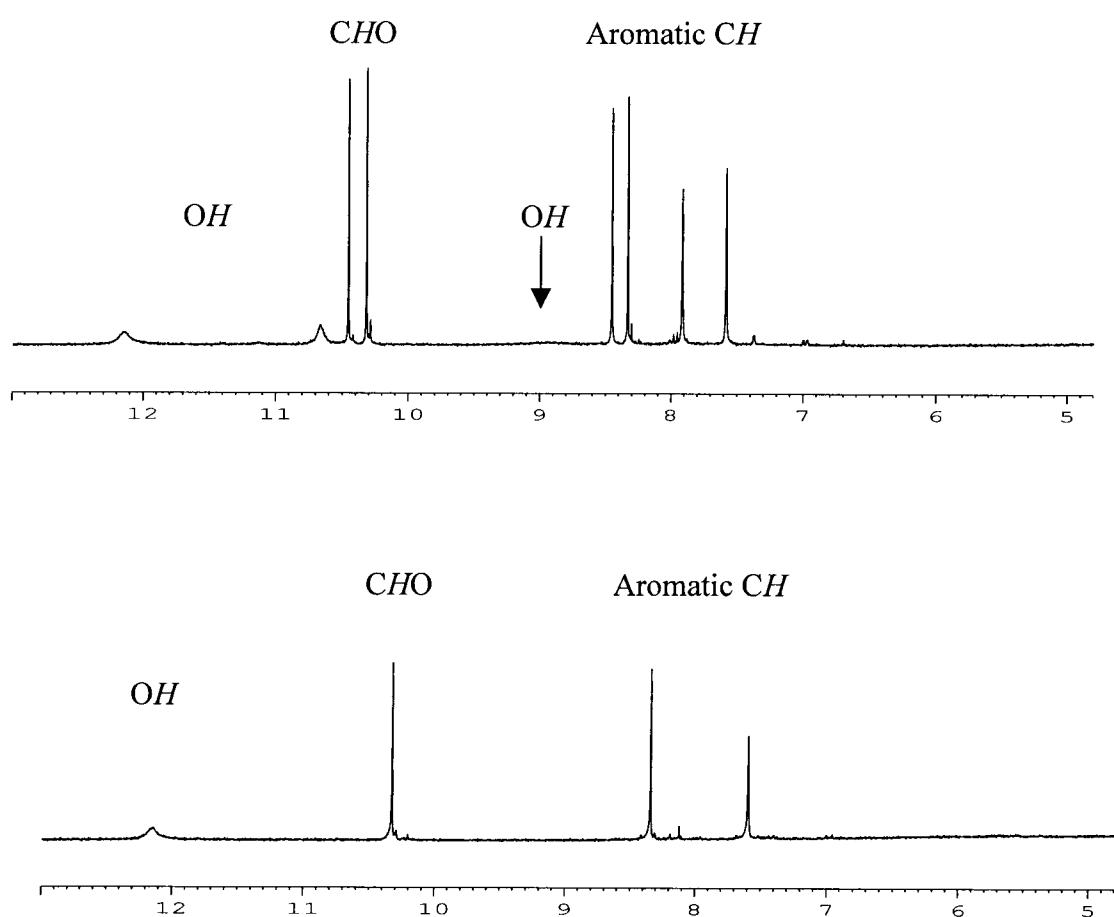


**Figure 2.7** <sup>1</sup>H NMR (300 MHz, DMSO-*d*<sub>6</sub>) of **100/101** (top) and **101** (bottom).

Single crystals of **101** suitable for X-ray diffraction were obtained from DMSO. The structure, solved by Dr. Brian O. Patrick and shown in Figure 2.8, confirms the identity of **101**. Typically in structures of salicylates, the formyl groups are hydrogen

bonded to the hydroxyl groups. However, the structure for **101** shows the oxygen of the aldehydes pointing away from the alcohol and the hydroxyl moieties are instead hydrogen bonding with the oxygen in crystallized DMSO. The extended structure shows phenanthrene molecules stacked in a staggered arrangement with intermolecular separations of 3.1-3.3 Å, characteristic of  $\pi$ - $\pi$  interactions.<sup>28</sup> The view from above shows the aromatic rings almost directly above one another.

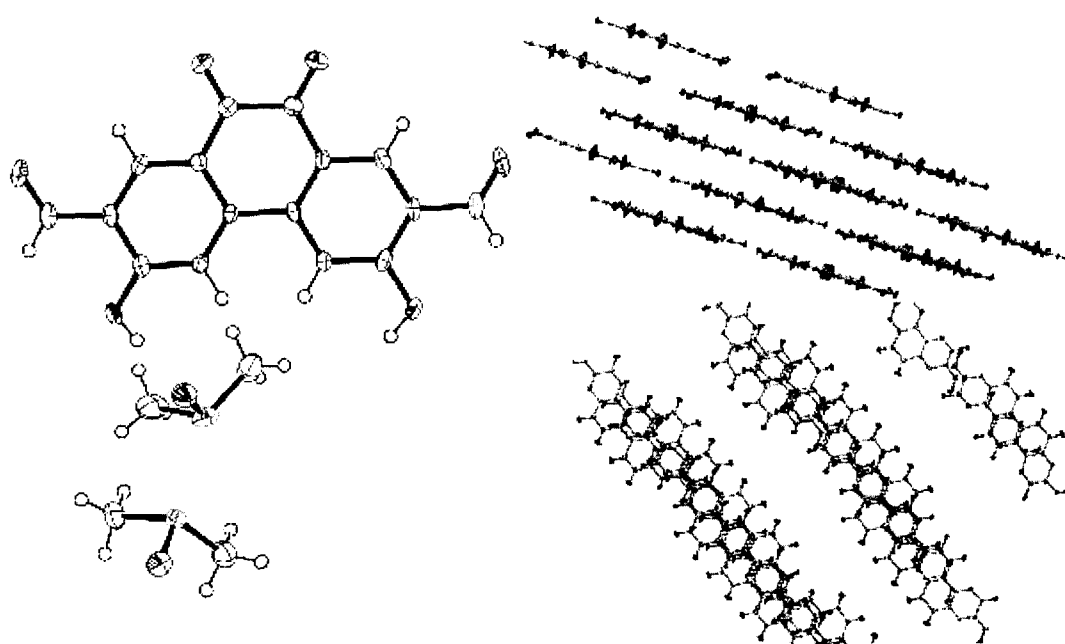


**Figure 2.8** ORTEP representation of the crystal structure of **101·2 DMSO**. DMSO molecules are omitted from the extended structure for clarity.

It stands to reason that the initial kinetic product formed, **100**, is a tautomer of **101**, while **101** is thermodynamically more stable. Mass spectrometry of both species gives similar ionization patterns. Similar to **96**, **101** darkens and appears to revert to **100** upon addition of base such as pyridine, resulting in prevention of protection of the 3,6 positions of the phenanthrene.

Attempts have been made to identify **100**; however, determination of the structure of **100** is hindered by its thermodynamic instability. Four possible structures for this compound, shown in Figure 2.9, were proposed. After stirring **101** with Na<sub>2</sub>S<sub>2</sub>O<sub>4</sub> to reduce the quinone, a pale yellow product was observed that eliminated the tetrahydroxy phenanthrene (Figure 2.9a) as a possible intermediate. Because the <sup>1</sup>H NMR spectrum of **100** contains one formyl resonance and two aromatic resonances, we can eliminate the possibility of an unsymmetrical charge transfer compound (Figure 2.9b). This leaves two tautomers remaining (Figure 2.9c and 2.9d), although neither of these appear stable.

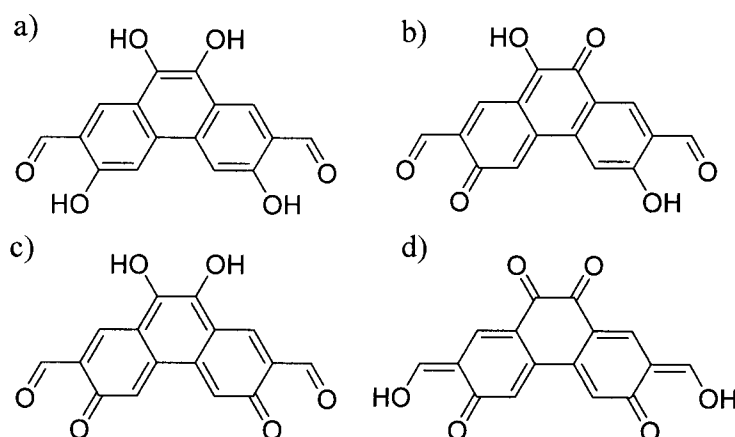
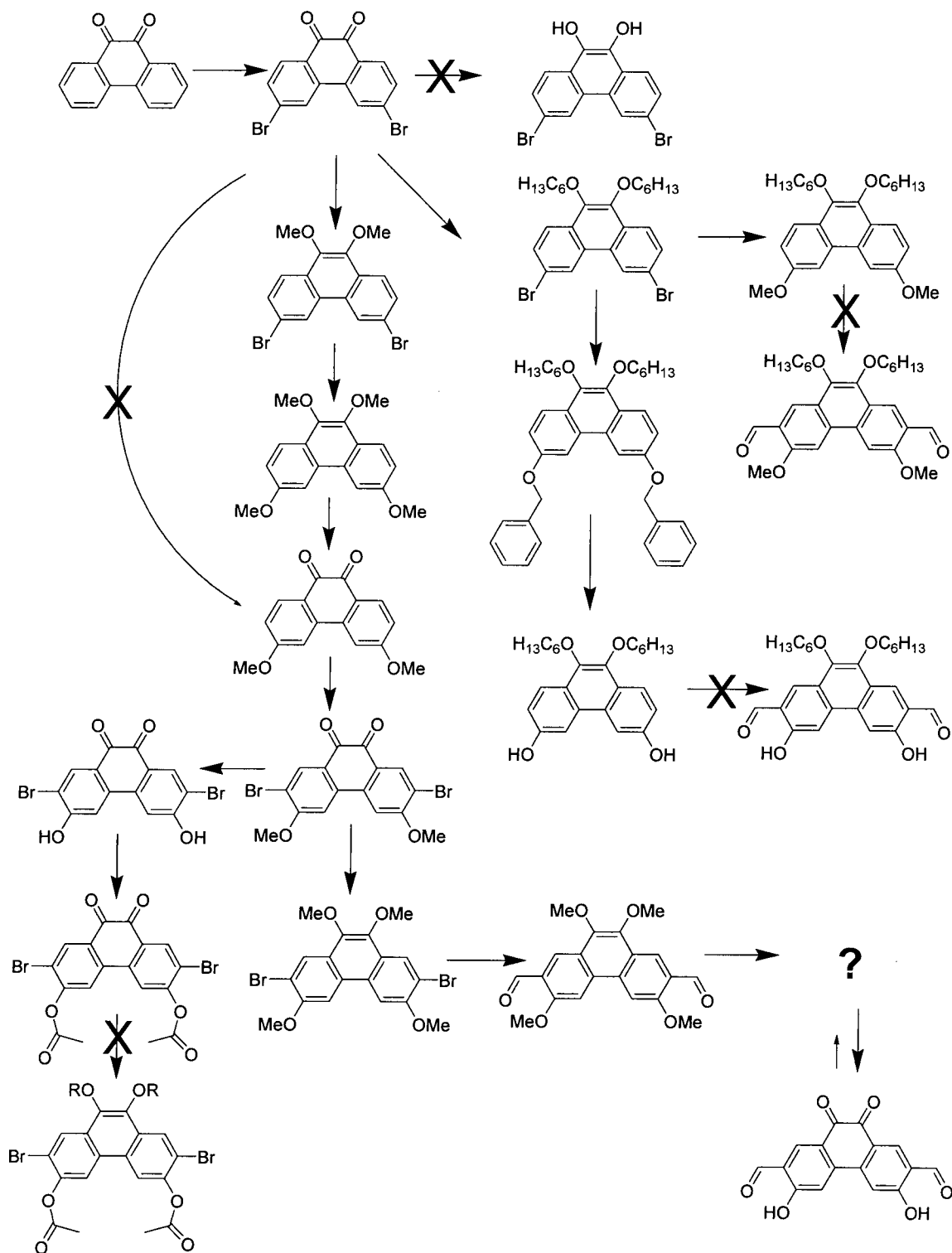


**Figure 2.9** Hypothetical structures for **100**.

Although the pursuit to synthesize precursor **70b** was unsuccessful, a variety of new compounds that have potential as foundations for other useful molecules were synthesized. Phenanthrene with halogens in the 2,7 or 3,6 positions have tremendous promise for substitution using organometallic coupling methods, such as Suzuki, Stille, Sonogashira and Heck reactions. Scheme 2.16 contains an overview of all the attempted routes to **70b**. For our purposes, the constant protection and deprotection of the quinone makes the synthesis of **70b** impractical.

**Scheme 2.16** Attempted routes to **70b**.



### 2.2.3 Synthesis of Precursor 71

As our attempts to solubilize phenanthrene were hindered by the reactions of the quinone, we decided to expand outward and use triphenylene. The necessary triphenylene precursor, **71**, has peripheral alkyl groups rather than alkoxy chains to ensure the macrocycle will be soluble and prevent the difficulties encountered in the attempted synthesis of **70b**. The synthesis of **71**, shown in Scheme 2.17, was based on previous research of unsymmetrically hexasubstituted triphenylenes.<sup>16, 17</sup>

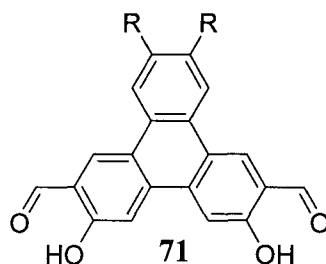


**Figure 2.10** Precursor **71**, where R = <sup>n</sup>C<sub>6</sub>H<sub>13</sub>.

In the first step, terphenyl **103** was formed via Suzuki coupling of 1,2-dibromo-4,5-dihexylbenzene (**102**) and 4-methoxyphenylboronic acid (Scheme 2.17). Optimal yields were obtained using a precise solvent ratio of 3:3:1 toluene/ethanol/water as well as decreasing the reaction times to about three hours rather than sixteen hours. Triphenylene **104** was produced by photocyclization of **103** in the presence of iodine. While this reaction yields a low percentage of triphenylene, unreacted starting material can easily be isolated using recrystallization. Selective double bromination of triphenylene **104** occurred at the 6,11 positions, yielding **105**. Subsequent metal-halogen exchange with <sup>n</sup>BuLi and reaction with DMF gave the diformyldimethoxytriphenylene **106** after work-up. In the last step, the phenol was deprotected with BBr<sub>3</sub> to afford the



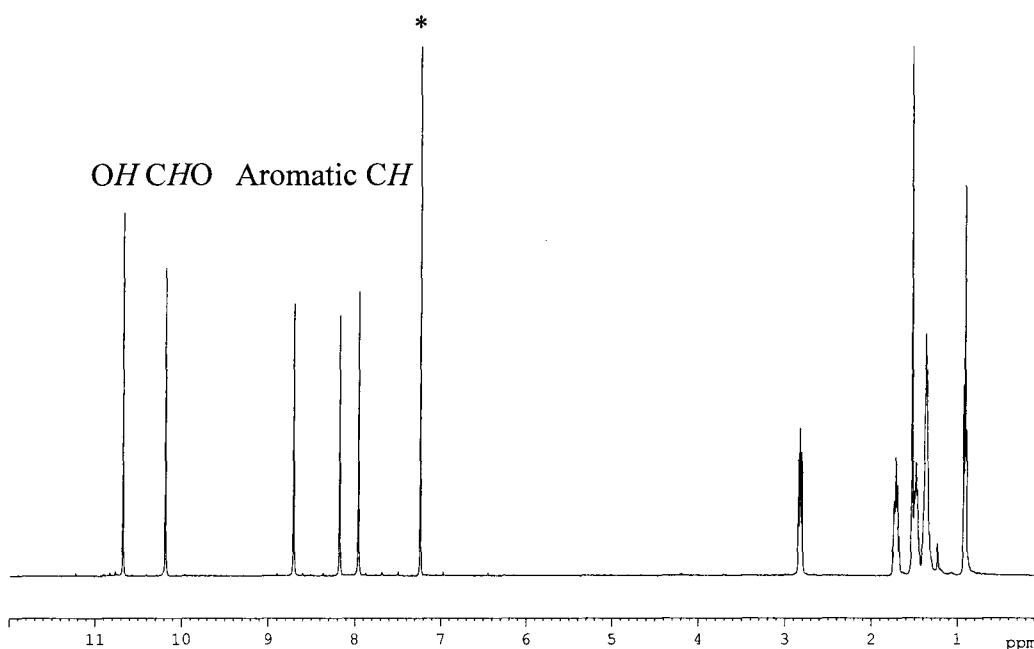


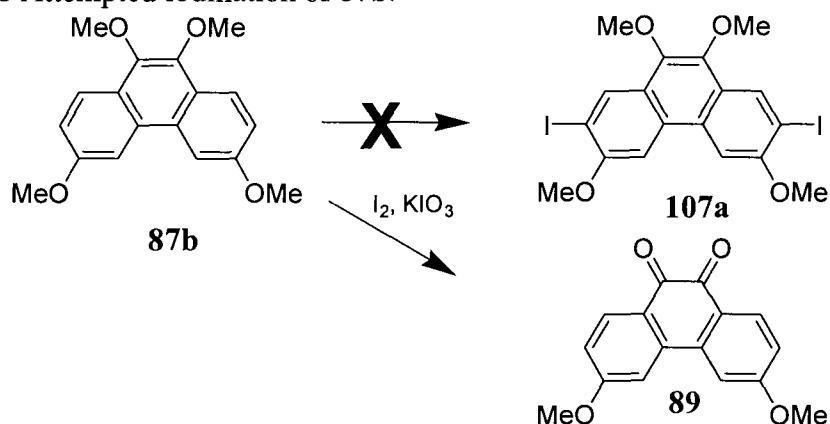
**Figure 2.11**  $^1\text{H}$  NMR (400 MHz,  $\text{CDCl}_3$ ) spectrum of **71** (\* =  $\text{CDCl}_3$ ).

#### 2.2.4 Synthesis of Precursor **72**

Brominated aromatic compounds are useful for halogen exchange reactions using  $n\text{BuLi}$ , as demonstrated with **99** and **105**. However, iodinated compounds can be used in Sonogashira-Hagihara couplings. This provides the means to include ethynyl moieties in a diol, which would greatly increase macrocycle size and conjugation.

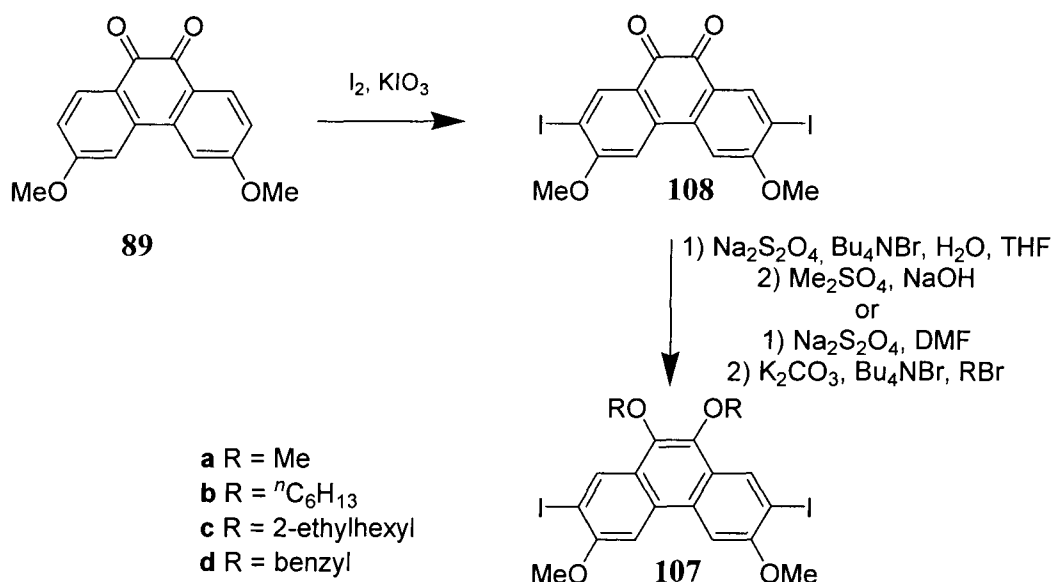
Iodination using  $\text{I}_2$  and  $\text{KIO}_3$  in a mixture of sulfuric acid, water and acetic acid was attempted to iodinate phenanthrene in the 2,7 positions. Unfortunately, using **87b** as a starting material failed to yield **107**, producing only phenanthrenequinone **89** as the product instead (Scheme 2.18). Fortunately, iodination of **89** afforded compound **108** selectively in good yield (Scheme 2.19).

**Scheme 2.18** Attempted iodination of **87b**.



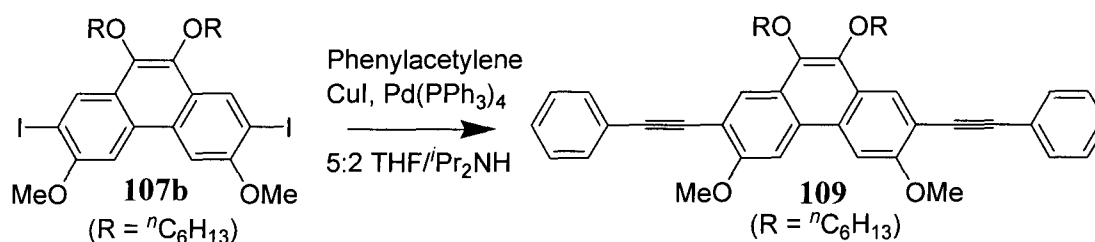
Compound **108** was further reduced and alkylated to afford **107**. To demonstrate the versatility of this compound, methoxy, hexyloxy, ethylhexyloxy and benzyloxy groups were successfully substituted in the 9,10 positions to acquire **107a-d**. Purification of **107a-d** involved both column chromatography and recrystallization, reducing the yield of the pure product. Decomposition of **107** to the quinone occurred if it remained in solution for extended periods of time. Once recrystallized, the solid is stable for several months without observable decomposition.

**Scheme 2.19** Synthesis of **108** and **107**.



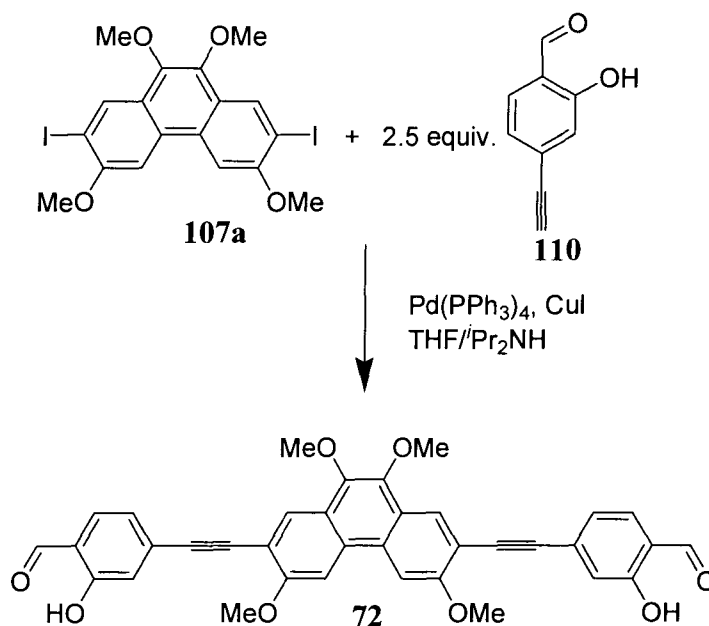
Once **107** was prepared, a model compound was synthesized using the hexyl derivative to test and optimize Sonogashira-Hagihara coupling conditions according to Scheme 2.20. Compound **109** could be prepared in nearly quantitative yield by Pd(0)-catalyzed cross-coupling of **107** with phenylacetylene.

**Scheme 2.20** Synthesis of model compound **109**.



The same cross-coupling reaction to obtain precursor **72** to form large, conjugated macrocycles was carried out using 4-ethynylsalicylaldehyde, **110** (Scheme 2.21).

**Scheme 2.21** Synthesis of diol **72**.



The  $^1\text{H}$  NMR spectrum of diol **72** is shown in Figure 2.12. The signal for the ethynyl proton is absent, while the aromatic resonances from the protons of the salicylaldehyde remain, confirming that the starting material reacted quantitatively with the phenanthrene. Additionally, only one set of aromatic resonances for the phenanthrene is present, indicating the reaction produced only the desired disubstituted product.

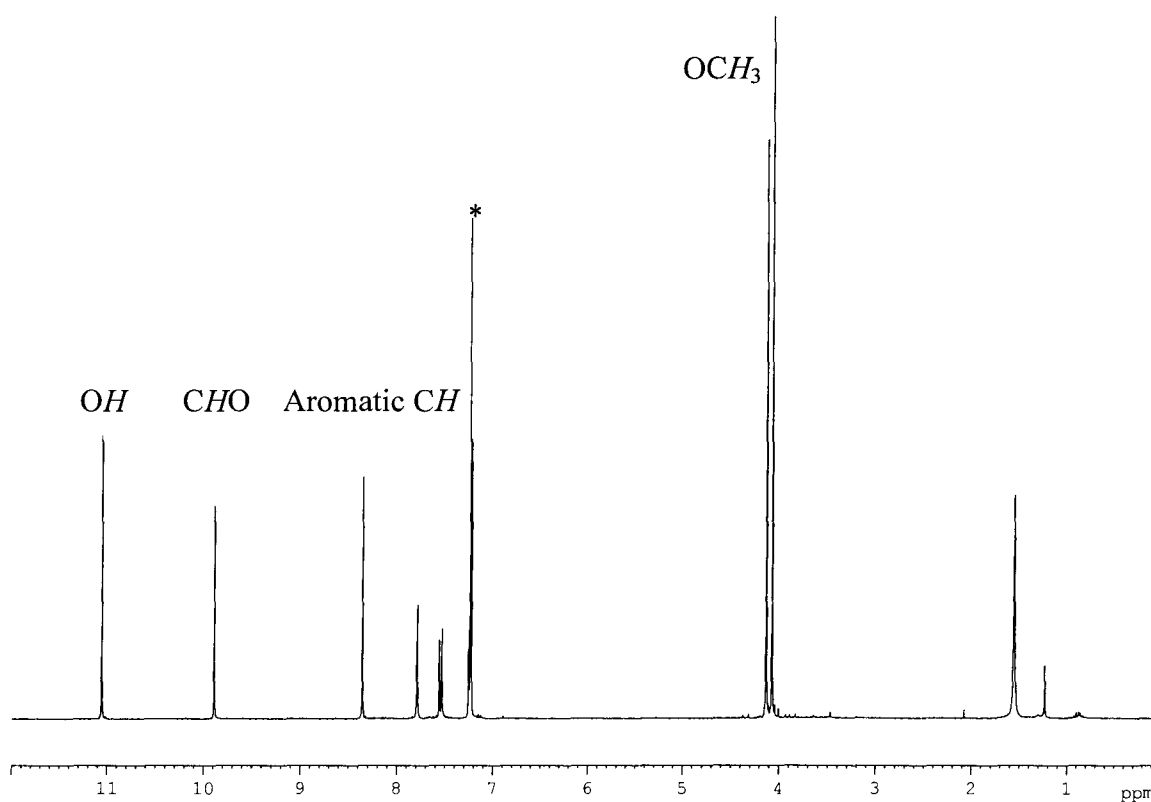


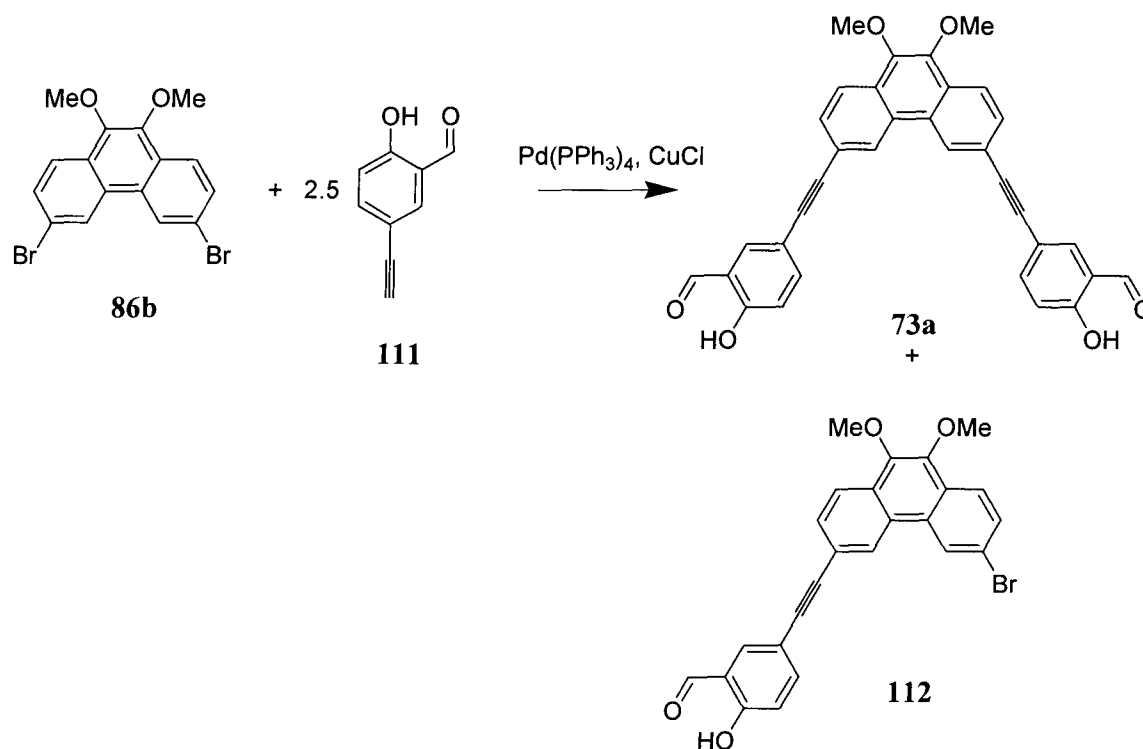
**Figure 2.12**  $^1\text{H}$  NMR (300 MHz,  $\text{CDCl}_3$ ) spectrum of diol **72** (\* =  $\text{CDCl}_3$ ).

Both diol **72** and model compound **109** are fluorescent, a result of the phenanthrene fluorophore, although the diol is markedly less so. This property will be discussed more in depth in later chapters.

### 2.2.5 Synthesis of Precursor 73

A similar compound, precursor **73**, can be used to synthesize macrocycle **75**, which will be discussed in Chapters 3 and 4. 5-Ethynylsalicylaldehyde (**111**) was initially reacted with **86b** using Sonogashira-Hagihara conditions (Scheme 2.22) in a convergent method, like the synthesis of **72**. A mixture of products was observed in the  $^1\text{H}$  NMR spectrum of the crude product. Two products were isolated via column chromatography and it was found that only a small yield of each mono and disubstituted products (**112** and **73a**, respectively) was obtained. It appears that the salicylate functionalities may compromise the reaction.

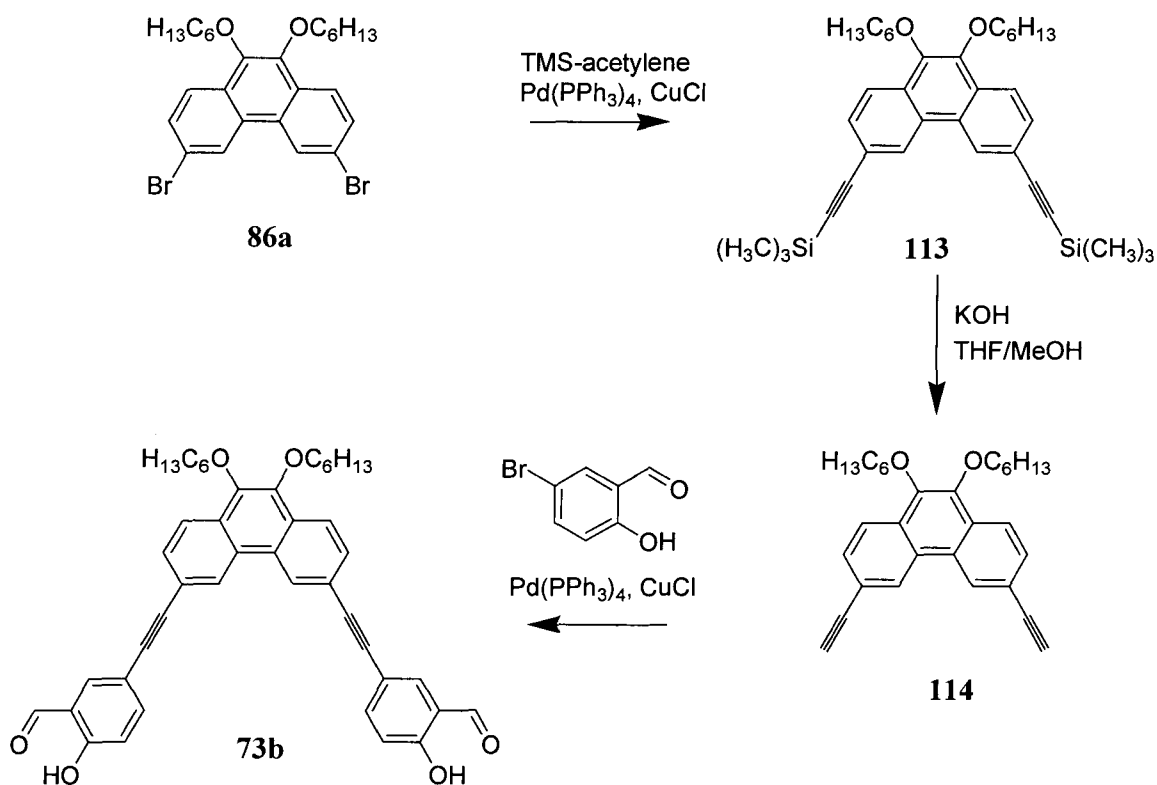
**Scheme 2.22** Initial synthesis of **73a**.



An alternative route to synthesize precursor **73** used a more divergent synthetic pathway (Scheme 2.23). Compound **86a** was reacted with TMS-acetylene using a

Sonogashira-Hagihara coupling to form **113**, a viscous oil which eventually crystallized into fine needles. Compound **113** was then deprotected using KOH in methanol and THF to afford **114**. While these reactions are straightforward, and give high yields (92% for **113** and 88% for **114**), rigorous purification is needed between each step for optimal results. In addition, it is sometimes necessary to perform several columns to successfully remove the impurities between each synthetic step. A second Sonogashira coupling was performed using **114** and 5-bromosalicylaldehyde to make precursor **73b**. After chromatography, this compound was recrystallized from ethanol to obtain a pure compound.

**Scheme 2.23** Synthesis of **113**, **114** and **73b**.



The  $^1\text{H}$  NMR spectrum of **73b** is shown in Figure 2.13. Absence of an ethynyl resonance as well as 1:1 integration of the formyl and hydroxyl resonances to the phenanthrene peaks indicates that the reaction of the phenanthrene with the salicylaldehyde went to completion. Both the phenanthrene and salicylaldehyde resonances are split through either *ortho* or *meta* coupling, and can be distinguished using the coupling constants.

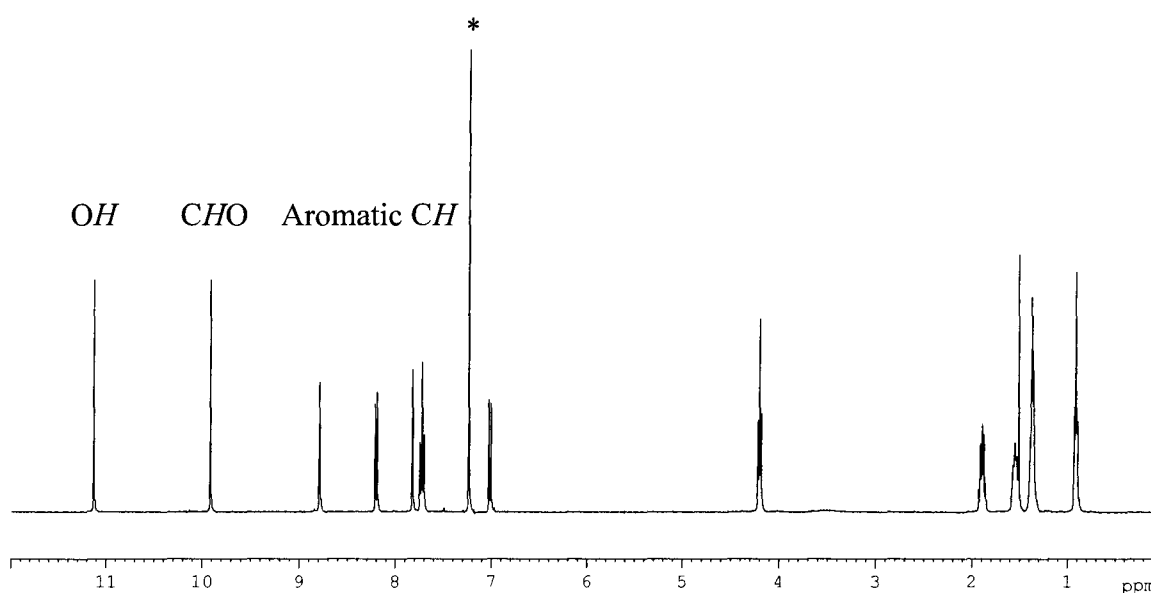


**Figure 2.13**  $^1\text{H}$  NMR (400 MHz,  $\text{CDCl}_3$ ) spectrum of diol **73b** (\* =  $\text{CDCl}_3$ ).

## 2.2.6 Conclusions

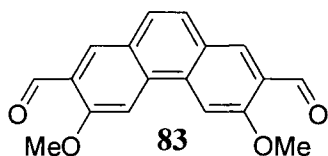
This chapter discussed our syntheses of new phenanthrene and triphenylene precursors **70-73** for Schiff base condensation of [3+3] macrocycles, which is discussed in Chapter 3. Difficulties in the syntheses arose from the stability of the 9,10-phenanthrenequinone over the 9,10-dialkoxyphenanthrene. Fortunately, we found a series of reactions to form **107**, a useful precursor for Pd-catalyzed couplings.

## 2.3 Experimental

### 2.3.1 General Methods and Materials

THF was distilled over Na and benzophenone under N<sub>2</sub>. Triethylamine and diisopropylamine were dried over NaOH or KOH and distilled under N<sub>2</sub>. Compounds **83**,<sup>21</sup> **85**,<sup>11</sup> **102**,<sup>29</sup> **110**<sup>30</sup> and **111**,<sup>31</sup> as well as 4-methoxyphenylboronic acid,<sup>32</sup> were prepared according to literature procedures. Tetrakis(triphenylphosphine)palladium(0) and bis(triphenylphosphine)palladium(II)dichloride were obtained from Strem Chemicals, Inc. Deuterated solvents were obtained from Cambridge Isotope Laboratories, Inc. All other chemicals were purchased from Aldrich or Fisher and used as received. All reactions were carried out under nitrogen unless otherwise noted. <sup>1</sup>H NMR (300 or 400 MHz) and <sup>13</sup>C NMR (75.5 or 100.7 MHz) spectra were recorded on Bruker Avance 300 or Bruker Avance 400 spectrometers and were referenced internally to residual protonated solvent. Infrared spectra were obtained as KBr discs or on NaCl plates with a Bomem MB-100 spectrometer or a Nicolet 4700 FTIR spectrometer. UV-Vis spectra were obtained in HPLC grade DCM, distilled THF or DMSO on a Varian Cary 5000 UV-Vis/near IR spectrometer using a 1 cm cuvette. Fluorescence spectra were obtained in CH<sub>2</sub>Cl<sub>2</sub> on a PTI QuantaMaster fluorimeter using a 1 cm quartz cuvette. Electron impact (EI), electrospray ionization (ESI) and matrix-assisted laser desorption ionization time of flight (MALDI-TOF) mass spectra were obtained in the UBC Mass Spectrometry facility. Elemental analyses were obtained at the UBC Microanalytical facility. Melting points were obtained on a Fisher John's melting point apparatus.

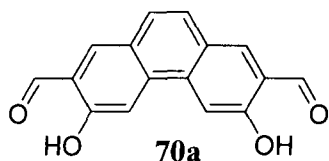
### 2.3.2 Synthetic Procedures



#### Synthesis of 2,7-diformyl-3,6-dimethoxyphenanthrene

**(83)** – 3,6-Dimethoxyphenanthrene **82** (0.718 g, 3.01 mmol) was dissolved in 20 mL THF. <sup>n</sup>BuLi (6.1 mL, 1.6 M in hexanes) was added and the solution was stirred for 30 min, after which anhydrous DMF (0.77 mL, 9.98 mmol) was added. The reaction solution was poured into aqueous HCl and extracted with DCM. After drying over MgSO<sub>4</sub>, the solvent was removed by rotary evaporation to reveal an orange solid. The product was chromatographed over silica with DCM and recrystallized from DCM to obtain 0.150 g (0.51 mmol) of yellow solid (17% yield).

**Data for 83.** <sup>1</sup>H NMR (300 MHz, CDCl<sub>3</sub>) δ 10.63 (s, 2H, CHO), 8.36 (s, 2H, aromatic CH), 7.92 (s, 2H, aromatic CH), 7.65 (s, 2H, aromatic CH), 4.17 (s, 6H, OCH<sub>3</sub>); <sup>13</sup>C NMR (75.5 MHz, CDCl<sub>3</sub>) δ 189.7, 159.0, 134.3, 130.6, 127.3, 126.1, 126.0, 103.8, 55.9; ESI-MS: *m/z* = 295 ([M+H]<sup>+</sup>); IR (KBr): ν = 2947, 2862, 1681, 1615, 1502, 1457, 1406, 1369, 1265, 1220, 1181, 1136, 1109, 1017, 970, 842, 655 cm<sup>-1</sup>; UV-Vis (CH<sub>2</sub>Cl<sub>2</sub>): λ<sub>max</sub> (ε) = 281 (5.6 × 10<sup>4</sup>), 338 (2.5 × 10<sup>4</sup>), 440 (2.2 × 10<sup>3</sup>) nm (L mol<sup>-1</sup>cm<sup>-1</sup>); Mp. ~ 280 °C (dec.); Anal. Calc'd for C<sub>18</sub>H<sub>14</sub>O<sub>4</sub>·0.5H<sub>2</sub>O: C, 71.28, H, 4.98. Found C, 71.35, H, 4.80.

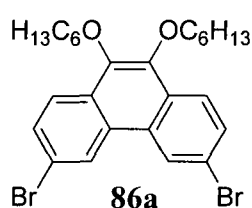


#### Synthesis of 2,7-diformyl-3,6-dihydroxyphenanthrene

**(70a)** – To an ice-cooled solution of compound **83** (0.413 g, 1.40 mmol) in DCM was added BBr<sub>3</sub> (1 mL, 10.6 mmol). After stirring overnight, the solution was poured into 200 mL of ice water to obtain an orange solid. The solid was filtered and the remaining aqueous solution was extracted

with DCM. The organic layer was dried and combined with the solid. After flashing the product through silica with DCM, 0.268 g (1.01 mmol) of orange crystals were obtained (72% yield).

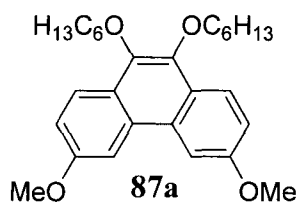
**Data for 70a.**  $^1\text{H}$  NMR (300 MHz, DMSO- $d_6$ )  $\delta$  10.96 (s, 2H, OH), 10.46 (s, 2H, CHO), 8.29 (s, 2H, aromatic CH), 7.99 (s, 2H, aromatic CH), 7.67 (s, 2H, aromatic CH);  $^{13}\text{C}$  NMR (75.5 MHz, DMSO- $d_6$ )  $\delta$  191.3, 157.6, 134.0, 130.6, 125.9, 125.1, 124.2, 109.2; EI-MS:  $m/z$  = 266 ( $M^+$ ); IR (KBr):  $\nu$  = 3449, 3253, 3017, 2884, 1652, 1530, 1338, 1205, 1157, 1106, 899  $\text{cm}^{-1}$ ; UV-Vis ( $\text{CH}_2\text{Cl}_2$ ):  $\lambda_{\text{max}}$  ( $\epsilon$ ) = 284, 304, 326, 465 nm; Mp. > 300  $^\circ\text{C}$ ; Anal. Calc'd for  $\text{C}_{16}\text{H}_{10}\text{O}_4$ : C, 72.18, H, 3.79. Found C, 72.05, H, 4.00.



**Synthesis of 3,6-dibromo-9,10-dihexyloxyphenanthrene (86a) –**

3,6-dibromophenanthrene-9,10-quinone **85** (6.557 g, 17.9 mmol) was dissolved in 50 mL DMF and degassed with  $\text{N}_2$  for 5 min.  $\text{Na}_2\text{S}_2\text{O}_4$  (10.105 g, 58.0 mmol) was added to the solution and stirred for 15 min, after which  $\text{K}_2\text{CO}_3$  (8.30 g, 60.1 mmol),  $\text{Bu}_4\text{NBr}$  (0.100 g, 0.310 mmol), and 1-bromohexane (9 mL, 64.0 mmol) were added. The solution was heated for 16 h at 80  $^\circ\text{C}$ . After cooling, the yellow solution was poured into  $\text{H}_2\text{O}$  and extracted with EtOAc (3 x 125 mL). The organic layer was dried with  $\text{MgSO}_4$ , filtered and dried under vacuum. Chromatography on silica with 1:4 DCM/hexanes afforded a colourless oil which was recrystallized from EtOH and DCM to give white crystals. Yield: 4.572 g, 8.52 mmol, 48%

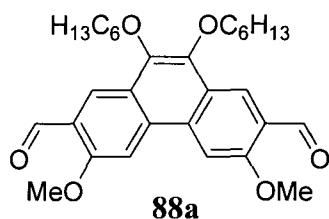
**Data for 86a.**  $^1\text{H}$  NMR (300 MHz,  $\text{CDCl}_3$ )  $\delta$  8.62 (d, 2H,  $J = 1.7$  Hz, aromatic CH), 8.07 (d, 2H,  $J = 8.8$  Hz, aromatic CH), 7.68 (dd, 2H,  $J_1 = 8.8$  Hz,  $J_2 = 1.7$  Hz, aromatic CH), 4.16 (t, 4H,  $\text{OCH}_2$ ), 1.91-0.88 (m, 22H, hexyl chain);  $^{13}\text{C}$  NMR (100.7 MHz,  $\text{CDCl}_3$ )  $\delta$  143.4, 130.7, 129.1, 129.0, 125.6, 124.4, 120.5, 74.0, 31.9, 30.6, 26.1, 22.9, 14.3; EI-MS:  $m/z = 536$  ( $\text{M}^+$ ); IR (KBr):  $\nu = 2954, 2923, 2869, 1619, 1590, 1468, 1381, 1343, 1312, 1171, 1122, 1073, 1056, 870, 821$   $\text{cm}^{-1}$ ; UV-Vis ( $\text{CH}_2\text{Cl}_2$ ):  $\lambda_{\text{max}}$  ( $\epsilon$ ) = 253 ( $5.0 \times 10^4$ ), 261 ( $5.6 \times 10^4$ ), 283 ( $1.9 \times 10^4$ ), 304 ( $1.3 \times 10^4$ ), 316 ( $1.4 \times 10^4$ ) nm ( $\text{L mol}^{-1}\text{cm}^{-1}$ ); Mp. = 54-56  $^\circ\text{C}$ ; Anal. Calc'd for  $\text{C}_{26}\text{H}_{32}\text{O}_2\text{Br}_2$ : C, 58.22, H, 6.01. Found C, 58.62, H, 6.24.



**Synthesis of 9,10-dihexyloxy-3,6-dimethoxyphenanthrene**

**(87a)** - EtOAc (1 mL) and toluene (1 mL) were added to **86a** (0.627 g, 1.17 mmol), under  $\text{N}_2$ . To this mixture was added NaOMe/MeOH (25 wt%, 17 mL) and CuBr (0.087 g, 0.606 mmol). The mixture was heated to 80  $^\circ\text{C}$  for 16 h. After cooling to room temperature, the solution was poured into 75 mL water and extracted with DCM (3 x 75 mL), dried over  $\text{MgSO}_4$ , and filtered. Rotary evaporation of the solution gave a brown oil which was passed through silica in 1:1 hexanes/DCM to afford 0.476 g (1.08 mmol, 93%) of a pale yellow oil.

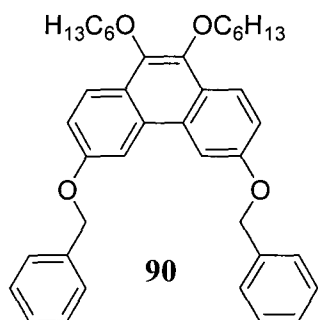
**Data for 87a.**  $^1\text{H}$  NMR (300 MHz,  $\text{CDCl}_3$ )  $\delta$  8.13 (d, 2H,  $J = 9.0$  Hz, aromatic CH), 7.89 (d, 2H,  $J = 2.4$  Hz, aromatic CH), 7.24 (dd, 2H,  $J_1 = 9.0$  Hz,  $J_2 = 2.4$  Hz, aromatic CH), 4.15 (t, 4H,  $\text{OCH}_2$ ), 3.99 (s, 6H,  $\text{OCH}_3$ ) 1.91-0.87 (m, 22H, hexyl chain);  $^{13}\text{C}$  NMR (75.5 MHz,  $\text{CDCl}_3$ )  $\delta$  157.8, 141.8, 129.4, 124.8, 124.2, 116.6, 104.9, 73.9, 55.8, 32.0, 30.7, 26.2, 22.9, 14.3; EI-MS:  $m/z = 438$  ( $\text{M}^+$ ); High Res. MS Calc'd for  $\text{C}_{28}\text{H}_{38}\text{O}_4$ : 438.27701. Found: 438.27581.



**Synthesis of 2,7-diformyl-9,10-dihexyloxy-3,6-dimethoxyphenanthrene (88a)** – Compound **87a** (0.627 g, 1.43 mmol) was dissolved in 20 mL THF.  $n$ BuLi (3.2 mL, 1.6 M in hexanes) was added and the solution was allowed to stir

for 30 min, after which anhydrous DMF (0.7 mL, 8.8 mmol) was added. The reaction solution was poured into aqueous HCl and extracted with DCM. After drying over  $MgSO_4$ , the solvent was removed by rotary evaporation to reveal an orange solid. The product was chromatographed over silica with DCM resulting in 0.040 g (0.09 mmol, 6% yield). Starting material and the monoformylated product were also isolated in different fractions.

**Data for 88a.**  $^1H$  NMR (400 MHz,  $CDCl_3$ )  $\delta$  10.63 (s, 2H, CHO), 8.71 (s, 2H, aromatic CH), 7.88 (s, 2H, aromatic CH), 4.17 (t, 4H,  $OCH_2$ ), 4.16 (s, 6H,  $OCH_3$ ), 1.94-0.92 (m, 22H, hexyl chain);  $^{13}C$  NMR (100.7 MHz,  $CDCl_3$ )  $\delta$  190.0, 158.6, 142.7, 132.5, 126.2, 125.8, 125.6, 104.3, 74.2, 56.2, 32.0, 30.5, 26.1, 22.9, 14.3; EI-MS:  $m/z$  = 494 ( $M^+$ ); IR (KBr):  $\nu$  = 2959, 2927, 2868, 1687, 1615, 1445, 1365, 1272, 1243, 1208, 1139, 1001, 913, 844, 608  $cm^{-1}$ ; UV-Vis ( $CH_2Cl_2$ ):  $\lambda_{max}$  ( $\epsilon$ ) = 288 ( $5.1 \times 10^4$ ), 342 ( $2.0 \times 10^4$ ) nm ( $L \text{ mol}^{-1} \text{ cm}^{-1}$ ); Mp. = 132-135  $^{\circ}C$ ; High Res. MS Calc'd for  $C_{30}H_{38}O_6$ : 494.26684. Found: 494.26616.

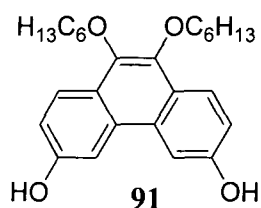


### Synthesis of 3,6-dibenzylxy-9,10-dihexyloxyphenanthrene

**(90)** – To a Schlenk flask was added 30 mL dried, distilled benzyl alcohol. NaH (1.340 g, 55.8 mmol) was added and stirred until bubbling stopped, after which **86a** (0.997 g, 1.82 mmol), CuBr (0.088 g, 0.613 mmol), EtOAc (1 mL) and

toluene (1 mL) were added. The reaction mixture was heated to 87 °C for 16 h. Dilution with water was followed by extraction with DCM. The organic layer was dried over MgSO<sub>4</sub>, filtered and the solvent was removed under vacuum. The residue was chromatographed with 3:1 hexanes/DCM to recover 0.927 g (1.57 mmol, 86% yield) of a colourless oil.

**Data for 90.** <sup>1</sup>H NMR (300 MHz, CDCl<sub>3</sub>) δ 8.12 (d, 2H, *J* = 9.0 Hz, aromatic *CH*), 7.92 (d, 2H, *J* = 2.3 Hz, aromatic *CH*), 7.52-7.27 (m, 12H, aromatic *CH*), 5.24 (s, 2H, benzyl OCH<sub>2</sub>), 4.16 (t, 4H, OCH<sub>2</sub>), 1.90-0.88 (m, 22H, hexyl chain); <sup>13</sup>C NMR (100.7 MHz, CDCl<sub>3</sub>) δ 157.1, 141.9, 137.3, 129.4, 128.9, 128.3, 127.81, 124.9, 124.2, 117.4, 106.2, 73.9, 70.7, 32.0, 30.7, 26.2, 22.9, 14.3; EI-MS: *m/z* = 590 (M<sup>+</sup>); High Res. MS Calc'd for C<sub>40</sub>H<sub>46</sub>O<sub>4</sub>: 590.33961. Found: 590.33806.



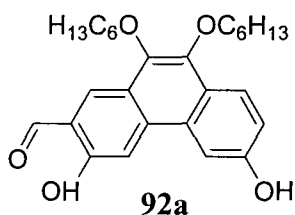
### Synthesis of 9,10-dihexyloxy-3,6-dihydroxyphenanthrene (**91**) -

Compound **90** (0.296 g, 0.501 mmol) was placed in a Schlenk flask and EtOH (10 mL) was added. To the mixture was added Pd/C (0.100 g), and hydrazine (1.2 mL, 24.6 mmol), which gave a grey and bubbly mixture. The mixture was heated for 16 h. While monitoring the reaction by TLC, additional hydrazine or catalyst was added to the flask as needed. Filtration through celite

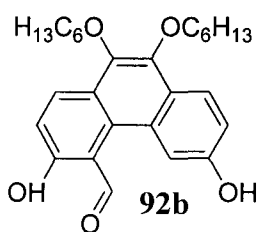
followed by precipitation with water gave a pale brown solid. Yield: 0.163 g, 0.401 mmol, 80%.

**Data for 91.**  $^1\text{H}$  NMR (400 MHz,  $\text{CD}_3\text{OD}$ )  $\delta$  7.98 (d, 2H,  $J = 8.8$  Hz, aromatic  $\text{CH}$ ), 7.84 (d, 2H,  $J = 2.3$  Hz, aromatic  $\text{CH}$ ), 7.12 (dd, 2H,  $J_1 = 8.8$  Hz,  $J_2 = 2.3$  Hz, aromatic  $\text{CH}$ ), 4.11 (t, 4H,  $\text{OCH}_2$ ), 1.90-0.90 (m, 22H, hexyl chain);  $^{13}\text{C}$  NMR (100.7 MHz,  $\text{CD}_3\text{OD}$ )  $\delta$  156.8, 142.5, 131.0, 124.9, 124.8, 118.2, 107.9, 74.7, 33.1, 31.7, 27.3, 23.9, 14.6; EI-MS:  $m/z = 410$  ( $\text{M}^+$ ); IR (KBr):  $\nu = 3385, 3224, 2955, 2927, 2855, 1606, 1510, 1438, 1356, 1229, 1115, 1072, 1052, 862, 814$   $\text{cm}^{-1}$ ; UV-Vis ( $\text{CH}_2\text{Cl}_2$ ):  $\lambda_{\text{max}}$  ( $\epsilon$ ) = 252 ( $4.4 \times 10^4$ ), 290 ( $1.8 \times 10^4$ ) nm ( $\text{L mol}^{-1}\text{cm}^{-1}$ ); Mp. = 162-163  $^\circ\text{C}$ ; High Res. MS Calc'd for  $\text{C}_{26}\text{H}_{34}\text{O}_4$ : 410.24571. Found: 410.24506.

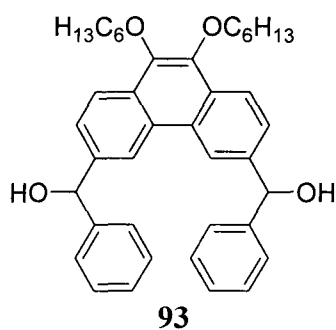
**Attempted synthesis of 2,7-diformyl-9,10-dihexyloxy-3,6-dihydroxyphenanthrene** - Compound **91** and anhydrous  $\text{MgCl}_2$  were placed in a Schlenk flask and dried under vacuum. Solvent (either dried MeCN or PhCN),  $\text{Et}_3\text{N}$  and paraformaldehyde were added and heated to various temperatures (80  $^\circ\text{C}$ , 100  $^\circ\text{C}$  or 115  $^\circ\text{C}$ ) for 16 h. The reaction solution was poured into aqueous HCl solution and extracted with DCM. Column chromatography with DCM as a solvent was used to purify recovered starting material. Additional fractions yielded monoformylated products **92a** and **92b**, which were inseparable.



**Data for 92a.**  $^1\text{H}$  NMR (300 MHz, DCM- $d_2$ )  $\delta$  10.58 (s, 1H, OH), 10.11 (s, 1H, CHO), 8.49 (s, 1H, aromatic CH), 8.11 (d, 1H, aromatic CH), 7.95 (s, 1H, aromatic CH), 7.90 (d, 1H, aromatic CH), 7.28 – underneath **92b** resonance (aromatic CH), 4.16 (q, 4H, overlapping inequivalent  $\text{OCH}_2$ ), 2.0-0.90 (m, 22H, hexyl chain); EI-MS:  $m/z = 438$  ( $\text{M}^+$ ); High Res. MS Calc'd for  $\text{C}_{27}\text{H}_{34}\text{O}_5$ : 438.24062. Found: 438.24180.



**Data for 92b.**  $^1\text{H}$  NMR (300 MHz, DCM- $d_2$ )  $\delta$  12.31 (s, 1H, OH), 10.47 (s, 1H, CHO), 8.41 (d, 1H, aromatic CH), 8.22 (d, 1H, aromatic CH), 7.43 (d, 1H, aromatic CH), 7.27 (dd, 1H, aromatic CH), 7.25 (d, 1H, aromatic CH), 4.16 (q, 4H, overlapping inequivalent  $\text{OCH}_2$ ), 2.0-0.90 (m, 22H, hexyl chain); EI-MS:  $m/z = 438$  ( $\text{M}^+$ ); High Res. MS Calc'd for  $\text{C}_{27}\text{H}_{34}\text{O}_5$ : 438.24062. Found: 438.24180.

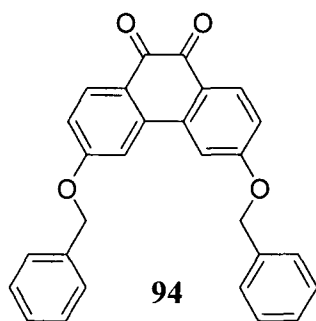


**Attempted synthesis of 3,6-dibenzyloxy-2,7-diformyl-9,10-dihexyloxyphenanthrene** – Compound **90** (0.240 g, 0.406 mmol) was dissolved in diethyl ether (18 mL) and TMEDA (1 mL) in a Schlenk flask under  $\text{N}_2$ .  $n\text{BuLi}$  (1.3 mL, 1.6 M in hexanes) was added to the flask, which caused the solution to initially turn orange then brown. After letting the solution stir overnight, DMF (0.5 mL, 6.48 mmol) was added. The reaction solution was poured into aqueous HCl and extracted with DCM. Residual solvent was removed under vacuum and the residue was

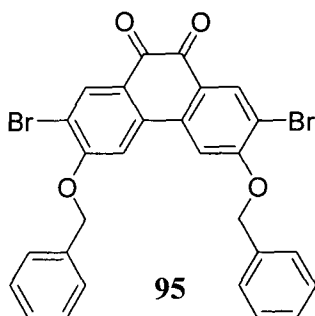
purified via column chromatography using DCM with an increasing percentage of acetone to yield compound **93** (0.038 g, 0.06 mmol, 16%).

**Data for 93.**  $^1\text{H}$  NMR (400 MHz,  $\text{CDCl}_3$ )  $\delta$  8.69 (d, 2H, aromatic *CH*), 8.15 (d, 2H, aromatic *CH*), 7.51 (d, 2H, aromatic *CH*), 7.42 (d, 4H, aromatic *CH*), 7.32 (dd, 4H, aromatic *CH*), 7.26 (d, 2H, aromatic *CH*), 6.06 (s, 2H, benzyl *H*), 4.15 (t, 4H,  $\text{OCH}_2$ ),  $\sim$ 2.5 (br s, 2H, *OH*), 1.9-0.85 (m, 22H, hexyl chain);  $^{13}\text{C}$  NMR (100.7 MHz,  $\text{CDCl}_3$ )  $\delta$  143.8, 143.2, 141.0, 129.2, 128.5, 128.4, 127.6, 126.7, 125.5, 122.8, 120.4, 120.3, 73.7, 31.7, 30.4, 25.9, 22.6, 14.0; EI-MS:  $m/z = 613$  ( $[\text{M} + \text{Na}]^+$ ).

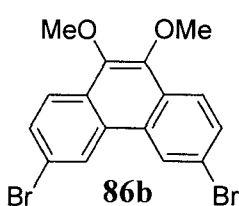
**Attempted Bromination of 3,6-dibenzoyloxy-9,10-dihexyloxyphenanthrene** – To a solution of compound **90** dissolved in MeCN, was added varying amounts of NBS (2.1, 4, 10 equivalents). The solution initially turned green, then orange. After stirring overnight, the solution was poured into water, and extracted with DCM. The organic layer was dried with  $\text{MgSO}_4$ , filtered and the solvent was removed by rotary evaporation. The isolated material contained both compounds **94** and **95**.



**Data for 94.**  $^1\text{H}$  NMR (400 MHz,  $\text{CDCl}_3$ )  $\delta$  8.16 (d, 2H, aromatic *CH*), 7.47-7.36 (m, 12H, aromatic *CH*), 6.98 (d, 2H, aromatic), 5.19 (s, 4H, benzyl  $\text{OCH}_2$ ); ESI-MS:  $m/z = 443$  ( $[\text{M} + \text{Na}]^+$ ).



**Data for 95.**  $^1\text{H}$  NMR (400 MHz,  $\text{CDCl}_3$ )  $\delta$  8.31 (s, 2H, aromatic CH), 7.51-7.37 (s, 10H, aromatic CH), 5.30 (s, 4H, benzyl  $\text{OCH}_2$ ); EI-MS:  $m/z = 578$  ( $\text{M}^+$ ).



**Synthesis of 3,6-dibromo-9,10-dimethoxyphenanthrene**

**(86b)** - Compound **85** (11.12 g, 30.3 mmol),  $\text{Bu}_4\text{NBr}$  (2.85 g, 8.82 mmol),  $\text{Na}_2\text{S}_2\text{O}_4$  (16.018 g, 91.9 mmol), THF (100 mL) and  $\text{H}_2\text{O}$  (100 mL) were combined in a separatory funnel and shaken for 5 min, after which dimethylsulfate (15 mL, 159 mmol) was added, followed by aqueous sodium hydroxide (30 mL, 14.1 M). The mixture was shaken for 3 min, during which time, 100 g of ice was added, then the mixture was shaken for 12 additional minutes. The aqueous layer was separated and extracted with EtOAc (3 x 150 mL), after which the combined organic layers were washed with water (3 x 100 mL),  $\text{NH}_4\text{OH}$  solution (2 x 100 mL) and brine (1 x 100 mL). The organic layer was dried with  $\text{MgSO}_4$ , filtered and the solvents were removed under vacuum, resulting in a fluffy yellow solid. Washing the product with MeOH gave a white solid. Additional impurities were removed by flashing the product through silica with a 1:1 mixture of hexanes and DCM. Yield: 10.86 g, 27.4 mmol, 90%.

**Data for 86b.**  $^1\text{H}$  NMR (400 MHz,  $\text{CDCl}_3$ )  $\delta$  8.63 (d, 2H,  $J = 1.8$  Hz, aromatic CH), 8.07 (d, 2H,  $J = 8.8$  Hz, aromatic CH), 7.70 (dd, 2H,  $J_1 = 8.8$  Hz,  $J_2 = 1.8$  Hz, aromatic CH), 4.05 (s, 6H,  $\text{OCH}_3$ );  $^{13}\text{C}$  NMR (75.5 MHz,  $\text{CDCl}_3$ )  $\delta$  144.0, 130.8, 129.1, 128.4, 125.6, 124.2, 120.7, 61.2; ESI-MS:  $m/z = 419$  ( $[\text{M}+\text{Na}]^+$ ); IR (KBr):  $\nu = 2964, 2934, 1619,$

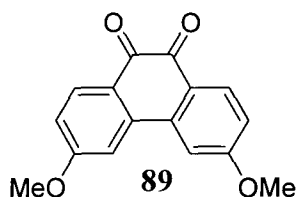
1589, 1483, 1424, 1347, 1313, 1121, 1094, 1066, 981, 868, 813  $\text{cm}^{-1}$ ; UV-Vis ( $\text{CH}_2\text{Cl}_2$ )  $\lambda_{\text{max}}(\epsilon) = 253 (4.9 \times 10^4), 260 (5.4 \times 10^4), 282 (1.8 \times 10^4), 302 (1.3 \times 10^4), 315 (1.4 \times 10^4)$  nm ( $\text{L mol}^{-1} \text{cm}^{-1}$ ); Mp. = 162-163  $^\circ\text{C}$ ; Anal. Calc'd for  $\text{C}_{16}\text{H}_{12}\text{O}_2\text{Br}_2$ : C, 48.52, H, 3.05. Found C, 48.39, H, 3.21.



#### Synthesis of 3,6,9,10-tetramethoxyphenanthrene (**87b**) -

EtOAc (1 mL) and toluene (1 mL) were added to **86b** (2.26 g, 5.71 mmol), under  $\text{N}_2$ . To this mixture was added NaOMe/MeOH (25 wt%, 50 mL) and CuBr (0.081 g, 0.571 mmol). The mixture was heated to 80  $^\circ\text{C}$  for 16 h. After cooling to room temperature, the solution was poured into 150 mL water and extracted with DCM (3 x 150 mL), dried over  $\text{MgSO}_4$ , and filtered. Rotary evaporation of the solution gave a brown oil which was passed through silica in 1:1 hexanes to DCM. Recrystallization of the product from EtOH afforded 1.66 g (5.58 mmol, 98%) of a white solid.

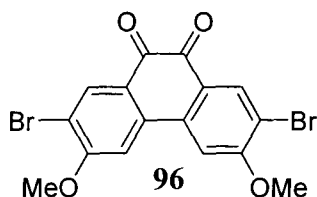
**Data for 87b.**  $^1\text{H}$  NMR (300 MHz,  $\text{CDCl}_3$ )  $\delta$  8.11 (d, 2H,  $J = 9.0$  Hz, aromatic CH), 7.89 (d, 2H,  $J = 2.5$  Hz, aromatic CH), 7.25 (dd, 2H,  $J_1 = 9.0$  Hz,  $J_2 = 2.5$  Hz, aromatic CH), 4.04 (s, 6H,  $\text{OCH}_3$ ), 3.99 (s, 6H,  $\text{OCH}_3$ );  $^{13}\text{C}$  NMR (75.5 MHz,  $\text{CDCl}_3$ )  $\delta$  157.9, 142.5, 129.5, 124.2, 124.0, 116.7, 104.9, 61.2, 55.8; ESI-MS:  $m/z = 321$  ( $[\text{M} + \text{Na}]^+$ ); IR (KBr):  $\nu = 2996, 2960, 2936, 2835, 1603, 1508, 1450, 1430, 1354, 1319, 1260, 1233, 1172, 1122, 1068, 1029, 986, 849, 832 \text{ cm}^{-1}$ ; UV-Vis ( $\text{CH}_2\text{Cl}_2$ )  $\lambda_{\text{max}}(\epsilon) = 252 (4.1 \times 10^4), 291 (1.7 \times 10^4), 313 (1.1 \times 10^4)$  nm ( $\text{L mol}^{-1} \text{cm}^{-1}$ ); Mp. = 74-76  $^\circ\text{C}$ ; Anal. Calc'd for  $\text{C}_{18}\text{H}_{18}\text{O}_4$ : C, 72.47; H, 6.08. Found: C, 72.18; H, 6.12.



### Synthesis of 3,6-dimethoxyphenanthrene-9,10-quinone (**89**) -

Compound **87b** (1.017 g, 3.4 mmol) was dissolved in MeCN (20 mL). A solution of ammonium cerium(IV) nitrate (3.73 g, 6.8 mmol) in MeCN (50 mL) was added, followed by 150 mL water. The solution was filtered and washed with water. Recrystallization from EtOH afforded 0.819 g (3.05 mmol, 90% yield) of a yellow solid.

**Data for 89.**  $^1\text{H}$  NMR (300 MHz,  $\text{CDCl}_3$ )  $\delta$  8.18 (d, 2H,  $J = 8.8$  Hz, aromatic CH), 7.37 (d, 2H,  $J = 2.4$  Hz, aromatic CH), 6.94 (dd, 2H,  $J_1 = 8.8$  Hz,  $J_2 = 2.4$  Hz, aromatic CH), 3.95 (s, 6H,  $\text{OCH}_3$ );  $^{13}\text{C}$  NMR (75.5 MHz,  $\text{CDCl}_3$ )  $\delta$  179.3, 166.0, 137.9, 133.6, 125.5, 114.6, 110.1, 56.1; ESI-MS:  $m/z = 291$  ( $[\text{M} + \text{Na}]^+$ ); IR (KBr):  $\nu = 3083, 2976, 2938, 2843, 1660, 1594, 1559, 1499, 1342, 1310, 1248, 1230, 1014, 864$   $\text{cm}^{-1}$ ; UV-Vis ( $\text{CH}_2\text{Cl}_2$ )  $\lambda_{\text{max}}$  ( $\epsilon$ ) = 238 ( $2.3 \times 10^4$ ), 284 ( $3.0 \times 10^4$ ), 347 ( $1.4 \times 10^4$ ) nm ( $\text{L mol}^{-1} \text{cm}^{-1}$ ); Mp. = 226-230  $^\circ\text{C}$ ; Anal. Calc'd for  $\text{C}_{16}\text{H}_{12}\text{O}_4$ : C, 71.64; H, 4.51. Found: C, 71.90, H, 4.77.

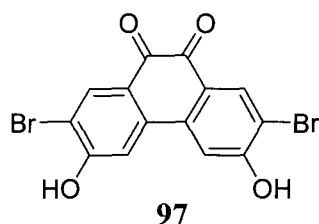


### Synthesis of 2,7-dibromo-3,6-dimethoxyphenanthrene-

**9,10-quinone (96)** – To a solution of 3,6-dimethoxy-9,10-phenanthrenequinone **89** (1.090 g, 4.06 mmol) in 25 mL each DCM and MeCN was added  $\text{Br}_2$  (1 mL, 19.5 mmol) and  $\text{FeCl}_3$  (1.317 g, 8.12 mmol). The solution was heated to reflux until an orange solid precipitated. After filtration of the solid, the filtrate was poured in  $\text{H}_2\text{O}$  and extracted with DCM. The solvent was removed under vacuum until further precipitation. Both solids were combined and recrystallized

from DCM to yield 1.298 g (3.05 mmol, 75%). The product was chromatographed on silica with DCM.

**Data for 96.**  $^1\text{H}$  NMR (300 MHz,  $\text{CDCl}_3$ )  $\delta$  8.33 (s, 2H, aromatic CH), 7.22 (s, 2H, aromatic CH), 4.11 (s, 6H,  $\text{OCH}_3$ );  $^{13}\text{C}$  NMR (100.7 MHz,  $\text{CDCl}_3$ )  $\delta$  177.7, 162.0, 136.5, 136.1, 125.9, 114.7, 105.9, 57.0; EI-MS:  $m/z = 426$  ( $\text{M}^+$ ); IR (KBr):  $\nu = 3448, 2946, 1670, 1578, 1545, 1436, 1333, 1312, 1274, 1262, 1203, 1040, 854, 696, 678$   $\text{cm}^{-1}$ ; UV-Vis ( $\text{CH}_2\text{Cl}_2$ ):  $\lambda_{\text{max}}$  ( $\epsilon$ ) = 247 ( $1.6 \times 10^4$ ), 297 ( $5.8 \times 10^4$ ), 344 ( $1.3 \times 10^4$ ) nm ( $\text{L mol}^{-1}\text{cm}^{-1}$ ); Mp.  $> 300$   $^\circ\text{C}$ ; Anal. Calc'd for  $\text{C}_{16}\text{H}_{10}\text{O}_4\text{Br}_2$ : C, 45.10, H, 2.37. Found C, 44.95, H, 2.66.

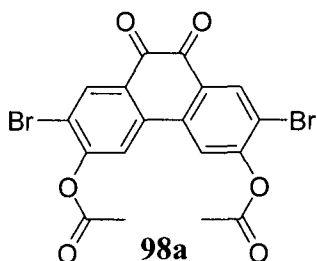


**Synthesis of 2,7-dibromo-3,6-dihydroxyphenanthrene-9,10-quinone (97)** – To an ice-cooled solution of **96** (0.957 g,

2.25 mmol) in DCM, 2.3 mL (24.3 mmol)  $\text{BBr}_3$  was added.

After stirring the solution overnight, it was poured onto ice to produce an orange solid. The solid was filtered and dried under vacuum. Yield: 0.662 g, 1.67 mmol, 74%.

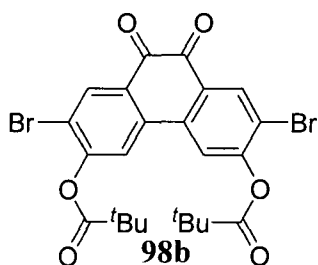
**Data for 97.**  $^1\text{H}$  NMR (300 MHz,  $\text{DMSO-d}_6$ )  $\delta$  11.97 (s, 2H, OH), 8.06 (s, 2H, aromatic CH), 7.43 (s, 2H, aromatic CH);  $^{13}\text{C}$  NMR (100.7 MHz,  $\text{DMSO-d}_6$ )  $\delta$  176.5, 160.6, 135.7, 134.6, 124.7, 111.3, 110.4; EI-MS:  $m/z = 398$  ( $\text{M}^+$ ); IR (KBr):  $\nu = 3461, 3192, 2509, 2364, 2259, 1658, 1580, 1443, 1329, 1190, 1061, 883, 814, 674$   $\text{cm}^{-1}$ ; UV-Vis ( $\text{CH}_2\text{Cl}_2$ ):  $\lambda_{\text{max}} = 294, 336$  nm; Mp.  $> 300$   $^\circ\text{C}$ ; High Res. MS Calc'd for  $\text{C}_{14}\text{H}_6\text{O}_4\text{Br}_2$ : 395.86328. Found: 395.86246.



**Synthesis of 3,6-diacetyl-2,7-dibromophenanthrene-9,10-quinone (98a)** – Compound **97** (0.488 g, 12.3 mmol) was dissolved in 9 mL acetic anhydride and heated to 80 °C overnight. The resulting brown solution was poured into water

and stirred. A yellow solid was filtered from the solution. Yield: 0.245 g, 0.508 mmol, 41%

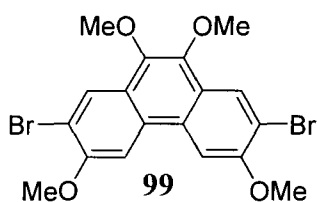
**Data for 98a.**  $^1\text{H}$  NMR (400 MHz,  $\text{CDCl}_3$ )  $\delta$  8.41 (s, 2H, aromatic CH), 7.65 (s, 2H, aromatic CH), 2.41 (s, 6H,  $\text{O}_2\text{CCH}_3$ );  $^{13}\text{C}$  NMR (100.7 MHz,  $\text{CDCl}_3$ )  $\delta$  178.2, 168.6, 155.5, 136.9, 136.1, 130.6, 120.6, 119.9, 21.8; EI-MS:  $m/z = 482$  ( $\text{M}^+$ ); IR (KBr):  $\nu = 3107, 3049, 2933, 1782, 1765, 1692, 1594, 1478, 1387, 1310, 1229, 1191, 1047, 1017, 917, 863, 730\text{ cm}^{-1}$ ; UV-Vis ( $\text{CH}_2\text{Cl}_2$ ):  $\lambda_{\text{max}}$  ( $\epsilon$ ) = 284 ( $5.1 \times 10^4$ ) nm ( $\text{L mol}^{-1}\text{cm}^{-1}$ ); Mp.  $\sim 275\text{ }^\circ\text{C}$  (dec.); High Res. MS Calc'd for  $\text{C}_{13}\text{H}_{10}\text{O}_6\text{Br}_2$ : 479.88441. Found: 479.88288.



**Synthesis of 3,6-di(pivaloyl)-dibromophenanthrene-9,10-quinone (98b)** - To a suspension of compound **97** (0.458 g, 1.15 mmol) in 20 mL THF was added pivaloyl chloride (5 mL, 41.6 mmol), then pyridine (3 mL, 37.2 mmol). A white precipitate formed as the reaction was stirred. After 2 h of stirring, the suspension was

poured into water and extracted with DCM. The organic layer was washed with aqueous  $\text{K}_2\text{CO}_3$ , dried with  $\text{MgSO}_4$ , filtered and the solvent was evaporated under vacuum. The solid was washed with petroleum ether and was filtered to give 0.200 g (0.36 mmol, 31% yield) of yellow product.

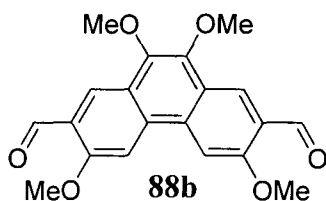
**Data for 98b.**  $^1\text{H}$  NMR (400 MHz,  $\text{CDCl}_3$ )  $\delta$  8.40 (s, 2H, aromatic CH), 7.61 (s, 2H, aromatic CH), 1.44 (s, 18H, t-butyl H);  $^{13}\text{C}$  NMR (100.7 MHz,  $\text{CDCl}_3$ )  $\delta$  177.5, 175.6, 155.1, 136.2, 135.3, 129.7, 119.9, 119.2, 39.9, 27.4; EI-MS:  $m/z = 266$  ( $\text{M}^+$ ); IR (KBr):  $\nu = 3100, 3071, 2973, 2935, 2877, 1766, 1689, 1590, 1473, 1386, 1306, 1220, 1090, 1043, 1030, 912, 692, 682$   $\text{cm}^{-1}$ ; UV-Vis ( $\text{CH}_2\text{Cl}_2$ ):  $\lambda_{\text{max}}$  ( $\epsilon$ ) = 284 ( $4.9 \times 10^4$ ) nm ( $\text{L mol}^{-1}\text{cm}^{-1}$ ); Mp.  $\sim 268$   $^\circ\text{C}$  (dec.); High Res. MS Calc'd for  $\text{C}_{24}\text{H}_{22}\text{O}_6\text{Br}_2$ : 563.97831. Found: 563.97891.



**Synthesis of 2,7-dibromo-3,6,9,10-tetramethoxy**

**phenanthrene (99)** – Compound **96** (0.567 g, 1.33 mmol),  $\text{Bu}_4\text{NBr}$  (0.113 g, 0.351 mmol),  $\text{Na}_2\text{S}_2\text{O}_4$  (0.610 g, 3.50 mmol), THF (50 mL) and  $\text{H}_2\text{O}$  (50 mL) were combined in a round-bottomed flask and stirred for 10 min, after which dimethylsulfate (3 mL, 31.7 mmol) was added, followed by aqueous sodium hydroxide (2 mL, 14 M). After stirring for 1 h, the aqueous layer was separated and extracted with EtOAc (3 x 50 mL). The combined organic layers were washed with water (3 x 50 mL),  $\text{NH}_4\text{OH}$  solution (2 x 50 mL) and brine (1 x 50 mL). The organic layer was dried with  $\text{MgSO}_4$ , filtered and the solvents were removed under vacuum, resulting in a brown solid. Washing the product with MeOH gave an orange solid. Additional impurities were removed by flashing the product through silica with a 1:1 mixture of hexanes/DCM, followed by recrystallization from DCM. Yield: 0.473 g, 1.0 mmol, 78%.

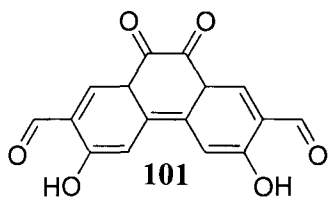
**Data for 99.**  $^1\text{H}$  NMR (400 MHz,  $\text{CDCl}_3$ )  $\delta$  8.38 (s, 2H, aromatic CH), 7.77 (s, 2H, aromatic CH), 4.09 (s, 6H,  $\text{OCH}_3$ ), 4.02 (s, 6H,  $\text{OCH}_3$ );  $^{13}\text{C}$  NMR (100.7 MHz,  $\text{CDCl}_3$ )  $\delta$  154.2, 142.1, 128.0, 127.5, 125.2, 114.1, 103.9, 61.3, 56.8; EI-MS:  $m/z$  = 456 ( $\text{M}^+$ ); IR (KBr):  $\nu$  = 3448, 2933, 1597, 1491, 1451, 1432, 1364, 1245, 1074, 1056, 993, 676  $\text{cm}^{-1}$ ; UV-Vis ( $\text{CH}_2\text{Cl}_2$ ):  $\lambda_{\text{max}}$  ( $\epsilon$ ) = 264 ( $5.3 \times 10^4$ ), 225 ( $3.8 \times 10^4$ ), 384 ( $1.0 \times 10^3$ ) nm ( $\text{L mol}^{-1} \text{cm}^{-1}$ ); Mp. = 217-218  $^\circ\text{C}$ ; Anal. Calc'd for  $\text{C}_{18}\text{H}_{16}\text{O}_4\text{Br}_2$ : C, 47.40, H, 3.54. Found C, 47.2, H, 3.66.



**Synthesis of 2,7-diformyl-3,6,9,10-tetramethoxyphenanthrene-9,10-quinone (88b)** – Compound **99** (0.373 g,

0.818 mmol) was dissolved in 18 mL THF and cooled to 0  $^\circ\text{C}$ . To the solution was added  $n\text{BuLi}$  (1.2 mL, 1.6 M in hexanes). After stirring for 10 min, DMF (0.3 mL, 3.87 mmol) was added. The solution was poured into acidified  $\text{H}_2\text{O}$  and extracted with DCM. Evaporation of the solvent gave a yellow solid (0.188 g, 0.531 mmol, 65% yield).

**Data for 88b.**  $^1\text{H}$  NMR (300 MHz,  $\text{CDCl}_3$ )  $\delta$  10.62 (s, 2H, CHO), 8.68 (s, 2H, aromatic CH), 7.68 (s, 2H, aromatic CH), 4.15 (s, 6H,  $\text{OCH}_3$ ), 4.05 (s, 6H,  $\text{OCH}_3$ );  $^{13}\text{C}$  NMR (75.5 MHz,  $\text{CDCl}_3$ )  $\delta$  190.0, 158.8, 143.3, 132.6, 126.3, 125.3, 104.3, 61.4, 56.2; EI-MS:  $m/z$  = 354 ( $\text{M}^+$ ); IR (KBr):  $\nu$  = 3448, 2935, 2858, 1686, 1610, 1491, 1452, 1429, 1358, 1278, 1249, 1205, 1145, 1128, 1014, 976, 570  $\text{cm}^{-1}$ ; UV-Vis ( $\text{CH}_2\text{Cl}_2$ ):  $\lambda_{\text{max}}$  ( $\epsilon$ ) = 287 ( $5.2 \times 10^4$ ), 342 ( $2.0 \times 10^4$ ), 448 ( $2.0 \times 10^3$ ) nm ( $\text{L mol}^{-1} \text{cm}^{-1}$ ); Mp.  $\sim$  294  $^\circ\text{C}$  (dec.); High Res. MS Calc'd for  $\text{C}_{20}\text{H}_{18}\text{O}_6$ : 354.11034. Found 354.11005.

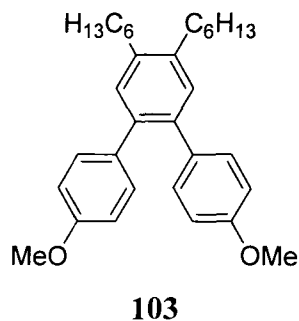


**Synthesis of 2,7-diformyl-3,6-dihydroxyphenanthrene-9,10-quinone (101) and unknown (100) - Compound 88b**

was dissolved in 10 mL dry DCM and cooled to 0 °C. To the solution was added BBr<sub>3</sub>. After stirring overnight, the dark solution was poured into H<sub>2</sub>O to precipitate a purple solid (**100/101**). After filtration, some of the solid was dissolved in THF to make an initially purple solution, which slowly became yellow. The solvent was removed to give a brown solid (**101**).

**Data for 101.** <sup>1</sup>H NMR (300 MHz, DMSO-d<sub>6</sub>) δ 12.12 (s, 2H, OH), 10.33 (s, 2H CHO), 8.34 (s, 2H, aromatic CH), 7.59 (s, 2H, aromatic CH); EI-MS: *m/z* = 296 (M<sup>+</sup>); IR (KBr):  $\nu$  = 3422, 2925, 2856, 1692, 1665, 1613, 1551, 1361, 1320, 1252, 1197, 1154, 947, 789, 652 cm<sup>-1</sup>; UV-Vis (DMSO):  $\lambda_{\text{max}}$  = 314 nm; Mp. > 300 °C; High Res. MS Calc'd for C<sub>16</sub>H<sub>8</sub>O<sub>6</sub>: 296.03209. Found 296.03142.

**Data for 100.** <sup>1</sup>H NMR (300 MHz, DMSO-d<sub>6</sub>) δ 12.15 (s, 1H, OH), 10.67 (s, 1H, OH), 10.46 (s, 1H CHO), 10.32 (s, 1H CHO), 8.45 (s, 2H, aromatic CH), 8.33 (s, 2H, aromatic CH), 7.92 (s, 2H, aromatic CH), 7.58 (s, 2H, aromatic CH).

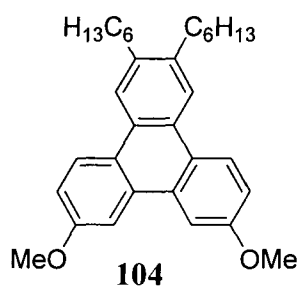


**Synthesis of 4',5'-dihexyl-4,4''-dimethoxy-1,1':2',1''-terphenyl (103)**

– A mixture of 1,2-dibromo-4,5-dihexylbenzene **102** (1.049 g, 2.59 mmol), 4-methoxyphenylboronic acid (0.971 g, 6.39 mmol), sodium carbonate (0.971 g, 9.16 mmol), and tetrakis(triphenylphosphine)palladium (0.050 g, 0.043 mmol) was stirred under reflux in

a mixture of toluene (18 mL), EtOH (18 mL) and water (6 mL) for 4 h. The solution was poured in water and extracted with DCM (3 x 100 mL). After drying with MgSO<sub>4</sub> and evaporating the solvent, a brown oil was obtained and purified by chromatography in 3:1 hexanes/DCM. Additional impurities were recrystallized out from EtOH. The product was a colourless oil. Yield: 0.732 g, 1.60 mmol, 62%.

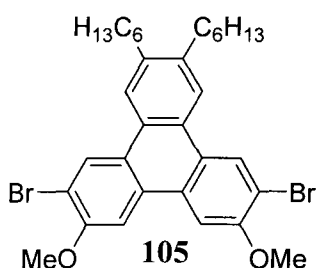
**Data for 103.** <sup>1</sup>H NMR (400 MHz, CDCl<sub>3</sub>) δ 7.14 (s, 2H, aromatic CH), 7.06 (d, 4H, *J* = 8.7 Hz, aromatic CH), 7.74 (d, 4H, *J* = 8.7 Hz, aromatic CH), 3.76 (s, 6H, OCH<sub>3</sub>), 2.64 (m, 4H, CH<sub>2</sub>), 1.62 (m, 4H, hexyl chain), 1.41 (m, 4H, hexyl chain), 1.33 (m, 8H, hexyl chain), 0.89 (t, 6H, hexyl CH<sub>3</sub>); <sup>13</sup>C NMR (100.7 MHz, CDCl<sub>3</sub>) δ 158.3, 139.8, 137.5, 134.5, 131.5, 131.1, 113.5, 55.4, 32.7, 32.0, 31.6, 29.8, 22.9, 14.3; EI-MS: *m/z* = 458 (M<sup>+</sup>); IR (KBr): ν = 2955, 2928, 2855, 1608, 1512, 1490, 1467, 1290, 1245, 1107, 1033, 831 cm<sup>-1</sup>; UV-Vis (CH<sub>2</sub>Cl<sub>2</sub>): λ<sub>max</sub> (ε) = 251 (4.7 x 10<sup>4</sup>) nm (L mol<sup>-1</sup>cm<sup>-1</sup>); High Res. MS Calc'd for C<sub>32</sub>H<sub>42</sub>O<sub>2</sub>: 458.31848. Found: 458.31810.



**Synthesis of 2,3-dihexyl-7,10-dimethoxytriphenylene (104) –**

Compound **103** (0.778 g, 1.69 mmol) and iodine (0.667 g, 2.6 mmol) were dissolved in 250 mL dry toluene. The solution was poured into a quartz flask and irradiated with UV light (253.7 nm) for 72 h in a Rayonet photochemical reactor. Excess iodine was removed by washing the solution with aq. Na<sub>2</sub>SO<sub>3</sub> and the resulting organic layer was dried with MgSO<sub>4</sub> and the solvent was removed under vacuum. Recrystallization of the product from EtOH afforded 0.098 g (0.215 mmol, 66% yield) of off-white crystals, and 0.629 g of terphenyl **103** was recovered and reused in subsequent reactions.

**Data for 104.**  $^1\text{H}$  NMR (400 MHz,  $\text{CDCl}_3$ )  $\delta$  8.52 (d, 2H,  $J = 9.1$  Hz, aromatic CH), 8.24 (s, 2H, aromatic CH), 7.92 (d, 2H,  $J = 2.5$  Hz, aromatic CH), 7.23 (dd, 2H,  $J_1 = 9.1$  Hz,  $J_2 = 2.5$  Hz, aromatic CH), 4.00 (s, 6H,  $\text{OCH}_3$ ), 2.80 (m, 4H,  $\text{CH}_2$ ), 1.71 (m, 4H, hexyl chain), 1.50 (m, 4H, hexyl chain), 1.24 (m, 8H, hexyl chain), 0.92 (t, 6H, hexyl  $\text{CH}_3$ );  $^{13}\text{C}$  NMR (100.7 MHz,  $\text{CDCl}_3$ )  $\delta$  158.6, 139.6, 130.8, 127.1, 125.0, 124.5, 123.1, 115.6, 106.3, 55.7, 33.4, 32.1, 31.8, 29.8, 22.9, 14.4; EI-MS:  $m/z = 456$  ( $\text{M}^+$ ); IR (KBr):  $\nu = 2953, 2926, 2852, 1619, 1508, 1464, 1416, 1367, 1231, 1203, 1178, 1050, 1027, 835, 812$   $\text{cm}^{-1}$ ; UV-Vis ( $\text{CH}_2\text{Cl}_2$ ):  $\lambda_{\text{max}}$  ( $\epsilon$ ) = 262 ( $9.3 \times 10^4$ ), 271 ( $1.2 \times 10^5$ ) nm ( $\text{L mol}^{-1}\text{cm}^{-1}$ ); Mp. = 73-75  $^\circ\text{C}$ ; Anal. Calc'd for  $\text{C}_{32}\text{H}_{40}\text{O}_2$ : C, 84.16, H, 8.83. Found: C, 84.32, H, 8.61.



**Synthesis of 6,11-dibromo-2,3-dihexyl-7,10-**

**dimethoxytriphenylene (105)** – To an ice-cooled solution of

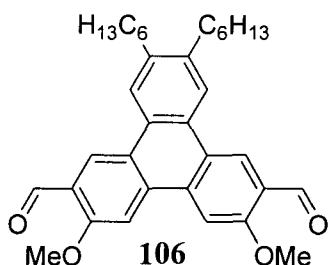
**104** (0.532 g, 1.16 mmol) in DCM (20 mL), bromine (0.1 mL,

1.9 mmol) was added dropwise. The solution was stirred for 2

h. After washing with aq.  $\text{Na}_2\text{SO}_3$ , the organic layer was dried with  $\text{MgSO}_4$  and the solvent was removed under vacuum. Recrystallization from EtOH and DCM afforded white fibrous crystals. Yield: 0.563 g, 0.916 mmol, 79%.

**Data for 105.**  $^1\text{H}$  NMR (400 MHz,  $\text{CDCl}_3$ )  $\delta$  8.71 (s, 2H, aromatic CH), 8.13 (s, 2H, aromatic CH), 7.76 (s, 2H, aromatic CH), 4.11 (s, 6H,  $\text{OCH}_3$ ), 2.81 (m, 4H,  $\text{CH}_2$ ), 1.70 (m, 4H, hexyl chain), 1.47 (m, 4H, hexyl chain), 1.34 (m, 8H, hexyl chain), 0.91 (t, 6H, hexyl  $\text{CH}_3$ );  $^{13}\text{C}$  NMR (100.7 MHz,  $\text{CDCl}_3$ )  $\delta$  154.7, 140.7, 129.4, 128.6, 126.2, 125.7, 123.2, 114.0, 104.9, 56.7, 33.4, 32.0, 31.9, 29.8, 22.9, 14.4; EI-MS:  $m/z = 614$  ( $\text{M}^+$ ); IR

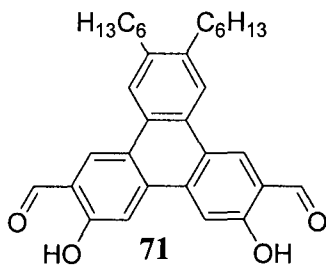
(KBr):  $\nu = 2956, 2926, 2853, 1600, 1494, 1464, 1401, 1252, 1201, 1059, 866, 830, 701$   $\text{cm}^{-1}$ ; UV-Vis ( $\text{CH}_2\text{Cl}_2$ ):  $\lambda_{\text{max}} (\epsilon) = 274 (1.6 \times 10^5) \text{ nm (L mol}^{-1}\text{cm}^{-1})$ ; Mp. = 166-168 °C; Anal. Calc'd for  $\text{C}_{32}\text{H}_{38}\text{O}_2\text{Br}_2$ : C, 62.55, H 6.23. Found: C, 62.70, H, 6.54.



**Synthesis of 6,11-diformyl-2,3-dihexyl-7,10-dimethoxytriphenylene (106)** – To a solution of **105** (0.795

g, 1.29 mmol) in dry THF (40 mL) cooled to -78 °C, 1.6 M  $n\text{BuLi}$  in hexanes (4 mL, 6.4 mmol) was added to produce a milky white solution. After 10 minutes, anhydrous DMF (0.8 mL, 10.3 mmol) was added to form a pale yellow solution. The solution was warmed to room temperature, then poured into aqueous HCl (1 M). Extraction with DCM, drying with  $\text{MgSO}_4$  and evaporation of the solvent afforded a brown oil. Yellow solid precipitated out upon addition of EtOH. Yield: 0.534 g, 1.04 mmol, 81%.

**Data for 106.**  $^1\text{H NMR}$  (400 MHz,  $\text{CDCl}_3$ )  $\delta$  10.60 (s, 2H, CHO), 8.94 (s, 2H, aromatic CH), 8.22 (s, 2H, aromatic CH), 7.67 (s, 2H, aromatic CH), 4.07 (s, 6H,  $\text{OCH}_3$ ), 2.79 (m, 4H,  $\text{CH}_2$ ), 1.68 (m, 4H, hexyl chain), 1.48 (m, 4H, hexyl chain), 1.36 (m, 8H, hexyl chain), 0.92 (t, 6H, hexyl  $\text{CH}_3$ );  $^{13}\text{C NMR}$  (100.7 MHz,  $\text{CDCl}_3$ )  $\delta$  190.0, 159.4, 141.2, 134.3, 126.9, 125.4, 125.2, 124.8, 123.5, 105.0, 55.9, 33.5, 32.1, 32.0, 29.9, 22.9, 14.4; EI-MS:  $m/z = 512 (\text{M}^+)$ ; IR (KBr);  $\nu = 2960, 2927, 2860, 1687, 1614, 1472, 1421, 1412, 1255, 1207, 1165, 1047, 869, 830 \text{ cm}^{-1}$ ; UV-Vis ( $\text{CH}_2\text{Cl}_2$ ):  $\lambda_{\text{max}} (\epsilon) = 264 (7.0 \times 10^4), 279 (6.2 \times 10^4), 384 (1.2 \times 10^4) \text{ nm (L mol}^{-1}\text{cm}^{-1})$ ; Mp. = 165-167 °C; Anal. Calc'd for  $\text{C}_{34}\text{H}_{40}\text{O}_4$ : C, 79.65, H, 7.86. Found: C, 79.52, H, 7.93.

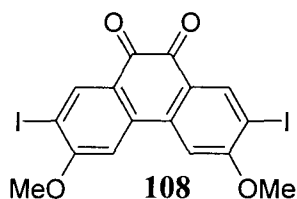


### Synthesis of 6,11-diformyl-2,3-dihexyl-7,10-

**dihydroxytriphenylene (71)** – To an ice-cooled solution of **106** (0.495 g, 0.965 mmol) in dry DCM (50 mL), boron tribromide (2.2 mL, 23.3 mmol) was added to produce a dark

brown solution, which subsequently faded to orange. The solution was warmed to room temperature overnight, then was poured into ice water (200 mL). After the mixture had warmed, it was filtered and the filtrate was extracted with  $\text{CHCl}_3$  (3 x 50 mL). The filtered solid and organic layer from extraction were combined and the solvent was removed under vacuum. The residue was passed through silica in  $\text{CHCl}_3$ . After removal of the solvent, the product was recrystallized from  $\text{CHCl}_3$  to obtain 0.357 g (0.736 mmol, 76% yield) of a yellow solid.

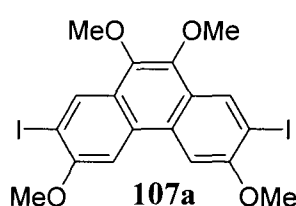
**Data for 71.**  $^1\text{H}$  NMR (400 MHz,  $\text{CDCl}_3$ )  $\delta$  10.68 (s, 2H, OH), 10.19 (s, 2H, CHO), 8.71 (s, 2H, aromatic CH), 8.18 (s, 2H, aromatic CH), 7.96 (s, 2H, aromatic CH), 2.82 (m, 4H,  $\text{CH}_2$ ), 1.72 (m, 4H, hexyl chain), 1.49 (m, 4H, hexyl chain), 1.36 (m, 8H, hexyl chain), 0.91 (t, 6H, hexyl  $\text{CH}_3$ );  $^{13}\text{C}$  NMR (75.5 MHz,  $\text{CDCl}_3$ )  $\delta$  196.8, 158.7, 141.1, 135.4, 130.4, 126.4, 124.8, 123.1, 121.9, 112.1, 33.4, 33.0, 31.9, 29.8, 22.9, 14.4; EI-MS:  $m/z$  = 484 ( $\text{M}^+$ ); IR (KBr):  $\nu$  = 3444, 2952, 2926, 2855, 1659, 1584, 1543, 1467, 1341, 1230, 1184, 880, 826, 790, 725, 600  $\text{cm}^{-1}$ ; UV-Vis ( $\text{CH}_2\text{Cl}_2$ ):  $\lambda_{\text{max}}$  ( $\epsilon$ ) = 248 ( $3.5 \times 10^4$ ), 274 ( $6.1 \times 10^4$ ), 393 ( $8.0 \times 10^3$ ) nm ( $\text{L mol}^{-1}\text{cm}^{-1}$ ); Mp. = 260-262  $^\circ\text{C}$ ; Anal. Calc'd for  $\text{C}_{32}\text{H}_{36}\text{O}_4$ : C, 79.31, H, 7.49. Found: C, 79.06, H, 7.52.



**Synthesis of 2,7-diiodo-3,6-dimethoxy-9,10-phenanthrenequinone (108)** - In a flask, **89** (3.99 g, 14.8

mmol), I<sub>2</sub> (4.16 g, 16.3 mmol), KIO<sub>3</sub> (1.27 g, 5.92 mmol), H<sub>2</sub>O (15.6 mL), H<sub>2</sub>SO<sub>4</sub> (1.56 mL), and HOAc (156 mL) were combined and heated to reflux. After 5 h, the solution was cooled, filtered and washed with copious amounts of H<sub>2</sub>O. The solid was stirred in an aqueous Na<sub>2</sub>SO<sub>3</sub> solution, filtered and washed with EtOH. Recrystallization from ethanol gave a brown solid, and from acetone gave an orange solid. Yield: 6.68 g, 12.8 mmol, 86%

**Data for 108.** <sup>1</sup>H NMR (300 MHz, CDCl<sub>3</sub>) δ 8.58 (s, 2H, aromatic CH), 7.17 (s, 2H, aromatic CH), 4.10 (s, 6H, OCH<sub>3</sub>); <sup>13</sup>C NMR (75.5 MHz, CDCl<sub>3</sub>) δ 177.5, 164.1, 142.5, 137.5, 126.4, 104.5, 88.7, 57.1; ESI-MS: *m/z* = 543 ([M+Na]<sup>+</sup>); IR (KBr): ν = 3027, 2926, 1670, 1573, 1492, 1453, 1330, 1310, 1268, 1206, 1058, 1041, 846, 756 cm<sup>-1</sup>; UV-Vis (CH<sub>2</sub>Cl<sub>2</sub>) λ<sub>max</sub> (ε) = 241 (1.5 x 10<sup>4</sup>), 306 (6.3 x 10<sup>4</sup>), 345 (1.3 x 10<sup>4</sup>) nm (L mol<sup>-1</sup> cm<sup>-1</sup>); Mp. > 300 °C; Anal. Calc'd for C<sub>16</sub>H<sub>10</sub>O<sub>4</sub>I<sub>2</sub>: C, 36.95, H, 1.94. Found C, 37.35, H 2.14.

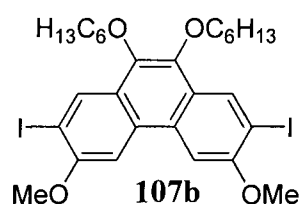


**Synthesis of 2,7-diiodo-3,6,9,10-tetramethoxyphenanthrene**

**(107a)** - Compound **108** (2.715 g, 5.22 mmol), Bu<sub>4</sub>NBr (0.561 g, 1.74 mmol), Na<sub>2</sub>S<sub>2</sub>O<sub>4</sub> (3.027 g, 17.3 mmol), THF (50 mL) and H<sub>2</sub>O (50 mL) were combined in a round-bottomed flask and stirred for 5 min, after which dimethyl sulfate (2.7 mL, 28.5 mmol) was added, followed by aqueous sodium hydroxide (4.4 mL, 14 M). After stirring for 2 h, the aqueous layer was separated and extracted with EtOAc (3 x 50 mL). The combined organic layers were washed with water

(3 x 50 mL), NH<sub>4</sub>OH solution (2 x 50 mL) and brine (1 x 50 mL). The organic layer was dried with MgSO<sub>4</sub>, filtered and the solvents were removed under vacuum, resulting in a brown solid. Washing the product with MeOH gave an orange solid. Additional impurities were removed by flashing the product through silica with a 1:3 mixture of DCM/hexanes, followed by recrystallization in DCM. Yield: 1.282 g, 2.33 mmol, 45%.

**Data for 107a.** <sup>1</sup>H NMR (300 MHz, CDCl<sub>3</sub>) δ 8.62 (s, 2H, aromatic CH), 7.69 (s, 2H, aromatic CH), 4.07 (s, 6H, OCH<sub>3</sub>), 4.02 (s, 6H, OCH<sub>3</sub>); <sup>13</sup>C NMR (75.5 MHz, CDCl<sub>3</sub>) δ 156.2, 141.9, 134.2, 129.0, 126.0, 102.8, 88.7, 61.2, 56.9; ESI-MS: *m/z* = 551 ([M + H]<sup>+</sup>); IR (KBr): ν = 3002, 2941, 2830, 1590, 1480, 1448, 1427, 1357, 1242, 1130, 1041, 990, 904, 840, 669, 593 cm<sup>-1</sup>; UV-Vis (CH<sub>2</sub>Cl<sub>2</sub>): λ<sub>max</sub> (ε) = 269 (3.7 x 10<sup>4</sup>), 298 (3.3 x 10<sup>4</sup>), 312 (2.7 x 10<sup>4</sup>) nm (L mol<sup>-1</sup>cm<sup>-1</sup>); Mp. = 251-254 °C; Anal. Calc'd for C<sub>18</sub>H<sub>16</sub>O<sub>4</sub>I<sub>2</sub>: C, 39.30, H, 2.93. Found C, 39.50, H, 3.15.

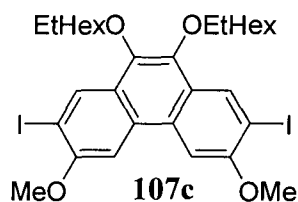


**Synthesis of 9,10-dihexyloxy-2,7-diiodo-3,6-dimethoxyphenanthrene (107b)** - Compound **108** (1.015 g, 2.125 mmol) was dissolved in 50 mL DMF and degassed with

N<sub>2</sub> for 5 min Na<sub>2</sub>S<sub>2</sub>O<sub>4</sub> (1.995 g, 11.46 mmol) was added to the solution and it was stirred for 15 min, after which K<sub>2</sub>CO<sub>3</sub> (1.175 g, 8.50 mmol), Bu<sub>4</sub>NBr (0.050 g, 0.154 mmol), and 1-bromohexane (0.90 mL, 4.64 mmol) were added. The solution was heated for 16 h at 80 °C. After cooling, the yellow solution was poured into H<sub>2</sub>O and extracted with EtOAc (3 x 125 mL). The organic layer was dried with MgSO<sub>4</sub>, filtered and dried under vacuum. Chromatography on silica with 1:3 DCM/hexanes afforded a colourless oil which

crystallized from EtOH and DCM to give white crystals. Yield: 0.398 g, 0.576 mmol, 27%

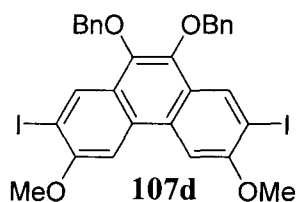
**Data for 107b.**  $^1\text{H}$  NMR (300 MHz,  $\text{CDCl}_3$ )  $\delta$  8.62 (s, 2H, aromatic CH), 7.69 (s, 2H, aromatic CH), 4.12 (t, 4H,  $\text{OCH}_2$ ), 4.06 (s, 6H,  $\text{OCH}_3$ ), 1.85 (m, 4H, hexyloxy chain), 1.55 (m, 4H, hexyloxy chain), 1.37 (m, 8H, hexyloxy chain), 0.89 (t, 6H, hexyloxy chain);  $^{13}\text{C}$  NMR (75.5 MHz,  $\text{CDCl}_3$ )  $\delta$  155.8, 141.0, 134.3, 128.8, 126.4, 102.4, 88.6, 73.9, 56.8, 31.9, 30.6, 26.1, 22.9, 14.3;  $R_F$  (1:3 DCM/hexanes): 0.11; ESI-MS:  $m/z = 713$  ( $[\text{M}+\text{Na}]^+$ ); IR (KBr):  $\nu = 2999, 2952, 2925, 2856, 1589, 1480, 1453, 1438, 1409, 1355, 1240, 1152, 1080, 1045, 891, 833, 658 \text{ cm}^{-1}$ ; UV-Vis ( $\text{CH}_2\text{Cl}_2$ )  $\lambda_{\text{max}}$  ( $\epsilon$ ) = 232 ( $3.7 \times 10^4$ ), 269 ( $5.9 \times 10^4$ ), 299 ( $5.3 \times 10^4$ ), 313 ( $4.3 \times 10^4$ ) nm ( $\text{L mol}^{-1} \text{ cm}^{-1}$ ); Mp. = 78-81 °C; Anal. Calc'd for  $\text{C}_{28}\text{H}_{36}\text{O}_4\text{I}_2$ : C, 48.71, H, 5.26. Found C, 48.91, H, 5.43.



**Synthesis of 9,10-di-2-ethylhexyloxy-2,7-diiodo-3,6-dimethoxyphenanthrene (107c) - Compound 108** (1.199 g,

2.31 mmol) was dissolved in 50 mL DMF and degassed with  $\text{N}_2$  for 5 min  $\text{Na}_2\text{S}_2\text{O}_4$  (1.204 g, 6.92 mmol) was added to the solution and stirred for 15 min, after which  $\text{K}_2\text{CO}_3$  (1.274 g, 9.21 mmol),  $\text{Bu}_4\text{NBr}$  (0.050 g, 0.154 mmol), and 2-ethylhexylbromide (1.23 mL, 6.92 mmol) were added. The solution was heated for 16 h at 80 °C. After cooling, the yellow solution was poured into  $\text{H}_2\text{O}$  and extracted with EtOAc (3 x 125 mL). The organic layer was dried with  $\text{MgSO}_4$ , filtered and dried under vacuum. Chromatography on silica with 1:3 DCM/hexanes afforded a colourless oil which crystallized from EtOH and DCM to give white crystals. Yield: 0.750 g, 1.00 mmol, 44%

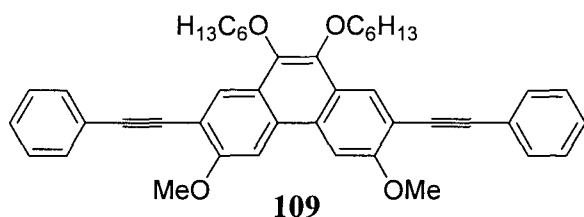
**Data for 107c.**  $^1\text{H}$  NMR (300 MHz,  $\text{CDCl}_3$ )  $\delta$  8.64 (s, 2H, aromatic CH), 7.71 (s, 2H, aromatic CH), 4.07 (s, 6H,  $\text{OCH}_3$ ) 4.00 (d, 4H,  $\text{OCH}_2$ ), 1.83 (m, 2H, CH), 1.57 (m, 4H, EtHex chain), 1.36 (m, 12H, EtHex chain), 0.96 (m, 12H, EtHex  $\text{CH}_3$ );  $^{13}\text{C}$  NMR (100.6 MHz,  $\text{CDCl}_3$ )  $\delta$  155.8, 141.3, 134.3, 128.9, 126.3, 102.5, 88.4, 76.7, 56.8, 40.8, 30.8, 29.4, 24.0, 23.4, 14.4, 11.4;  $R_F$  (1:3 DCM/hexanes): 0.14; ESI-MS:  $m/z = 769$  ( $[\text{M}+\text{Na}]^+$ ); IR (KBr):  $\nu = 3001, 2959, 2926, 2871, 1589, 1464, 1439, 1355, 1241, 1144, 1043, 886, 832, 656\text{ cm}^{-1}$ ; UV-Vis ( $\text{CH}_2\text{Cl}_2$ )  $\lambda_{\text{max}}$  ( $\epsilon$ ) = 232 ( $2.9 \times 10^4$ ), 269 ( $4.8 \times 10^4$ ), 299 ( $4.5 \times 10^4$ ), 313 ( $3.7 \times 10^4$ ) nm ( $\text{L mol}^{-1}\text{ cm}^{-1}$ ); Mp. = 110-112  $^\circ\text{C}$ ; Anal. Calc'd for  $\text{C}_{32}\text{H}_{44}\text{O}_4\text{I}_2$ : C, 51.49, H, 5.94. Found C, 51.69, H 6.18.



**Synthesis of 9,10-dibenzyloxy-2,7-diiodo-3,6-dimethoxyphenanthrene (107d)** - Compound **108** (0.157 g, 0.302 mmol) was dissolved in 20 mL DMF and degassed with  $\text{N}_2$  for 5 min  $\text{Na}_2\text{S}_2\text{O}_4$  (0.158 g, 0.907 mmol) was added to the solution and stirred for 15 min, after which  $\text{K}_2\text{CO}_3$  (0.405 g, 2.93 mmol),  $\text{Bu}_4\text{NBr}$  (0.050 g, 0.154 mmol), and benzyl chloride (0.5 mL, 4.34 mmol) were added. The solution was heated for 16 h at 80  $^\circ\text{C}$ . After cooling, the yellow solution was poured into  $\text{H}_2\text{O}$  and extracted with EtOAc (3 x 75 mL). The organic layer was dried with  $\text{MgSO}_4$ , filtered and dried under vacuum. Chromatography on silica with 1:3 DCM/hexanes afforded white crystals. Yield: 0.073 g, 0.104 mmol, 34%

**Data for 107d.**  $^1\text{H}$  NMR (400 MHz,  $\text{CDCl}_3$ )  $\delta$  8.62 (s, 2H, aromatic CH), 7.70 (s, 2H, aromatic CH), 7.47 (d, 4H, aromatic CH), 7.36 (m, 6H, aromatic CH), 5.21 (s, 4H,  $\text{OCH}_2$ ), 4.07 (s, 6H,  $\text{OCH}_3$ );  $^{13}\text{C}$  NMR (100.6 MHz,  $\text{CDCl}_3$ )  $\delta$  156.1, 141.2, 137.3, 134.5,

129.1, 128.8, 128.7, 128.5, 126.1, 102.4, 88.7, 75.9, 56.8; EI-MS:  $m/z = 702$  ( $M^+$ ); IR (KBr):  $\nu = 2999, 2932, 2875, 2855, 1586, 1455, 1436, 1350, 1275, 1132, 1044, 955, 896, 841, 758, 696 \text{ cm}^{-1}$ ; UV-Vis ( $\text{CH}_2\text{Cl}_2$ )  $\lambda_{\text{max}} (\epsilon) = 233 (3.2 \times 10^4), 270 (5.0 \times 10^4), 299 (4.7 \times 10^4), 312 (3.7 \times 10^4) \text{ nm}$  ( $\text{L mol}^{-1} \text{ cm}^{-1}$ ); Mp. 213-215 °C.



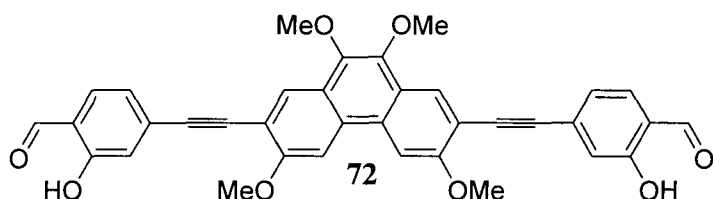
#### Synthesis of Model Compound 109 -

Compound **107b** (0.153 g, 0.222 mmol), phenylacetylene (0.2 mL, 1.82 mmol) and

CuI (30 mg, 0.16 mmol) were dissolved in 10 mL toluene and 4 mL diisopropylamine. After the solution was degassed, Pd(PPh<sub>3</sub>)<sub>4</sub> (50 mg, 0.043 mmol) was added. The reaction was heated for 1 h at 50 °C. Upon cooling, the solution was poured into water and extracted with DCM. The organic layer was dried with MgSO<sub>4</sub>, filtered and dried under vacuum to obtain a brown oil. The product was chromatographed with 3:1 hexanes/DCM to obtain a yellow oil. Yellow needles crystallized from EtOH and DCM. Yield: 0.114 g, 0.178 mmol, 80%

**Data for 109.** <sup>1</sup>H NMR (400 MHz, CDCl<sub>3</sub>)  $\delta$  8.33 (s, 2H, aromatic CH), 7.79 (s, 2H, aromatic CH), 7.61 (m, 4H, aromatic CH), 7.35 (m, 6H, aromatic CH), 4.17 (t, 4H, OCH<sub>2</sub>), 4.12 (s, 6H, OCH<sub>3</sub>), 1.89 (m, 4H, hexyloxy chain), 1.51 (m, 4H, hexyloxy chain), 1.38 (m, 8H, hexyloxy chain), 0.91 (t, 6H, hexyloxy chain); <sup>13</sup>C NMR (75.5 MHz, CDCl<sub>3</sub>)  $\delta$  157.6, 141.7, 132.0, 128.7, 128.5, 124.9, 123.6, 114.3, 102.9, 94.4, 86.3, 73.9, 56.4, 31.9, 30.6, 26.2, 23.0, 14.3; ESI-MS:  $m/z = 662$  ( $[M+Na]^+$ ); IR (KBr):  $\nu = 2953, 2930, 2854, 1591, 1499, 1443, 1365, 1235, 1118, 1009, 832, 756, 694 \text{ cm}^{-1}$ ; UV-Vis ( $\text{CH}_2\text{Cl}_2$ )  $\lambda_{\text{max}} (\epsilon) = 295 (4.0 \times 10^4), 353 (4.4 \times 10^4) \text{ nm}$  ( $\text{L mol}^{-1} \text{ cm}^{-1}$ ); Fluorescence

(CH<sub>2</sub>Cl<sub>2</sub>):  $\lambda_{em}$  = 456 nm ( $\lambda_{exc}$  = 354 nm); Mp. = 70-72 °C; Anal. Calc'd for C<sub>44</sub>H<sub>46</sub>O<sub>4</sub>: C, 82.72, H, 7.26. Found C, 82.40, H, 7.29.



#### Synthesis of Diol 72 - 4-

Ethynylsalicylaldehyde 110

(0.528 g, 3.61 mmol) and 107a

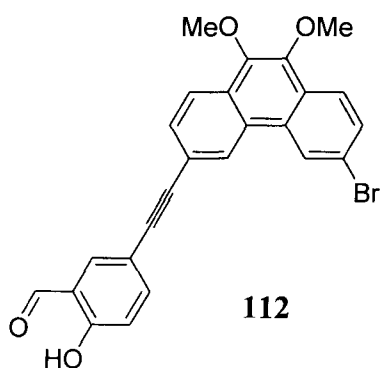
(0.793 g, 1.44 mmol) were

combined in a Schlenk flask along with Pd(PPh<sub>3</sub>)<sub>4</sub> (0.160 g, 0.138 mmol) and CuI (0.028 g, 0.147 mmol). To the flask were added diisopropylamine (4.5 mL) and THF (20 mL). The reaction mixture was refluxed for 16 h, after which the solution was poured into aqueous acetic acid (1 M). Yellow solid precipitated and was filtered and washed with copious amounts of water. After dissolving the solid in DCM, it was filtered again and then passed through silica. The solvent was removed under vacuum and the solid was recrystallized in DCM. Yield: 0.633 g, 2.71 mmol, 75%.

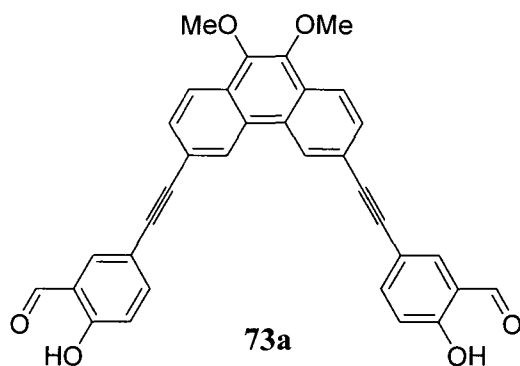
**Data for 72.** <sup>1</sup>H NMR (300 MHz, CDCl<sub>3</sub>)  $\delta$  11.06 (s, 2H, OH), 9.89 (s, 2H, CHO), 8.36 (s, 2H, aromatic CH), 7.79 (s, 2H, aromatic CH), 7.54 (d, 2H,  $J$  = 8.5 Hz, aromatic CH), 7.22-7.26 (m, 4H, aromatic CH), 4.13 (s, 6H, OCH<sub>3</sub>), 4.08 (s, 6H, OCH<sub>3</sub>); <sup>13</sup>C NMR (75.5 MHz, CDCl<sub>3</sub>)  $\delta$  196.0, 188.5, 161.6, 157.9, 142.4, 133.7, 132.3, 129.3, 128.9, 124.5, 123.4, 120.7, 120.3, 113.7, 103.0, 90.9, 61.3, 56.5; ESI-MS:  $m/z$  = 587 ([M+H]<sup>+</sup>); IR (KBr):  $\nu$  = 3426, 2942, 2833, 2207, 1657, 1626, 1505, 1455, 1369, 1324, 1255, 1231, 1195, 1100, 1009, 979, 956, 829, 704 cm<sup>-1</sup>; UV-Vis (CH<sub>2</sub>Cl<sub>2</sub>):  $\lambda_{max}$  ( $\epsilon$ ) = 295 (1.6 x 10<sup>4</sup>), 379 (3.4 x 10<sup>4</sup>) nm (L mol<sup>-1</sup> cm<sup>-1</sup>); Fluorescence (CH<sub>2</sub>Cl<sub>2</sub>):  $\lambda_{em}$  = 520 nm ( $\lambda_{exc}$  = 379 nm);

Mp. = 286-289 °C; Anal. Calc'd for C<sub>36</sub>H<sub>26</sub>O<sub>8</sub>: C, 73.71, H, 4.47. Found C, 73.43, H, 4.63.

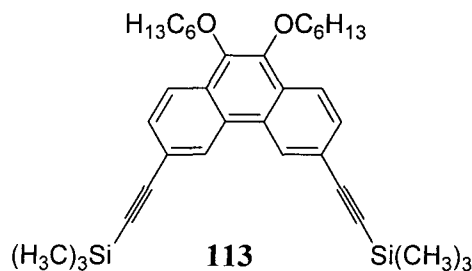
**Attempted Convergent Synthesis of 73a** - 4-Ethynylsalicylaldehyde **111** (0.141 g, 0.356 mmol) and **86b** (0.145 g, 0.992 mmol) were combined in a Schlenk flask along with Pd(PPh<sub>3</sub>)<sub>2</sub>Cl<sub>2</sub> (0.030 g, 0.0427 mmol), PPh<sub>3</sub> (0.020 g, 0.0763 mmol) and CuCl (0.052 g, 0.525 mmol). To the flask were added Et<sub>3</sub>N (15 mL). The reaction mixture was heated at 60 °C for 3 days, during which the reaction was monitored by TLC. More catalyst and cocatalyst was added as needed. After heating, the solution was poured into aqueous acetic acid (1 M) and extracted with CHCl<sub>3</sub>. The organic layer was washed with water, dried with MgSO<sub>4</sub>, filtered and the solvent was removed by rotary evaporation. After chromatography of the product first with 1:1 DCM/hexanes, then with pure DCM, both monosubstituted **112** (0.039 g, 0.085 mmol, 24%) and disubstituted products **73a** (0.022 g, 0.041 mmol, 11%) were isolated in separate fractions.



**Data for 112.** <sup>1</sup>H NMR (300 MHz, CDCl<sub>3</sub>) δ 11.13 (s, 1H, OH), 9.91 (s, 1H CHO), 8.70, (dd, 2H, aromatic CH), 8.18 (d, 1H, aromatic CH), 8.08 (d, 1H, aromatic CH), 7.82 (d, 1H, aromatic CH), 7.70-7.74 (m, 3H, aromatic CH), 7.01 (d, 1H, aromatic CH), 4.07 (s, 6H, OCH<sub>3</sub>); EI-MS: *m/z* = 462 (M<sup>+</sup>); High Res. MS Calc'd for C<sub>25</sub>H<sub>17</sub>O<sub>4</sub>Br: 460.03102. Found: 460.02997.



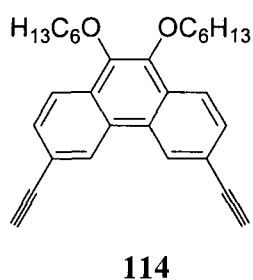
**Data for 73a.**  $^1\text{H NMR}$  (300 MHz,  $\text{CDCl}_3$ )  $\delta$  11.13 (s, 2H, OH), 9.91 (s, 2H, CHO), 8.79 (d, 2H, aromatic CH), 8.20 (d, 2H, aromatic CH), 7.82 (d, 2H, aromatic CH), 7.74 (dd, 2H aromatic CH), 7.71 (dd, 2H, aromatic CH), 7.02 (d, 2H, aromatic CH), 4.09 (t, 4H,  $\text{OCH}_3$ ); EI-MS:  $m/z = 526$  ( $\text{M}^+$ ); High Res. MS Calc'd for  $\text{C}_{34}\text{H}_{22}\text{O}_6$ : 526.14164. Found: 526.14078.



**Synthesis of 3,6-di(trimethylsilyl)ethynyl-9,10-dihexyloxyphenanthrene (113)** - To a mixture of compound **86a** (4.572 g, 8.52 mmol),  $\text{Pd}(\text{PPh}_3)_4$  (0.424 g, 0.367 mmol) and  $\text{CuCl}$  (0.075 g, 0.757 mmol), was added  $\text{Et}_3\text{N}$  (40 mL) and trimethylsilylacetylene (3 mL, 21.4 mmol). The mixture was heated to reflux for 16 h. After diluting the solution with water, the product was extracted with DCM and the solvent was evaporated under reduced pressure. The residue was purified through chromatography using 3:1 hexanes/DCM. The product was recrystallized from DCM and EtOH. Yield: 4.478 g, 7.84 mmol, 92%.

**Data for 113.**  $^1\text{H NMR}$  (400 MHz,  $\text{CDCl}_3$ )  $\delta$  8.71 (d, 2H,  $J = 1.0$  Hz, aromatic CH), 8.12 (d, 2H,  $J = 8.5$  Hz, aromatic CH), 7.64 (dd, 2H,  $J_1 = 8.5$  Hz,  $J_2 = 1.0$  Hz, aromatic CH), 4.17, (t, 4H,  $\text{OCH}_2$ ), 1.89-0.89 (m, 22H, hexyl chain), 0.30 (s, 18H, TMS  $\text{CH}_3$ );  $^{13}\text{C NMR}$  (100.7 MHz,  $\text{CDCl}_3$ )  $\delta$  144.1, 130.2, 129.8, 127.9, 126.4, 122.5, 120.7, 105.8, 95.1, 74.0, 31.9, 30.6, 26.1, 22.9, 14.3, 0.3; EI-MS:  $m/z = 570$  ( $\text{M}^+$ ); IR (KBr):  $\nu = 2957, 2929, 2870, 2154, 1606, 1435, 1251, 1124, 1063, 861, 846, 764$   $\text{cm}^{-1}$ ; UV-Vis ( $\text{CH}_2\text{Cl}_2$ ):  $\lambda_{\text{max}}$  ( $\epsilon$ ) =

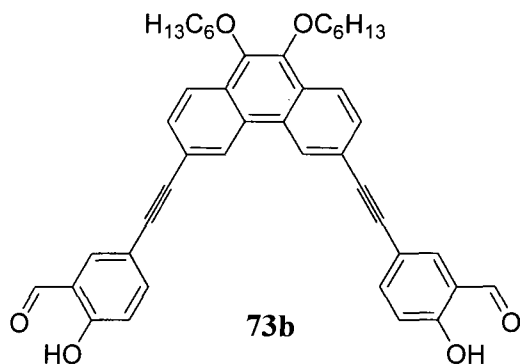
269 ( $8.5 \times 10^4$ ), 332 ( $2.7 \times 10^4$ ), 348 ( $2.4 \times 10^4$ ) nm ( $\text{L mol}^{-1}\text{cm}^{-1}$ ); Mp. = 77-79 °C; Anal. Calc'd for  $\text{C}_{36}\text{H}_{50}\text{O}_2\text{Si}_2$ : C, 75.73, H, 8.83. Found C, 75.90, H, 9.15.



**Synthesis of 3,6-diethynyl-9,10-dihexyloxyphenanthrene (114) –**

To a solution of compound **113** (1.082 g, 1.89 mmol) in THF (15 mL) was added a solution of KOH (0.335 g, 5.97 mmol) in MeOH (30 mL). After stirring for 16 h, the solution was poured into a dilute acetic acid solution and extracted with DCM. The organic layer was dried with  $\text{MgSO}_4$  and filtered and the solvent was removed under vacuum to give a brown oil. Chromatography through silica with 3:1 hexanes/DCM, followed by recrystallization in EtOH gave pure product. Yield: 0.711 g, 1.66 mmol, 88%.

**Data for 114.**  $^1\text{H}$  NMR (300 MHz,  $\text{CDCl}_3$ )  $\delta$  8.74 (d, 2H,  $J=1.2$  Hz, aromatic CH), 8.16 (d, 2H,  $J=8.5$  Hz, aromatic CH), 7.67 (dd, 2H  $J_1=8.5$  Hz,  $J_2=1.2$  Hz, aromatic CH), 4.18 (t, 4H,  $\text{OCH}_2$ ), 3.20 (s, 2H,  $\text{HC}\equiv\text{C}$ ), 1.92-0.88 (m, 22H, hexyl chain);  $^{13}\text{C}$  NMR (75.5 MHz,  $\text{CDCl}_3$ )  $\delta$  144.1, 130.3, 130.0, 127.8, 127.1, 122.7, 119.7, 84.3, 78.0, 73.9, 31.9, 30.6, 26.1, 22.9, 14.3; EI-MS:  $m/z = 426$  ( $\text{M}^+$ ); IR (KBr):  $\nu = 3287, 2956, 2927, 2871, 2858, 2107, 1609, 1503, 1470, 1440, 1355, 1324, 1241, 1169, 1122, 1067, 1052, 884, 827, 627$   $\text{cm}^{-1}$ ; UV-Vis ( $\text{CH}_2\text{Cl}_2$ ):  $\lambda_{\text{max}}$  ( $\epsilon$ ) = 257 ( $7.7 \times 10^4$ ), 324 ( $2.3 \times 10^4$ ), 339 ( $2.2 \times 10^4$ ) nm ( $\text{L mol}^{-1}\text{cm}^{-1}$ ); Mp. = 43-45 °C; Anal. Calc'd for  $\text{C}_{30}\text{H}_{34}\text{O}_2$ : C, 84.47, H, 8.03. Found C, 84.38, H, 8.41.



**Synthesis of Compound 73b** - Compound **114** (0.488 g, 1.14 mmol), 5-bromosalicylaldehyde (0.624 g, 3.10 mmol), Pd(PPh<sub>3</sub>)<sub>4</sub> (0.061 g, 0.053 mmol) and CuCl (0.014 g, 0.140 mmol), were dissolved in Et<sub>3</sub>N (40 mL) and the mixture was heated to reflux for 16 h. After diluting the solution with water and neutralizing it with acetic acid, it was extracted with DCM and washed with aqueous NaHCO<sub>3</sub>. The solvent was evaporated under reduced pressure and the product was purified using column chromatography with a gradient of 3:1 hexanes/DCM to 1:1 hexanes/DCM to pure DCM. The product was recrystallized from DCM and EtOH. Yield: 0.365 g, 0.55 mmol, 48%.

**Data for 73b.** <sup>1</sup>H NMR (400 MHz, CDCl<sub>3</sub>) δ 11.13 (s, 2H, OH), 9.94 (s, 2H, CHO), 8.81 (d, 2H, *J* = 1.3 Hz, aromatic CH), 8.22 (d, 2H, *J* = 8.5 Hz, aromatic CH), 7.85 (d, 2H, *J* = 2.0 Hz, aromatic CH), 7.73 (dd, 2H, *J*<sub>1</sub> = 8.7 Hz, *J*<sub>2</sub> = 2.0 Hz, aromatic CH), 7.71 (dd, 2H, *J*<sub>1</sub> = 8.5 Hz, *J*<sub>2</sub> = 1.3 Hz, aromatic CH), 7.04 (d, 2H, *J* = 8.7 Hz, aromatic CH), 4.23 (t, 4H, OCH<sub>2</sub>), 1.96-0.88 (m, 22H, hexyl chain); <sup>13</sup>C NMR (100.7 MHz, CDCl<sub>3</sub>) δ 196.3, 161.7, 144.1, 140.0, 137.2, 129.9, 128.0, 126.3, 122.8, 120.8, 120.5, 118.5, 115.4, 89.8, 88.5, 74.0, 31.9, 30.7, 26.1, 22.9, 14.3; EI-MS: *m/z* = 666 (M<sup>+</sup>); IR (KBr): ν = 2950, 2933, 2859, 2209 1665, 1606, 1484, 1319, 1292, 1280, 1177, 1121, 1059, 887, 831 cm<sup>-1</sup>; UV-Vis (CH<sub>2</sub>Cl<sub>2</sub>): λ<sub>max</sub> (ε) = 260 (6.5 × 10<sup>4</sup>), 303 (6.9 × 10<sup>4</sup>), 350 (3.6 × 10<sup>4</sup>) nm (L mol<sup>-1</sup> cm<sup>-1</sup>); Fluorescence (CH<sub>2</sub>Cl<sub>2</sub>): λ<sub>em</sub> = 541 nm (λ<sub>exc</sub> = 350 nm); Mp. = 172-174 °C; Anal. Calc'd for C<sub>44</sub>H<sub>42</sub>O<sub>6</sub>: C, 79.25, H, 6.35. Found C, 79.63, H, 6.50.

## 2.4 References

- (1) Bendig, J.; Beyermann, M.; Kreysig, D. *Tetrahedron Lett.* **1977**, *41*, 3659-3660.
- (2) Dickerman, S. C.; Zimmermann, I. *J. Org. Chem.* **1974**, *23*, 3429-3430.
- (3) Giles, R. G. F.; Sargent, M. V. *J. Chem. Soc., Chem. Commun.* **1974**, 215-216.
- (4) Letcher, R. M.; Nhamo, L. R. M.; Gumiro, I. T. *J. Chem. Soc. Perkin I* **1972**, 206-210.
- (5) Blackburn, E. V.; Timmons, C. J. *Q. Rev., Chem. Soc.* **1969**, *23*, 482-503.
- (6) Liu, Z.; Larock, R. C. *Angew. Chem. Int. Ed.* **2007**, *46*, 2535-2538.
- (7) Yang, C.; Scheiber, H.; List, E. J. W.; Jacob, J.; Müllen, K. *Macromolecules* **2006**, *39*, 5213-5221.
- (8) Fuson, R. C.; Tomboulion, P. *J. Am. Chem. Soc.* **1957**, *79*, 956-960.
- (9) Linstead, R. P.; Doering, W. E. *J. Am. Chem. Soc.* **1942**, *64*, 1991-2003.
- (10) Mukherjee, T. K. *J. Phys. Chem.* **1967**, *71*, 2277-2282.
- (11) Bhatt, M. V. *Tetrahedron* **1964**, *20*, 803-821.
- (12) Paruch, K.; Katz, T. J.; Incarvito, C.; Lam, K. -C.; Rhatigan, B.; Rheingold, A. L. *J. Org. Chem.* **2000**, *65*, 7602-7608.
- (13) Buess, C. M.; Lawson, D. D. *Chem. Rev.* **1960**, *60*, 313-330.
- (14) Pérez, D.; Guitián, E. *Chem. Soc. Rev.* **2004**, *33*, 274-283.
- (15) Beattie, D. R.; Hindmarsh, P.; Goodby, J. W.; Haslan, S. D.; Richardson, R. M. *J. Mater. Chem.* **1992**, *2*, 1261-1266.
- (16) Bushby, R. J.; Hardy, C. *J. Chem. Soc. Perkin Trans. I* **1986**, 721-723.
- (17) Cammidge, A. N.; Gopee, H. *J. Mater. Chem.* **2001**, *11*, 2773-2783.
- (18) Henderson, P.; Kumar, S.; Rego, J. A.; Ringsdorf, H.; Schuhmacher, P. *J. Chem. Soc., Chem. Commun.* **1995**, 1059-1060.
- (19) Boden, N.; Bushby, R. J.; Cammidge, A. N.; Headdock, G. *J. Mater. Chem.* **1995**, *5*, 2275-2281.
- (20) Kumar, S.; Manickam, M.; Balagurusamy, V. S. K.; Schonherr, H. *Liquid Crystals* **1999**, *26*, 1455-1466.

- (21) Buquet, A.; Couture, A.; Lablache-Combier, A. *J. Org. Chem.* **1979**, *44*, 2300-2303.
- (22) Snieckus, V. *Chem. Rev.* **1990**, *90*, 879-933.
- (23) Capdevielle, P.; Maumy, M. *Tetrahedron Lett.* **1993**, *34*, 1007.
- (24) Jacob, P. 3.; Callery, P. S.; Shulgin, A. T.; Castagnoli, N. J. *J. Org. Chem.* **1976**, *41*, 3627-3629.
- (25) Barluenga, J.; Fananas, F. J.; Sanz, R.; Marcos, C.; Trabada, M. *Org. Lett.* **2002**, *4*, 1587-1590.
- (26) Garst, J. F.; Smith, C. D. *J. Am. Chem. Soc.* **1976**, *98*, 1526-1537.
- (27) Lindsay Smith, J. R.; O'Brian, P.; Reginato, G. *Tetrahedron: Asymmetry* **1997**, *8*, 3415-3420.
- (28) Zhao, D.; Moore, J. S. *J. Org. Chem.* **2002**, *67*, 3548-3554.
- (29) Hanack, M.; Haisch, P.; Lehmann, H.; Subramanian, L. R. *Synthesis* **1993**, 387-390.
- (30) Ma, C.; Lo, A.; Abdolmaleki, A.; MacLachlan, M. J. *Org. Lett.* **2004**, *6*, 3841-3844.
- (31) Chang, K. -H.; Huang, C. -C.; Liu, Y. -H.; Hu, Y. -H.; Chou, P. -T.; Lin, Y. -C. *Dalton Trans.* **2004**, 1731-1738.
- (32) Schmid, M.; Eberhardt, R.; Kukral, J.; Rieger, B. *Z. Naturforsch* **2002**, *57b*, 1141-1146.

## Chapter 3

# Synthesis of Phenanthrene and Triphenylene Macrocycles<sup>§</sup>

### 3.1 Introduction

Chapter 2 discussed the synthetic routes to useful precursors for Schiff base condensation. The focus of this chapter is the synthesis of macrocycles using compounds **70-73**, with the characterization of the products.

#### 3.1.1 Synthesis of [3+3] Macrocycles

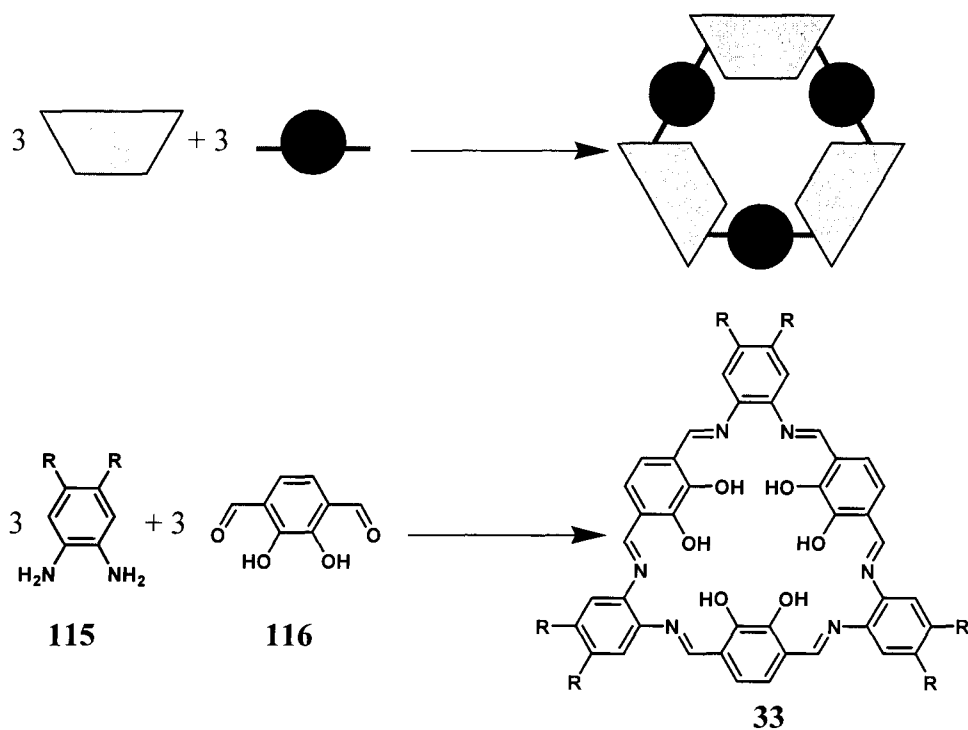
Even though there is a large variety of Schiff base macrocycles that have been synthesized over the past several decades, only recently have [3+3] Schiff base macrocycles been of interest. As previously mentioned in Chapter 1, Reinhoudt was the first to synthesize a [3+3] macrocycle, using a template of Ba<sup>2+</sup>, which could not be removed.<sup>1</sup> Macrocycle **33** is a shape-persistent [3+3] Schiff base macrocycle containing three N<sub>2</sub>O<sub>2</sub> salphen pockets for metal coordination.<sup>2,3</sup> It has a conjugated backbone, but the crystal structure shows that the aromatic rings in the spacer are tilted out of the plane of the macrocycle.<sup>4</sup> In addition, **33** has six hydroxyl groups arranged in a similar hexagonal geometry to 18-crown-6, allowing it to coordinate to alkali metals.<sup>3</sup> The size of the macrocycle can be increased by using larger bis(salicylate) spacers, as

---

<sup>§</sup> A version of this chapter has been accepted for publication/will be submitted for publication: (a) Boden, B.N.; Abdolmaleki, A.; Ma, C. T.-Z.; and MacLachlan, M. J. "New Diformyldihydroxyaromatic Precursors for Luminescent Schiff base Macrocycles: Synthesis, Characterization, and Condensation Studies" *Can. J. Chem.* (b) Boden, B. N.; MacLachlan, M. J. "Aggregation of Giant Luminescent Schiff Base Macrocycles".

demonstrated by macrocycle **34**, which is made with a phenyleneethynylene diol.<sup>5</sup> Both of these macrocycles are synthesized using a template-free synthesis and a general representation of this reaction is shown in Scheme 3.1. The same principles can be applied in the synthesis of [6+6] Schiff base macrocycles, such as **35**,<sup>6</sup> which have a *meta* geometry of the formyl groups rather than the *para* geometry that produces [3+3] macrocycles.

**Scheme 3.1** General representation of the synthesis of a [3+3] Schiff base macrocycle (top) and synthesis of **33**.



The same procedure can successfully be employed with different diol spacers to form the macrocycles. Combining three equivalents of each diol, for example **116**, with an appropriate diamine **115** yields the corresponding macrocycle in good yield. Often for larger spacers or diamines with longer chains, a longer reaction time is needed. Also, to

achieve crystallization of the final macrocycle, the solvent combination must be tuned, and this is often determined with trial and error.

The synthesis of diols **70b**, **71**, **72** and **73b** was discussed in Chapter 2. Diols **70b** and **71** can be used to make macrocycles that are slightly larger than **33**, with a total of 42 covalently-bonded atoms forming a ring. Giant [3+3] Schiff base macrocycles that have a total of 78 bonds around the backbone can be made with diols **72** and **73b**.

## 3.2 Discussion

Typically, [3+3] macrocycles are formed when equimolar amounts of diol and diamine are heated to reflux in a mixture of  $\text{CHCl}_3$  and MeCN. After cooling the reaction, crystals of the product precipitate out of the solution. This procedure was applied to the various diols synthesized in Chapter 2.

### 3.2.1 Attempted Synthesis of Macrocycle **68**

In the formation of macrocycle **68**, we had the versatility of using different lengths of alkoxy chains on the diamine to achieve a soluble macrocycle, despite the low solubility of **70a**. Synthesis of **68a** was first attempted using 1,2-dihexyloxy-4,5-diaminobenzene **115a** (Scheme 3.2), but after a few hours of reaction, an insoluble orange precipitate **117** had formed. The IR spectra, shown in Figure 3.1, revealed that fragments of the macrocycle had formed, apparent from the presence of an imine band at  $1611\text{ cm}^{-1}$ , but the product still exhibited the carbonyl stretch at  $1636\text{ cm}^{-1}$ . The starting material shows a carbonyl stretch at  $1652\text{ cm}^{-1}$ .

**Scheme 3.2** Attempted synthesis of **68a**.

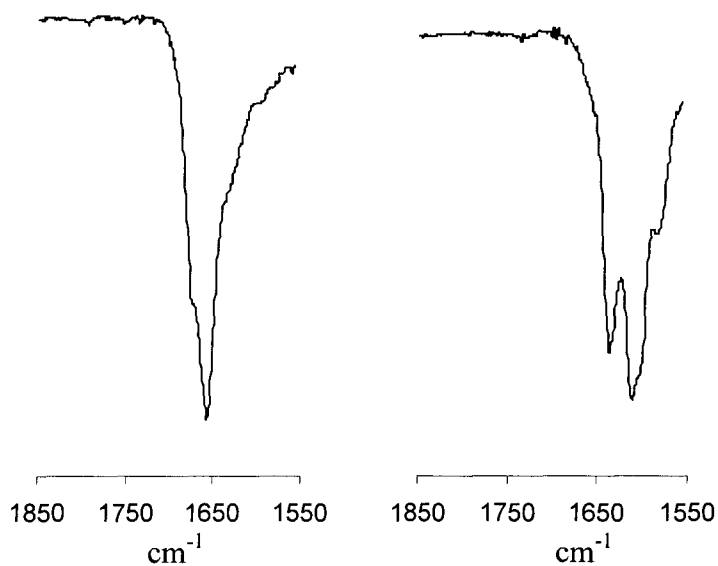
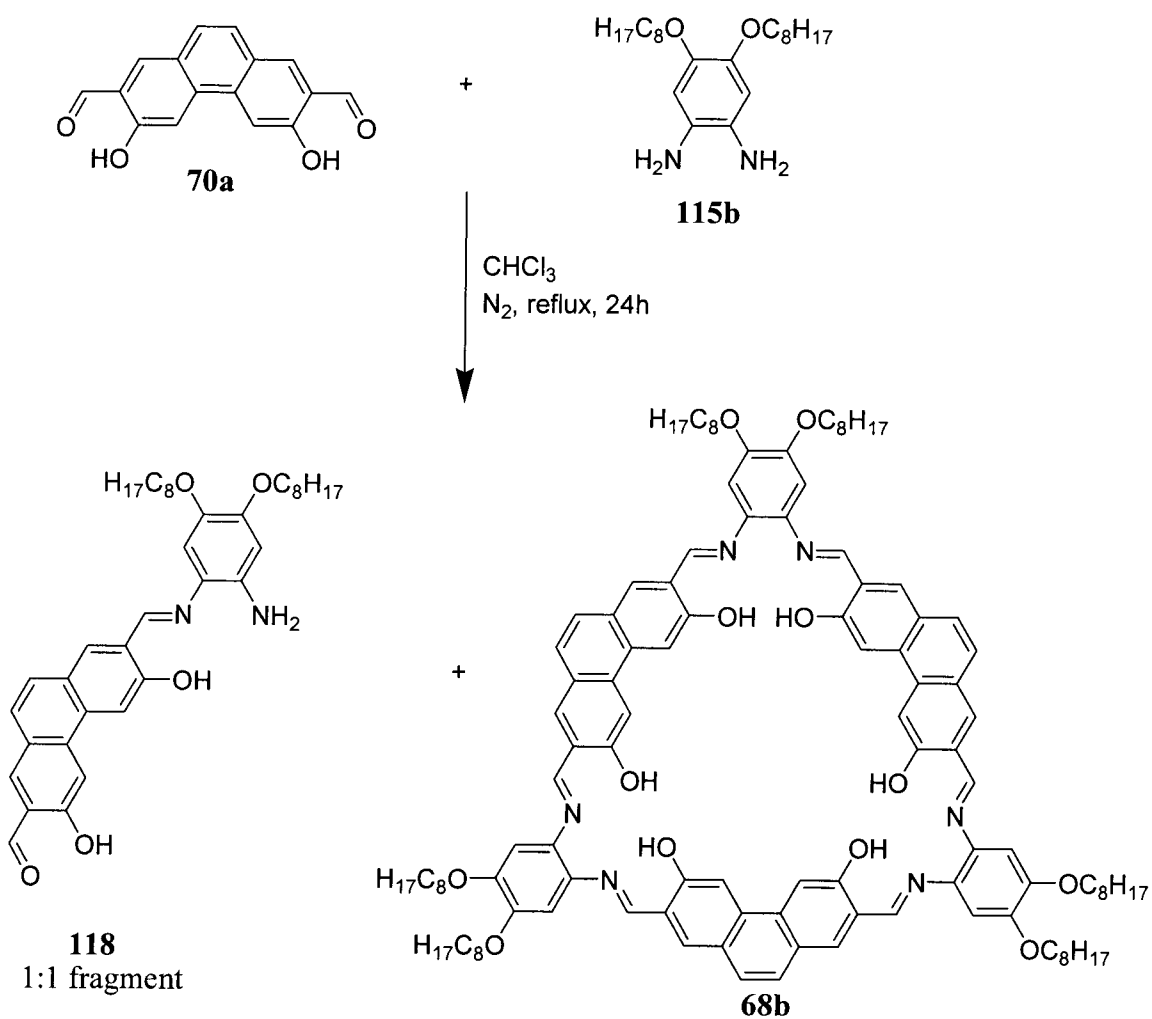


**Figure 3.1** IR spectra of **70a** (left) and **117** (right) as KBr discs.

Reaction of **70a** with 1,2-dioctyloxy-4,5-diaminobenzene **115b** in  $\text{CHCl}_3$  resulted in a more soluble product. This time, no precipitate formed during reflux. After cooling and addition of MeCN, a small amount of orange precipitate formed. The  $^1\text{H}$  NMR spectra of both the filtrate and the solid showed different sets of peaks, indicating multiple species were formed, and they could not be separated. The filtrate was composed mainly of macrocyclic fragments that were identified by electrospray ionization mass spectrometry (ESI-MS). Based on the  $^1\text{H}$  NMR spectrum (Figure 3.2, top) and ESI-MS, it is clear that the bulk of the product is a 1:1 (diol:diamine) fragment **118**, with traces of larger 2:1 and 2:2 fragments. Further reflux of the products did not

change the composition of the product, as the 1:1 fragment remained the most prominent species.

**Scheme 3.3** Synthesis of **68b**.



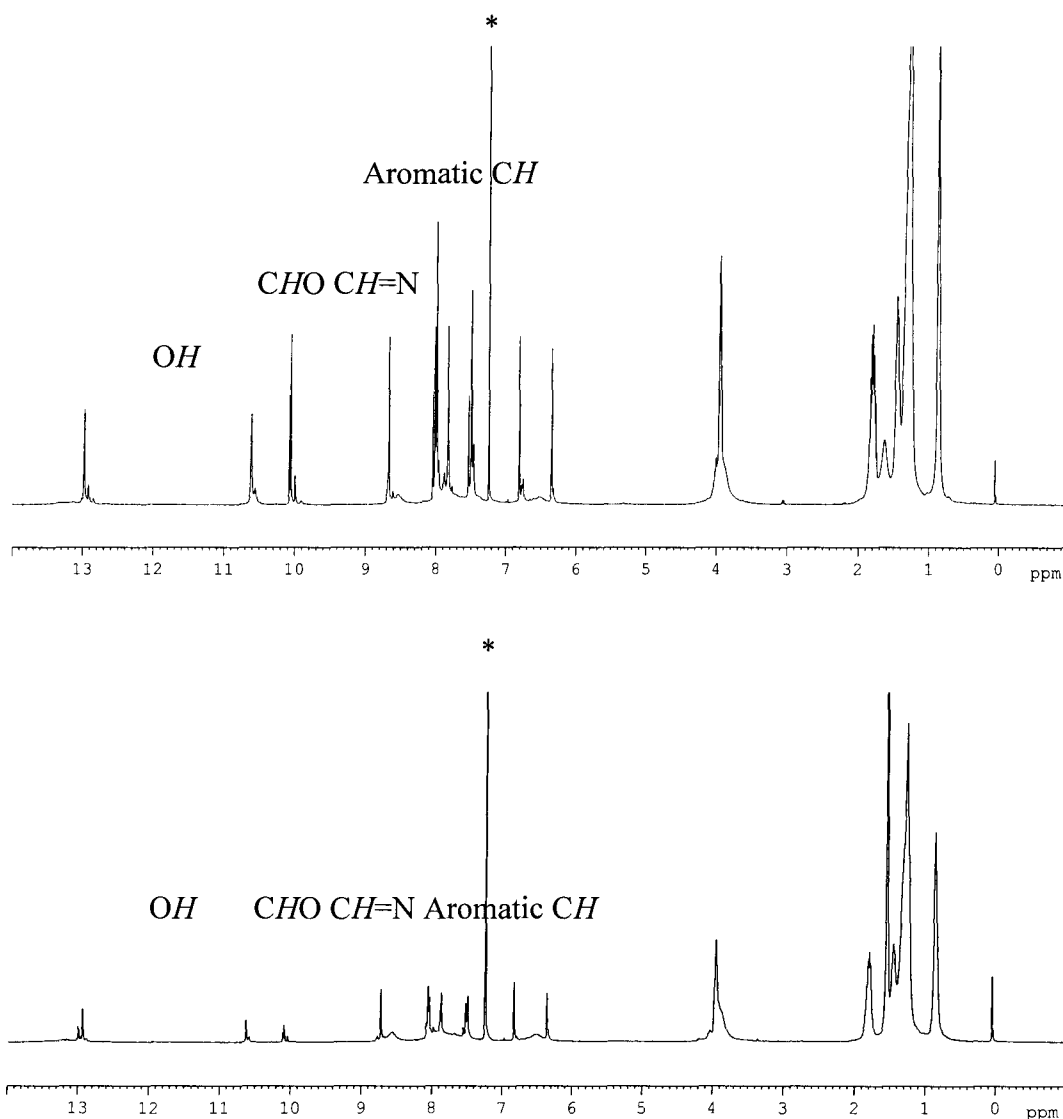


**Figure 3.2** <sup>1</sup>H NMR spectra (400 MHz, CDCl<sub>3</sub>) of filtrate (top) and solid (bottom) of **68b** synthesis (\* = CDCl<sub>3</sub>).

Matrix-assisted laser desorption ionization time-of-flight (MALDI-TOF) mass spectrometry of the solid showed the presence of the full macrocycle **68b**, (Figure 3.3) though the <sup>1</sup>H NMR spectrum (Figure 3.2, bottom) showed that the solid contained a mixture of products, including several fragments. Interestingly, the MALDI-TOF mass spectrum prepared from a more concentrated solution showed evidence for a larger [4+4] macrocycle.

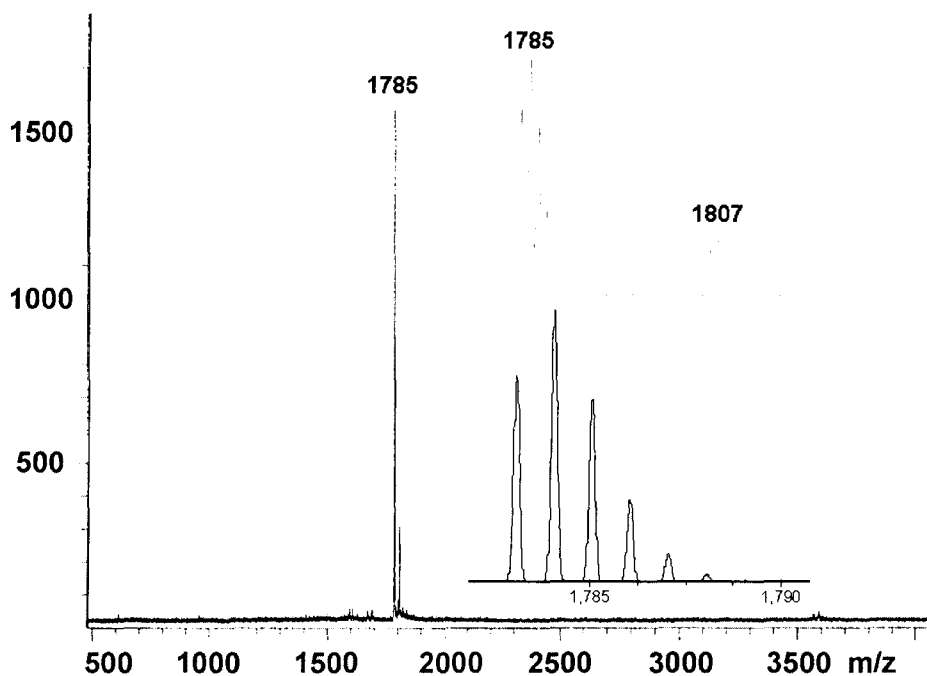


**Figure 3.3** MALDI-TOF spectrum of macrocycle **68b**. The insets show a simulation of the simulated isotope distribution for the  $[\mathbf{68b} + \text{H}]^+$  ion (bottom) and the expanded experimental data for this peak (top).

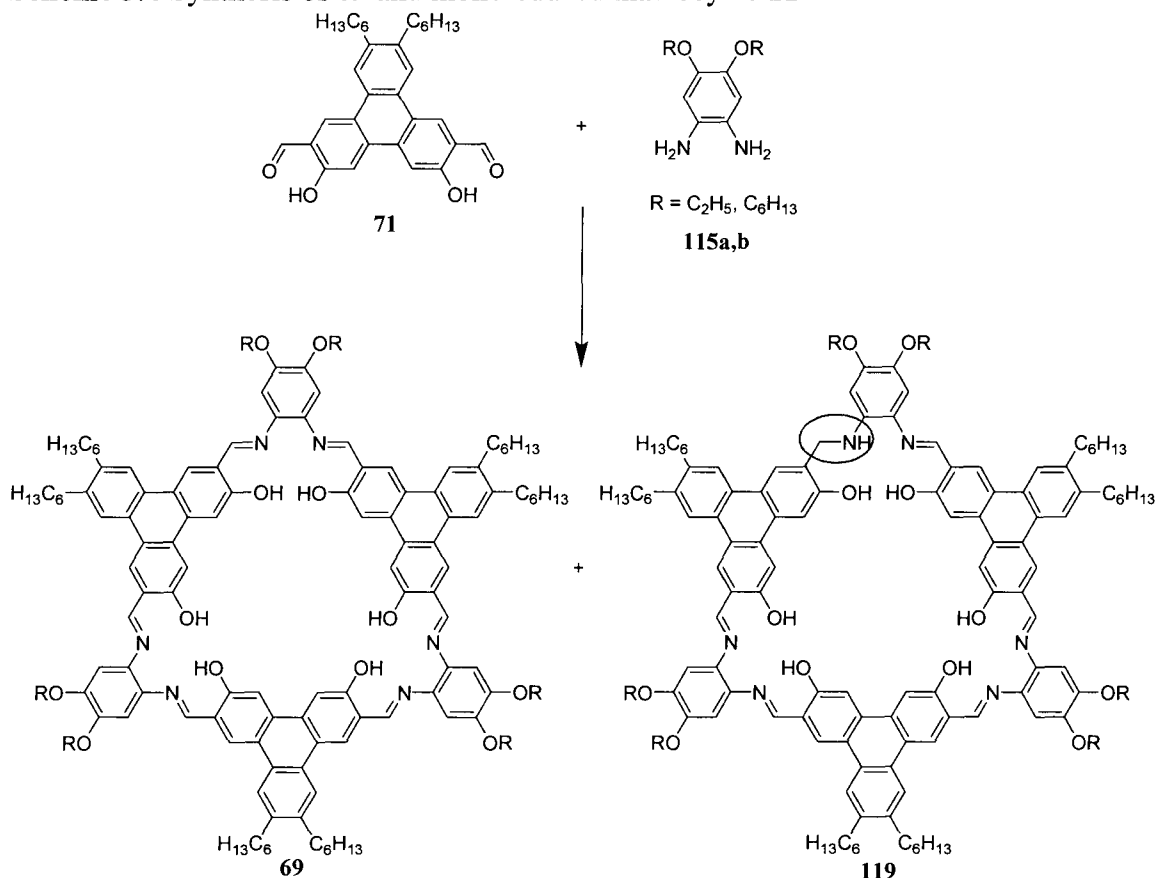
While there was moderate success in this reaction, the combination of poor yields, low solubility of the precursor, and inseparable mixture of products emphasized the need for an alternative spacer.

### 3.2.2 Synthesis of Macrocycle **69**

Triphenylene diol **71** was synthesized with greater yields and better solubility than **70a**, so it was hoped that we would obtain a soluble macrocycle with interesting properties. Initially, we tried to make macrocycle **69** by reacting **71** with 1,2-dihexyloxy-4,5-phenylenediamine **115a** in  $\text{CHCl}_3/\text{MeCN}$ , conditions that have worked well for other [3+3] Schiff base macrocycle reactions. Unfortunately, this reaction yielded a mixture of products that could not be separated, and with the hexyloxy chains, the products were too soluble. The  $^1\text{H}$  NMR spectrum of the orange solid (Figure 3.4) collected from the

reaction showed several hydroxyl protons between 11.6 and 14.8 ppm. While the largest resonance at 13.2 ppm is characteristic of a hydroxyl group hydrogen bonded to an imine, as in the intended Schiff base macrocycle, the other peaks are similar to those observed for the monoreduced macrocycle of **33**, where exactly one of the six imines has been reduced.<sup>7</sup> In addition, many other Schiff base macrocycles are often formed as partially reduced species.<sup>8</sup> Additional <sup>1</sup>H NMR evidence of a reduced macrocycle would be a N-CH<sub>2</sub> resonance, which would be present just above 4 ppm. This region in the spectrum of **69** is a broad overlap of alkoxy resonances, and it is difficult to confirm the presence of this peak. However, there are more than seven hydroxyl resonances in the spectrum, indicating that there is another unidentified species present in the product.

**Scheme 3.4** Synthesis of **69** and monoreduced macrocycle **119**.



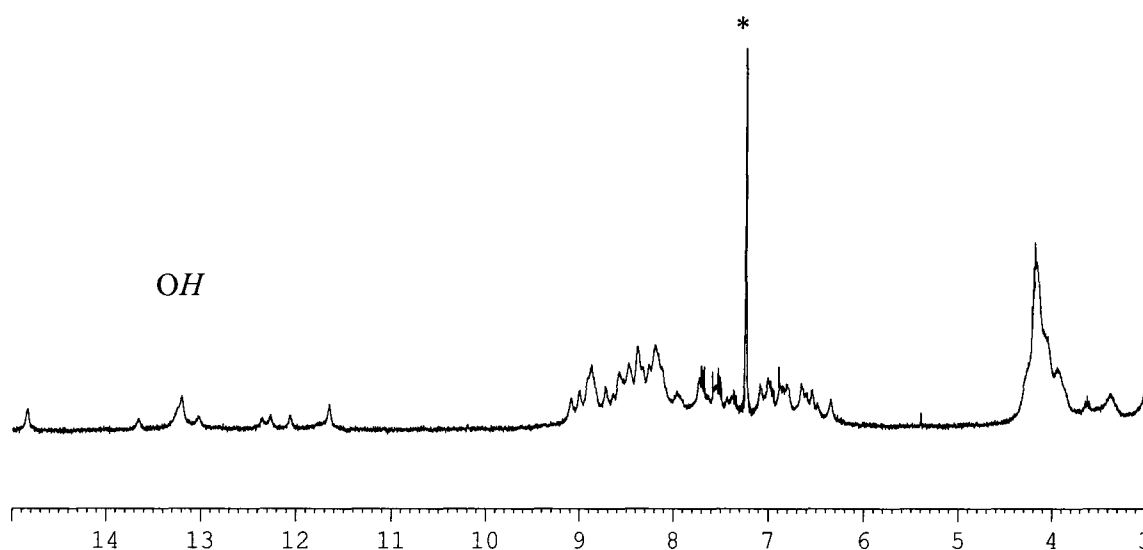


**Figure 3.4**  $^1\text{H}$  NMR spectrum (300 MHz,  $\text{CDCl}_3$ ) of reaction products from attempted synthesis of **69** (\* =  $\text{CDCl}_3$ ).

Subsequent attempts used diamine **115c** with shorter ethoxy chains, but the outcomes of the reactions were similar. In investigations of monoreduction of macrocycle **33**, Amanda Gallant identified the reducing agent to be a benzimidazoline formed in situ.<sup>7</sup> The reduction of the macrocycle could be prevented by removing all acid from the reaction solvent. In an effort to selectively form the unreduced macrocycle **69**, a variety of conditions was used (Table 3.1). In all cases, the same series of resonances was present in the  $^1\text{H}$  NMR spectrum of the recrystallized solid, as well as fragments of the macrocycle. Through  $^1\text{H}$  NMR spectroscopy and electrospray mass spectrometry, the dried filtrate of the reaction was shown to consist of fragments of the macrocycle. The 1:1 fragment was isolated by flushing the filtrate through silica using a solution of 1% MeOH in dichloromethane.

**Table 3.1** Synthetic conditions for the formation of macrocycle **69**.

Solvent	R	Metal	Product
CHCl <sub>3</sub> /MeCN	C <sub>6</sub> H <sub>13</sub>	N/A	<b>69, 119</b>
CH <sub>2</sub> Cl <sub>2</sub> /MeCN	C <sub>2</sub> H <sub>5</sub>	N/A	<b>69, 119</b> , fragment
THF	C <sub>2</sub> H <sub>5</sub>	N/A	<b>69, 119</b> , fragment
Toluene	C <sub>2</sub> H <sub>5</sub>	N/A	<b>69, 119</b> , fragment
EtOH	C <sub>2</sub> H <sub>5</sub>	Ni(OAc) <sub>2</sub>	metallated fragment
EtOH	C <sub>2</sub> H <sub>5</sub>	Zn(OAc) <sub>2</sub>	starting material

MALDI-TOF mass spectrometry of the orange product confirmed that the macrocycle had indeed formed. In fact, only the ring-closed [3+3] macrocycle is observed in the MALDI-TOF mass spectrum. By comparison of the experimental data with simulations for both unreduced and the monoreduced species (Figure 3.5), the molecular ion appears to be the protonated macrocycle. We cannot see any evidence in the mass spectrum for the monoreduced macrocycle **119**, but it may be that the conjugated macrocycle is ionized more readily.

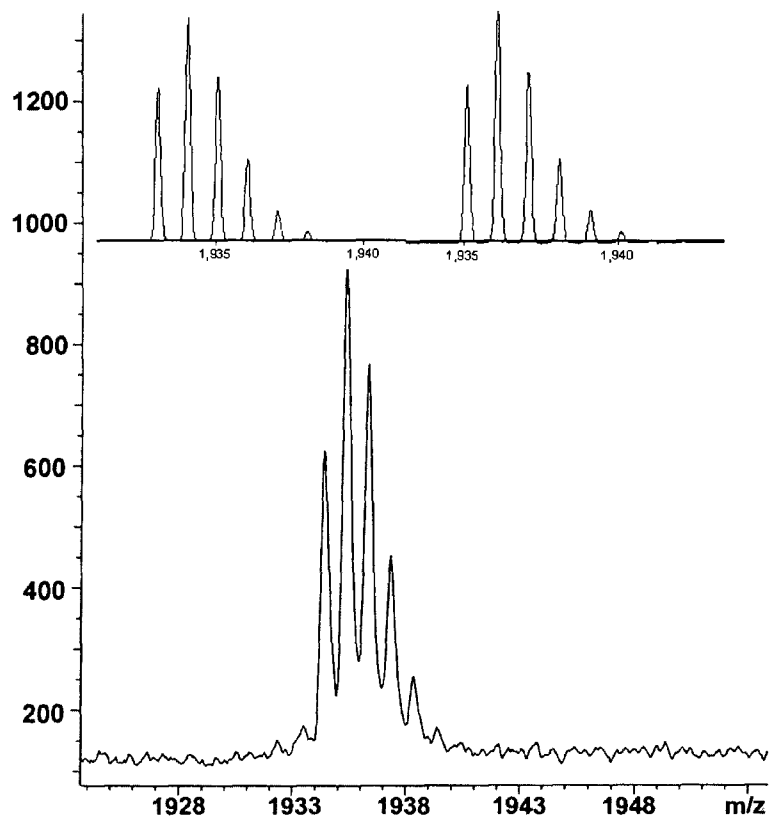


**Figure 3.5** MALDI-TOF mass spectrum of **69**. Simulations of isotope distribution for macrocycle **69** (top, left) and monoreduced macrocycle **119** (top, right).

Metal templation, which has proved to be critical in the synthesis of many Schiff base macrocycles,<sup>9</sup> was also unsuccessful. Reaction of the diol and diamine in the presence of Ni(II) gave a black solid, which was revealed to be a 2:1 diol to diamine fragment coordinated to the metal through MALDI-TOF (Figure 3.6). The same reaction in the presence of Zn(II) gave only starting material and a soluble red product.

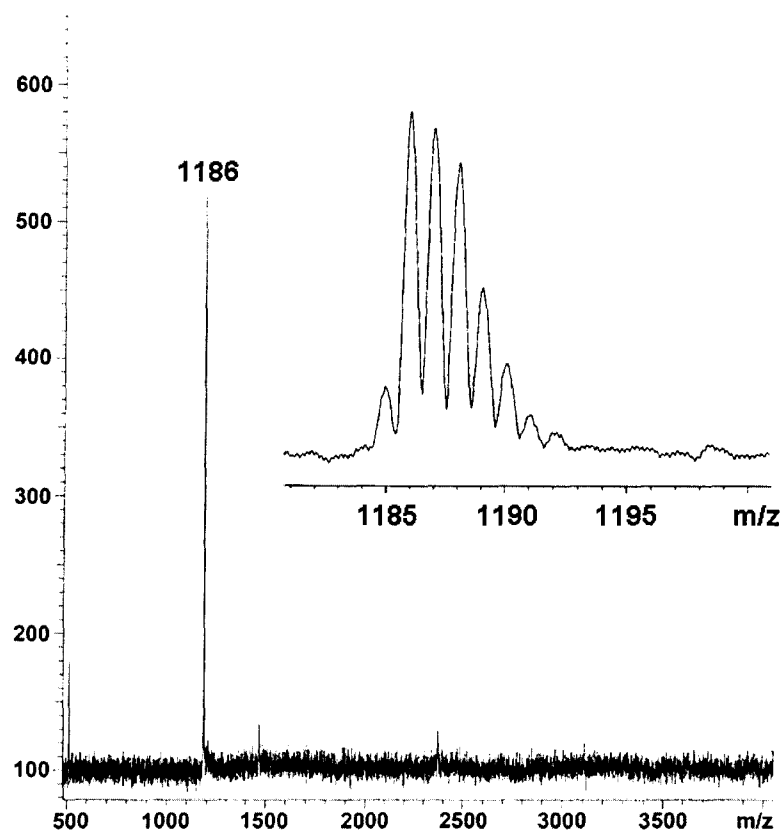
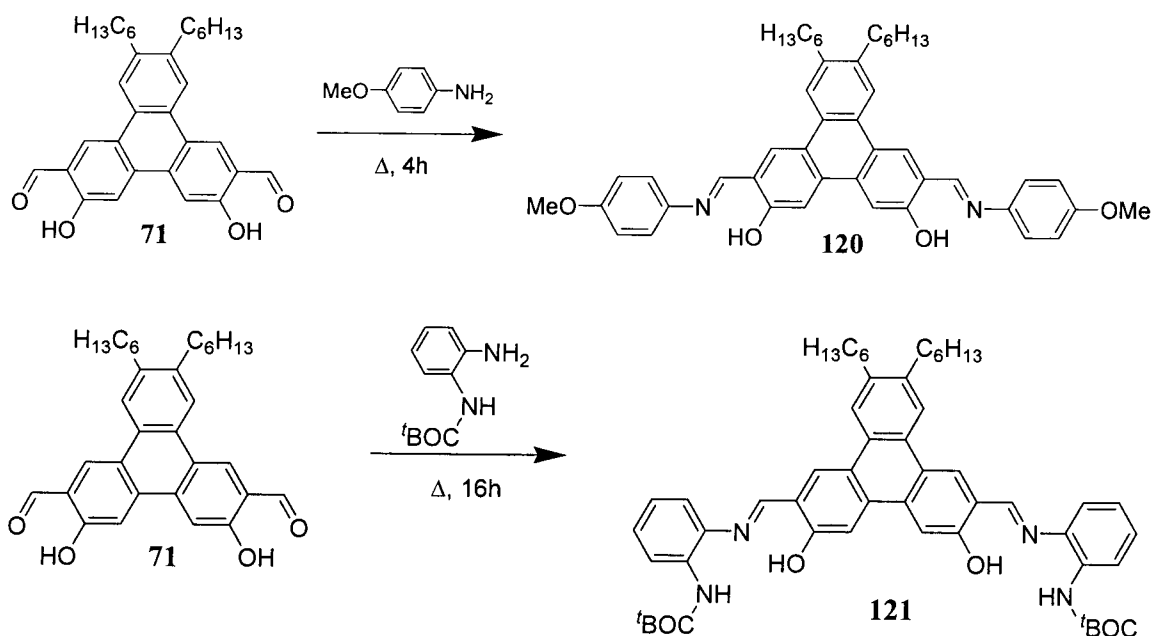


**Figure 3.6** MALDI-TOF mass spectrum of Ni(II)-templated product, with magnification inset.

After initial attempts to form the pure macrocycle failed, two model compounds were synthesized to ensure that **71** could react with amines without reduction. Model compounds **120** and **121** were synthesized by reacting excess amine with **71** and yielded crystalline solids (Scheme 3.5). The  $^1\text{H}$  NMR spectra of these compounds show imine resonances at 8.86 and 8.90 ppm, respectively. There is no indication of either reduction of the imine bond or isomerization to the keto-enamine tautomer of the macrocycle, which was observed previously with a naphthalene diol.<sup>10</sup>

**Scheme 3.5** Synthesis of model compounds **120** and **121**.

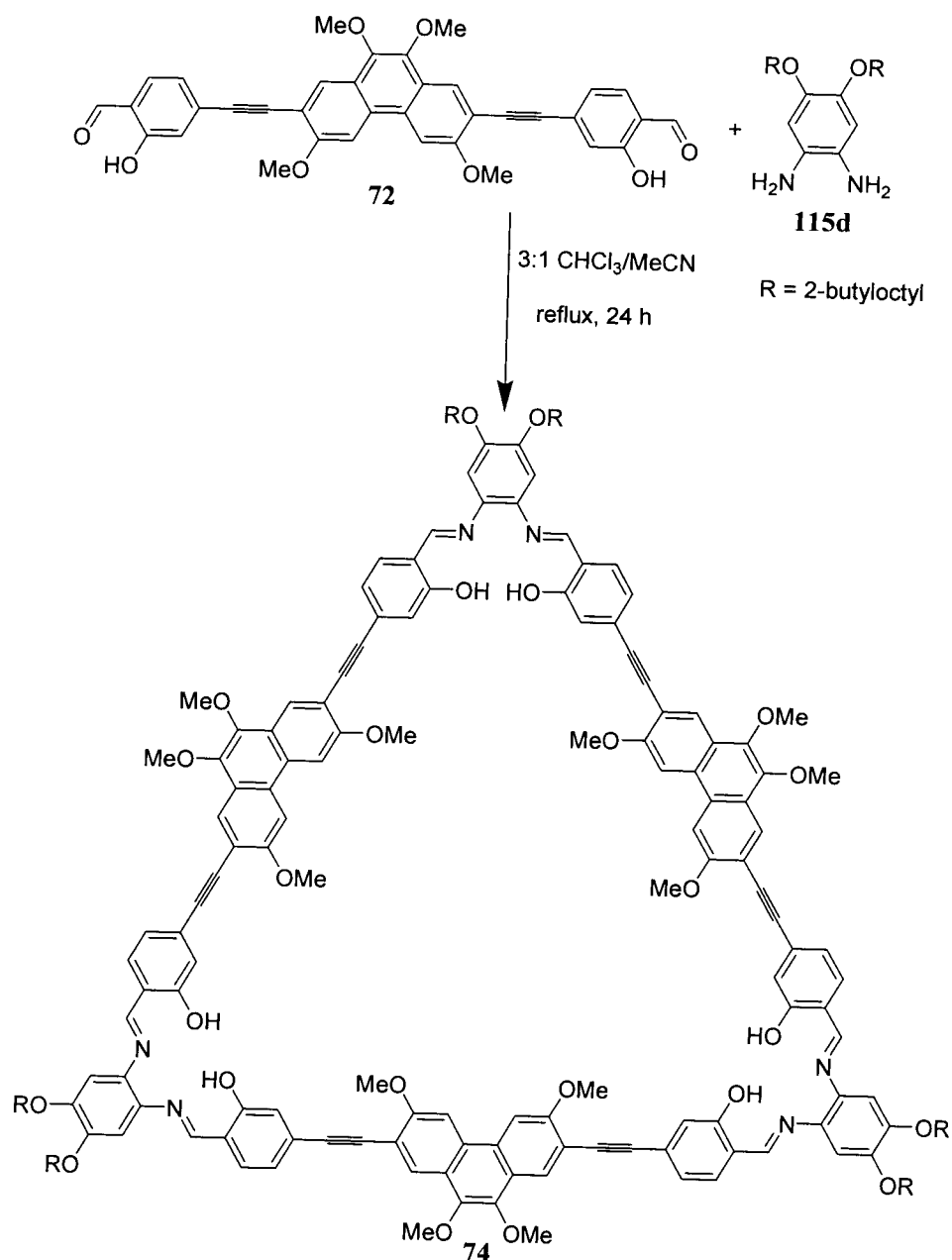


Although spectral data indicate that macrocycles **68** and **69** were formed, they were both synthesized in low yield and purity. In each case, the salicylate groups are on the polycyclic aromatic spacer, but it is unclear why this hinders macrocycle formation.

### 3.2.3 Synthesis of Macrocycle **74** and Macrocycle **75**

While synthesis of macrocycles with the salicylate moieties incorporated directly into a polycyclic aromatic system seems to be complicated by other factors, larger diols containing ethynyl groups, such as **72**, have been found to proceed without problems. Diol **72** has short alkoxy chains, therefore reaction with a diamine bearing longer alkoxy chains is needed to produce a soluble macrocycle (Scheme 3.6). This is achieved using diamine **115d** with 2-butyloctyloxy chains.

**Scheme 3.6** Synthesis of macrocycle **74**.



Unfortunately, long chains prevent easy recrystallization. After reflux of the precursors to form macrocycle, more MeCN was added while the solution was still hot. Dark red solid formed upon cooling, but after filtration, a great deal of product still remained in the filtrate. Heating of the filtrate in a mixture of CHCl<sub>3</sub> and MeCN until the

solid is just dissolved, followed by slow cooling allows for additional recrystallization. Often, the solid cannot be filtered and must be separated by centrifugation of the mixture. This procedure is repeated until the  $^1\text{H}$  NMR spectrum of the macrocycle (Figure 3.7) does not show resonances for the 1:1 fragment, which has a characteristic resonance assigned to a formyl group at 9.9 ppm. The  $^1\text{H}$  NMR spectrum of the macrocycle shows the *OH* resonance at 13.32 ppm and the imine resonance at 8.62 ppm.

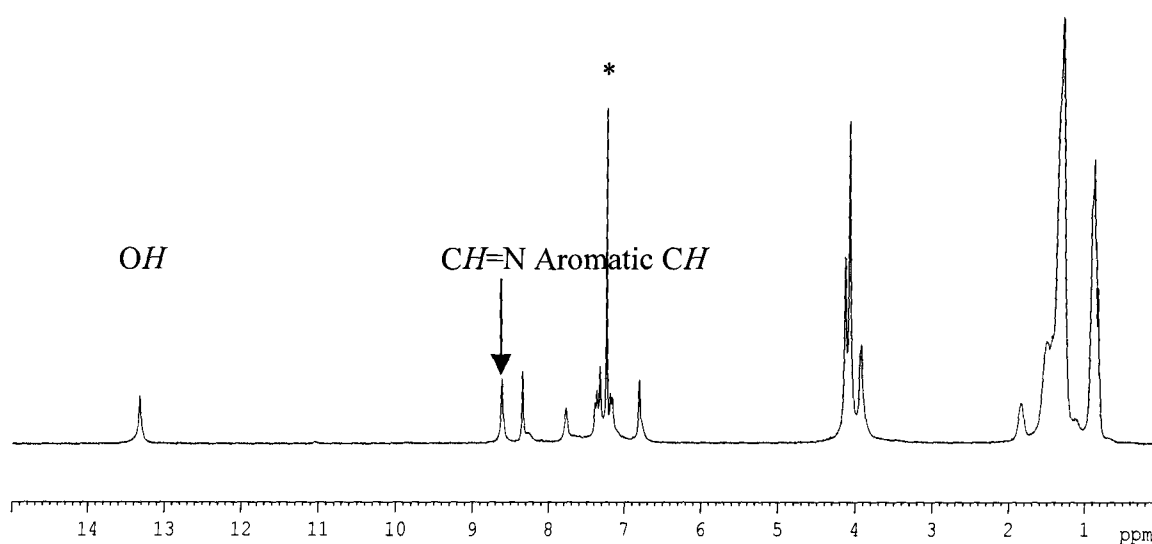


**Figure 3.7**  $^1\text{H}$  NMR spectrum (300 MHz) of **74** in  $\text{CDCl}_3$  (\* =  $\text{CDCl}_3$ ).

The MALDI-TOF mass spectrum for the macrocycle is seen in Figure 3.8. The spectrum shows the peak corresponding to the fully formed [3+3] macrocycle plus one proton at  $m/z = 3083$ . There is also a small peak at  $m/z = 1045$  corresponding to the 1:1 fragment, which is never fully removed, as well as a small peak at  $m/z = 3100$ , which corresponds to the macrocycle plus a molecule of water.

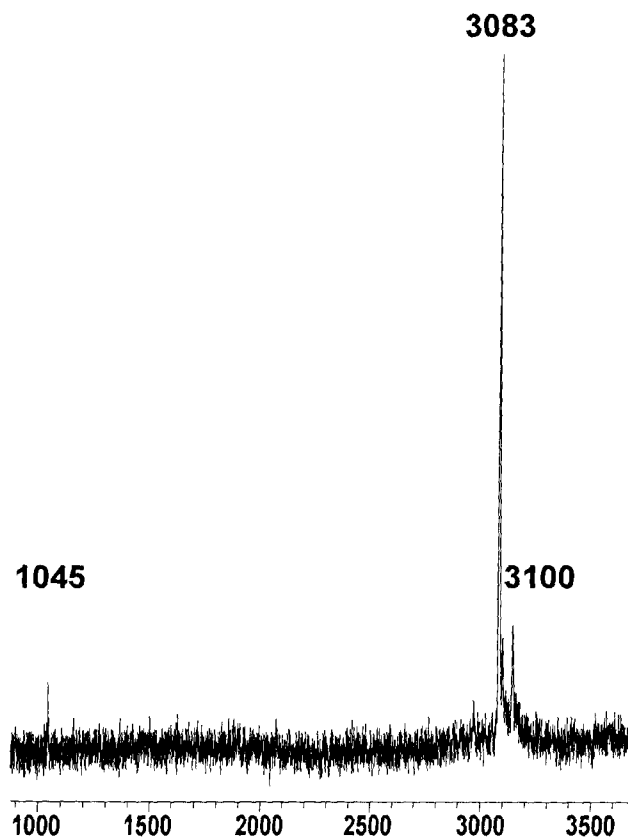
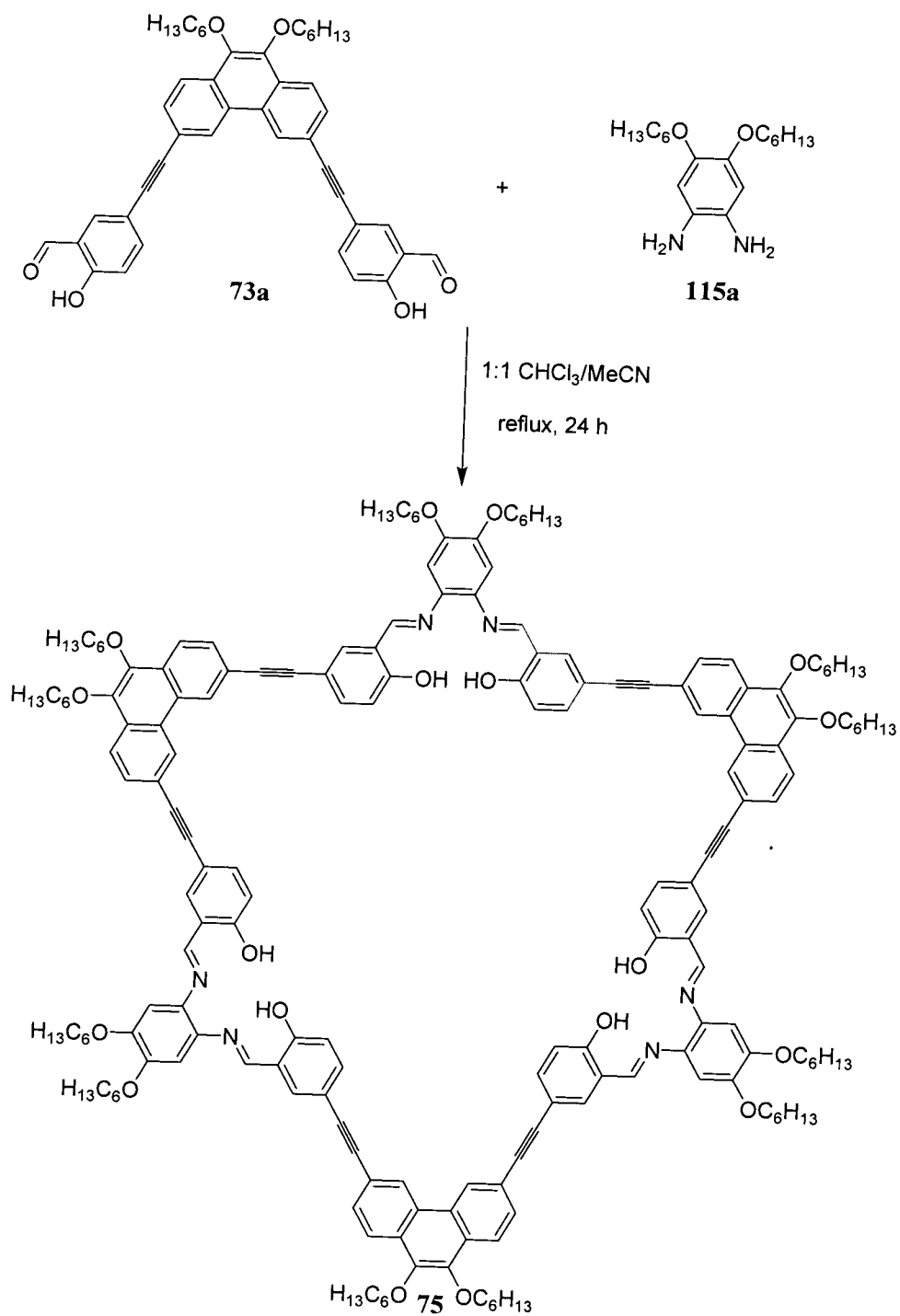


**Figure 3.8** MALDI-TOF mass spectrum of **74**.

The reaction of **73b** with diamine **115a** in  $\text{CHCl}_3$  and MeCN makes a [3+3] macrocycle that precipitates upon cooling of the reaction mixture. Macrocycle **75** is recrystallized in the same solvent and is a bright orange solid. Unlike **74**, **75** can be represented such that it is not fully conjugated through the backbone. In Scheme 3.7, some adjacent single bonds are denoted in red, highlighting the break in conjugation.

**Scheme 3.7** Synthesis of **75**. Breaks in the conjugation are denoted in red.



The  $^1\text{H}$  NMR spectrum of **75** shows the expected hydroxyl resonance as well as the imine resonance which overlaps with one of the phenanthrene peaks. The phenylenediimine proton at 6.36 ppm is broad as is the phenylenediimine alkoxy peak at 3.81 ppm. At room temperature, the  $^1\text{H}$  NMR sample was not fully dissolved, so the sample was heated to 40 °C. The peaks sharpened and it was noted that many of the peaks moved significantly downfield. This observation and additional NMR data will be further discussed in Chapter 4.

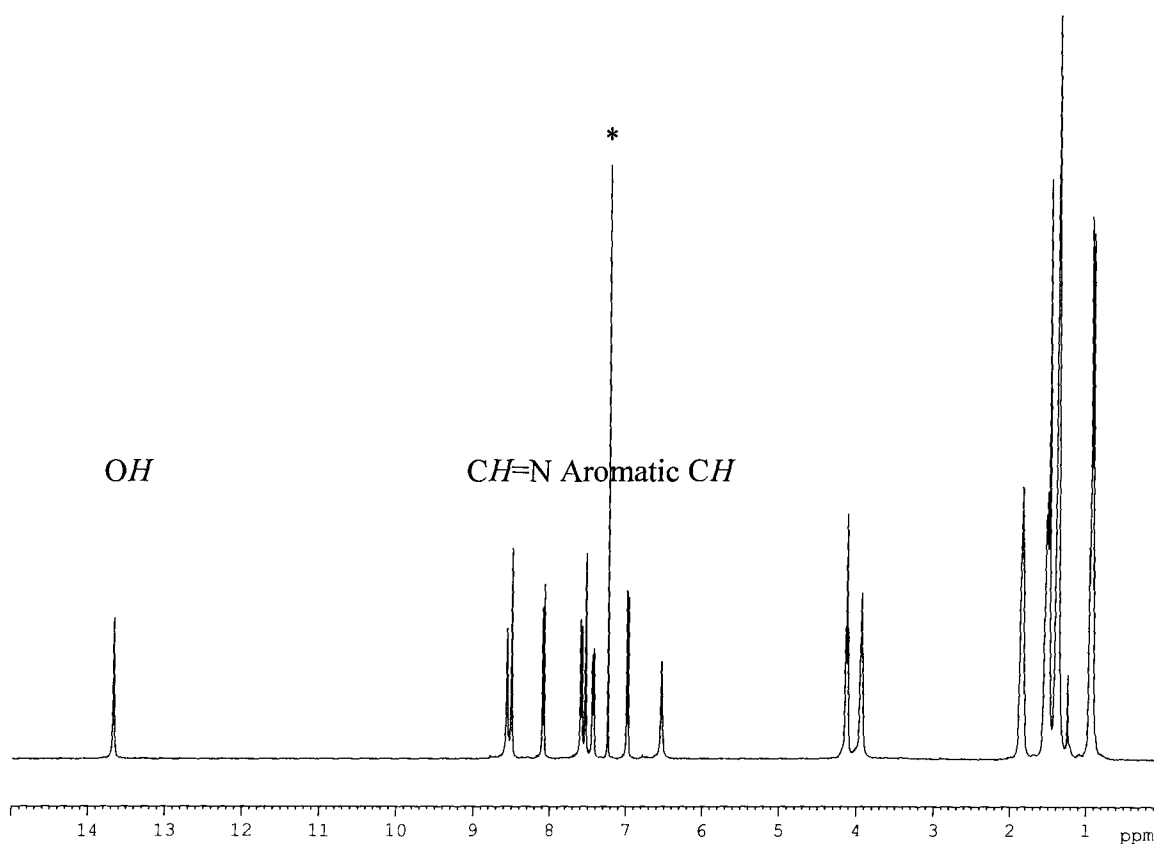


**Figure 3.9**  $^1\text{H}$  NMR spectrum (400 MHz) of **75** in  $\text{CDCl}_3$  (\* =  $\text{CDCl}_3$ ).

The MALDI-TOF mass spectrum of **75**, in Figure 3.10 shows the peak for the protonated macrocycle at  $m/z = 2819$ , confirming the formation of the [3+3] macrocycle.

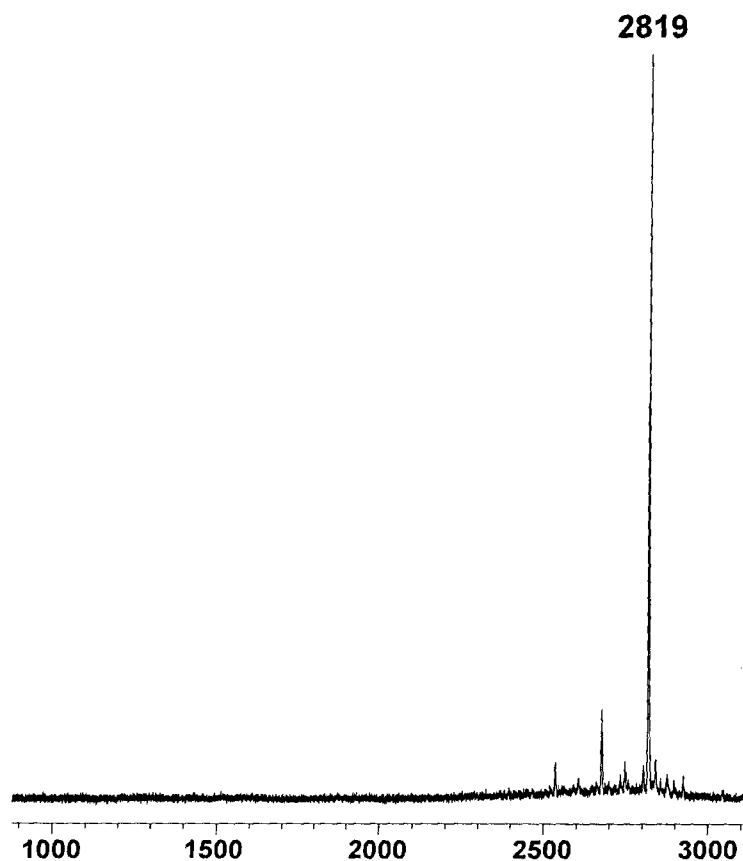


**Figure 3.10** MALDI-TOF mass spectrum of **75**.

Crystals of this macrocycle were grown in DCM and MeCN through slow cooling of a solution. However, once removed from the solution by the crystallographer, the crystals fell apart due to evaporation of the solvent from the large internal cavity of the macrocycle.

### 3.2.4 Conclusions

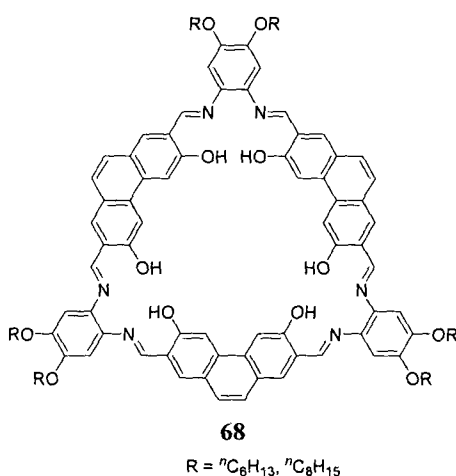
Phenanthrene and triphenylene-containing Schiff base macrocycles **68** and **69** can be synthesized but in poor yield and purity. Large Schiff base macrocycles **74** and **75**, which contain phenanthrene ethynylene spacers can be made in good yield and purity. The properties of these macrocycles will be discussed in Chapter 4.

### 3.3 Experimental

#### 3.3.1 General Methods and Materials

$\text{CHCl}_3$  and MeCN were dried over molecular sieves and degassed before use. Diamines **115a-d**<sup>11</sup> and BOC-protected phenylenediamine<sup>12</sup> were prepared according to literature procedure. Matrix-assisted laser desorption ionization time of flight (MALDI-TOF) mass spectra were obtained in the UBC Mass Spectrometry facility using dithranol as a matrix. All other methods and materials are as outlined in Section 2.3.1.

#### 3.3.2 Synthetic Procedures



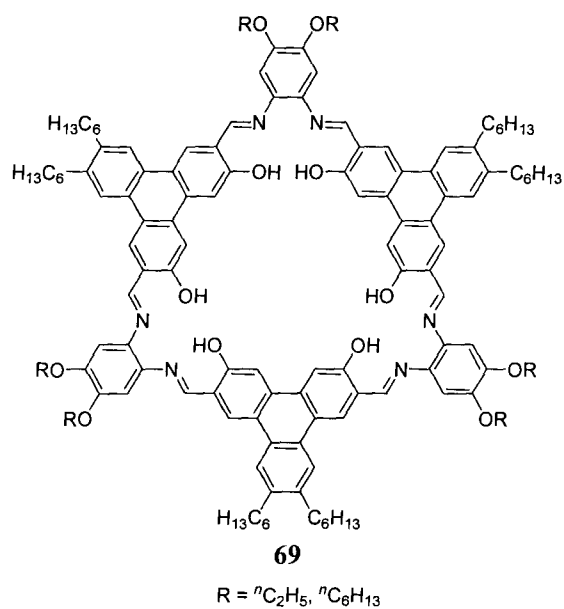
**Attempted Synthesis of Macrocycle 68** – Equimolar amounts of compound **70a** and 1,2-dialkoxy-4,5-diaminobenzene **115a** or **115b** were combined in a Schlenk flask. Degassed  $\text{CHCl}_3$  was added and the resulting solution was heated to reflux for 24 h. After cooling, any precipitate was filtered, or MeCN was added until precipitate

formed. The products are unstable to chromatographic separation on silica or alumina.

**Data for the insoluble product 117 when R = <sup>n</sup>C<sub>6</sub>H<sub>13</sub>.** IR (KBr):  $\nu = 3051, 2952, 2928, 2857, 1636, 1611, 1506, 1465, 1370, 1256, 1190, 1165, 1120, 1017, 959 \text{ cm}^{-1}$ .

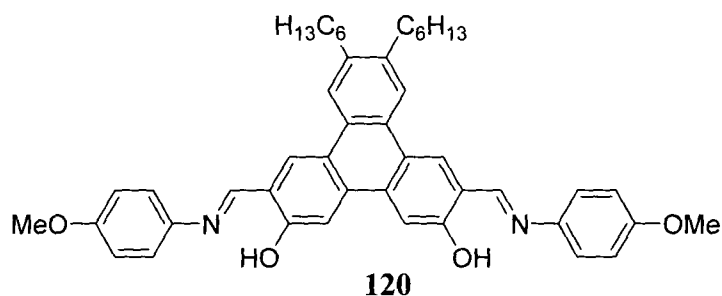
**Data obtained for filtrate when R =  ${}^n\text{C}_8\text{H}_{17}$ .**  ${}^1\text{H}$  NMR (400 MHz,  $\text{CDCl}_3$ , 25 °C):  $\delta$  12.97, 10.61, 10.07, 10.05, 8.66, 8.01, 7.99, 7.82, 7.49, 6.80, 6.34, 3.95, 1.82-0.86 (hexyloxy chain); ESI-MS:  $m/z = 614$  ( $\text{M}^+$ , 1:1 fragment **118**).

**Data for solid obtained from reaction with R =  ${}^n\text{C}_8\text{H}_{17}$ .**  ${}^1\text{H}$  NMR (400 MHz,  $\text{CDCl}_3$ , 25 °C):  $\delta$  13.00, 12.93, 10.63, 10.11, 10.09, 8.72, 8.52, 8.06, 8.03, 7.87, 7.51, 7.49, 6.83, 6.36, 3.95, 1.83-0.86 (hexyloxy chain); MALDI-TOF:  $m/z = 1785$  ( $[\text{68b} + \text{H}]^+$ ).



**Attempted Synthesis of Macrocycle 69 –** Equimolar amounts of compound **71** and 1,2-dialkoxy-4,5-diaminobenzene **115a** or **115c** were combined in a Schlenk flask. Solvent was added and the resulting solution was heated to reflux. For specific conditions, see Table 3.1.

**Data for 69.**  ${}^1\text{H}$  NMR (300 MHz,  $\text{CDCl}_3$ , 25 °C):  $\delta$  14.84, 13.66, 13.21, 13.02, 12.35, 12.28, 12.06, 11.65, 9.2-6.3, 4.2-3.8, 2.9-2.7, 2.0-0.8; MALDI-TOF-MS:  $m/z = 1935$  ( $[\text{M} + \text{H}]^+$ ).



## Synthesis of Model

### Compound 120 – Compound

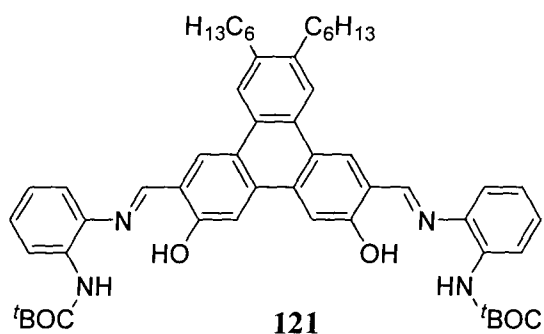
71 (0.058 g, 0.120 mmol) and

*p*-anisidine (0.46 g, 0.373

mmol) were combined in a

flask and dissolved in dry THF to form a yellow solution. After refluxing for 4 h, the solution was cooled, and the volume of solvent was reduced. Upon addition of MeOH, an orange solid precipitated, was filtered, and was washed with MeOH and petroleum ether to yield 0.071 g (0.102 mmol, 86%) of product.

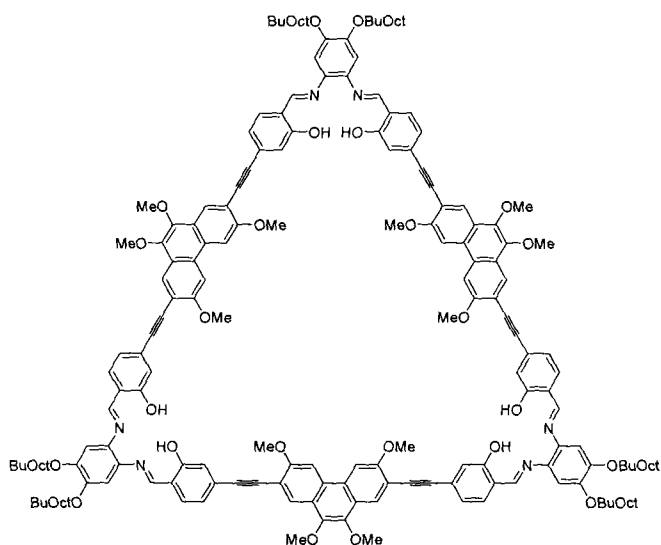
**Data for 120.** <sup>1</sup>H NMR (300 MHz, CDCl<sub>3</sub>, 25 °C): δ 13.21 (s, 2H, OH), 8.86 (s, 2H, CH=N), 8.50 (s, 2H, aromatic CH), 8.16 (s, 2H, aromatic CH), 8.01 (s, 2H, aromatic CH), 7.36 (d, 4H, aromatic CH), 6.96 (d, 4H, aromatic CH), 3.85 (s, 6H, OCH<sub>3</sub>), 2.81 (m, 4H, CH<sub>2</sub>), 1.73 (m, 4H, hexyl chain), 1.48 (m, 4H, hexyl chain), 1.36 (m, 8H, hexyl chain), 0.92 (t, 6H, hexyl CH<sub>3</sub>); <sup>13</sup>C NMR (75.5 MHz, CDCl<sub>3</sub>, 25 °C): δ 160.1, 159.3, 158.9, 141.5, 140.0, 132.9, 127.8, 126.8, 123.7, 122.9, 122.7, 120.9, 114.9, 110.9, 55.8, 33.5, 32.1, 31.9, 29.9, 23.0, 14.4; EI-MS: *m/z* = 694 (M<sup>+</sup>); IR (KBr): ν = 3424, 3029, 2952, 2926, 2861, 1616, 1507, 1457, 1366, 1297, 1250, 1183, 1032, 832, 696 cm<sup>-1</sup>; UV-Vis (CH<sub>2</sub>Cl<sub>2</sub>): λ<sub>max</sub> (ε) = 287 (5.8 x 10<sup>4</sup>), 340 (2.8 x 10<sup>4</sup>), 359 (3.2 x 10<sup>4</sup>), 401 (5.2 x 10<sup>4</sup>) nm (L mol<sup>-1</sup>cm<sup>-1</sup>); Mp. = 212-213 °C; Anal. Calc'd for C<sub>46</sub>H<sub>50</sub>N<sub>2</sub>O<sub>4</sub>: C, 79.51, H, 7.25, N, 4.03. Found: C, 79.74, H, 7.41, N, 4.19.



### Synthesis of Model Compound 121 –

Compound **71** (0.062 g, 0.128 mmol) and *N*-(*tert*-butyloxycarbonyl)1,2-diaminobenzene (0.087 g, 0.418 mmol) were combined in a flask and dissolved in 10 mL THF. After refluxing the solution overnight, the solvent was reduced and precipitated by MeOH. The product was recrystallized in DCM and hexanes. Filtration of the yellow solid yielded 0.091 g (0.105 mmol, 83%) of product.

**Data for 121.**  $^1\text{H}$  NMR (400 MHz,  $\text{CDCl}_3$ , 25 °C):  $\delta$  12.22 (s, 2H, OH), 8.90 (s, 2H, N=CH), 8.63 (s, 2H, aromatic CH), 8.21 (s, 2H, aromatic CH), 8.20 (d, 2H, NH), 8.12 (s, 2H, aromatic CH), 7.31 (m, 2H, aromatic CH), 7.17-7.07 (m, 6H, aromatic CH), 2.82 (m, 4H,  $\text{CH}_2$ ), 1.73 (m, 4H, hexyl chain), 1.53 (s, 18H, *t*-butyl H), 1.48 (m, 4H, hexyl chain), 1.36 (m, 8H, hexyl chain), 0.90 (t, 6H, hexyl  $\text{CH}_3$ );  $^{13}\text{C}$  NMR (100.7 MHz,  $\text{CDCl}_3$ , 25 °C):  $\delta$  164.2, 158.5, 152.8, 140.4, 138.1, 133.4, 132.9, 128.8, 128.5, 126.7, 124.2, 123.5, 123.0, 120.9, 119.6, 118.6, 111.2, 81.2, 33.4, 32.0, 31.9, 29.8, 28.6, 22.9, 14.4; ESI-MS:  $m/z = 865$  ( $\text{M}^+$ ); IR (KBr):  $\nu = 3436, 2955, 2925, 1736, 1639, 1609, 1595, 1510, 1447, 1366, 1216, 1159, 1048, 898, 751$   $\text{cm}^{-1}$ ; UV-Vis ( $\text{CH}_2\text{Cl}_2$ ):  $\lambda_{\text{max}}$  ( $\epsilon$ ) = 263 ( $5.2 \times 10^4$ ), 289 ( $5.5 \times 10^4$ ), 410 ( $3.8 \times 10^4$ ) nm ( $\text{L mol}^{-1}\text{cm}^{-1}$ ); Mp. = 223-226 °C; Anal. Calc'd for  $\text{C}_{54}\text{H}_{64}\text{N}_4\text{O}_6 \cdot 2 \text{H}_2\text{O}$ : C, 71.97, H, 7.61, N, 6.22. Found: C, 71.88, H, 7.29, N, 6.40.



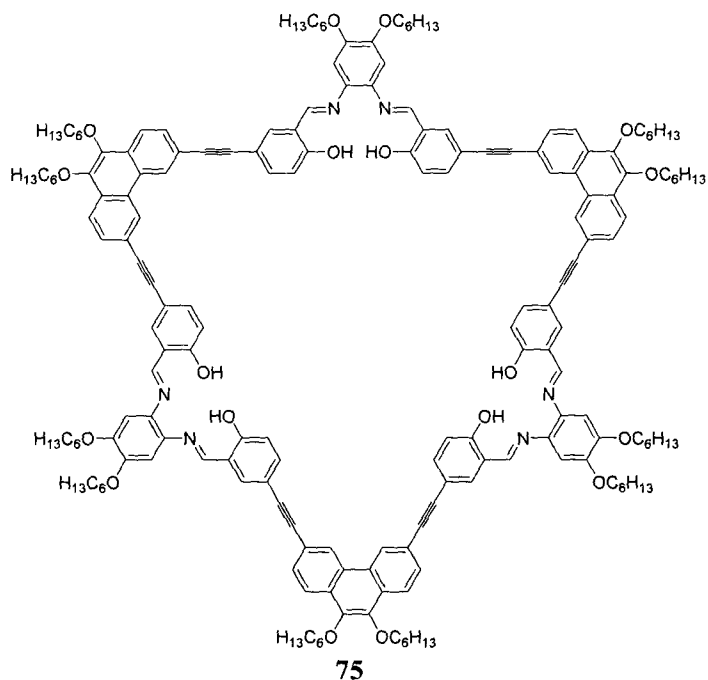
74

### Synthesis of Macrocycle 74 -

Compounds **72** (0.145 g, 0.247 mmol) and **115d** (0.118 g, 0.247 mmol) were combined in a Schlenk flask in the glovebox. Degassed  $\text{CHCl}_3$  (15 mL) and MeCN (5 mL) were added to the flask and the solution was heated to reflux. After heating for 24 h,

the solution was cooled and the solid was precipitated by addition of MeCN. The solid was recrystallized from DCM and MeCN. Yield: 0.180 g, 0.0584 mmol, 71%.

**Data for 74.**  $^1\text{H}$  NMR (300 MHz,  $\text{CDCl}_3$ )  $\delta$  13.32 (s, 6H, OH), 8.62 (s, 6H, CH=N), 8.34 (s, 6H, aromatic CH), 7.78 (s, 6H, aromatic CH), 7.38 (d, 6H,  $J = 8.0$  Hz, aromatic CH), 7.31 (s, 6H, aromatic CH), 7.17 (d, 6H,  $J = 8.0$  Hz, aromatic CH), 6.81 (2, 6H, phenylenediimine CH), 4.13 (s, 18H,  $\text{OCH}_3$ ), 4.08, (s, 18H,  $\text{OCH}_3$ ), 3.93 (d, 12H,  $\text{OCH}_2$ ), 2.0-0.80 (m, 138H, BuOct H);  $^{13}\text{C}$  NMR (75.5 MHz,  $\text{CDCl}_3$ )  $\delta$  161.1, 157.9, 149.8, 142.4, 135.3, 132.1, 129.0, 128.5, 127.9, 124.4, 122.5, 120.8, 119.7, 114.2, 103.0, 94.5, 88.7, 72.5, 61.4, 56.5, 38.4, 32.2, 31.6, 31.3, 30.0, 29.4, 27.2, 23.3, 23.0, 14.4; MALDI-TOF-MS:  $m/z = 3084$  ( $[\text{M}+\text{H}]^+$ ); IR (KBr):  $\nu = 3430, 2952, 2932, 2859, 2204, 1606, 1511, 1457, 1367, 1252, 1207, 1172, 1103, 1015, 813, 696$   $\text{cm}^{-1}$ ; UV-Vis ( $\text{CH}_2\text{Cl}_2$ ):  $\lambda_{\text{max}}$  ( $\epsilon$ ) = 300 ( $1.3 \times 10^5$ ), 384 ( $2.2 \times 10^5$ ) nm ( $\text{L mol}^{-1}\text{cm}^{-1}$ ); Fluorescence ( $\text{CH}_2\text{Cl}_2$ ):  $\lambda_{\text{em}} = 567$  nm ( $\lambda_{\text{exc}} = 383$  nm); Mp. > 300 °C; Anal. Calc'd for  $\text{C}_{198}\text{H}_{234}\text{N}_6\text{O}_{24} \cdot 2\text{H}_2\text{O}$ : C, 76.27, H, 7.69, N, 2.70. Found C, 75.94, H, 7.79, N, 3.11.



### Synthesis of Macrocycle 75 –

To a mixture of compound **73a** (0.206 g, 0.309 mmol) and diamine **115a** (0.096 g, 0.311 mmol) was added 10 mL of each CHCl<sub>3</sub> and MeCN. The resulting solution was refluxed for 24 h after which an orange solid precipitated and was filtered. For additional

purification, the product was recrystallized in hot CHCl<sub>3</sub> and MeCN, and washed with petroleum ether. Yield: 0.156 g, 0.0554 mmol, 53%.

**Data for 75.** <sup>1</sup>H NMR (400 MHz, CDCl<sub>3</sub>) δ 13.78 (s, 6H, OH), 8.50 (s, 6H, CH=N), 8.47 (s, 6H, aromatic CH), 8.08 (d, 6H, *J* = 8.5 Hz, aromatic CH), 7.60 (d, 6H, *J* = 8.5 Hz, aromatic CH), 7.53 (s, 6H, *J* = 1.3 Hz, aromatic CH), 7.40 (dd, 6H, *J*<sub>1</sub> = 8.6 Hz, *J*<sub>2</sub> = 1.4 Hz, aromatic CH), 6.98 (d, 6H, *J* = 8.6 Hz, aromatic CH), 6.36 (s, 6H, aromatic CH), 4.15 (t, 12H, phenanthryl OCH<sub>2</sub>), 3.81 (t, 12H, phenylenediimine OCH<sub>2</sub>), 1.87-0.94 (m, 132H, hexyl chains); <sup>13</sup>C NMR (100.7 MHz, CDCl<sub>3</sub>) δ 161.8, 159.5, 149.1, 143.8, 136.4, 135.7, 134.8, 129.2, 128.1, 126.3, 122.4, 120.8, 119.6, 118.1, 113.8, 90.2, 88.9, 73.6, 69.3, 32.1, 31.9, 30.8, 29.4, 26.2, 26.0, 23.0, 22.9, 14.4, 14.3; MALDI-TOF-MS: *m/z* = 2818.9 ([M+H]<sup>+</sup>); IR (KBr): ν = 3413, 2958, 2933, 2857, 2204, 1617, 1608, 1503, 1488, 1437, 1352, 1317, 1292, 1263, 1179, 1121, 1062, 828 cm<sup>-1</sup>; UV-Vis (CH<sub>2</sub>Cl<sub>2</sub>): λ<sub>max</sub> (ε) = 279

( $1.9 \times 10^5$ ), 309 ( $2.0 \times 10^5$ ), 357 ( $1.5 \times 10^5$ ) nm ( $\text{L mol}^{-1}\text{cm}^{-1}$ ); Fluorescence ( $\text{CH}_2\text{Cl}_2$ ):  
 $\lambda_{\text{em}} = 588$  nm ( $\lambda_{\text{exc}} = 357$  nm); Mp.  $> 300$  °C; Anal. Calc'd for  $\text{C}_{186}\text{H}_{210}\text{N}_6\text{O}_{18}$ : C, 79.28,  
H, 7.51, N, 2.98. Found C, 79.00, H, 7.67, N, 3.22.

### 3.4 References

- (1) Huck, W. T. S.; van Veggel, F. C. J. M.; Reinhoudt, D. N. *Recl. Trav. Chim. Pays-Bas* **1995**, *114*, 273-276.
- (2) Akine, S.; Taniguchi, T.; Nabeshima, T. *Tetrahedron Lett.* **2001**, *42*, 8861-8864.
- (3) Gallant, A. J.; MacLachlan, M. J. *Angew. Chem. Int. Ed.* **2003**, *42*, 5307-5310.
- (4) Gallant, A. J.; Hui, J. K. -H.; Zahariev, F. E.; Wang, Y. A.; MacLachlan, M. J. *J. Org. Chem.* **2005**, *70*, 7936-7949.
- (5) Ma, C.; Lo, A.; Abdolmaleki, A.; MacLachlan, M. J. *Org. Lett.* **2004**, *6*, 3841-3844.
- (6) Hui, J. K. -H.; MacLachlan, M. J. *Chem. Commun.* **2006**, 2480-2482.
- (7) Gallant, A. J.; Patrick, B. O.; MacLachlan, M. J. *J. Org. Chem.* **2004**, *69*, 8739-8744.
- (8) Tian, Y.; Tong, J.; Frenzen, G.; Sun, J. -Y. *J. Org. Chem.* **1999**, *64*, 1442-1446.
- (9) Atkins, A. J.; Black, D.; Blake, A. J.; Marin-Becerra, A.; Parsons, S.; Ruiz-Ramirez, L.; Schröder, M. *Chem. Commun.* **1996**, 457-464.
- (10) Gallant, A. J.; Yun, M.; Sauer, M.; Yeung, C. S.; MacLachlan, M. J. *Org. Lett.* **2005**, *7*, 4827-4830.
- (11) Kim, D. -J.; Choi, M. J.; Chang, S. -K. *Bull. Korean Chem. Soc.* **2000**, *21*, 145-147.
- (12) Seto, C. T.; Mathias, J. T.; Whitesides, G. M. *J. Am. Chem. Soc.* **1993**, *115*, 1321-1329.

## Chapter 4

# Self-Assembly, Metal Complexation and Sensing Studies of Phenanthrene Ethynylene Macrocycles<sup>§</sup>

### 4.1 Introduction

Having successfully synthesized our target macrocycles in good yield and purity, we were interested in further studying the properties and reactions of macrocycles **74** and **75**. It was noted in Chapters 2 and 3 that **72**, **73b**, **74** and **75** were brightly coloured and luminescent. Also, the <sup>1</sup>H NMR spectrum of macrocycle **75** showed a change in chemical shift upon a change in temperature. These observations prompted the study of the optical properties and self-assembly of the macrocycles.

#### 4.1.1 Aggregation of Macrocycles

As mentioned in Chapter 1, macrocycle **13** aggregates in polar solvents such as dichloromethane and acetone (Figure 4.1), while in aromatic solvents, there is less tendency to aggregate.<sup>1, 2</sup> Shape-persistent macrocycles that include aromatic rings are able to stack as a result of  $\pi$ -interactions and dissolution of these macrocycles in aromatic solvents can disrupt this aggregation. Macrocycle **13** contains *m*-linked phenyleneethynylene groups, so it is forced into a planar conformation and can aggregate into larger structures. Dimeric structures can also form through aggregation if the

---

<sup>§</sup>A version of this chapter will be submitted for publication: (a) Boden, B. N.; MacLachlan, M. J. "Aggregation of Giant Luminescent Schiff Base Macrocycles"

conformation of the macrocycles within the dimer hinders further stacking<sup>3</sup> or if the electronic environment of the macrocycle is stabilized by dimerization.<sup>4</sup> To this point, aggregation of unmetallated [3+3] Schiff base macrocycles such as **33** and **34** have not been observed.

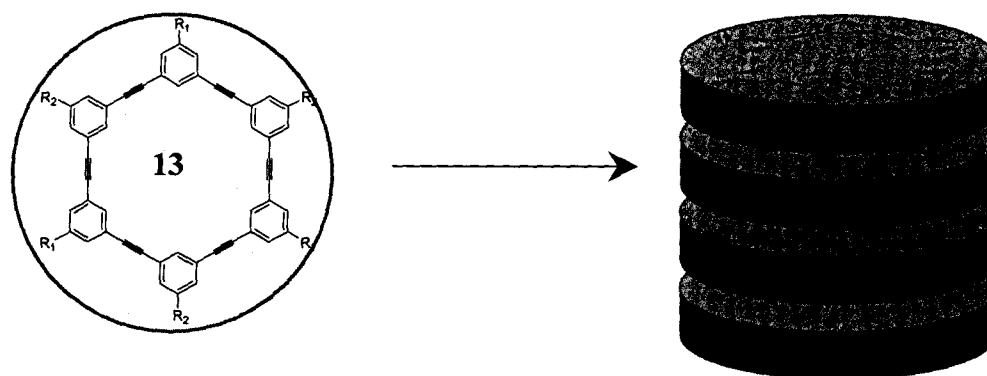


**Figure 4.1** Representation of macrocycle aggregation.

Aggregation can be studied in several ways, including vapour pressure osmometry and NMR spectroscopy. <sup>1</sup>H NMR spectroscopy is a straightforward method for the study of aggregation, as protons are in different environments in an aggregate compared to a free molecule.<sup>5</sup> For example, aromatic protons may be subjected to different ring currents, shifting the frequency of the resonance. Decreasing the concentration of the solution decreases aggregate formation, generally resulting in a downfield shift for aromatic protons. Similarly, changes in temperature also affect aggregation, as heating breaks  $\pi$ -stacking interactions.

Mathematical models can be used to determine the extent of aggregation and to quantify the association constants,  $K_E$ .<sup>6</sup> The peaks in the NMR spectrum represent a time average of the different environments present in the sample. Models of indefinite

association are represented by the following equations which enable the study of dimerization (eqn. 4.1)<sup>6</sup> and extended aggregation (eqn. 4.2),<sup>6</sup> where P is the observed chemical shift, P<sub>m</sub> is the chemical shift of the monomer, P<sub>d</sub> is the chemical shift of the dimer, P<sub>a</sub> is the chemical shift of the aggregate, C is the concentration of the solution and K<sub>E</sub> is the association constant.

$$P = (P_d - P_m) \left( 1 + \frac{(1 - \sqrt{8K_E C + 1})}{4K_E C} \right) + P_m \quad 4.1$$

$$P = (P_a - P_m) \left( 1 + \frac{(1 - \sqrt{4K_E C + 1})}{2K_E C} \right) + P_m \quad 4.2$$

While these models alone cannot distinguish between dimers and indefinite aggregates, the magnitude of the change in chemical shift also can be indicative of the extent of aggregation.

#### 4.1.2 Metallation of Macrocycles

An interesting feature of Schiff base macrocycles is their ability to coordinate metals. Macrocycles with salen or salphen pockets are often synthesized by metal templation, much like the Robson macrocycle **27** (Figure 4.2).<sup>7</sup> Surprisingly, this route is not needed for the conjugated [3+3] macrocycles discussed in this thesis, and a variety of metals can be coordinated after condensation.

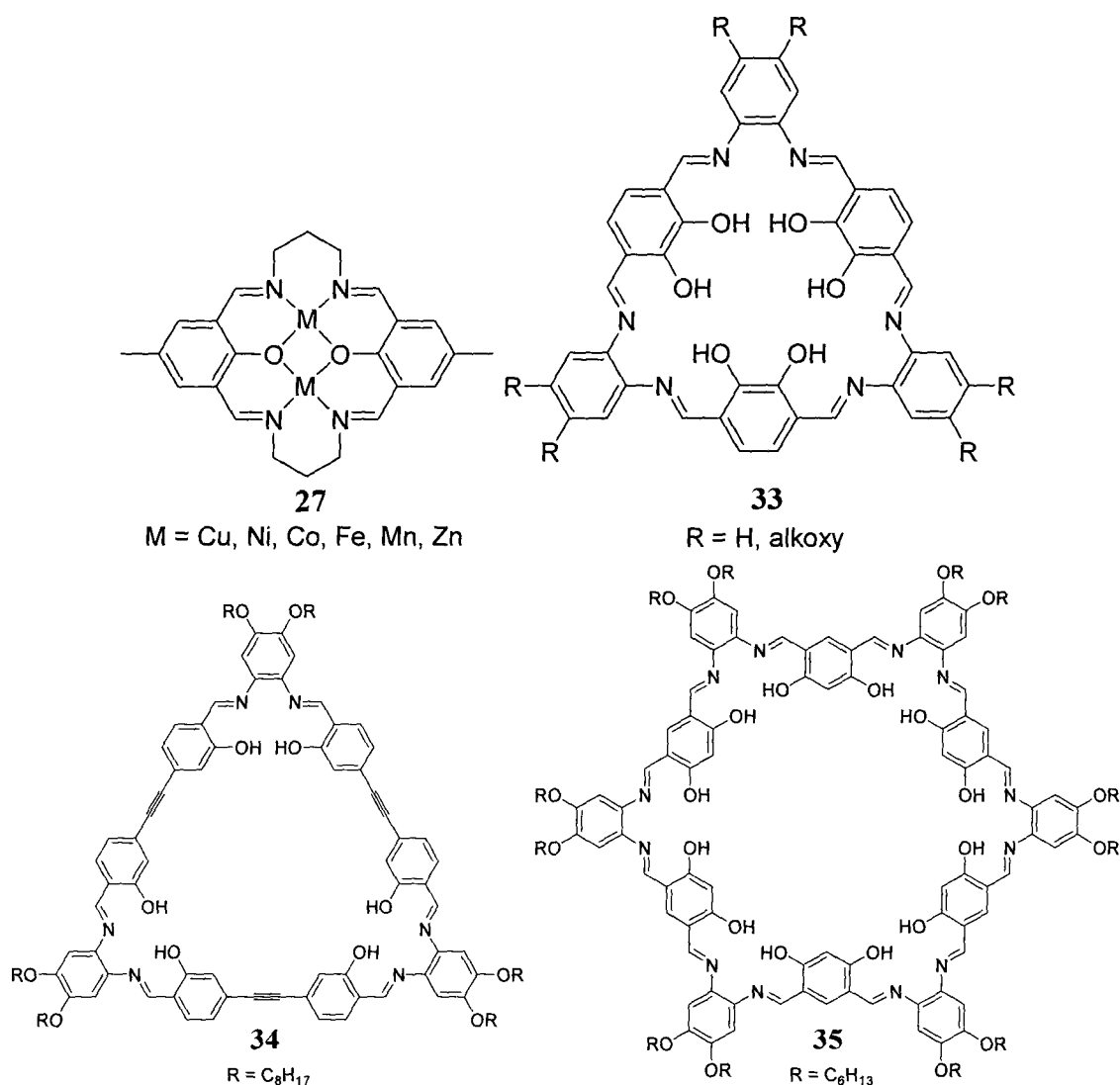


**Figure 4.2** Macrocycles **27**, **33-35**.

Macrocycle **33** templates the formation of large metal clusters including Zn(II), Cd(II), Ni(II) and Mn(II).<sup>8-10</sup> Additionally, the Zn(II) and Cd(II) metallated macrocycles form dimeric structures in the solid state and in solution.<sup>11</sup> Other Schiff base macrocycles, like **34** and **35**, are too big for cluster formation and only coordinate metals in the N<sub>2</sub>O<sub>2</sub> pockets.<sup>12, 13</sup> Coordination of metals to **34** alters the optical properties of the macrocycle through self-assembly. Macrocycle **34** is weakly luminescent on its own, and coordination of Zn(II) to the salphen units increases the luminescence sixfold, while

coordination of Ni(II) quenches the luminescence entirely. Besides luminescence, metallated [2+2] and [3+3] macrocycles are useful catalysts or have interesting magnetic properties.<sup>14-17</sup>

### 4.1.3 Macrocyclic Sensors

Chapter 1 mentioned that macrocycles can be modified with chromophores or fluorophores to act as supramolecular sensors. For sensors such as these, sensing ability is limited by the specific number of binding sites in the sensor. For example, twistophane **19** exhibits increasingly quenched emission with incremental additions of Ag(I) up to a 1:1 ratio of **19**:Ag(I).<sup>18</sup>

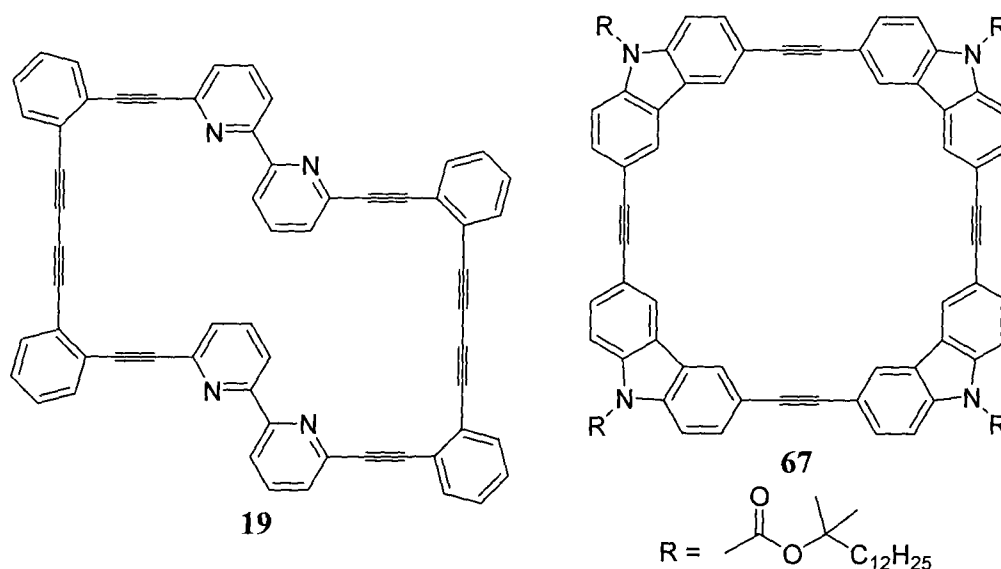


**Figure 4.3** Macrocyclic sensors **19** and **67**.

Macrocycle **67** is not a supramolecular sensor, but it senses nitroaromatic compounds, such as dinitrotoluene (DNT) and trinitrotoluene (TNT), through transfer of photoexcited electrons from the macrocycle to the analyte rather than interactions such as hydrogen bonding or coordination.<sup>19</sup> Macrocycle **67** aggregates into tubes and can be cast into nanofibrous films,<sup>20</sup> which are porous and allow the nitroaromatic vapour to diffuse

efficiently into the films. Exciton migration arises from cofacial intermolecular coupling between individual rings in the nanofibers. In conjugated polymer films, which are typically studied for sensing of nitroaromatics, thicker films decrease the efficiency of luminescence quenching and exciton migration comes from delocalization of the polymer chain.

#### 4.1.4 Properties of Macrocycles **74** and **75**

Macrocycles **74** and **75** have several attributes that encourage the study of aggregation, metal complexation and sensing. The phenanthrene moieties, shown in violet, may allow for aggregation through  $\pi$ -stacking interactions. The three  $N_2O_2$  sites, denoted in red, allow for coordination of metals, which will change the optical properties of the macrocycle and possibly affect aggregation. Lastly, the phenanthrene ethynylene spacers in blue are electron donors, which may cause the macrocycle to behave as sensors of electron accepting molecules such as nitroaromatic compounds. The focus of this chapter is the study of these properties in macrocycles **74** and **75**.

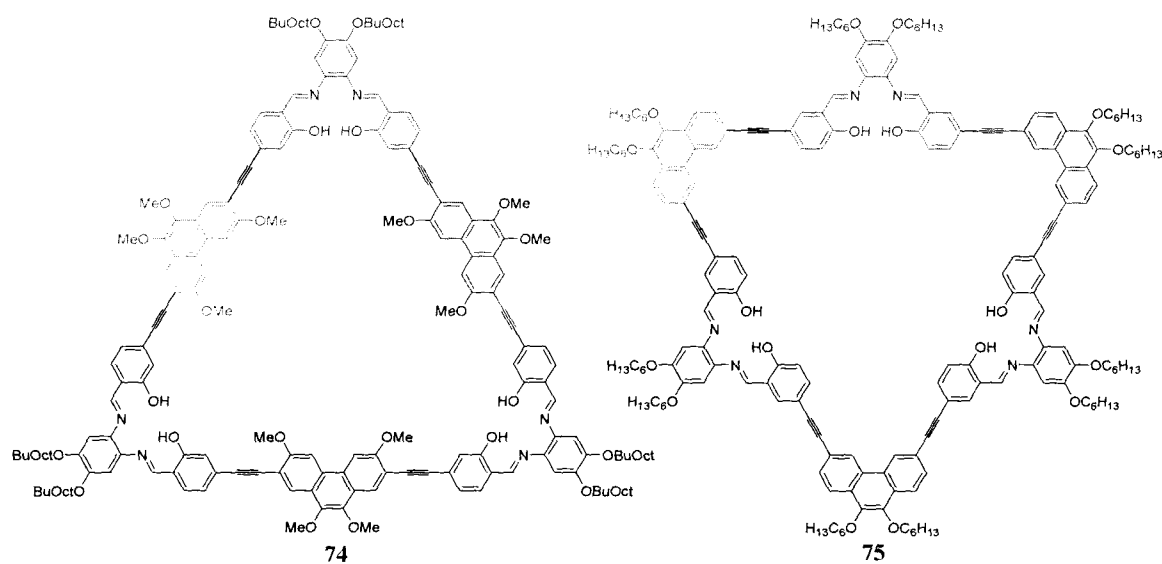


**Figure 4.4** Macrocycles **74** and **75**.

## 4.2 Discussion

### 4.2.1 Aggregation of Macrocycles 74 and 75

Polycyclic aromatic hydrocarbons are well known to stack as a result of  $\pi$ -interactions between layers of the various compounds. Macrocycles **74** and **75** both contain many aromatic units that have potential to interact with each other. In order to study aggregation in these compounds, we can observe this phenomenon through variable temperature and variable concentration  $^1\text{H}$  NMR (VT/VC NMR) spectroscopy.

As an initial test to determine whether the macrocycles aggregate, solutions of two different concentrations of each macrocycle were prepared and  $^1\text{H}$  NMR spectra were obtained at four different temperatures, ranging from 25 – 55 °C at 10 °C intervals. Macrocycle **74** was prepared as 0.25 and 1.5 mM solutions in  $\text{CDCl}_3$ .

Upon changing the temperature, the only peak that exhibits a large change in chemical shift is the *OH* resonance (Figure 4.5). It moves downfield from 13.30 to 13.13 ppm over the 30 °C temperature range. The aromatic and the alkoxy resonances shift only by less than 0.02 ppm. If the concentration is changed (Figure 4.6), there is virtually no difference between the chemical shifts of each solution at the same temperature. This suggests that **74** does not aggregate in  $\text{CDCl}_3$ .

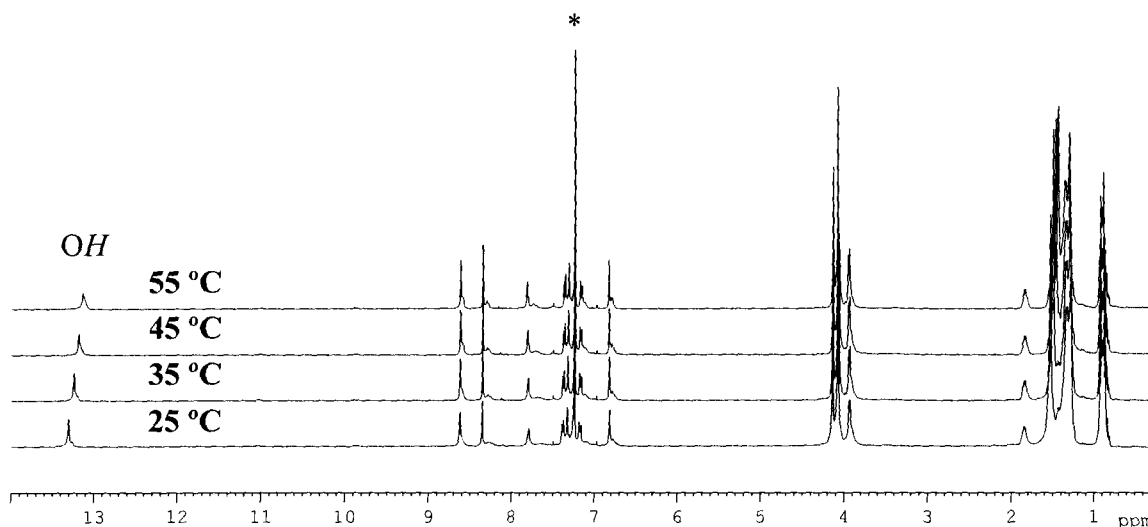


**Figure 4.5** Stacked  $^1\text{H}$  NMR spectra (400 MHz,  $\text{CDCl}_3$ , 1.5 mM) of **74** at various temperatures (\* =  $\text{CDCl}_3$ ).

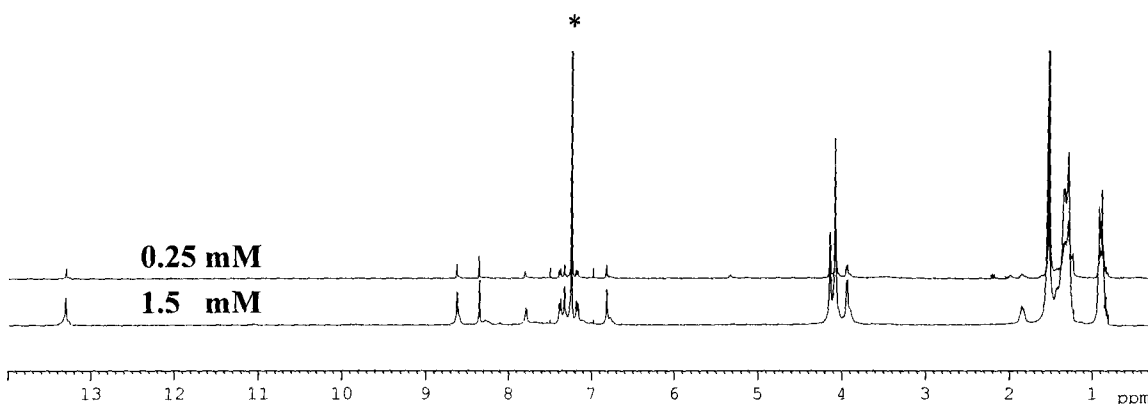


**Figure 4.6** Stacked  $^1\text{H}$  NMR spectra (400 MHz,  $\text{CDCl}_3$ , RT) of **74** at two concentrations (\* =  $\text{CDCl}_3$ ).

Initial VT/VC NMR experiments with macrocycle **75** gave a different result. The macrocycle was dissolved in  $\text{CDCl}_3$  to give 0.23 and 1.4 mM solutions. Chemical shifts of the same resonances are different for each concentration and temperature (Figures 4.7 and 4.8). Hydroxyl resonances shift downfield with increasing temperature and decreasing concentration, while all aromatic resonances shift upfield. The most notable shifts come from the imine proton, the aromatic phenylenediimine proton and alkoxy  $\text{OCH}_2$ . Additionally, the overlapping imine and the phenanthrene proton resonances, found near 8.5 ppm, separate and sharpen with increasing temperature.

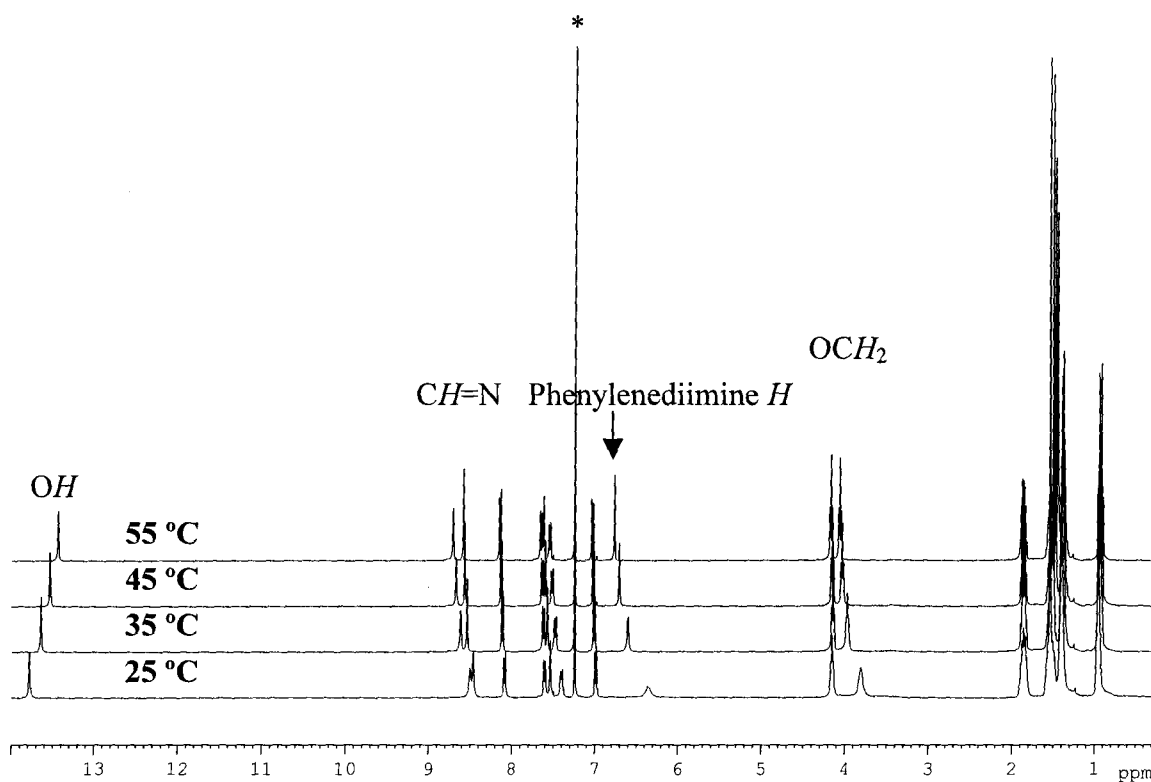


**Figure 4.7** Stacked  $^1\text{H}$  NMR spectra (400 MHz, CDCl<sub>3</sub>, 1.4 mM) of **75** at various temperatures (\* = CDCl<sub>3</sub>).

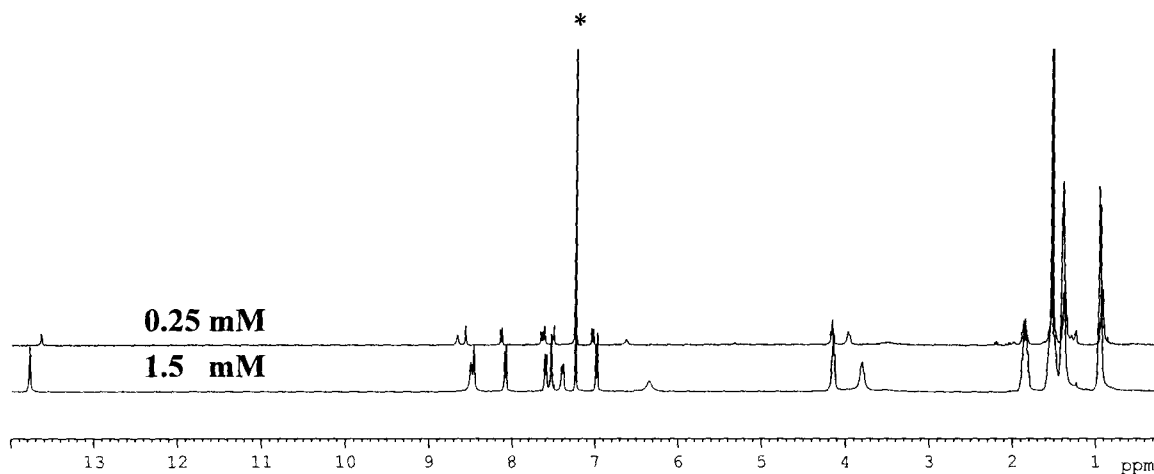


**Figure 4.8** Stacked  $^1\text{H}$  NMR spectra (400 MHz, CDCl<sub>3</sub>, RT) of **75** at two concentrations (\* = CDCl<sub>3</sub>).

These initial results suggest that macrocycle **75** aggregates in solution. The monomer to aggregate equilibrium is affected by changes in temperature and concentration. By collecting a larger sampling of NMR data at more temperatures and concentrations, we can calculate association constants for aggregation of the macrocycle.

Plots of chemical shift versus concentrations (ranging from 0.045 mM to 2.27 mM) at various temperatures (from 5 to 55 °C) are shown in Figure 4.9. The graphs for the alkoxy  $OCH_2$  resonance, the phenylenediimine peak and the imine resonance show the same trend, as the curves appear to merge towards one chemical shift at low concentration. The hydroxyl resonances show a different trend, as there does not appear to be a convergence of the data at a specific chemical shift. While change in concentration affects the aggregation, heating affects both aggregation and the hydrogen bonding between the hydroxyl proton and the nitrogen of the imine.

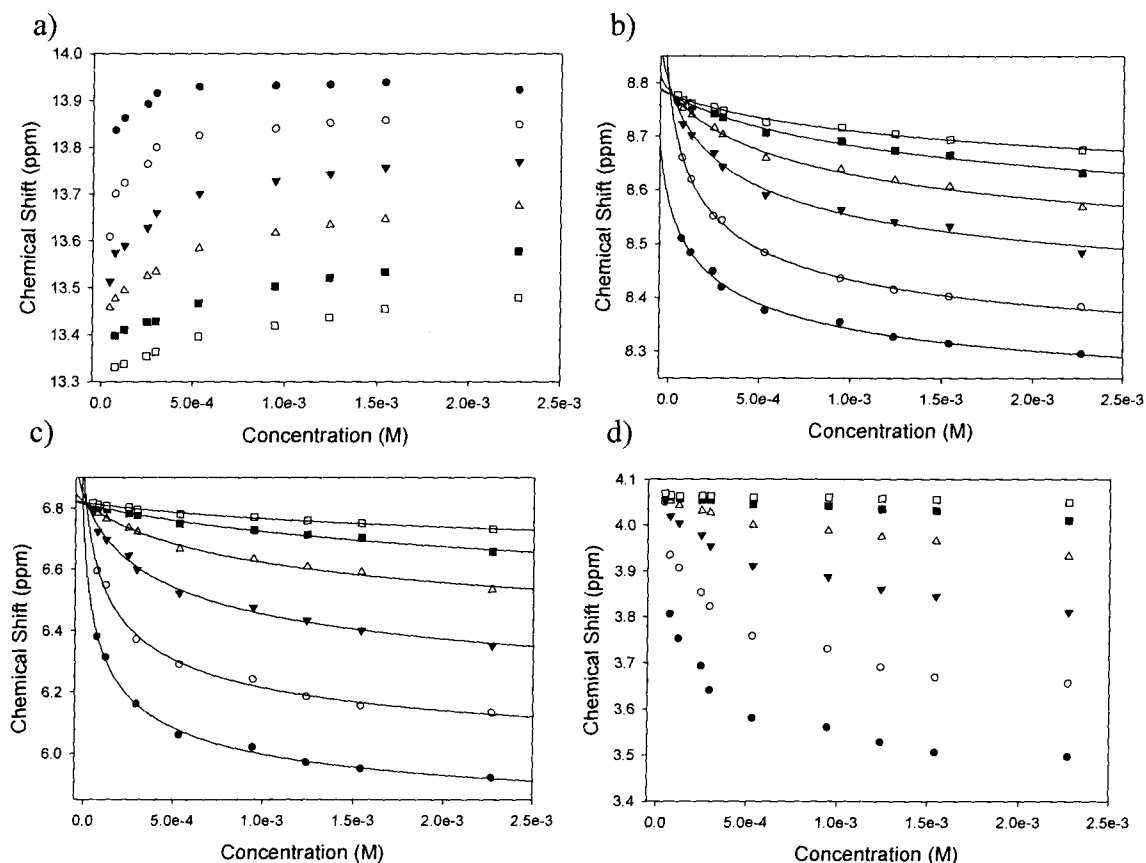


**Figure 4.9** Plots of chemical shift vs. concentration of **75** for a)  $OH$ , b)  $CH=N$ , c) phenylenediimine proton, and d) phenylenediimine  $OCH_2$  at different temperatures ( $\bullet = 5\text{ }^\circ\text{C}$ ,  $\circ = 15\text{ }^\circ\text{C}$ ,  $\blacktriangledown = 25\text{ }^\circ\text{C}$ ,  $\triangle = 35\text{ }^\circ\text{C}$ ,  $\blacksquare = 45\text{ }^\circ\text{C}$ ,  $\square = 55\text{ }^\circ\text{C}$ ) in  $CDCl_3$ . The curves in b) and c) represent the best fit of these data to the dimer model, equation 4.1.

The changes in the  $^1\text{H}$  NMR chemical shift can be fitted to mathematical models 4.1 and 4.2 to help determine association constants and whether a dimer or an indefinite stack is likely present. The data fits to both models, but considering that the magnitude of the change in chemical shift, dimer formation seems more probable. Upfield shifts for aromatic rings that are less than 1 ppm can be indicative of either a dimer or an indefinite stack, while changes in chemical shift greater than 1 ppm are evidence for association beyond dimerization.<sup>6</sup> The data for the hydroxyl resonance in Figure 4.9a cannot be fitted to the mathematical models as the change in chemical shift is affected by other interactions, such as hydrogen bonding.

Each curve in Figure 4.9b and 4.9c gives a value for  $K_E$ , shown in Table 4.1. As expected, the association constants decrease as temperature increases, indicative of weaker aggregation at elevated temperatures. The association constants obtained on the basis of the imine chemical shifts and the phenylenediimine chemical shifts are different, but on the same order of magnitude. This difference has been noted for other macrocycles as well.<sup>21</sup>

**Table 4.1** Association constants  $K_E$  for dimerization of **75** in  $\text{CDCl}_3$ .

T (°C, K)	$K_E$ (imine) ( $\text{M}^{-1}$ )	$K_E$ (diimine) ( $\text{M}^{-1}$ )
5, 278	$1600 \pm 410$	$5000 \pm 1200$
15, 288	$2700 \pm 290$	$3700 \pm 1100$
25, 298	$1200 \pm 380$	$1000 \pm 280$
35, 308	$580 \pm 150$	$420 \pm 120$
45, 318	$290 \pm 90$	$140 \pm 60$
55, 328	$280 \pm 90$	$150 \pm 60$

The magnitude of the association constant  $K_E$  is dependent on many factors. The data in Table 4.1 demonstrate the dependence of  $K_E$  on temperature. Other factors that affect association are solvent and side chains on the macrocycle. The value of  $K_E$  for **75** in  $\text{CDCl}_3$  at room temperature is 100 times higher than  $K_E$  for **13** in  $\text{CDCl}_3$  but is 10 times lower than that for **13** in acetone.<sup>2</sup> Macrocycle **13** has higher  $K_E$  for more electron-withdrawing side chains, such as esters, rather than electron-donating side groups, such as alkoxy chains.<sup>22</sup> Other imine-containing macrocycles have values  $K_E$  in the same order of magnitude as **75**.<sup>21</sup>

The association constants can be fit to a van't Hoff plot (Figure 4.10), showing the natural logarithm of  $K_E$  vs. the inverse of the absolute temperature. Using the van't Hoff equation (4.3), the changes in enthalpy and entropy of association can be determined.

$$\ln(K_E) = -\frac{\Delta H}{R} \left[ \frac{1}{T} \right] + \frac{\Delta S}{R} \quad 4.3$$

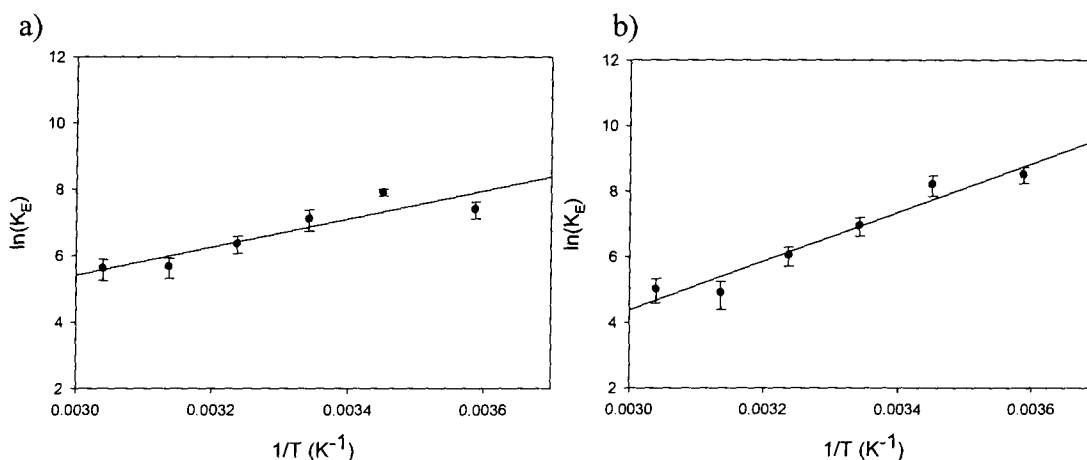


**Figure 4.10** van't Hoff plots for the dimerization of **75** a) imine  $K_E$  and b) phenylenediimine  $K_E$ .

The values of  $\Delta H$  and  $\Delta S$  are shown in Table 4.2. These data show that dimerization is enthalpically driven, and entropically disfavoured. The values of  $\Delta H$  are slightly larger than those for **13**, but on the same order of magnitude.<sup>22</sup> The larger value of  $\Delta H$  may be due to several factors. In stacking the macrocycle, electron-rich phenanthrene groups are paired with electron-deficient aromatic rings in the salphen moiety, which increases the strength of association through electrostatic interactions. Also, the presence of phenanthrene incorporates more aromatic rings into the macrocycle, which encourages  $\pi$ -stacking. Values of  $\Delta S$  for **75** are comparable to values for derivatives of **13**. The negative change in entropy is not unexpected, as aggregation would increase order in solution. Given these results, it is apparent that at higher temperatures, the chemical shifts are nearly independent of concentration, indicating that elevated temperature effectively deaggregates the macrocycle and these spectra are most representative of the free macrocycle. Conversely, the most concentrated spectra obtained at the lowest temperature represent, in effect, the macrocycle in a fully aggregated environment.

**Table 4.2** Thermodynamic data for dimerization of **75** in  $\text{CDCl}_3$ .

Plot	$\Delta H$ (kcal/mol)	$\Delta S$ (cal/mol)
a) Imine	$-8.5 \pm 7$	$-15 \pm 21$
b) Phenylenediimine	$-15 \pm 8$	$-36 \pm 25$

Considering that **74** and **75** have isomeric macrocyclic backbones with 78 covalent bonds forming the ring, it is surprising that they behave differently in solution.

However, Figure 4.11, which shows hypothetical structures of the dimers, illustrates a possible reason why **74** does not aggregate while **75** does. The macrocycles are rotated in the figure because direct overlap of the aromatic rings would lead to repulsion of the macrocycles rather than attractive forces necessary for aggregation.<sup>23</sup> The dimer depicted in Figure 4.11 would allow attractive interactions between electron-deficient and electron-rich rings. Dimers of macrocycle **74** lack overlapping aromatic rings, greatly reducing its capacity for  $\pi$ -stacking and preventing aggregation. Model dimers of macrocycle **75** have salphen moieties directly aligned with the phenanthrene groups and the protons positioned over the aromatic rings, where they would experience the greatest effects of magnetic anisotropy, exhibit the greatest change in chemical shift in the VT/VC NMR spectra. For example, the phenylenediimine proton is positioned over the center of the phenanthrene rings, therefore the chemical shifts are considerably upfield at lower temperatures and higher concentrations because of the proximity to the ring current. Upon deaggregation, the peak shifts downfield by nearly one ppm because this proton is no longer in such an electronically shielded environment. Previous studies have confirmed that aromatic protons typically display upfield shifts when involved in stacking and hydrogen bonded protons shift downfield, both as a result of the ring current effects of adjacent molecules.<sup>5</sup>

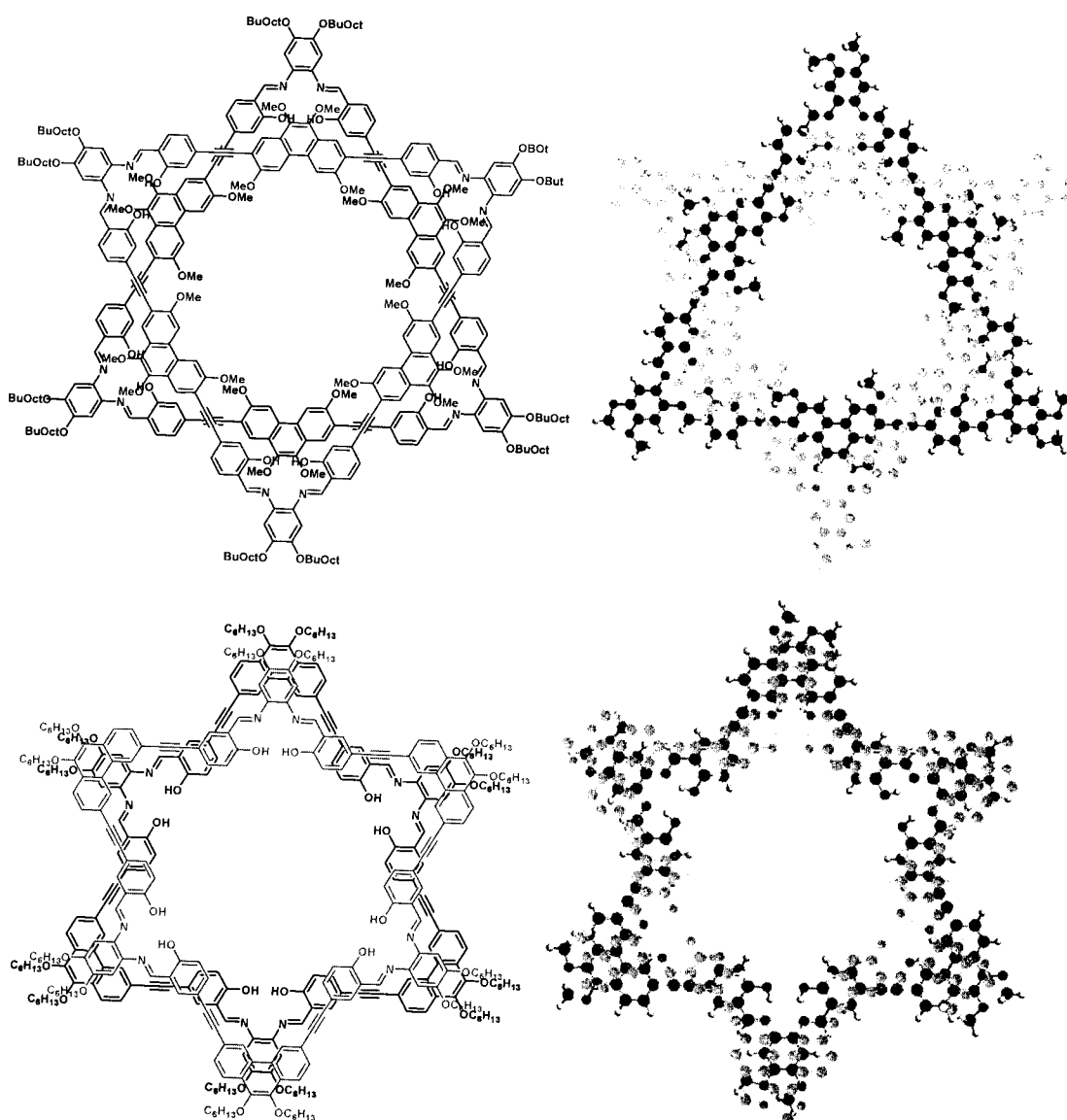


**Figure 4.11** Structures of hypothetical dimers of **74** (top) and **75** (bottom), with ChemDraw representations on the left and Spartan models on the right.

It is clear that aggregation occurs in solution, but it is unclear whether this translates to the solid state. The crystal structure was not determined because crystals suitable for diffraction could not be grown. Powder X-ray diffraction (PXRD) was applied to the solid in an attempt to elucidate additional solid state structural data. The PXRD pattern (Figure 4.12) showed several reflections at  $2\theta = 4.82^\circ$ ,  $5.56^\circ$  and  $7.42^\circ$ . At larger values of  $2\theta$ , there is a weak, broad peak, as well as a weak signal at  $27.0^\circ$ , which

corresponds to  $d = 3.30 \text{ \AA}$  and is indicative of  $\pi$ -stacking.<sup>21</sup> This reveals that the powder of **75** has microcrystalline domains, but more details could not be ascertained.

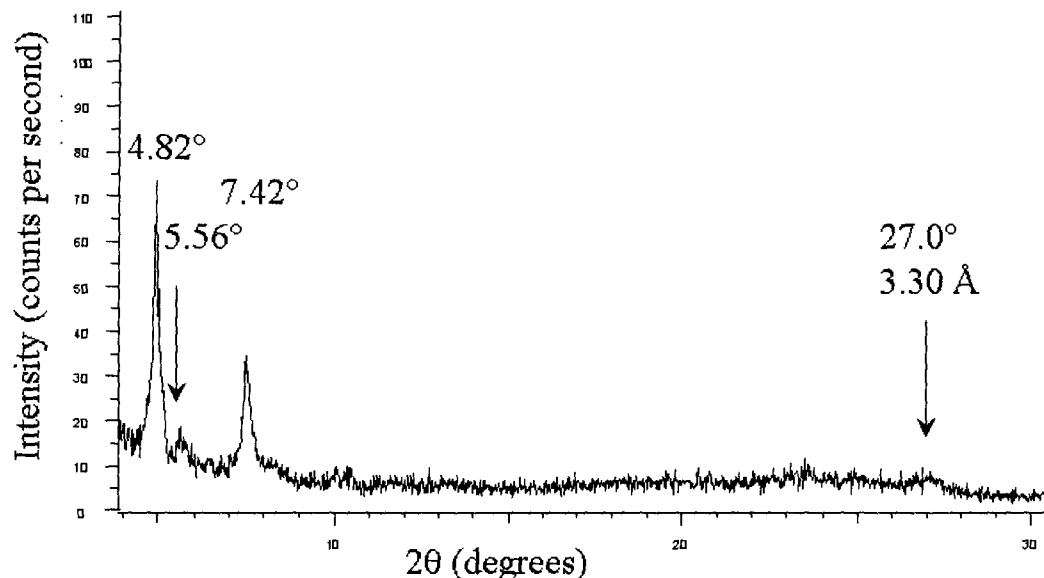
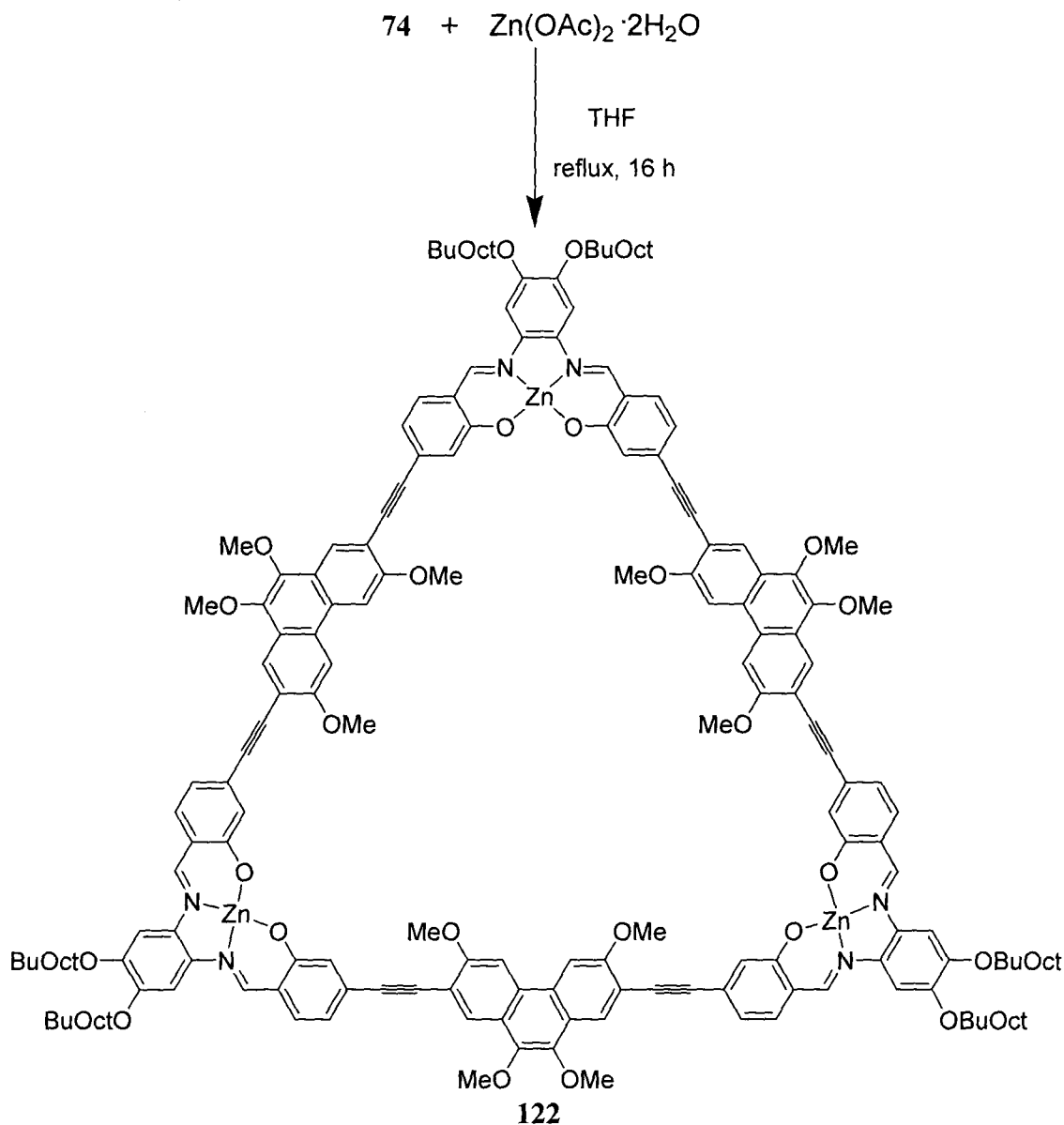


**Figure 4.12** Powder X-Ray diffraction pattern of **75**.

#### 4.2.2 Metal Complexation of Macrocycles **74** and **75**

Previous studies on macrocycles **33** and **34** have shown that aggregation can be induced by interaction with metals. As macrocycles **74** and **75** are large, it is not expected that the presence of alkali metals will induce aggregation of **74** and **75** as they do with **33**. However, coordination of Ni(II) or Zn(II) to **74** and **75** should affect similar behaviours to those that occur in metallated **34**. Aggregation in **75** should be strengthened in the presence of Zn(II), while it should be induced in **74** via Zn(II)-phenolic oxygen interactions. Luminescence may be enhanced, while coordination of Ni(II) should quench luminescence. Macrocycles **74** and **75** were refluxed in the presence of either Zn(OAc)<sub>2</sub> or Ni(OAc)<sub>2</sub>. When a mixture of **74** and Zn(II) were heated together, a solid precipitated, which was found to be insoluble in all solvents unless pyridine was added.

**Scheme 4.1** Synthesis of macrocycle **122**.



These results indicate that **122** is aggregating as **34** does through intermolecular Zn-O interactions, and breaks up upon coordination of pyridine to the metal center.<sup>12</sup> The lack of solubility caused difficulty in characterization, but MALDI-TOF mass spectrum (Figure 4.13) indicated that the expected product **122** is present through the appearance of a peak at  $m/z = 3274$ . It is accompanied by a second peak at  $m/z = 3211$ , which corresponds to  $74 + 2 \text{ Zn}$ .

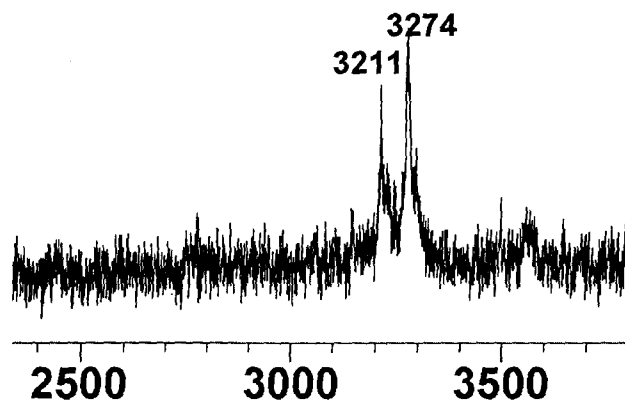
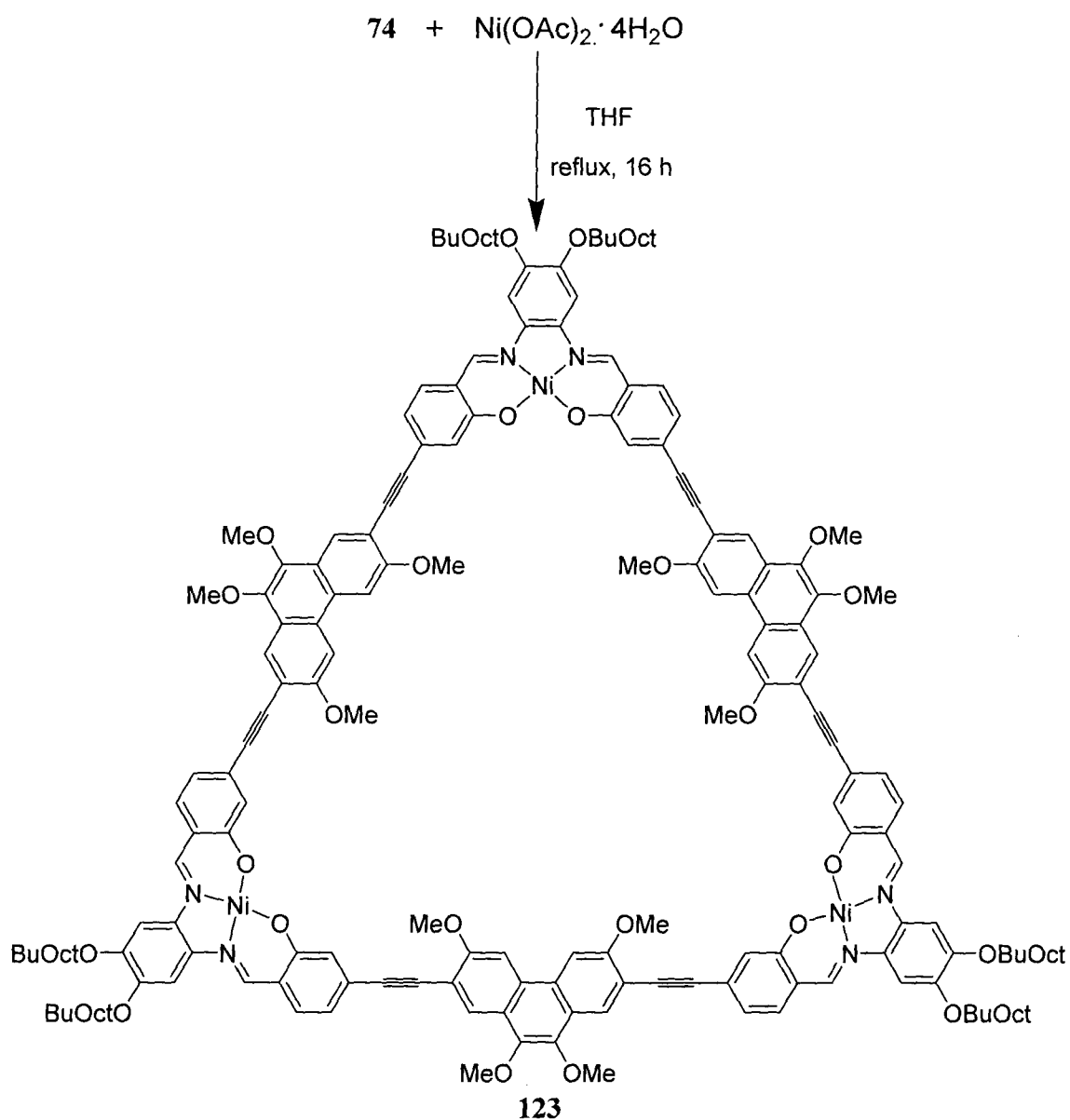


Figure 4.13 MALDI-TOF mass spectrum of **122**.

Adding pyridine- $d_5$  to a sample of **122** allowed  $^1\text{H}$  NMR data to be obtained, but the resonances in the spectrum appear as multiplets, as would be expected for a mixture of di- and trimetallated products. For example, the imine resonance at 8.7 ppm appears as a doublet, but is most likely two separate peaks. Attempts to recrystallize **122** were unsuccessful, as a result of its low solubility.

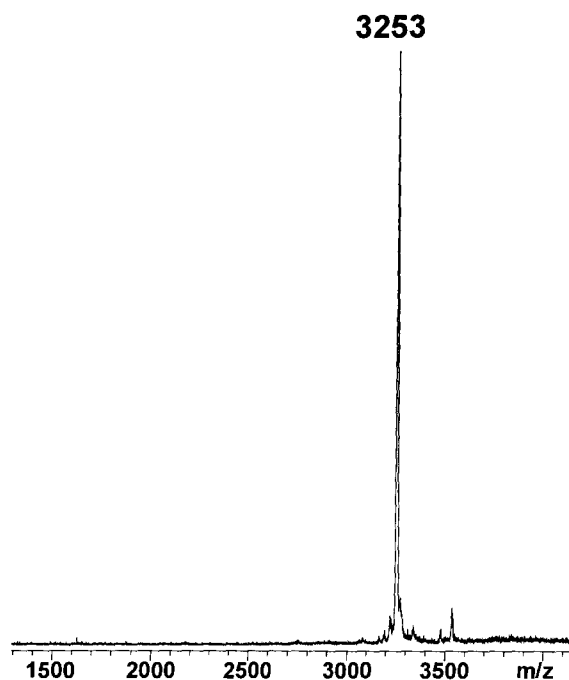
When **74** was heated in the presence of Ni(II), a much more soluble product, **123**, was obtained (Scheme 4.2). Once again, the  $^1\text{H}$  NMR spectrum contained peaks that were broad. The disappearance of the hydroxyl resonance indicates that Ni(II) coordinated to the  $\text{N}_2\text{O}_2$  site.

**Scheme 4.2** Synthesis of macrocycle **123**.



The initial MALDI-TOF spectrum of **123** showed several peaks, indicating the presence of multiple products. Compound **123** could be recrystallized and a cleaner spectrum was obtained with a peak at  $m/z = 3253$  (Figure 4.14), confirming the coordination of three Ni(II) to the  $\text{N}_2\text{O}_2$  sites to form **123**. As with **34**, compounds **122** and **123** show changes in luminescence from **74**. Macrocycle **122** exhibits enhanced

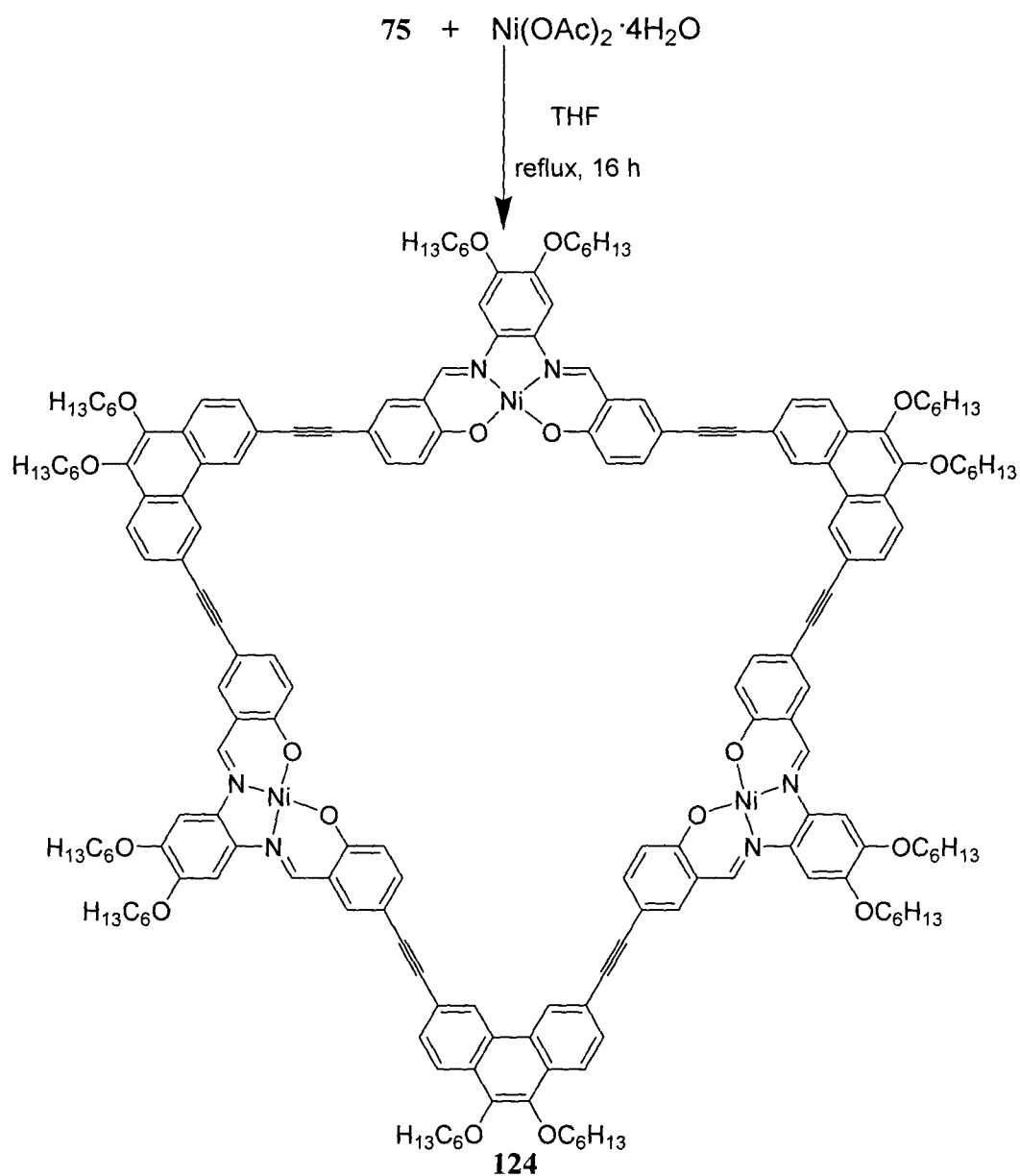
luminescence over unmetallated **74**, while Ni(II)-containing macrocycle **123** is not luminescent.



**Figure 4.14** MALDI-TOF mass spectrum of **123**.

When **75** was heated in the presence of Ni(II), a red powder precipitated out of solution (Scheme 4.3). This solid was completely insoluble making characterization of **124** difficult. The MALDI-TOF mass spectrum (Figure 4.15) of the initial reaction mixture was obtained and it showed three peaks indicative of **75** with one, two and three Ni(II) centers at  $m/z = 2875$ ,  $2933$  and  $2989$ , respectively. After heating the macrocycle with Ni(OAc)<sub>2</sub> for an extended duration, a second mass spectrum showed a change in the intensity of the peaks, indicating that all the coordination sites could be filled given ample reaction time.

**Scheme 4.3** Synthesis of macrocycle **124**.



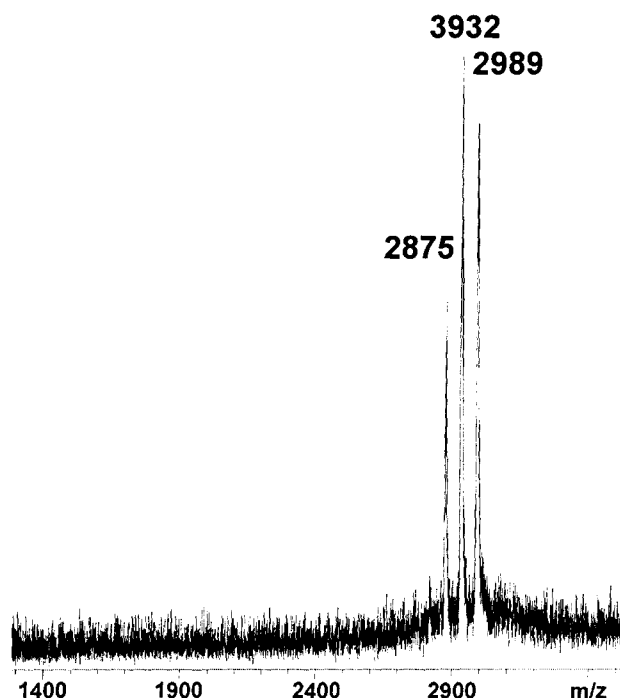


**Figure 4.15** MALDI-TOF mass spectrum of **124**, and mono- and dimetallated **75**.

As with **123**, coordination of Ni(II) to form **124** quenches the luminescence of the macrocycle. In light of these results, coordination of Zn(II) was not attempted as it was determined that the product would be insoluble and difficult to characterize.

#### 4.2.3 Optical Properties of Macrocycles **74** and **75**

[3+3] Schiff base macrocycles are generally brightly coloured and exhibit luminescence. Macrocycles **74** and **75** are dark red and bright orange, respectively, while diols **72** and **73b** are both yellow. All of these compounds are weakly luminescent. Figure 4.16 shows the optical spectra of **72** and **74** and Figure 4.17 shows that of **73b** and **75**. Figure 4.18 shows the absorption and emission spectra of **74** and **75** for a direct comparison of the optical spectra of the macrocycles. The absorption spectra of diols **72** and **73b** are similar to their respective macrocycles, but the peaks are narrower for the diols. The  $\lambda_{\text{max}}$  values of the diols are only slightly blue-shifted from their respective

macrocycles, but the tails of the peaks for **74** and **75** are bathochromically shifted from **72** and **73b** by 40-80 nm. Macrocycle **74** has two large bands at 300 and 384 nm, while macrocycle **75** has bands at 309 and 357 nm. The maximum absorbance for **75** is 27 nm blue-shifted from that of **74**, a trend that was expected due to the decreased conjugation of **75**.

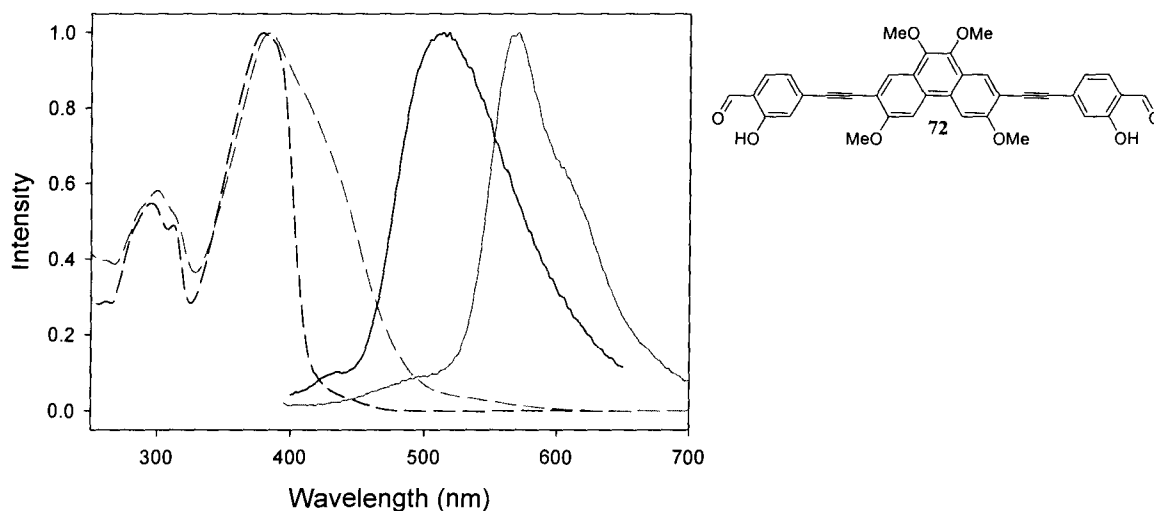


**Figure 4.16** Normalized absorption (dashed) and emission (solid) of **72** (black,  $7.6 \times 10^{-6}$  M) and **74** (red,  $4.2 \times 10^{-6}$  M) in DCM.

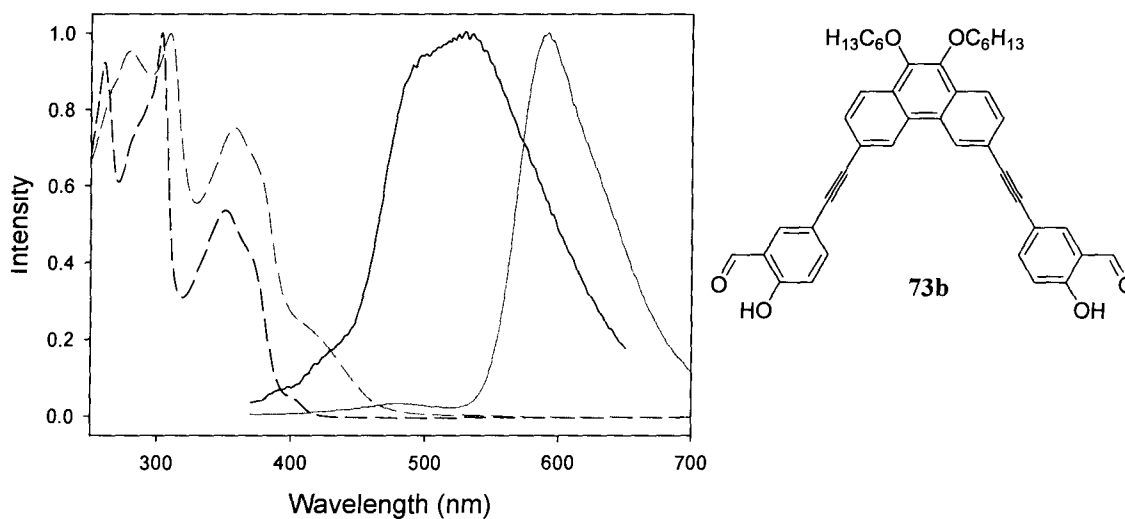


**Figure 4.17** Normalized absorption (dashed) and emission (solid) of **73b** (black,  $7.6 \times 10^{-6}$  M) and **75** (red,  $2.9 \times 10^{-6}$  M) in DCM.

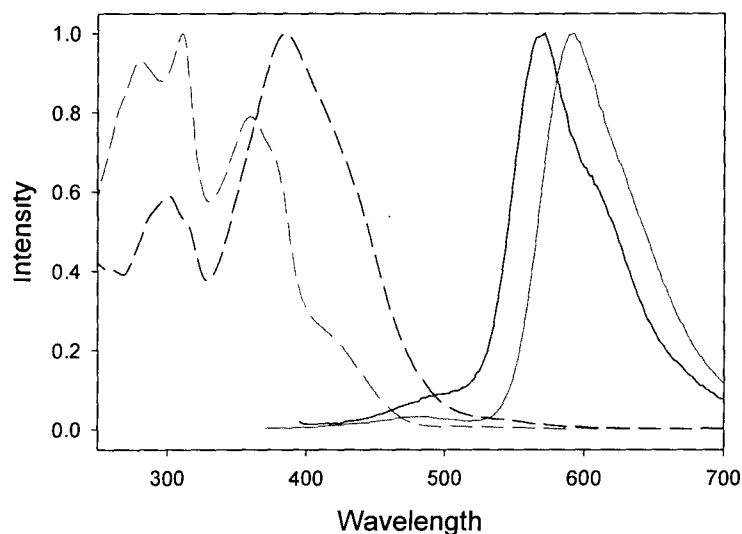


**Figure 4.18** Normalized absorption (dashed) and emission (solid) of **74** (black,  $4.2 \times 10^{-6}$  M) and **75** (red,  $2.9 \times 10^{-6}$  M) in DCM.

The emission spectra of **72** and **73b** both show maximum emission peaks that are blue-shifted from their respective macrocycles by approximately 50 nm. Interestingly, the trend for the wavelength of the macrocycle emission is reversed, with the emission of **72** and **74** ( $\lambda_{\text{max}} = 520$  nm and 567 nm, respectively) blue-shifted 21 nm from the emission of **73b** and **75** ( $\lambda_{\text{max}} = 541$  nm and 588 nm, respectively). Both macrocycles exhibit a Stokes shift that is approximately the same energy as for most phenanthrene compounds.<sup>24</sup> Because of the large red shift between absorption and emission, it was initially wondered whether excimers were forming in solution, however the concentration is low enough (0.005 mM) compared to that of the NMR solutions discussed in Section 4.2.1 (as low as 0.045 mM) that the macrocycle should be entirely deaggregated at this point. Excimer peaks are generally broad and featureless and these are fairly sharp and well-defined. Furthermore, phenanthrene rarely forms excimers, unless submitted to extreme circumstances, such as very low temperatures.<sup>25, 26</sup>

Both macrocycles are only weakly luminescent. Quantum yield measurements compared to anthracene show that for **74**,  $\Phi_F = 0.4\%$  ( $\lambda_{em} = 386$  nm), while for **75**,  $\Phi_F = 1.2\%$  ( $\lambda_{em} = 359$  nm). Both macrocycles have much greater quantum yields of fluorescence than other unmetallated Schiff base macrocycles our group has investigated. For example, **33** is not luminescent and **34** has a quantum yield of only 0.14%.<sup>12</sup> Low quantum yields of luminescence for the macrocycles are likely due to quenching from the unmetallated salphen units in the macrocycle.

If fluorescent emission spectra of different aliquots of the same solution are taken several hours apart, there is a remarkable decrease in intensity (Figure 4.19). Solutions of **74** and **75** in DCM or THF also exhibit this behaviour. When the concentration is decreased, there is additional broadening and a slight increase in intensity of the small blue-shifted peak at 484 nm and 472 nm for **74** and **75**, respectively.

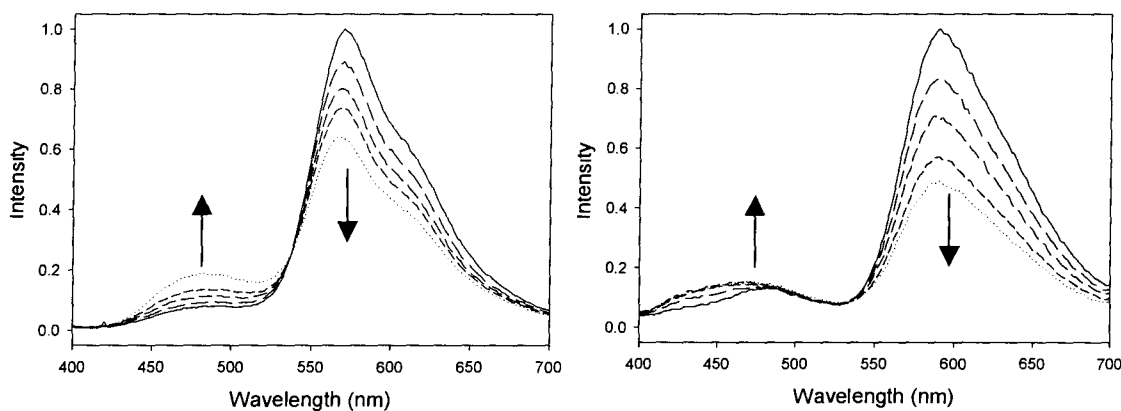


**Figure 4.19** Emission spectra of **74** ( $4.2 \times 10^{-7}$  M, left) and **75** ( $4.2 \times 10^{-7}$  M, right) in DCM over time where black is  $t = 0$  min and blue is  $t \approx 300$  min.

However, if the solvent is changed to toluene, the change in the intensity of  $\lambda_{max}$  of **74** is accompanied by a prominent increase in intensity of the small band at 480 nm (Figure 4.20). For **75**, this peak grows in at 488 nm. At lower concentrations, the increase

in this peak is even more noticeable. The colour of the solution remains the same, and there is little change in the absorption spectrum. Meanwhile, the colour of the luminescence changes from orange to yellow to green.

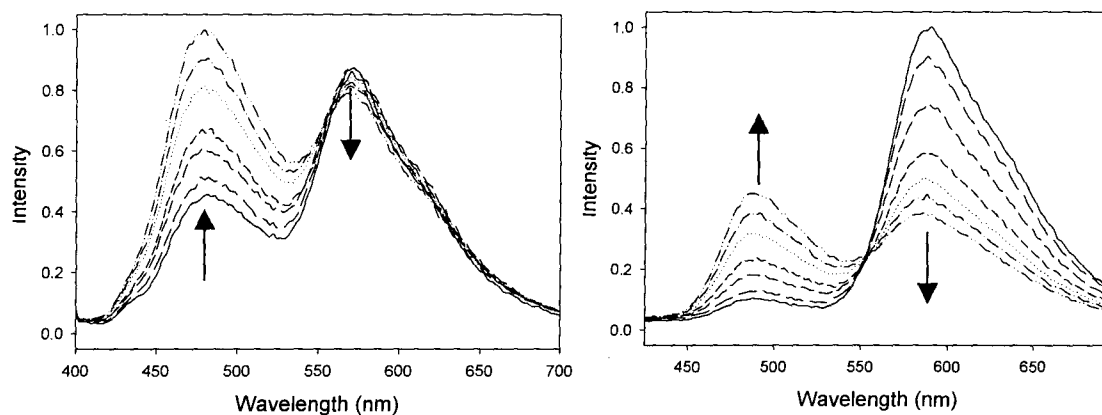


**Figure 4.20** Emission spectra of **74** (left) and **75** (right) in toluene ( $7.8 \times 10^{-7}$  M for both solutions) over time where black is  $t = 0$  min and blue is  $t \approx 420$  min.

As we were interested in the sensing abilities of the macrocycles, it was necessary to determine the source of the decrease in intensity of  $\lambda_{em}$  and the emergence of a new peak. The  $\lambda_{max}$  of this new peak is blue-shifted from the emission of diols **72** and **73b**, so the cause of this emission is not simply the hydrolysis reaction to the starting materials. Because this occurs with different samples of the same macrocycle, it is not an impurity from one reaction. It also occurs in a variety of solvents. A test experiment involved adding *p*-toluenesulfonic acid to solutions of the macrocycle in toluene, DCM and chloroform. In each case, the luminescence immediately changed colour to green or blue. In addition, it was noted that test solutions with some pyridine added did not change the wavelength of fluorescent emission with only small changes in the intensity of emission. To observe this reaction spectroscopically, solutions of each macrocycle were prepared and 100  $\mu$ L of a 0.53 mM solution of *p*-TsOH was added to observe the change in the

spectrum (Figure 4.21). In both cases, the solution with acid added provided a decrease in the  $\lambda_{\max}$  of each macrocycle. This confirms that decomposition of the macrocycle in solution can be caused by presence of acid in the solvent.

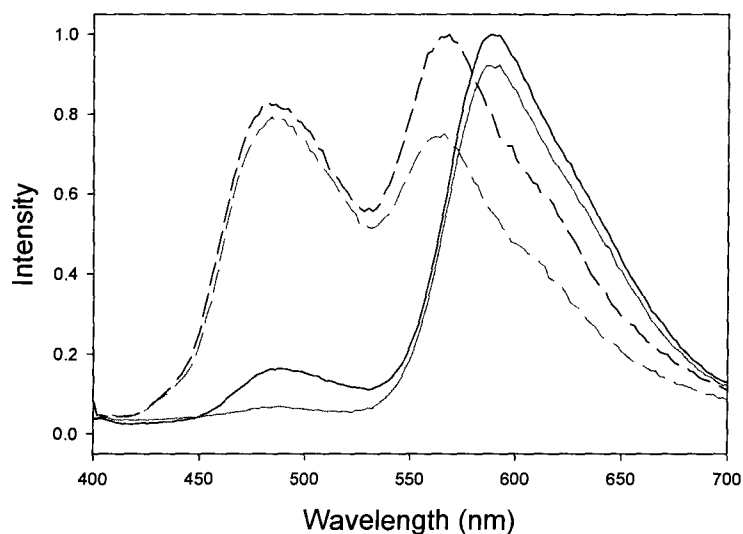
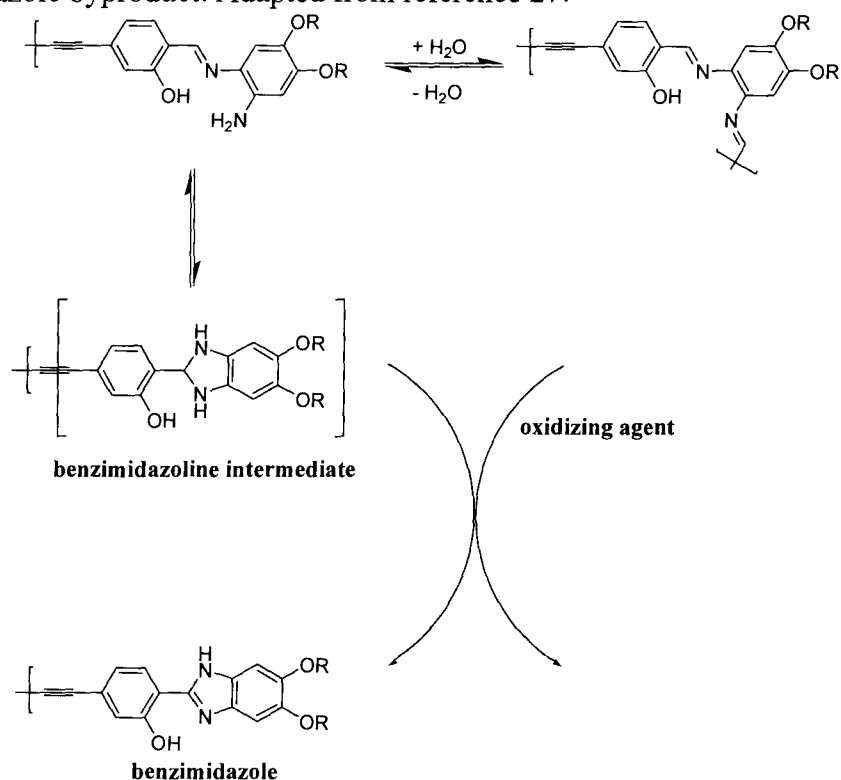


**Figure 4.21** Emission spectra of **74** ( $1.6 \times 10^{-6}$  M, dashed) and **75** ( $1.4 \times 10^{-6}$  M, solid) in toluene before (black) and after (red) addition of *p*-TsOH.

It was shown that the presence of acid plays a role in the decomposition. In addition, the presence of an oxidizing agent, such as air or the macrocycle itself, may contribute to this process. It is possible that the new peak is a result of formation of a benzimidazole, which has been identified as a byproduct in the reduction of imine bonds in Schiff base macrocycles (Scheme 4.4).<sup>27</sup> Benzimidazole and derivatives thereof have been observed to be very luminescent.<sup>28</sup> Addition of base to the spectra prevents a dramatic decrease in the  $\lambda_{\max}$ , however it can deprotonate the hydroxyl groups of the macrocycle, which may induce other behaviour.

**Scheme 4.4** Proposed mechanism of macrocycle decomposition, resulting in formation of a benzimidazole byproduct. Adapted from reference 27.



#### 4.2.4 Sensing of Nitroaromatics

The phenanthrene ethynylene group in the macrocycle spacer provides the means for these macrocycles to behave as sensors. PPEs have previously been shown to behave as sensors for nitroaromatic compounds<sup>29</sup> and this property has also been observed for macrocycle **67**.<sup>19</sup> As determined in the previous section, macrocycles **74** and **75** undergo decomposition in solution, making quantitative analysis of their sensing abilities problematic. Over the time needed to gather the necessary data points for Stern-Volmer constants, the intensity of luminescence would have quenched through decomposition, making it difficult to determine the extent of quenching from the analyte.

Qualitative tests for the sensing of nitroaromatics were attempted to determine whether the macrocycles have any sensing abilities. To 3 mL of  $5.0 \times 10^{-6}$  M solutions of

**74** and **75**, 250  $\mu\text{L}$  of 0.441 M DNT (roughly 13 equiv.) in DCM was added. As a comparison, the same volume of pure DCM was added to a second aliquot of the macrocycle solution to maintain concentration. The two samples were prepared at the same time and the spectra were obtained immediately to prevent the effects of decomposition from interfering with magnitude of intermolecular quenching. Figure 4.22 shows the results of this test. Macrocycle **74** shows only a slight change upon addition of the DNT solution, while the change is more pronounced in the spectrum of macrocycle **75**.

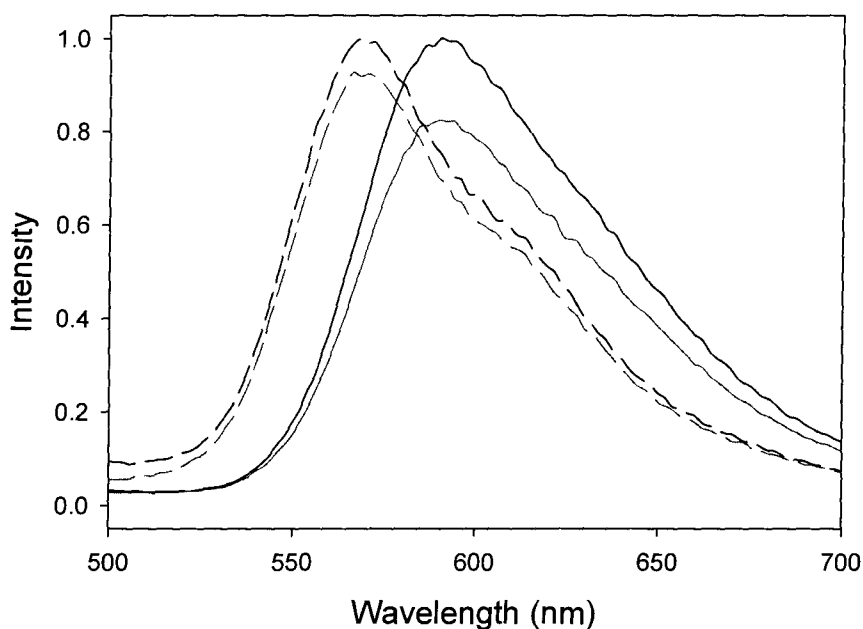


**Figure 4.22** Emission spectra of **74** (dashed) and **75** (solid) in DCM ( $5.0 \times 10^{-6}$  M) before (black) and after (red) the addition of DNT.

It has been determined that macrocycles **74** and **75** are poor sensors for nitroaromatics. A better macrocyclic sensor would require an improvement of the quantum yield of fluorescence of the macrocycle in order to provoke a larger response in the presence of DNT or TNT. Greater stability of the macrocycle in solution is also

needed to improve sensing abilities. A macrocycle that could form well-ordered porous films would also be advantageous in a sensor as it would be able to sense nitroaromatic vapour.

#### 4.2.5 Conclusions

Macrocycle **75** has been shown to associate in  $\text{CDCl}_3$ , while **74** does not. Association constants and changes in enthalpy and entropy were determined for dimerization of **75**, showing that it is enthalpically favourable, but entropically opposed. Metallation of **74** and **75** occurs upon reflux of the macrocycles in the presence of metal acetates, but purification and characterization of these compounds are difficult as a result of their low solubility. Both macrocycles are luminescent and show some quenching in the presence of DNT but decompose in solution, preventing a quantitative study of sensing abilities of **74** and **75**.

### 4.3 Experimental

#### 4.3.1 General Methods and Materials

Quantum yields of fluorescence for a sample (s) were determined using the equation

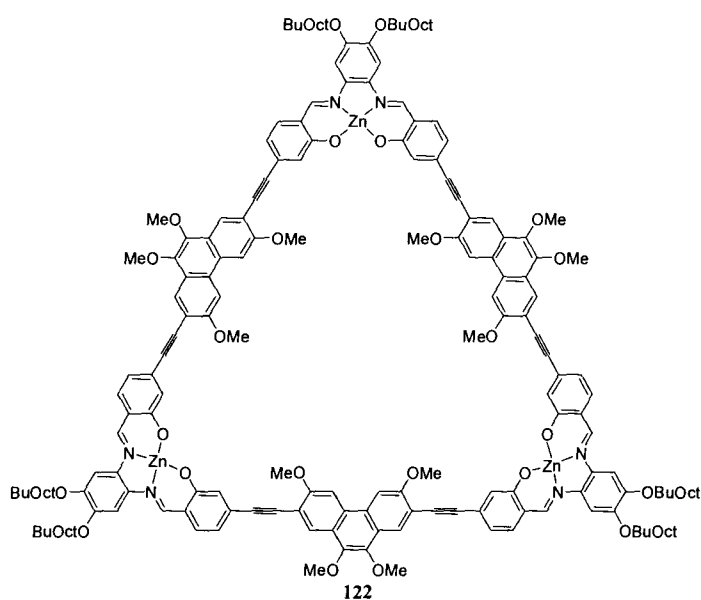
$$\Phi_s \cong \frac{\eta_s^2}{\eta_{ref}^2} \cdot \frac{F_s}{A_s} \cdot \frac{A_{ref}}{F_{ref}} \cdot \Phi_{ref} \cdot 100\%$$

where A = absorbance at the wavelength of excitation of the reference (ref) and the sample,  $\eta$  = refractive index of the solvent and F = integrated fluorescent intensity of the emission band. Quantum yields were referenced to a solution of anthracene in EtOH ( $\Phi_F$ )

= 0.30).<sup>30</sup> Solutions of **74** and **75** were approximately  $4.0 \times 10^{-7}$  M. Models for Figure 4.11 were drawn using Spartan '04, Copyright © 1991-2003 by Wavefunction Inc. The models were not energy minimized. Powder X-Ray diffraction was obtained using a Bruker D8 Advance diffractometer, with CuK $\alpha$  radiation and a graphite monochromator. The sample was prepared by suspension of **75** in MeOH on a zero-signal plate and evaporation of the solvent to form a thin film. All other methods and materials are as outlined in previous sections.

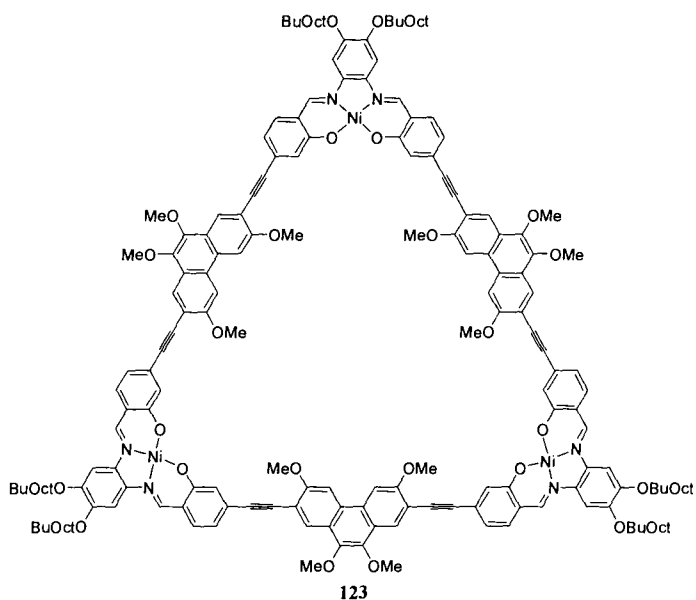
**Sample preparation for association studies** – A stock solution of **75** was prepared by dissolving 10.1 mg of **75** in CDCl<sub>3</sub> in a 2 mL volumetric flask (1.8 mM). Aliquots of the solution (0.45 mL, 0.4 mL, 0.25 mL, 0.15 mL, 0.10 mL) were diluted to 0.5 mL in an NMR tube. Additional samples were prepared in the same manner. VT/VC <sup>1</sup>H NMR spectra were collected on the Bruker Avance 400inv spectrometer at 10 °C intervals from 5 – 55 °C. Association constants were determined using eqn. 4.1<sup>6</sup> to fit the NMR data with SigmaPlot for Windows version 10, Copyright © 2006 by Systat Software, Inc. Error bars were determined by taking the natural logarithm of the maximum and minimum values of K<sub>E</sub> with the error applied.

### 4.3.2 Synthetic Procedures



remained a red solution with red precipitate. The solid was filtered and washed with methanol. Macrocycle **122** was found to be insoluble in common solvents except pyridine.

**Data for 122.** MALDI-TOF-MS:  $m/z = 3211$  ( $[74 + 2Zn]^+$ ),  $3274$  ( $[122 + H]^+$ ).

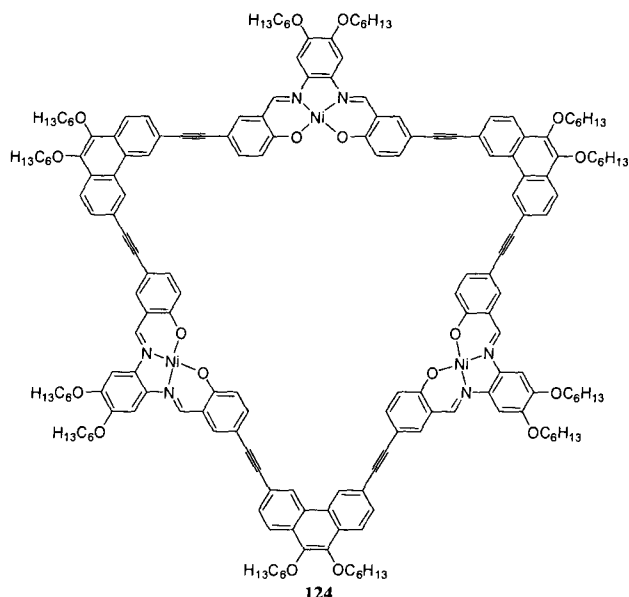


**Synthesis of Macrocycle 122 –**  
Compound **74** (0.071 g, 0.023 mmol) and  $Zn(OAc)_2 \cdot 2H_2O$  (0.019 g, 0.0104 mmol) were dissolved in THF. After heating the solution to reflux, a dark red solution formed and was allowed to reflux for 16 h. After cooling to room temperature, there

**Synthesis of Macrocycle 123 –**  
Compound **74** (0.071 g, 0.023 mmol) and  $Ni(OAc)_2 \cdot 4H_2O$  (0.026 g, 0.0104 mmol) were dissolved in THF. After heating the solution to reflux, a dark red solution formed and was allowed

to reflux for 16 h. The volume of solvent was reduced under vacuum and was precipitated with MeOH. The solid was filtered and washed with methanol. Macrocycle **123** was found to be sparingly soluble in many solvents and could be recrystallized from a combination of THF and MeOH.

**Data for 123.** MALDI-TOF-MS:  $m/z = 3253$  ( $[123 + H]^+$ ).



**Synthesis of Macrocycle 124** – Compound **75** (0.073 g, 0.026 mmol) and Ni(OAc)<sub>2</sub>·4H<sub>2</sub>O (0.027 g, 0.0108 mmol) were dissolved in THF. After heating the solution to reflux, a dark red solid precipitated out. The solid was filtered and washed with methanol. Macrocycle **124** was found to be insoluble in most

solvents, and only sparingly soluble in pyridine.

**Data for 124.** MALDI-TOF-MS:  $m/z = 2875$  ( $[75 + Ni]^+$ ), 2933 ( $[75 + 2Ni]^+$ ), 2990 ( $[124]^+$ ).

#### 4.4 References

- (1) Zhang, J.; Moore, J. S. *J. Am. Chem. Soc.* **1992**, *114*, 9701-9702.
- (2) Lahiri, S.; Thompson, J. L.; Moore, J. S. *J. Am. Chem. Soc.* **2000**, *122*, 11315-11319.
- (3) Klyatskaya, S.; Dingenouts, N.; Rosenauer, C.; Müller, B.; Höger, S. *J. Am. Chem. Soc.* **2006**, *128*, 3150-3151.
- (4) Abraham, R. J.; Fell, S. C. M.; Pearson, H.; Smith, K. M. *Tetrahedron* **1979**, *35*, 1759-1766.
- (5) Hamuro, Y.; Geib, S. J.; Hamilton, A. J. *J. Am. Chem. Soc.* **1997**, *119*, 10587-10593.
- (6) Martin, R. B. *Chem. Rev.* **1996**, *96*, 3043-3064.
- (7) Pilkington, N. H.; Robson, R. *Aust. J. Chem.* **1970**, *23*, 2225-2236.
- (8) Gallant, A. J.; Chong, J. H.; MacLachlan, M. J. *Inorg. Chem.* **2006**, *45*, 5248-5250.
- (9) Nabeshima, T.; Miyazaki, H.; Iwasaki, A.; Akine, S.; Saiki, T.; Ikeda, C. *Tetrahedron* **2007**, *63*, 3328-3333.
- (10) Nabeshima, T.; Miyazaki, H.; Iwasaki, A.; Akine, S.; Saiki, T.; Ikeda, C.; Sato, S. *Chem. Lett.* **2006**, *35*, 1070-1071.
- (11) Frischmann, P. D.; MacLachlan, M. J. *Chem. Commun.* **2007**, *in press*.
- (12) Ma, C.; Lo, A.; Abdolmaleki, A.; MacLachlan, M. J. *Org. Lett.* **2004**, *6*, 3841-3844.
- (13) Hui, J. K. -H.; MacLachlan, M. J. *Chem. Commun.* **2006**, 2480-2482.
- (14) Gao, J.; Reibenspies, J. H.; Martell, A. E. *Angew. Chem. Int. Ed.* **2003**, *42*, 6008-6012.
- (15) Gao, J.; Zingaro, R. A.; Reibenspies, J. H.; Martell, A. E. *Org. Lett.* **2004**, *6*, 2453-2455.
- (16) Pavlishchuck, V. V.; Kolotilov, S. V.; Addison, A. W.; Prushan, M. J.; Butcher, R. J.; Thompson, L. K. *Chem. Commun.* **2002**, 468-469.
- (17) Tandon, S. S.; Bunge, S. D.; Thompson, L. K. *Chem. Commun.* **2007**, 798-800.
- (18) Baxter, P. N. W. *Chem. Eur. J.* **2002**, *8*, 5250-5264.
- (19) Naddo, T.; Che, Y.; Zhang, W.; Balakrishnan, K.; Yang, X.; Yen, M.; Zhao, J.; Moore, J. S.; Zang, L. *J. Am. Chem. Soc.* **2007**, *129*, 6978-6979.

- (20) Balakrishnan, K.; Datar, A.; Zhang, W.; Yang, X.; Naddo, T.; Huang, J.; Zuo, J.; Yen, M.; Moore, J. S.; Zang, L. *J. Am. Chem. Soc.* **2006**, *128*, 6576-6577.
- (21) Zhao, D.; Moore, J. S. *J. Org. Chem.* **2002**, *67*, 3548-3554.
- (22) Shetty, A. S.; Zhang, J.; Moore, J. S. *J. Am. Chem. Soc.* **1996**, *118*, 1019-1027.
- (23) Hunter, C. A.; Sanders, J. K. M. *J. Am. Chem. Soc.* **1990**, *112*, 5525-5534.
- (24) Zimmermann, T. J.; Müller, T. J. J. *Eur. J. Org. Chem.* **2002**, 2269-2279.
- (25) Azumi, T.; McGlynn, S. P. *J. Chem. Phys.* **1964**, *41*, 3131-3138.
- (26) Nakamura, Y.; Tsuihiji, T.; Mita, T.; Minowa, T.; Tobita, S.; Shizuka, H.; Nishimura, J. *J. Am. Chem. Soc.* **1996**, *118*, 1006-1012.
- (27) Gallant, A. J.; Patrick, B. O.; MacLachlan, M. J. *J. Org. Chem.* **2004**, *69*, 8739-8744.
- (28) Tway, P. C.; Love, L. J. C. *J. Phys. Chem.* **1982**, *86*, 5223-5226.
- (29) Toal, S. J.; Trogler, W. C. *J. Mater. Chem.* **2006**, *16*, 2871-2883.
- (30) Parker, C. A. In *Photoluminescence of Solutions* 1st Ed. Elsevier Publishing Company: Amsterdam, 1968; pp 261.

## Chapter 5

# Synthesis and Characterization of Phenanthrene-containing Conjugated Polymers<sup>§</sup>

### 5.1 Introduction

Chapters 2, 3 and 4 discussed synthesis and properties of phenanthrene-containing macrocycles. Some of the compounds developed in these studies have potential use as precursors for other materials. This chapter focuses on the incorporation of phenanthrene into polymers.

#### 5.1.1 Conjugated Polymers

Conjugated polymers, such as polythiophene, poly(phenylenevinylene) (PPV), poly(*p*-phenylene), and poly(phenyleneethynylene) (PPE), have remarkable electronic and optical properties as a consequence of electron delocalization within  $\pi$ -orbitals.<sup>1-5</sup> These semiconducting properties, when combined with the processibility and purification of organic polymers, make these materials useful for flexible display and solar cell technologies.<sup>6, 7</sup> Luminescent polymers, particularly PPV and its derivatives (e.g., MEH-PPV), are being commercialized for application in organic light emitting diodes (LEDs) and chemical sensors.<sup>8, 9</sup> Fluorene-based polymers have been shown to emit blue light

---

<sup>§</sup> A version of this chapter has been published: Boden, B.N.; Jardine, K.J.; Leung, A.C.W.; MacLachlan, M.J. "Tetraalkoxyphenanthrene: A New Precursor for Luminescent Conjugated Polymers" *Org. Lett.* **2006**, *8*, 1855-1858.

The work in this chapter was done in collaboration with A. C. W. Leung, who synthesized and characterized compounds **125**, **127** and **128**.

with high quantum yields while having good processability and interesting solid-state behavior,<sup>10, 11</sup> and similar results have been observed for poly(2,7-carbazole) (Figure 5.1).<sup>12, 13</sup>

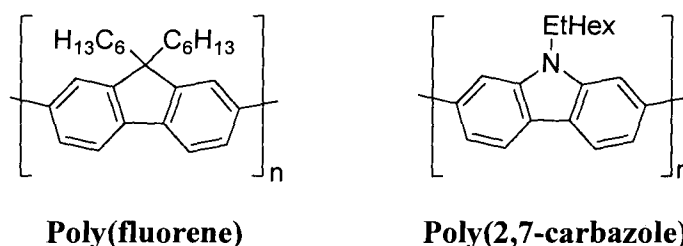


**Figure 5.1** Examples of poly(fluorene) and poly(carbazole).

Although the many derivatives of conjugated polymers now available offer a broad spectrum of color tunability, the continued development of polymers with improved stability, better quantum yields, and modified optical properties is important.

Though PPEs may be too unstable for semiconductor devices, they have been exploited for use in chemical sensors.<sup>14</sup> Modification of the side-chains in this polymer may permit control over solubility and may incorporate additional functionality. Some polymers that extend the conjugation between the alkyne groups were mentioned in Chapter 1. By incorporating zinc salphen moieties to synthesize **76** (Figure 5.2), for instance, dramatic red-shifting of the luminescence of the polymer is observed, with a resulting diminution of fluorescence intensity.<sup>15</sup> Adding triphenylene to the backbone of PPEs (**55**) can modulate the fluorescence lifetimes and can increase intrachain exciton migration.<sup>16</sup>

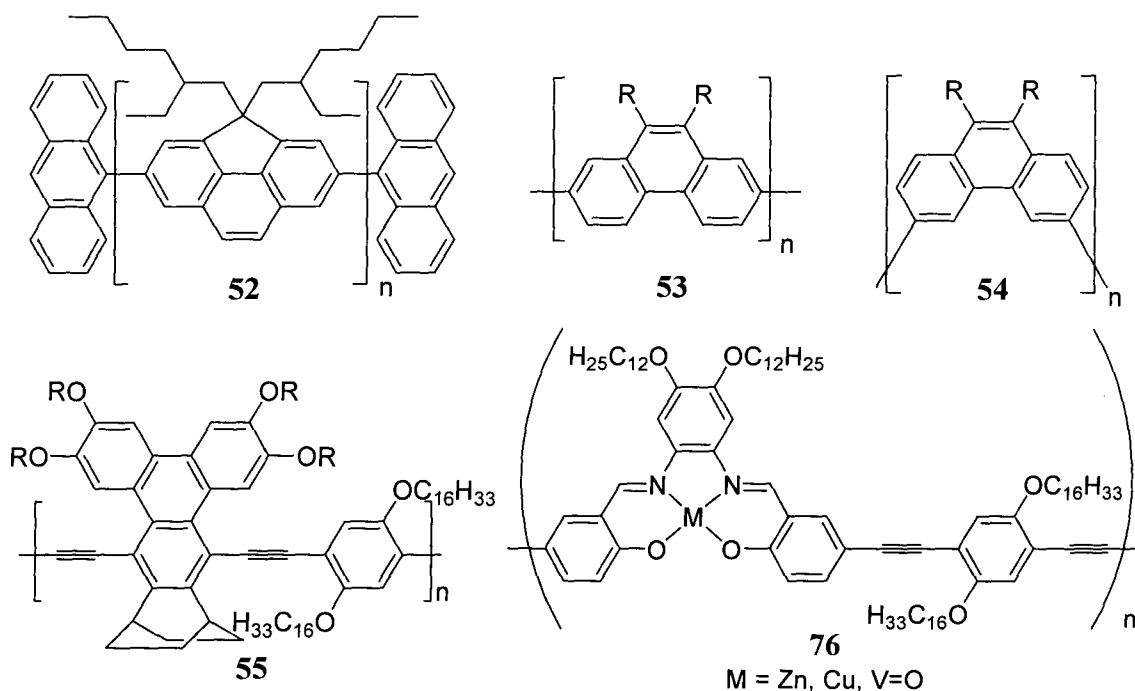


**Figure 5.2** Conjugated polymers **52-55** and **76**.

The incorporation of other conjugated species, such as phenanthrene, into PPEs and PPVs is still an underdeveloped area of exploration. Recent reports by Suh and Müllen suggest that phenanthrene may be a useful moiety for incorporation into conjugated polymers **52-54** for electroluminescent devices.<sup>17-19</sup> Unfortunately, the lack of suitable phenanthrene precursors has limited its utility in conjugated polymers. Tetraalkoxyphenanthrenes, whose syntheses were discussed in Chapter 2, are useful precursors to organic conjugated polymers. This chapter discusses the synthesis and characterization of new conjugated PPEs and PPVs which incorporate phenanthrene into the backbone and are highly luminescent.

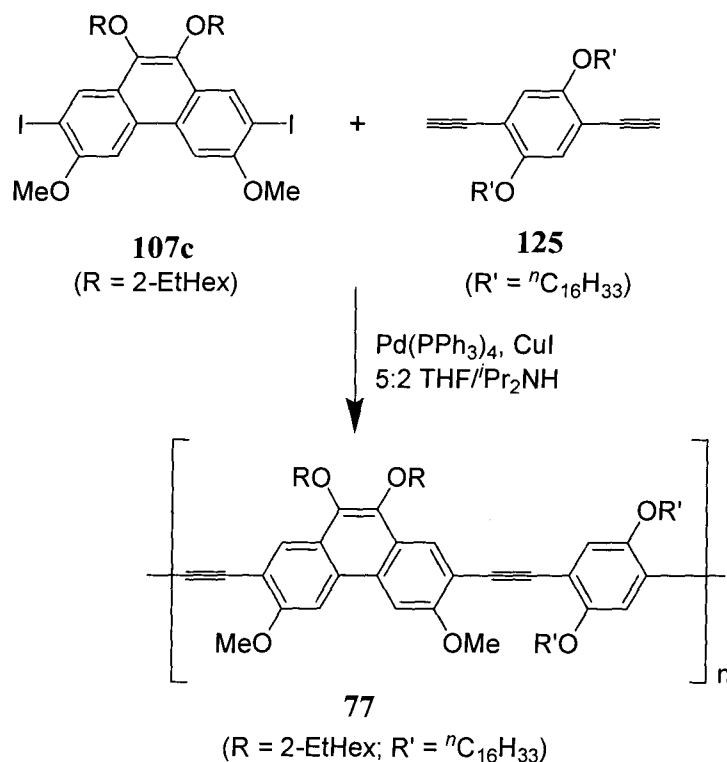
## 5.2 Discussion

### 5.2.1 Synthesis of Phenanthrene-containing PPEs

Chapter 2 introduced compounds **107a-d**, which were found to be promising reagents in the Sonogashira-Hagihara coupling. These results inspired the synthesis of a PPE derivative, similar to polymer **76**, which incorporates phenanthrene into the backbone rather than salphen. It was necessary to use derivative **107c** which has greater potential for yielding a soluble polymer. Compound **107c** can be purified by chromatography followed by recrystallization, and it is present as a mixture of diastereomers arising from the stereocenters in the branched alkyl substituents. This purification step is important to access high molecular weight polymers by step growth mechanisms.

Polymer **77** was prepared by the Pd(0)-catalyzed cross-coupling reaction of **107c** with **125** (Scheme 5.1).

**Scheme 5.1** Synthesis of polymer **77**.



Polymer **77** was purified first with an aqueous solution of KCN to remove excess copper and then precipitated out in methanol to give a rubbery yellow solid. The structure of the polymer was verified by elemental analysis and <sup>1</sup>H NMR spectroscopy (Figure 5.3). The <sup>1</sup>H NMR spectrum shows two aromatic resonances and three alkoxy peaks as required. Gel permeation chromatography (GPC) of polymer samples showed monomodal distributions with molecular weights (*M<sub>n</sub>*) between 5x10<sup>4</sup> and 1.5x10<sup>5</sup> Da (Figure 5.4), although comparison to polystyrene standards have been known to skew the molecular weight measurements of rigid rod polymers. Differential scanning calorimetry (DSC) was attempted on **77**, but no *T<sub>g</sub>* was observed.

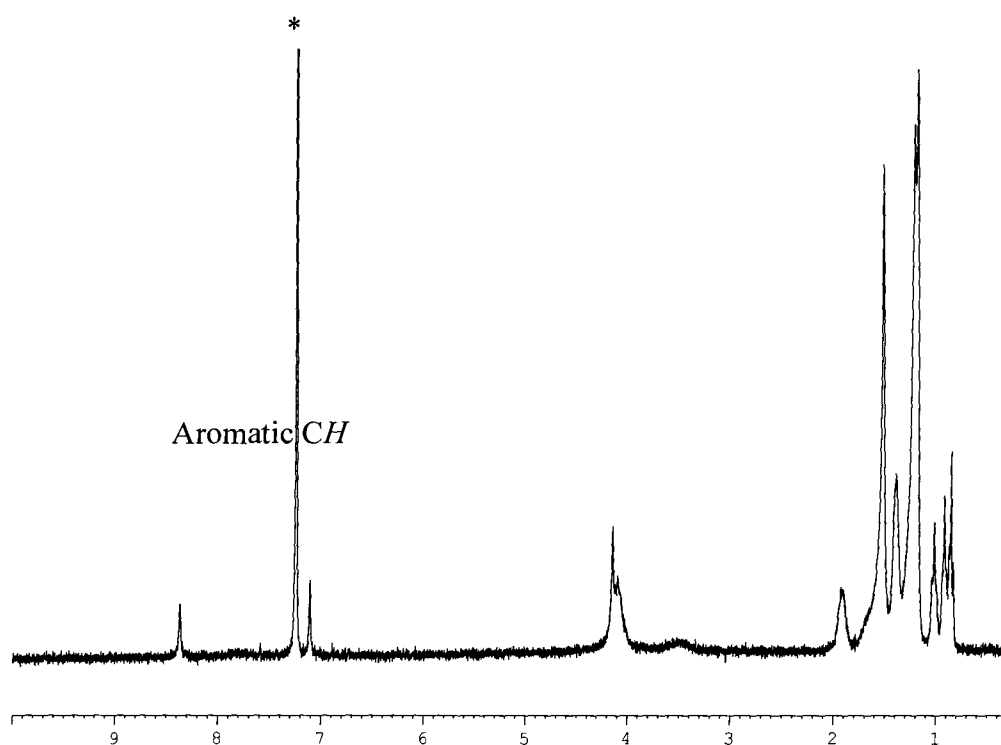


**Figure 5.3**  $^1\text{H}$  NMR spectrum (300 MHz,  $\text{CDCl}_3$ ) of **77** (\* =  $\text{CDCl}_3$ ).

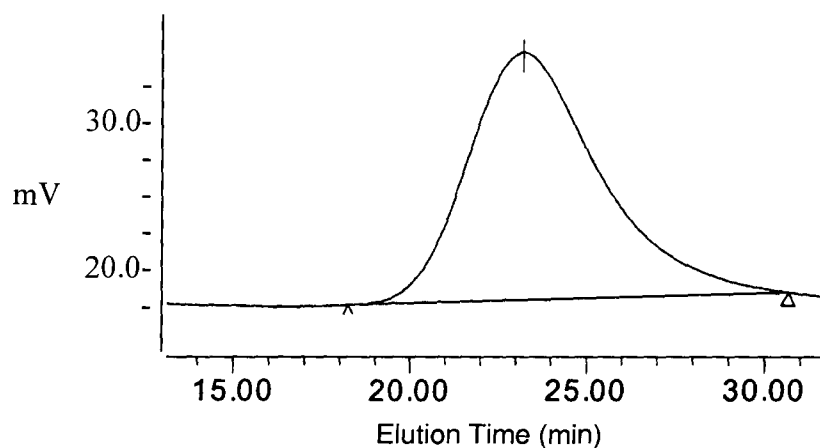


**Figure 5.4** GPC of polymer **77** in THF (ca. 1 mg/mL) measured relative to polystyrene standards.

Figure 5.5 shows the absorption and emission spectrum of both **109** and **77** in solution. The absorption maximum of **109** at 353 nm is attributed to the  $\pi$ - $\pi^*$  transition of the conjugated chain. Compound **109** also exhibits blue fluorescence ( $\lambda_{\text{em}} = 456$  nm) that is red-shifted by ca. 100 nm from the maximum absorbance. This is consistent with the Stokes shift of phenanthrene.<sup>20</sup> Polymer **77** has a  $\lambda_{\text{max}}$  that is considerably red-shifted

from **109**, indicating that the conjugation is greatly increased. The yellow polymer is fluorescent in solution ( $\lambda_{em} = 455 \text{ nm}$ ;  $\Phi_F = 70\%$ ) and in the solid state. The sample for solid state spectroscopy was obtained by spin coating a solution of the polymer onto a microscope slide. The solid-state fluorescence is only slightly red-shifted from the polymer in solution, but is significantly broadened, which may be due to  $\pi$ - $\pi$  interactions in the solid state or polymer segments locked into different conformations.

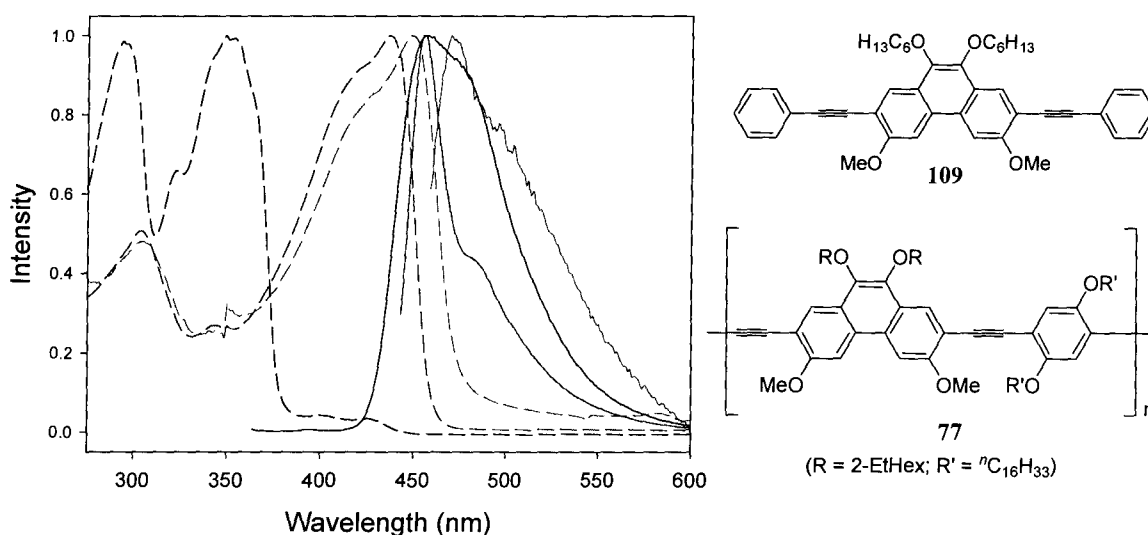


**Figure 5.5** Absorption (dashed line) and emission (solid line) spectra of model compound **109** (black,  $3.5 \times 10^{-6} \text{ M}$ ) and polymer **77** in DCM (blue,  $2.6 \text{ mg/L}$ ) and in the solid state (red).

### 5.2.2 Synthesis of Phenanthrene-containing PPVs

In an effort to develop PPV analogues, the model compound **126** was prepared by the Heck coupling of styrene with **107c**. Compound **126** is drawn as a *E,E* isomer in Scheme 5.2, but this stereochemistry cannot be confirmed, as the  $^1\text{H}$  NMR resonances for the vinyl protons overlap with other aromatic peaks. Coupling constants would indicate whether the vinyl has *E* or *Z* stereochemistry, although *trans*-stilbenes generally have downfield shifted vinyl proton resonances compared to *cis*-stilbenes.<sup>21</sup> This compound

exhibits green fluorescence at 475 nm. By reacting **107c** with divinylbenzene **127** under similar conditions, low molecular weight ( $M_n = 4400$ ) conjugated polymers **128** were formed, Scheme 5.2. The optical properties of compound **126** and polymer **128** are illustrated in Figure 5.6. The fluorescence spectrum of **128** shows emission at 499 nm (green).

**Scheme 5.2** Synthesis of **126** and **128**.

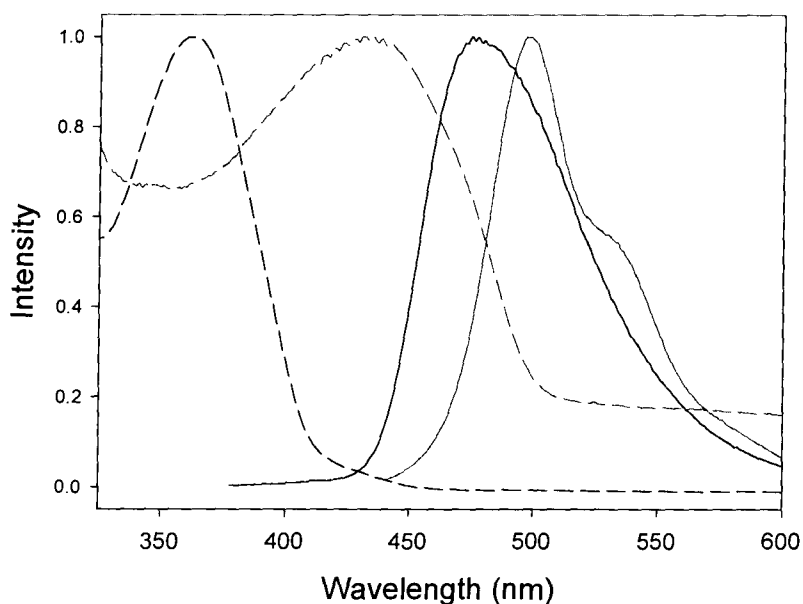
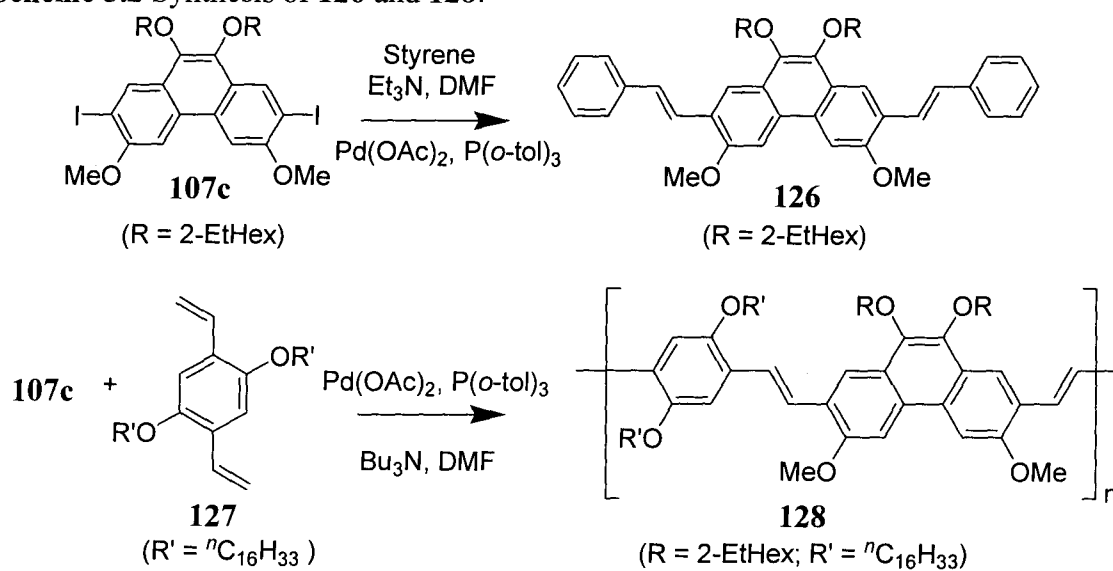
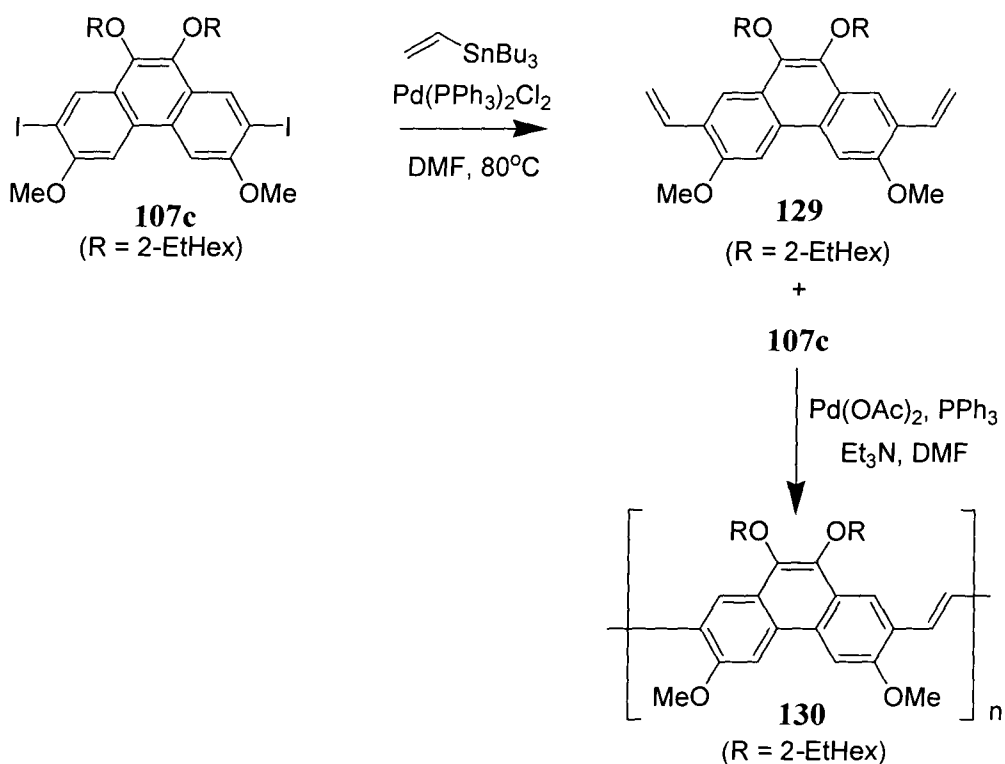


**Figure 5.6** Optical spectroscopy of **126** (black) and **128** (red) in DCM. Absorption spectra (dashed line,  $4.0 \times 10^{-6}$  M) and emission spectra (solid line, 2.0 mg/L).

To prepare an analogue of PPV incorporating only tetraalkoxyphenanthrene, we first prepared 2,7-divinyl-3,6-dimethoxy-9,10-di(2-ethylhexyloxy)phenanthrene **129** by the Stille coupling of vinyltributylstannane with compound **107c**. Compound **129** is a yellow oil that was purified by column chromatography to remove the  $\text{Bu}_3\text{SnI}$  byproduct. However, it was difficult to remove all of the impurities. Heck coupling of **107c** with **129** was undertaken, Scheme 5.3, but GPC of the product showed only oligomeric material **130**.

**Scheme 5.3** Synthesis of compound **129** and attempted polymerization.



### 5.2.3 Applications of 77

Based on studies of similar polymers,<sup>22, 23</sup> this PPE could be useful for polymer-based chemical sensors or solar cells. PPEs have been shown to efficiently sense nitroaromatic compounds.<sup>24, 25</sup> As a test to see if this was true of 77 as well, 0.11 mmol of DNT, dissolved in DCM was added to 3 mL of a 1.4 mg/L solution of 77 in DCM. The emission spectrum, Figure 5.7, shows a dramatic decrease in intensity upon addition of DNT. The change in emission intensity indicates that 77 is sensitive to the presence of DNT, but without a more detailed study of the system, it is difficult to determine how 77 compares to other PPE sensors. Also, previous research has investigated sensing of nitroaromatics using polymer thin films, rather than solutions of polymers.

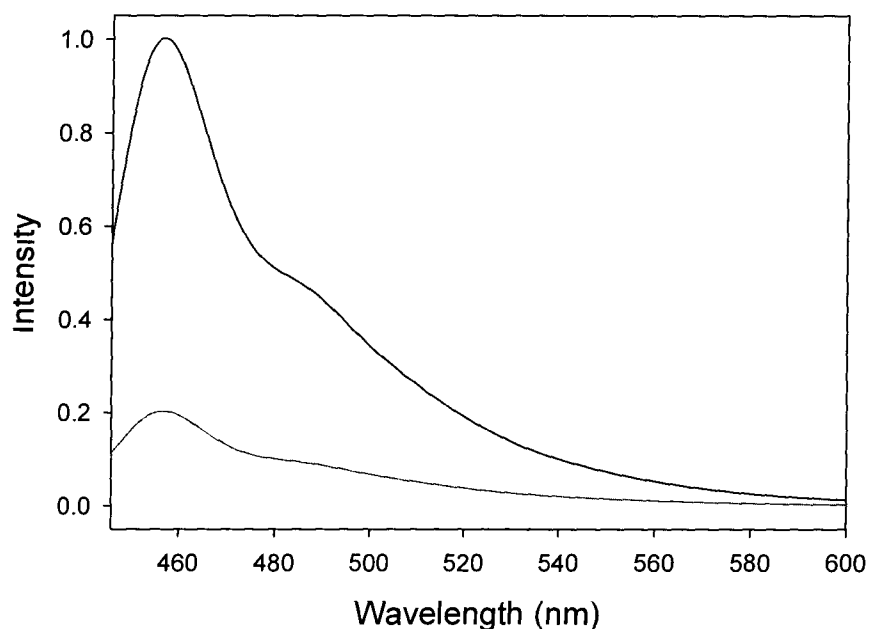


**Figure 5.7** Emission spectrum of 77 (black, 1.4 mg/L) and 77 after the addition of DNT (red).

### 5.2.4 Conclusions

Phenanthrene-containing PPE 77 was synthesized in good yield with high molecular weight, while PPV 128 was synthesized with a much lower molecular weight.

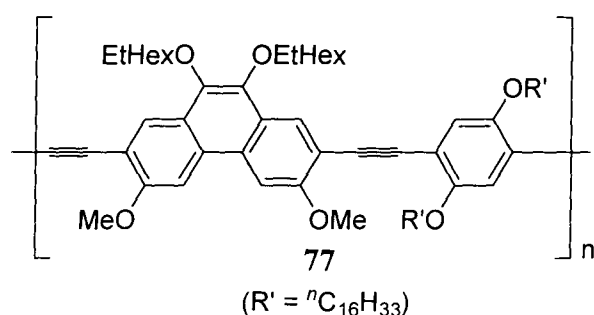
Polymer **77** is highly luminescent and has potential as a sensor for nitroaromatic compounds.

### 5.3 Experimental

#### 5.3.1 General Methods and Materials

Compounds **125**<sup>26</sup> and **127**<sup>27</sup> were synthesized from literature procedures. Molecular weights were estimated by gel permeation chromatography (GPC) using a Waters liquid chromatograph equipped with a Waters 515 HPLC pump, Waters 717 plus autosampler, Waters Styragel® columns (4.6% 300 mm) HR2, HR4 and HR5E and a Waters 2410 differential refractometer (refractive index detector). A flow rate of 0.3 mL/min was used and samples were dissolved in THF (ca. 1 mg/mL) and filtered before injection. Narrow molecular weight polystyrene standards were used for calibration purposes. Differential scanning calorimetry was performed using a Perkin Elmer Diamond DSC, scanning from -50 °C to 200 °C using 1 mg samples. All other methods and materials are as outlined in previous sections.

#### 5.3.2 Synthetic Procedures

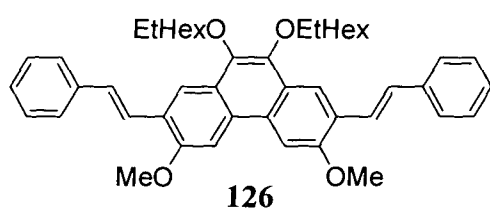


**Synthesis of Polymer 77** - Compound **107c** (0.2035 g, 0.2726 mmol) and 1,4-diethynyl-2,5-dihexadecyloxybenzene **125** (0.1688 g, 0.2781 mmol) were dissolved in 28 mL of a 5:2

THF/diisopropylamine solution and degassed by three freeze/pump/thaw cycles. CuI (30

mg, 0.16 mmol) and Pd(PPh<sub>3</sub>)<sub>4</sub> (50 mg, 0.043 mmol) were added to the solution in a nitrogen filled glovebox and the mixture underwent 2 additional freeze/pump/thaw cycles. The solution was heated to reflux under vacuum for 16 h to obtain a brown solution. The solution was filtered and the solvent was removed by vacuum. After redissolution in DCM, the solution was washed with aqueous KCN, then water. The solvent was evaporated until the polymer solution was viscous, and the solution was then precipitated in MeOH and filtered to obtain a yellow solid. This was repeated twice to remove impurities. Yield: 0.256 g, 86%. Resonances in the <sup>1</sup>H NMR spectrum were broad and only alkyl resonances could be observed in the <sup>13</sup>C NMR spectrum.

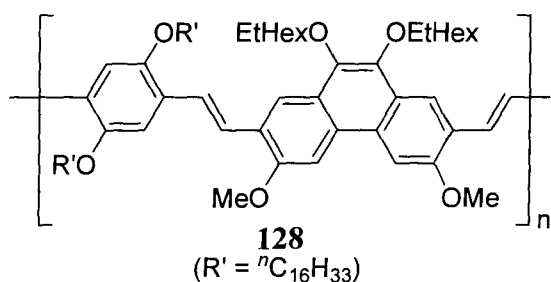
**Data for 77.** <sup>1</sup>H NMR (300 MHz, CDCl<sub>3</sub>) δ 8.35 (s, aromatic CH), 7.10 (s, aromatic CH), 4.14, 4.09 (m, alkoxy), 2.0-0.8 (br m, alkoxy); <sup>13</sup>C NMR (75.5 MHz, CDCl<sub>3</sub>) δ 40.9, 32.2, 30.8, 29.9, 29.7, 29.6, 29.4, 26.2, 24.1, 23.5, 22.9, 14.4, 14.3, 11.5, resonances from the aromatic region of the spectrum were not observed; IR (KBr): ν = 3028, 2924, 2851, 1736, 1603, 1494, 1453, 1211, 1025, 756, 697, 536 cm<sup>-1</sup>; UV-Vis (CH<sub>2</sub>Cl<sub>2</sub>) λ<sub>max</sub> = 304, 437 nm; UV-Vis (film) λ<sub>max</sub> = 449 nm; Mp. ~ 150 °C (dec.); Anal. Calc'd for C<sub>74</sub>H<sub>112</sub>O<sub>6</sub>: C, 80.97, H, 10.28. Found: C, 80.89, H, 10.00. GPC: M<sub>n</sub> = 146 000, M<sub>w</sub> = 1 370 000, PDI = 9.36. Fluorescence (CH<sub>2</sub>Cl<sub>2</sub>): λ<sub>em</sub> = 455 nm (λ<sub>exc</sub> = 438 nm), Φ<sub>F</sub> = 70%. Fluorescence (film): λ<sub>em</sub> = 470 nm (λ<sub>exc</sub> = 449 nm).



**Synthesis of Model Compound 126** - To a mixture of **107c** (0.205 g, 0.274 mmol), Pd(OAc)<sub>2</sub> (0.005 g, 0.022 mmol) and tri(o-

tolyl)phosphine (0.013 g, 0.043 mmol) were added anhydrous DMF (5 mL), triethylamine (3 mL) and styrene (0.3 mL, 2.6 mmol). The solution was heated at 130 °C for 20 h, after which it was diluted with CHCl<sub>3</sub> and washed with water. After drying with MgSO<sub>4</sub> and removing the solvent by evaporation, the residue was chromatographed using 3:1 hexanes/DCM to afford a yellow oil. Yield: 0.101 g, 0.145 mmol, 53%.

**Data for 126.** <sup>1</sup>H NMR (400 MHz, CDCl<sub>3</sub>) δ 8.46 (s, 2H, aromatic CH), 7.79 (s, 2H, aromatic CH), 7.66-7.58 (m, 6H, aromatic CH), 7.40-7.20 (m, 8H, aromatic and vinyl CH), 4.11 (d, 4H, OCH<sub>2</sub>), 4.10 (s, 6H, OCH<sub>3</sub>), 1.91 (m, 2H, CH), 1.81-1.34 (m, 18H, ethex chain), 1.05 (t, 6H, ethex chain), 0.91 (m, 6H, ethex CH<sub>3</sub>); <sup>13</sup>C NMR (75.5 MHz, CDCl<sub>3</sub>) δ 155.7, 142.2, 138.2, 130.3, 128.9, 128.6, 127.8, 127.7, 126.9, 124.6, 123.7, 120.5, 102.8, 76.7, 56.0, 41.0, 31.0, 29.6, 24.2, 23.5, 14.4, 11.5; EI-MS: *m/z* = 698 (M<sup>+</sup>); IR (NaCl): *v* = 2956, 2928, 2873, 2855, 1598, 1498, 1447, 1370, 1240, 1220, 1143, 1014, 965, 829, 752, 693 cm<sup>-1</sup>; UV-Vis (CH<sub>2</sub>Cl<sub>2</sub>) λ<sub>max</sub> (ε) = 235 (3.1 x 10<sup>4</sup>), 301 (4.6 x 10<sup>4</sup>), 362 (4.6 x 10<sup>4</sup>) nm (L mol<sup>-1</sup> cm<sup>-1</sup>); High Res MS Calc'd for C<sub>48</sub>H<sub>58</sub>O<sub>4</sub>: 698.43351. Found: 698.43323. Fluorescence (CH<sub>2</sub>Cl<sub>2</sub>): λ<sub>em</sub> = 475 nm (λ<sub>exc</sub> = 368 nm).

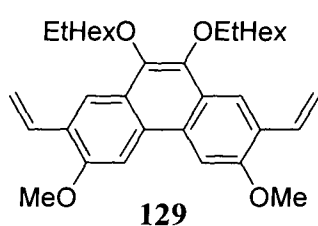


**Synthesis of Polymer 128 - Monomers**  
**107c** (0.0642 g, 0.086 mmol) and **127** (0.0526 g, 0.086 mmol) were combined in a 100 mL Schlenk tube. To these

solids were added 5 mL of dry DMF and 1 mL of distilled Bu<sub>3</sub>N via syringe. The reaction mixture was then degassed by three freeze/pump/thaw cycles. In a nitrogen filled

glovebox, Pd(OAc)<sub>2</sub> (50 mg, 0.043 mmol) and (o-tol)<sub>3</sub>P (0.013 g, 0.043 mmol) were added. The reaction mixture was subsequently freeze/pump/ thawed one more time. A fluorescent green solution was obtained after heating the reaction mixture at 85 °C for 40 h. After cooling to room temperature, the solution was filtered and precipitated into 200 mL of MeOH to yield a yellow precipitate. The polymer was further purified by precipitating the polymer from DCM into MeOH. The above procedure gave 0.095 g of polymer **128** in 45% yield. Resonances in the <sup>1</sup>H NMR spectrum were broad and only alkyl resonances could be observed in the <sup>13</sup>C NMR spectrum.

**Data for 128.** <sup>1</sup>H NMR (300 MHz, CDCl<sub>3</sub>) δ 8.46 (br), 7.80 (br), 7.69 (br), 7.21 (br), 6.8-6.6 (br), 4.2-3.7 (br), 2.0-0.8 (br); <sup>13</sup>C NMR (100.6 MHz, CDCl<sub>3</sub>) δ 56.0, 40.9, 32.1, 29.9, 29.5, 26.4, 23.4, 22.9, 14.3, 11.4, resonances from the aromatic region of the spectrum were not observed; IR (NaCl): ν = 2955, 2923, 2852, 1728, 1677, 1598, 1502, 1467, 1422, 1364, 1239, 1204, 1146, 1016 cm<sup>-1</sup>; UV-Vis (CH<sub>2</sub>Cl<sub>2</sub>) λ<sub>max</sub> = 431 nm; GPC: M<sub>n</sub> = 4439, M<sub>w</sub> = 8702, PDI = 1.96. Fluorescence (CH<sub>2</sub>Cl<sub>2</sub>): λ<sub>em</sub> = 499 nm (λ<sub>exc</sub> = 441 nm), Φ<sub>F</sub> = 59%.



#### Synthesis of 9,10-diethylhexyloxy-3,6-dimethoxy-2,7-

**divinylphenanthrene 129** - A solution of tributyl(vinyl)tin (0.84 mL, 2.6 mmol) in DMF (40 mL) was added to a mixture of **107c** (0.714 g, 0.957 mmol) and Pd(PPh<sub>3</sub>)<sub>2</sub>Cl<sub>2</sub> (0.067 g,

0.095 mmol). The resulting solution was heated to 80 °C for 3 h and cooled. Ether (100 mL) was added to the reaction and the solution was washed (3 x 100 mL) with aqueous

NH<sub>4</sub>Cl. The organic layer was flashed through silica and the solvent was removed under vacuum. Chromatography with 7:1 hexanes/DCM afforded a pale yellow oil. Yield: 0.237 g, 0.433 mmol, 45%.

**Data for 129.** <sup>1</sup>H NMR (300 MHz, CDCl<sub>3</sub>) δ 8.35 (s, 2H, aromatic CH), 7.76 (s, 2H, aromatic CH), 7.22 (dd, 2H,  $J_{\text{trans}} = 17.7$  Hz,  $J_{\text{cis}} = 11.1$  Hz, H<sub>2</sub>C=CH), 5.96 (dd, 2H,  $J_{\text{trans}} = 17.7$  Hz,  $J_{\text{gem}} = 1.5$  Hz, C=CH<sub>trans</sub>), 5.40 (dd, 2H,  $J_{\text{cis}} = 11.1$  Hz,  $J_{\text{gem}} = 1.5$  Hz, C=CH<sub>cis</sub>), 4.08 (d, 4H, OCH<sub>2</sub>), 4.05 (s, 6H, OCH<sub>3</sub>), 1.89 (m, 2H, ethex chain), 1.63 (m, 8H, ethex chain), 1.40 (m, 8H, ethex chain), 1.02 (t, 6H, ethex chain), 0.94 (t, 6H, ethex chain); <sup>13</sup>C NMR (75.5 MHz, CDCl<sub>3</sub>) δ 155.5, 142.2, 132.1, 130.4, 128.7, 128.8, 124.5, 120.8, 115.6, 102.6, 76.6, 55.9, 41.0, 30.9, 29.5, 24.1, 23.4, 14.3, 11.4; ESI-MS:  $m/z = 569$  ([M+Na]<sup>+</sup>); IR (NaCl)  $\nu = 2959, 2923, 2873, 2855, 1601, 1484, 1456, 1446, 1368, 1236, 1142, 1047, 997, 901, 834$  cm<sup>-1</sup>; UV-Vis (CH<sub>2</sub>Cl<sub>2</sub>)  $\lambda_{\text{max}} (\epsilon) = 284 (6.2 \times 10^4), 318 (3.3 \times 10^4)$  nm (L mol<sup>-1</sup> cm<sup>-1</sup>); High Res MS Calc'd for C<sub>36</sub>H<sub>50</sub>O<sub>4</sub>: 546.37091. Found: 546.37118. Fluorescence (CH<sub>2</sub>Cl<sub>2</sub>):  $\lambda_{\text{em}} = 449$  nm ( $\lambda_{\text{exc}} = 318$  nm).

**Heck coupling of 129 with 107c** - To a mixture of **107c** (0.073 g, 0.098 mmol), **129** (0.059 g, 0.11 mmol), Pd(OAc)<sub>2</sub> (0.001 g, 0.0045 mmol) and PPh<sub>3</sub> (0.010 g, 0.038 mmol) were added anhydrous DMF (4 mL) and triethylamine (2 mL). The resulting yellow solution was heated to reflux for 48 h, after which it was filtered and precipitated into MeOH to obtain a yellow solid. A second attempt at precipitation was unsuccessful and the product (**130**) was recovered through evaporation of the solvent.

**Data for 130.**  $^1\text{H}$  NMR (300 MHz,  $\text{CDCl}_3$ )  $\delta$  7.7 (br), 7.5 (br), 7.2 (br), 4.2 (br), 4.1 (br), 2.3-0.5 (br); IR (NaCl)  $\nu$  = 2954, 2929, 2873, 2860, 1725, 1594, 1461, 1368, 1265, 1239, 1131, 1017  $\text{cm}^{-1}$ ; GPC:  $M_n$  = 2200,  $M_w$  = 3300.

## 5.4 References

- (1) Heeger, A. J. *Angew. Chem. Int. Ed.* **2001**, *40*, 2591-2611.
- (2) Kraft, A.; Grimsdale, A. C.; Holmes, A. B. *Angew. Chem. Int. Ed.* **1998**, *37*, 402-428.
- (3) Perepichka, I. F.; Perepichka, D. F.; Meng, H.; Wudl, F. *Adv. Mater.* **2005**, *17*, 2281-2305.
- (4) Mikroyannidis, J. A. *Macromolecules* **2002**, *35*, 9289-9295.
- (5) Chan, K. L.; McKeirnan, M. J.; Towns, C. R.; Holmes, A. B. *J. Am. Chem. Soc.* **2005**, *127*, 7662-7663.
- (6) Burroughes, J. H.; Bradley, D. C. C.; Brown, A. R.; Marks, R. N.; Mackay, K.; Friend, R. H.; Burns, P. L.; Holmes, A. B. *Nature* **1990**, *347*, 539-541.
- (7) Gustaffson, G.; Cao, Y.; Treacy, G. M.; Klavetter, F.; Colaneri, N.; Heeger, A. J. *Nature* **1992**, *357*, 477-479.
- (8) Morin, J. -F.; LeClerc, M.; Adès, D.; Siove, A. *Macromol. Rapid Commun.* **2005**, *26*, 761-778.
- (9) Rose, A.; Zhu, Z.; Madigan, C. F.; Swager, T. M.; Bulovic, V. *Nature* **2005**, *434*, 876-879.
- (10) Ohmori, Y.; Uchida, M.; Muro, K.; Yoshino, K. *Jpn. J. Appl. Phys.* **1991**, *30*, L1941-L1943.
- (11) Scherf, U.; List, E. J. W. *Adv. Mater.* **2002**, *14*, 477-487.
- (12) Grazulevicius, J. V.; Strohriegl, P.; Pielichowski, J.; Pielichowski, K. *Prog. Polym. Sci.* **2003**, *28*, 1297-1353.
- (13) Iraqi, A.; Wataru, I. *Chem. Mater.* **2004**, *16*, 442-448.
- (14) Kim, I. -B.; Dunkhorst, A.; Gilbert, J.; Bunz, U. H. F. *Macromolecules* **2005**, *38*, 4560-4562.
- (15) Leung, A. C. W.; Chong, J. H.; Patrick, B. O.; MacLachlan, M. J. *Macromolecules* **2003**, *36*, 5051-5054.
- (16) Rose, A.; Lugmair, C. G.; Swager, T. M. *J. Am. Chem. Soc.* **2001**, *123*, 11298-11299.
- (17) Park, S. H.; Kim, J. Y.; Kim, S. H.; Jin, Y.; Kim, J.; Suh, H.; Lee, K. *Proc. of SPIE* **2005**, *5937*, 593710/1-593710/6.

- (18) Suh, H.; Jin, Y.; Park, S. H.; Kim, D.; Kim, J.; Kim, C.; Kim, J. Y.; Lee, K. *Macromolecules* **2005**, *38*, 6285-6289.
- (19) Yang, C.; Scheiber, H.; List, E. J. W.; Jacob, J.; Müllen, K. *Macromolecules* **2006**, *39*, 5213-5221.
- (20) Zimmermann, T. J.; Müller, T. J. J. *Eur. J. Org. Chem.* **2002**, 2269-2279.
- (21) Buquet, A.; Couture, A.; Lablache-Combier, A. *J. Org. Chem.* **1979**, *44*, 2300-2303.
- (22) Bunz, U. H. F. *Chem. Rev.* **2000**, *100*, 1605-1644.
- (23) Alam, M. M.; Jenekhe, S. E. *Chem. Mater.* **2004**, *16*, 4647-4656.
- (24) Chang, C. -P.; Chao, C. -Y.; Huang, J. H.; Li, A. -K.; Hsu, C. -S.; Lin, M. -S.; Hsieh, B. R.; Su, A. C. *Synth. Met.* **2004**, *144*, 297-301.
- (25) Yang, J. -S.; Swager, T. M. *J. Am. Chem. Soc.* **1998**, *120*, 11864-11873.
- (26) Swager, T. M.; Gil, C. J.; Wrighton, M. S. *J. Phys. Chem.* **1995**, *99*, 4886-4893.
- (27) Peng, Z.; Galvin, M. E. *Chem. Mater.* **1998**, *10*, 1785-1788.

## Chapter 6

# Synthesis and Characterization of Thienyl-Schiff Base Monomers<sup>§</sup>

### 6.1 Introduction

The previous chapters of this thesis have discussed new Schiff base macrocycles containing phenanthrene and triphenylene. This chapter discusses a side project involving the synthesis of new Schiff base monomers for use in electropolymerization.

#### 6.1.1 Schiff Base Polymers

Chapter 1 introduced macrocycles utilizing the Schiff base condensation, but there is a large body of research concerning Schiff base polymers as well. Polymers can incorporate salen and salphen in many ways, and although groups for polymerization are most often included on the salicylate moieties, the salen can be suspended from the polymer if the backbone connects only to the diamine. Additionally, the polymer can be formed through either chemical polymerization or electropolymerization.

Early examples from 1957 include metal-templated condensation polymerization of diamines and bis(salicylaldehydes) joined by a CH<sub>2</sub> or SO<sub>2</sub> spacer to synthesize

---

<sup>§</sup> A portion of this chapter has been submitted for publication: (a) Sih, B.C.; Pietrangelo, A.; Boden, B. N.; Wang, Z.; Li, Q.; Chou, K.C.; MacLachlan, M. J.; Wolf, M. O. "Nonlinear Optical Properties of Schiff-Base-Containing Conductive Polymer Films Electrodeposited in Microgravity"

The work in this chapter was done in collaboration with Dr. B. C. Sih, who studied electropolymerization of the monomers.

polymer **131**,<sup>1,2</sup> shown in Figure 6.1. These polymers have limited solubility, and cannot be properly characterized. They are thermally stable, although less so than corresponding salen model compounds. Polymer **131b** shows improved thermal stability over **131a** as a result of the more electron-withdrawing spacer.

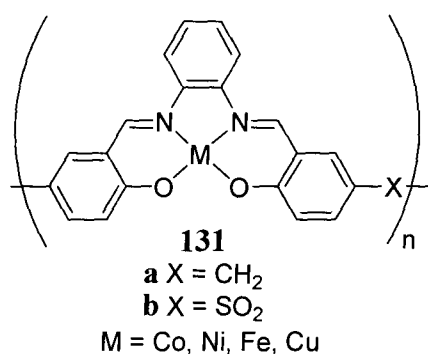
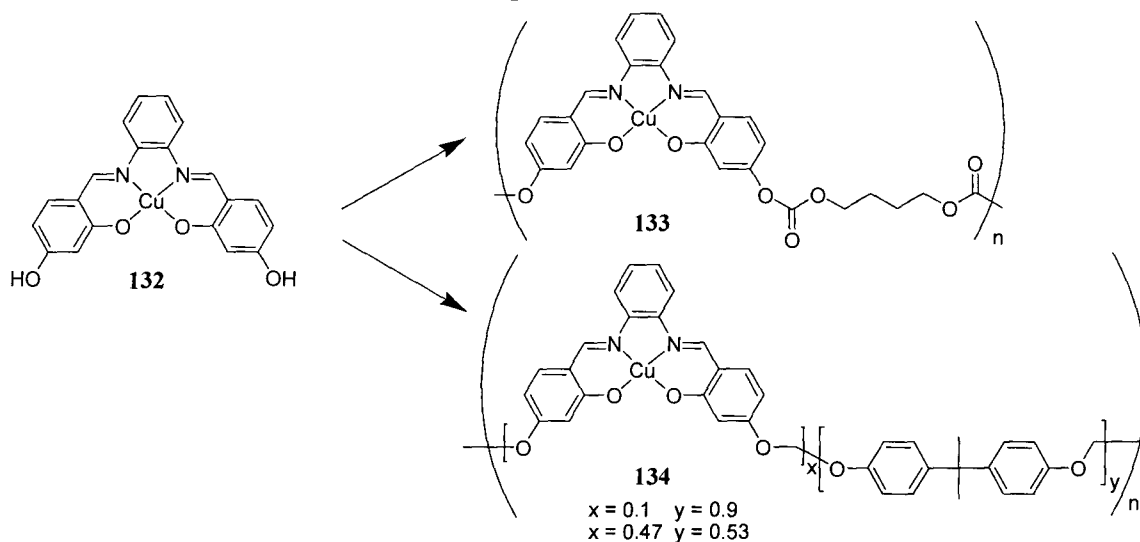


**Figure 6.1** Early examples of Schiff base polymers.

Copolymerization of salen complexes containing useful functional groups with complementary co-monomers has also been employed to obtain Schiff base polymers.<sup>3</sup> First, Schiff base monomers **132** with hydroxyl groups *para* to the imine were synthesized. Polycarbonates **133** and polyethers **134** can be made from the Cu-containing monomers and either a bischloroformate or a combination of dibromoethane, and Bisphenol A as co-monomers. The polycarbonate polymer was synthesized as an alternating copolymer, while the polyethers were formed as statistical copolymers, with different percentages of the salen unit in the polymer backbone. The molecular weights of **133** and **134** were low, indicating that only oligomers were formed.

**Scheme 6.1** Synthesis of condensation polymers **133** and **134**.



Using diiodo-substituted salphen monomers, Sonogashira coupling can be employed to make salphen-based poly(phenyleneethynylene)s **76**.<sup>4</sup> These polymers can be made with high molecular weight, but were not as luminescent as anticipated. Shifting the ethynyl group *para* to the imine makes a helical PPE **135** that has greater solubility and increased conjugation.<sup>5</sup> Zn(II) complexes of the polymers show decrease in luminescence upon titration of polymer solution with pyridine, indicating that the polymers may aggregate as a result of interaction between the phenolic oxygen with the Zn(II) centers. Ni(II) and Cu(II)-containing polymers do not exhibit spectral changes in the presence of coordinating bases.

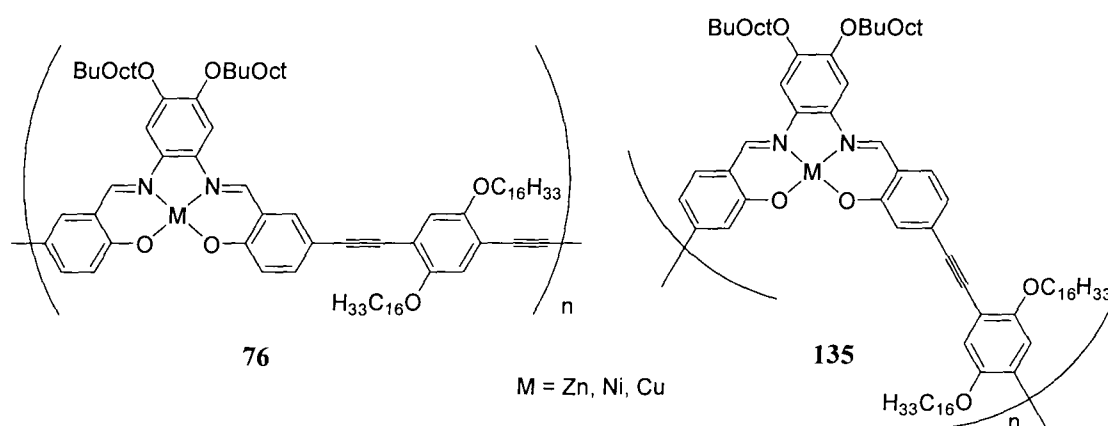


**Figure 6.2** Schiff base PPEs **76** and **135**.

Swager and Reynolds have synthesized thiophene-containing Schiff base monomers and studied electropolymerization of these compounds. Electropolymerization of monomers **136a** and **136b** ( $M = \text{Co}$ ) gave conductive polymers where the metal does not contribute to conductivity but is necessary for electropolymerization of these monomers.<sup>6</sup> Changing the substituents on **136b** from  $R = \text{H}$  to bulkier groups such as  $R = \text{Ph}$  increases the interchain spacing and results in a decrease in conductivity for  $\text{Cu(II)}$ -containing polymers.<sup>7</sup> Reynolds investigated electropolymerization of monomers **137** and **138**, and found that polymerization occurs at the phenylene for **137**.<sup>8,9</sup> In the case of **138**, polymerization could occur at either the thienyl or at the phenylene, unless  $R = \text{CH}_3$ , in which case polymerization occurs exclusively through the oligothiophene unit.

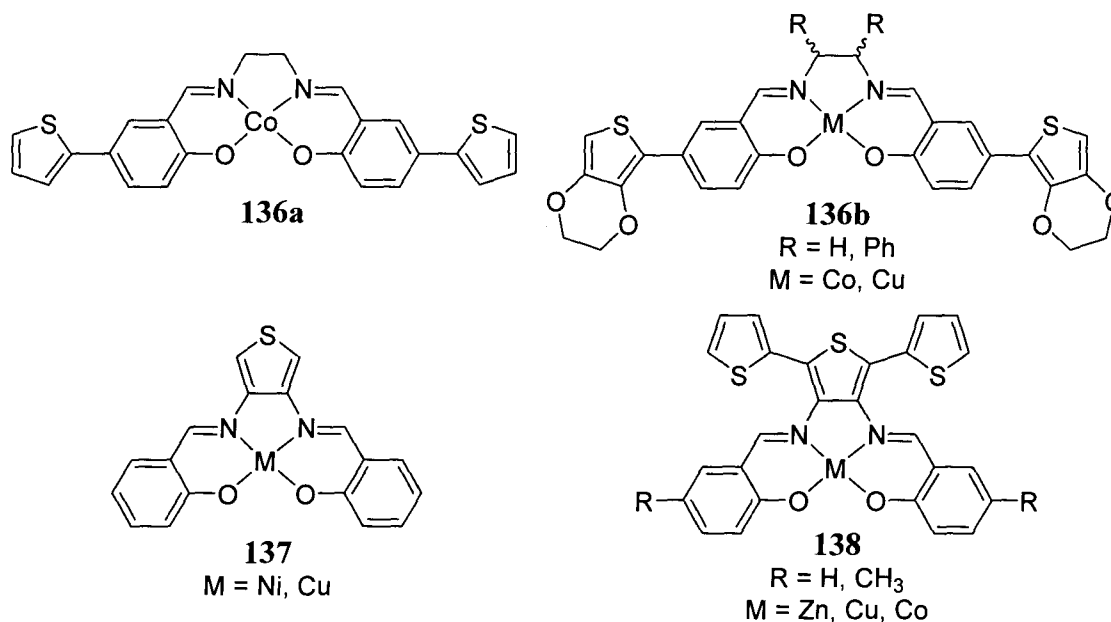


**Figure 6.3** Thiophene-containing Schiff base monomers **136-138**.

Our goals were to modify some of Swager's monomers for electropolymerization, synthesize polymer films in both gravity and microgravity, and study their nonlinear

optical properties. This chapter will deal mainly with synthesis of the monomers, with some brief discussion of initial electropolymerization experiments.

## 6.2 Discussion

### 6.2.1 Synthesis of 5-thienyl Salphen Monomers

Both conjugated polymers and Schiff base metal complexes have been found to have potential for non-linear optical materials.<sup>10</sup> Monomers **136a** and **136b** are known to electropolymerize but the monomers and resulting polymer films have not been studied for NLO properties. By producing a more ordered film, NLO properties can be enhanced, and electropolymerization under microgravity could provide improved film uniformity because gravity-driven convection currents are absent.<sup>11</sup> Modification of the monomers by using alkoxy-substituted phenylenediamines rather than ethylenediamine allows for tuning of the solubility of the monomer and the separation between individual polymer chains.

Salphen **140** was prepared by Schiff base condensation of 5-(2-thienyl)salicylaldehyde **139** and 1,2-dialkoxy-4,5-phenylenediamine derivatives **115** (Scheme 6.2). These reactions produced red-orange powders with varying solubility depending on the length of the alkoxy chain. <sup>1</sup>H NMR spectroscopy of these powders revealed a resonance at 8.63 ppm for **140a**, characteristic of the imine proton. An OH resonance was observed at 13.24 ppm (Figure 6.4).

**Scheme 6.2** Synthesis of compounds **140-144**.

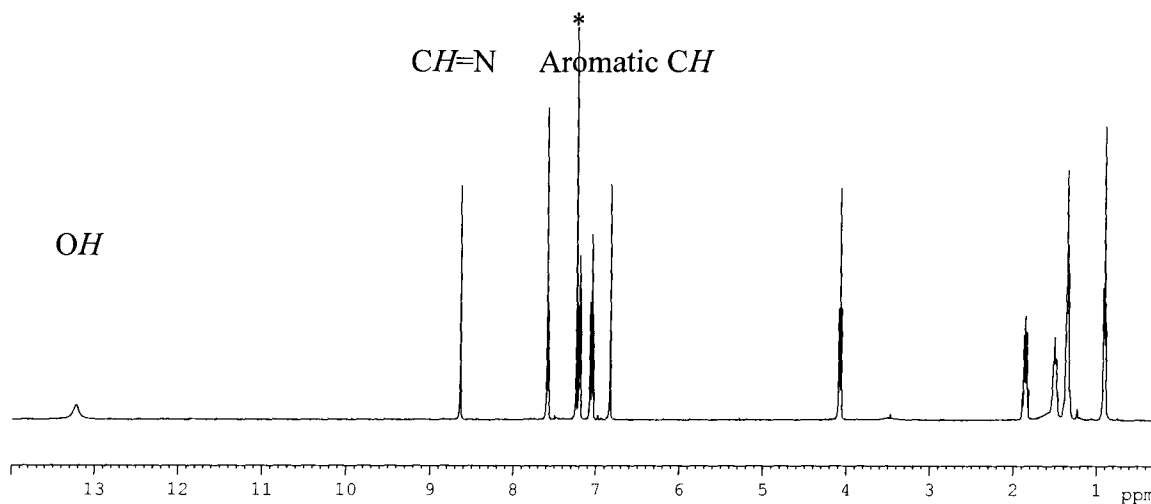
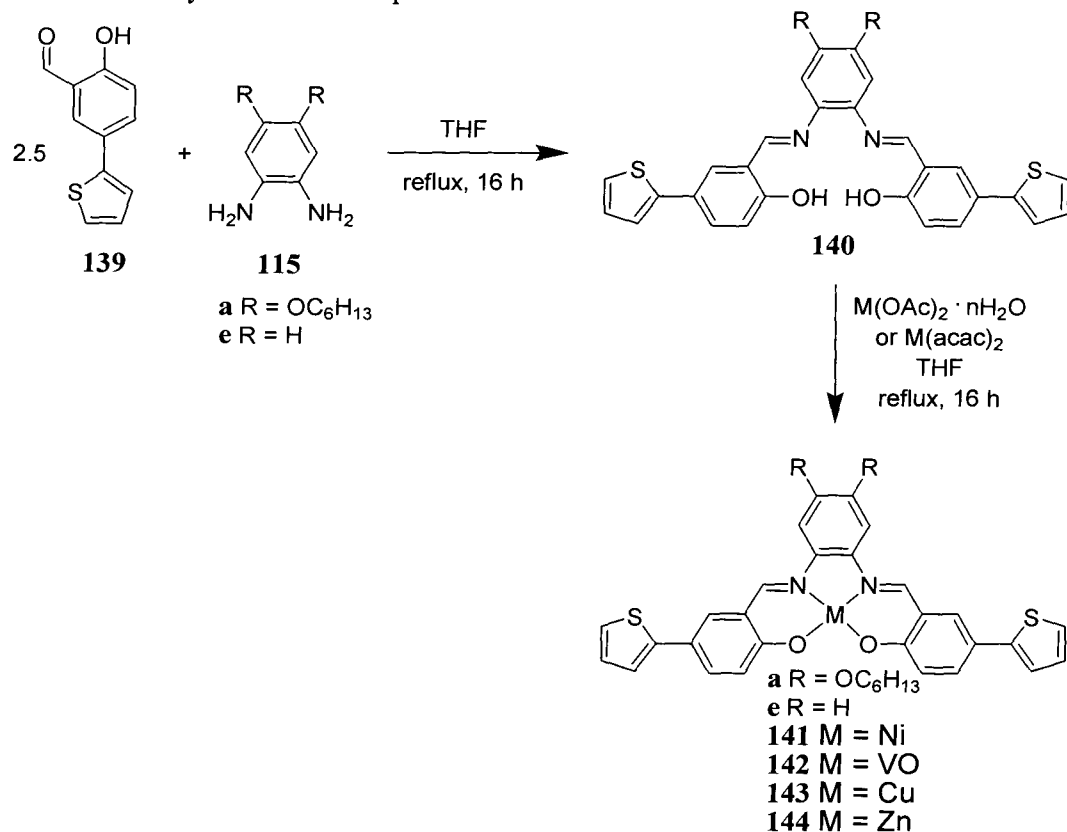


**Figure 6.4** <sup>1</sup>H NMR (300 MHz, CDCl<sub>3</sub>) spectrum of **140a** (\* = CDCl<sub>3</sub>).

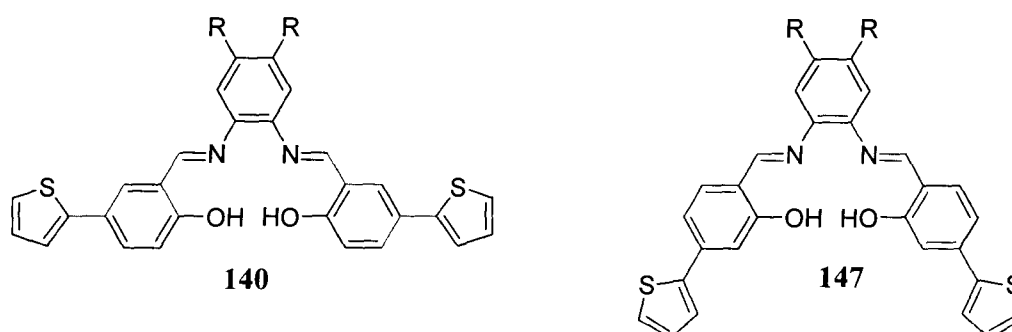
Formation of the metal complexes **141-144** was accomplished by refluxing solutions of metal and ligand overnight in THF. Complexation was identified by the disappearance of the hydroxyl resonance in the <sup>1</sup>H NMR spectrum for nickel and zinc

complexes **141** and **144**. The identities of the paramagnetic copper and vanadyl complexes **142** and **143** were confirmed through electrospray mass spectrometry. Complexes **141-143** were sufficiently soluble in methylene chloride for electropolymerization; however **141e-143e** were markedly less soluble than **141a-143a** due to the absence of an alkoxy chain. Zinc complex **144a** was insoluble in most solvents, rendering it useless for further study. All compounds were checked for purity using elemental analysis.

Electropolymerization for these compounds resulted in thin films deposited onto Au on glass. Monomers **140-143e** were found to produce thinner films resulting from their more limited solubility.

### 6.2.2 Synthesis of 4-thienyl Salphen Monomers

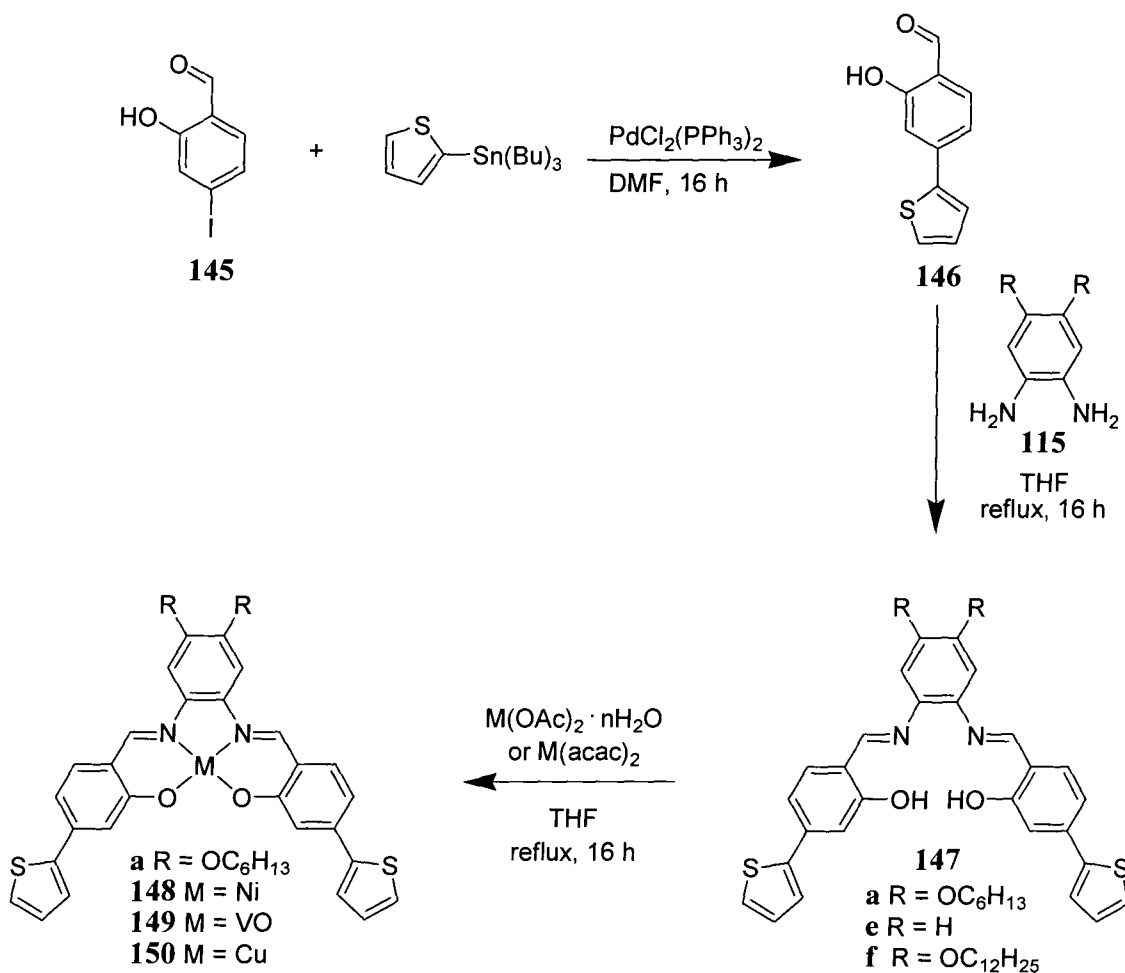
While electropolymerization is known for salphens formed from 5-(2-thienyl)salicylaldehyde, it has not been studied for salphens made from 4-(2-thienyl)salicylaldehyde. The structure of compound **140** can be represented with adjacent single bonds in the salphen backbone, resulting in a break in the conjugation through the phenylenediimine (Figure 6.5). By moving the thienyl group *para* to the imine, the conjugation extends through the entire organic backbone.



**Figure 6.5** Monomer **140**, with breaks in conjugation shown in red. Conjugated monomer **147**, with the path of conjugation in blue.

4-Iodosalicylaldehyde **145** is coupled with 2-tributylstannylthiophene using a Stille coupling to form salicylaldehyde **146**, in an analogous fashion to the synthesis of **139**. This reaction gives a beige product in 92% yield. Next, a Schiff base condensation of **146** with diamine **115** gives salphen **147**, an orange solid. With longer alkoxy chains on the salphen, a longer reaction time is required for complete conversion to the product. The  $^1\text{H}$  NMR spectrum of **147a** is similar to that of **140a**, showing an imine resonance at 8.56 ppm and a hydroxyl resonance at 13.34 ppm, with disappearance of the formyl peak at 9.84 ppm.

**Scheme 6.3** Synthesis of compounds **146-150**.



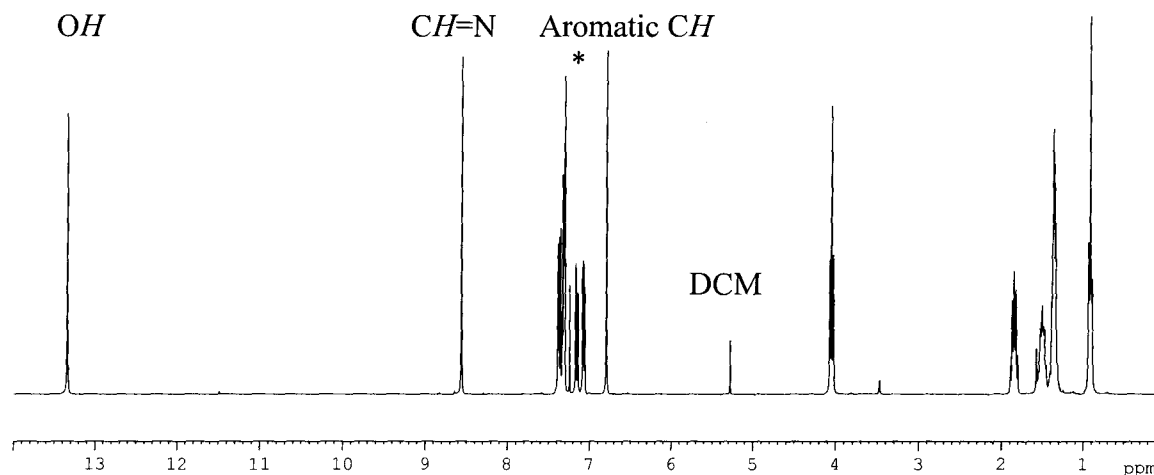


**Figure 6.6**  $^1\text{H}$  NMR (300 MHz,  $\text{CDCl}_3$ ) spectrum of **147a** (\* =  $\text{CDCl}_3$ ).

Reflux of **147a** in THF with the appropriate metal salt gives the metallated salphens **148a-150a**. All three metal complexes crystallize readily, but the resulting crystals are thin and unsuitable for X-ray diffraction. Once again, a  $^1\text{H}$  NMR spectrum can only be obtained for **148a** with a diamagnetic Ni(II) center, but elemental analysis confirmed the purity of both **149a** and **150a**.

Electropolymerization was attempted with all four compounds, but only the Ni(II) complex **148a** and Cu(II) complex **150a** reacted and the films obtained were of poor quality. The vanadyl complex **149a** and the metal free salphen **147a** did not electropolymerize at all.

In the literature, there are no examples of electropolymerization of thiophene-substituted benzene with an imine para to the thienyl group. The first step of electropolymerization of dithienylsalphen monomers involves oxidation of the thiophene to form a radical cation (Figure 6.7). The oxidized species of **147** has more resonance structures than the oxidized species of **140**, because of the increased conjugation of the salphen. As a result, the radical cation of **147** may be stable enough to prevent polymerization.

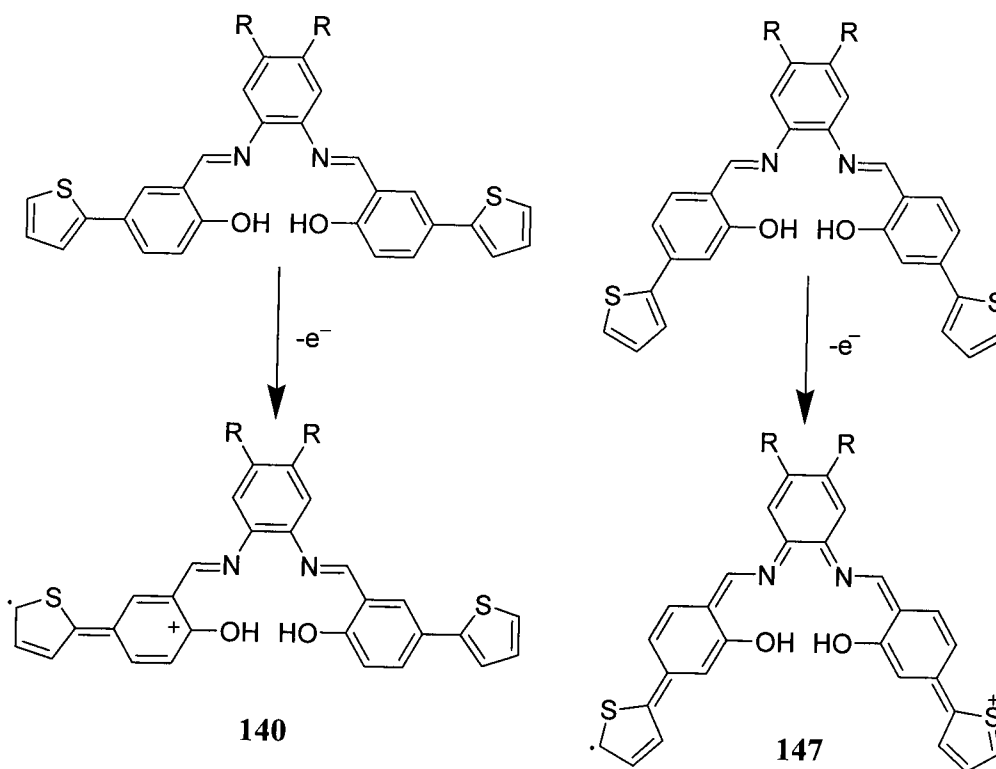


**Figure 6.7** Formation of the radical cations for **140** and **147**, showing one resonance structure for each monomer.

### 6.2.3 Absorption of Salphen Monomers

In order to confirm the difference in conjugation of the monomers, absorption spectra of the monomers were obtained. Like macrocycles **74** and **75**, there should be a bathochromic shift for the conjugated species. The optical spectra of **140a** - **143a** and **147a** - **150a** are included in Figure 6.8.

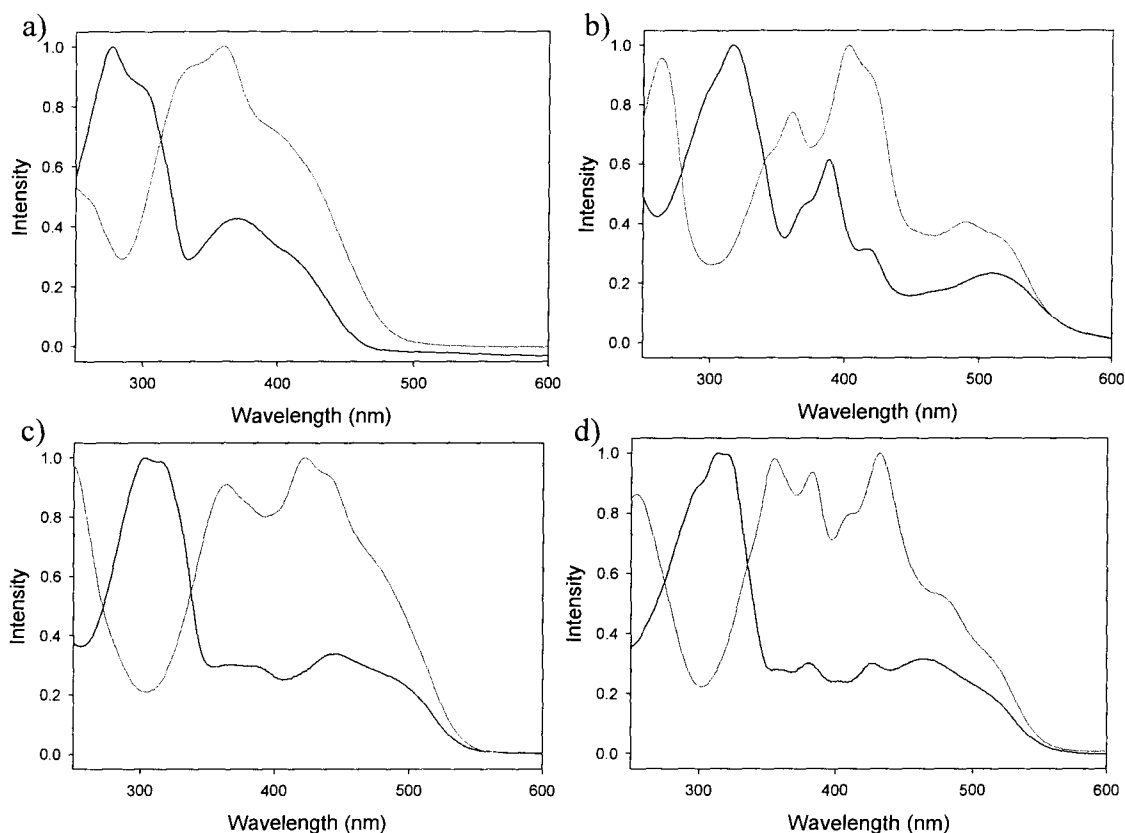


**Figure 6.8** Normalized absorption spectra of dithienylsalphen monomers in DCM (concentration  $4.0 - 5.0 \times 10^{-6}$  M), where a) **140a** (black), **147a** (red) b) **141a** (black), **148a** (red) c) **142a** (black), **149a** (red), d) **143a** (black), **150a** (red).

For the metal-free monomers, there is a clear red-shift by approximately 30 nm for **147** compared to **140**. In the metallated monomers, there does not appear to be a bathochromic shift for the 4-thienylsalphen complexes, resulting from overlap of the absorption bands of the coordination complex, and it is therefore difficult to determine whether the increased conjugation is present in **148a - 150a**. Interestingly, the most intense absorption bands for conjugated monomers **147a - 150a** have longer wavelengths than the other bands in the spectrum, while the most intense bands for the less conjugated monomers **140a - 143a** are blue-shifted compared to other bands in the spectrum. This trend is similar to that of the absorption bands of **74** and **75**.

## 6.2.4 Conclusions

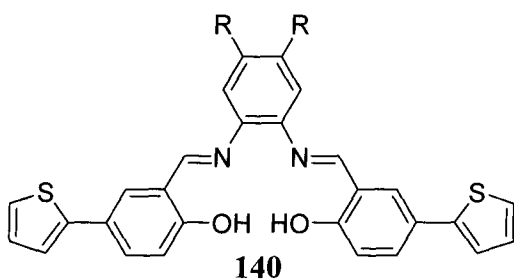
Compounds **140-143** were synthesized and found to be suitable monomers for electropolymerization. Previously unreported compounds **147-150** have been synthesized but were found to be poor monomers for electropolymerization.

## 6.3 Experimental

### 6.3.1 General Methods and Materials

Compounds **139**<sup>6</sup> and **145**<sup>12</sup> were prepared according to literature procedures. All other methods and materials are as outlined in previous sections.

### 6.3.2 Synthetic Procedures



#### Synthesis of *N,N'*-Phenylenebis(5-(2-thienyl)salicylideneimines) (**140a, e**) -

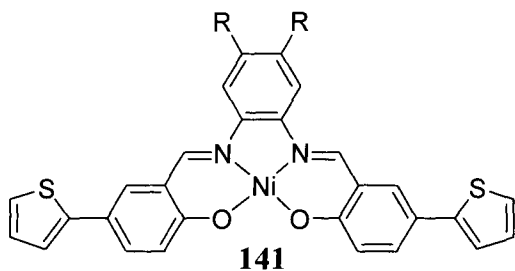
Compounds **115a** (0.306 g, 0.992 mmol) and 5-thienylsalicylaldehyde (0.475 g, 2.33 mmol)

were combined in a 100 mL Schlenk flask

under a nitrogen atmosphere. To the mixture was added 20 mL of dry THF to form an orange solution. After heating the reaction to reflux overnight, the solution was cooled to room temperature and the volume of solvent was reduced. Addition of methanol to the solution caused precipitation of an orange solid, which was collected on a Büchner funnel and washed with additional methanol. The same procedure was followed with **115e** to obtain **140e**. Yield for **140a**: 0.614 g, 0.90 mmol, 91%. Yield for **140e**: 0.566 g, 1.18 mmol, 66%.

**Data for 140a.**  $^1\text{H}$  NMR (300 MHz,  $\text{CDCl}_3$ )  $\delta$  13.24 (s, 2H, OH), 8.63 (s, 2H, CH=N), 7.60-7.56 (m, 4H, aromatic CH), 7.22-7.18 (m, 4H, aromatic CH), 7.07-7.02 (m, 4H, aromatic CH), 6.82 (s, 2H, aromatic CH) 4.07 (t, 4H,  $\text{OCH}_2$ ), 1.86-0.88 (m, 22H, hexyl chain);  $^{13}\text{C}$  NMR (100.7 MHz,  $\text{CDCl}_3$ )  $\delta$  161.37, 160.77, 149.30, 143.73, 135.16, 130.78, 129.29, 127.99, 125.77, 123.87, 122.15, 119.34, 118.07, 104.70, 69.79, 31.58, 29.24, 25.71, 22.61; ESI-MS:  $m/z$  = 681.5 ( $[\text{M}+\text{H}]^+$ ); IR (KBr):  $\nu$  = 3443, 2930, 2855, 1616, 1508, 1289, 1262, 1170, 816, 697  $\text{cm}^{-1}$ ; UV-Vis ( $\text{CH}_2\text{Cl}_2$ ):  $\lambda_{\text{max}}$  ( $\epsilon$ ) = 277 ( $5.0 \times 10^5$ ), 371 ( $2.1 \times 10^4$ ) nm ( $\text{L mol}^{-1} \text{cm}^{-1}$ ); Mp. = 182-189  $^\circ\text{C}$ ; High Res. MS Calc'd for  $\text{C}_{40}\text{H}_{45}\text{N}_2\text{O}_4\text{S}_2$ : 681.2823. Found: 681.2821; Anal. Calc'd for  $\text{C}_{40}\text{H}_{42}\text{N}_2\text{O}_4\text{S}_2$ : C, 70.56; N, 4.11; H, 6.51. Found: C, 70.45; N, 4.16; H, 6.60.

**Data for 140e.**  $^1\text{H}$  NMR (400MHz,  $\text{CDCl}_3$ )  $\delta$  13.09 (s, 2H, OH), 8.68 (s, 2H, CH=N), 7.61 (m, 4H, aromatic CH), 7.36 (dd, 2H,  $J_1 = 5.9$  Hz,  $J_2 = 3.4$  Hz, aromatic CH), 7.26 (dd, 2H,  $J_1 = 5.8$  Hz,  $J_2 = 3.5$  Hz, aromatic CH), 7.20 (d, 2H,  $J = 8.3$  Hz, aromatic CH), 7.19 (d, 2H,  $J = 6.8$  Hz, aromatic CH), 7.08-7.03 (m, 4H, aromatic CH);  $^{13}\text{C}$  NMR (75.5 MHz,  $\text{CDCl}_3$ )  $\delta$  163.39, 160.96, 143.61, 142.44, 131.24, 129.54, 128.00, 127.95, 125.90, 123.99, 122.25, 119.63, 119.23, 118.18; ESI-MS:  $m/z$  = 481.2 ( $[\text{M}+\text{H}]^+$ ); IR (KBr):  $\nu$  = 3443, 3022, 2923, 2855, 1617, 1481, 1285, 1166, 818, 753, 698  $\text{cm}^{-1}$ ; UV-Vis ( $\text{CH}_2\text{Cl}_2$ ):  $\lambda_{\text{max}}$  ( $\epsilon$ ) = 279 ( $6.8 \times 10^4$ ) nm ( $\text{L mol}^{-1} \text{cm}^{-1}$ ); Mp. = 206-209  $^\circ\text{C}$ ; High Res. MS Calc'd for  $\text{C}_{28}\text{H}_{21}\text{N}_2\text{O}_2\text{S}_2$ : 481.1044. Found: 481.1046; Anal. Calc'd for  $\text{C}_{28}\text{H}_{18}\text{N}_2\text{O}_2\text{S}_2$ : C, 62.59; N, 5.21; H, 3.38. Found: C, 62.20; N, 5.26; H, 3.52.



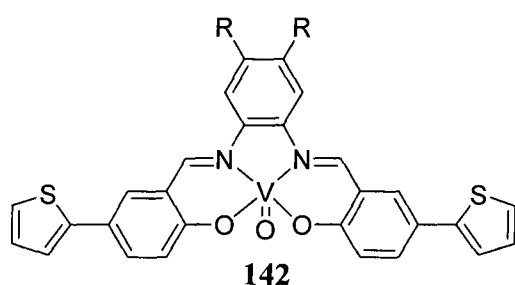
**Synthesis of Ni(II) salphen complexes 141a, e** – Dithienylsalphen **140a** or **140e** (1 equiv.) and nickel(II) acetate tetrahydrate (2 equiv.) were dissolved in 20 mL of THF. The resulting

solution was heated to reflux overnight. After cooling, the volume of the solvent was reduced and a red solid was precipitated with addition of methanol, isolated on a Büchner funnel and washed with methanol and hexanes. Yield for **141a**: 0.256 g, 0.35 mmol, 86%. Yield for **141e**: 0.295 g, 0.55 mmol, 96%.

**Data for 141a.**  $^1\text{H NMR}$  (300 MHz,  $\text{CDCl}_3$ )  $\delta$  7.91 (s, 2H,  $\text{CH}=\text{N}$ ), 7.52 (d, 2H,  $J = 2.3$  Hz, aromatic  $\text{CH}$ ), 7.47 (dd, 2H,  $J_1 = 9.0$  Hz,  $J_2 = 2.4$  Hz, aromatic  $\text{CH}$ ), 7.14-7.04 (m, 6H, aromatic  $\text{CH}$ ), 7.02 (s, 2H, aromatic  $\text{CH}$ ), 6.99 (dd, 2H,  $J_1 = 4.9$  Hz,  $J_2 = 3.7$  Hz, aromatic  $\text{CH}$ ), 4.06 (t, 2H,  $\text{OCH}_2$ ), 1.86-0.92 (m, 22H, hexyl chain); ESI-MS:  $m/z = 737$  ( $\text{M}^+$ ); IR (KBr):  $\nu = 3439, 2927, 2856, 1615, 1517, 1465, 1434, 1362, 1281, 1178, 816, 695$   $\text{cm}^{-1}$ ; UV-Vis ( $\text{CH}_2\text{Cl}_2$ ):  $\lambda_{\text{max}}$  ( $\epsilon$ ) = 508 ( $1.4 \times 10^4$ ), 388 ( $3.6 \times 10^4$ ), 317 ( $5.8 \times 10^4$ ) nm ( $\text{L mol}^{-1} \text{cm}^{-1}$ ); Mp.  $> 300$   $^\circ\text{C}$ ; High Res. MS Calc'd for  $\text{C}_{40}\text{H}_{43}\text{N}_2\text{O}_4\text{S}_2\text{Ni}$ : 737.2020. Found: 737.2018; Anal. Calc'd for  $\text{C}_{40}\text{H}_{42}\text{O}_4\text{N}_2\text{S}_2\text{Ni}$ : C, 65.13; H, 5.74; N, 3.80. Found: C, 64.86; H, 5.88; N, 4.30.

**Data for 141e.**  $^1\text{H NMR}$  (300 MHz,  $\text{DMSO-d}_6$ )  $\delta$  9.22 (s, 2H,  $\text{CH}=\text{N}$ ), 8.17 (dd, 2H,  $J_1 = 5.7$  Hz,  $J_2 = 3.1$  Hz, aromatic  $\text{CH}$ ), 7.91 (d, 2H,  $J = 2.0$  Hz, aromatic  $\text{CH}$ ), 7.69 (dd, 2H,  $J_1 = 9.0$  Hz,  $J_2 = 2.1$  Hz, aromatic  $\text{CH}$ ), 7.43 (d, 2H,  $J = 5.2$  Hz, aromatic  $\text{CH}$ ), 7.37 (dd, 2H,  $J_1 = 5.9$  Hz,  $J_2 = 2.8$  Hz, aromatic  $\text{CH}$ ), 7.33 (d, 2H,  $J = 3.6$  Hz, aromatic  $\text{CH}$ ), 7.09 (dd, 2H,  $J_1 = 4.8$  Hz,  $J_2 = 3.7$  Hz, aromatic  $\text{CH}$ ), 6.96 (d, 2H,  $J = 9.0$  Hz, aromatic  $\text{CH}$ );

ESI-MS:  $m/z = 559$  ( $[M+Na]^+$ ); IR (KBr):  $\nu = 3259, 3064, 2956, 1612, 1579, 1520, 1469, 1381, 1332, 1180, 1062, 926, 819, 745$   $\text{cm}^{-1}$ ; UV-Vis ( $\text{CH}_2\text{Cl}_2$ ):  $\lambda_{\text{max}} (\epsilon) = 504 (8.8 \times 10^3), 383 (2.5 \times 10^4), 317 (5.0 \times 10^4)$   $\text{nm}$  ( $\text{L mol}^{-1} \text{cm}^{-1}$ ); Mp.  $> 300$   $^\circ\text{C}$ ; High Res. MS Calc'd for  $\text{C}_{28}\text{H}_{19}\text{N}_2\text{O}_2\text{S}_2\text{Ni}$ : 537.0241. Found: 537.0245; Anal. Calc'd for  $\text{C}_{28}\text{H}_{18}\text{O}_2\text{N}_2\text{S}_2\text{Ni}$ : C, 62.59; H, 3.38; N, 5.21. Found: C, 62.20; H, 3.52; N, 5.26.



### Synthesis of vanadyl salen complexes

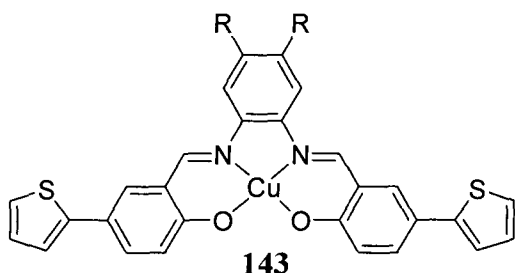
**142a, e** - Dithienylsalphen **140a** or **140e** (1 equiv.) and vanadyl acetylacetonate (2 equiv.) were dissolved in 20 mL of THF. The resulting

brown solution was heated to reflux overnight. After cooling, the volume of the solvent was reduced. Addition of methanol precipitated a brown solid, which was collected on a Büchner funnel and washed with methanol and hexanes. Yield for **140a**: 0.200 g, 0.27 mmol, 61%. Yield for **140e**: 0.093 g, 0.17 mmol, 85%.

**Data for 142a.** ESI-MS:  $m/z = 768$  ( $[M+Na]^+$ ); IR (KBr):  $\nu = 3448, 3068, 3017, 2924, 2858, 1612, 1582, 1520, 1506, 1464, 1371, 1310, 1271, 1176, 1116, 980, 822$   $\text{cm}^{-1}$ ; UV-Vis ( $\text{CH}_2\text{Cl}_2$ ):  $\lambda_{\text{max}} (\epsilon) = 446 (2.0 \times 10^4), 304 (6.0 \times 10^4)$   $\text{nm}$  ( $\text{L mol}^{-1} \text{cm}^{-1}$ ); Mp.  $> 300$   $^\circ\text{C}$ ; Anal. Calc'd for  $\text{C}_{40}\text{H}_{42}\text{N}_2\text{O}_5\text{S}_2\text{V}$ : C, 64.41; N, 3.76; H, 5.68. Found: C, 64.49; N, 3.93; H, 5.80.

**Data for 142e.** ESI-MS:  $m/z = 568$  ( $[M+Na]^+$ ); IR (KBr):  $\nu = 3455, 3067, 2923, 1610, 1576, 1521, 1465, 1377, 1311, 1178, 982, 815$   $\text{cm}^{-1}$ ; UV-Vis ( $\text{CH}_2\text{Cl}_2$ ):  $\lambda_{\text{max}} (\epsilon) = 458$

( $7.5 \times 10^3$ ), 315 ( $4.8 \times 10^4$ ) nm ( $\text{L mol}^{-1} \text{cm}^{-1}$ ); Mp. = 279-286 °C (dec.); Anal. Calc'd for  $\text{C}_{28}\text{H}_{18}\text{N}_2\text{O}_3\text{S}_2\text{V}$ : C, 61.65; N, 5.13; H, 3.33. Found: C, 61.57; N, 5.04; H, 3.73.



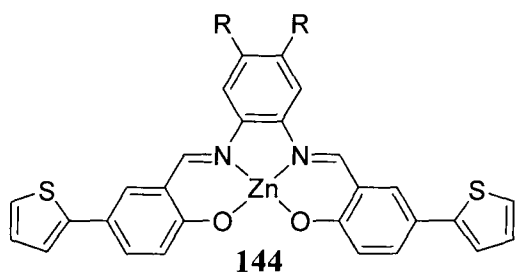
### Synthesis of Cu(II) salphen complexes

**143a, e** - Dithienylsalphen **140a** or **140e** (1 equiv.) and copper(II) acetylacetonate (2 equiv.) were dissolved in 20 mL of THF. The

resulting solution was heated to reflux overnight. After cooling, the volume of the solvent was reduced and an orange-red solid was precipitated with addition of methanol, which was collected on a Büchner funnel and washed with methanol and hexanes. Yield for **143a**: 0.218 g, 0.29 mmol, 55%. Yield for **143e**: 0.149 g, 0.28 mmol, 47%.

**Data for 143a.** ESI-MS:  $m/z = 764$  ( $[\text{M}+\text{Na}]^+$ ); IR (KBr):  $\nu = 3426, 3072, 2954, 2924, 2851, 1611, 1587, 1513, 1469, 1375, 1276, 1172, 815 \text{ cm}^{-1}$ ; UV-Vis ( $\text{CH}_2\text{Cl}_2$ ):  $\lambda_{\text{max}} (\epsilon) = 464$  ( $1.7 \times 10^4$ ), 314 ( $5.1 \times 10^4$ ) nm ( $\text{L mol}^{-1} \text{cm}^{-1}$ ); Mp. > 300 °C; High Res. MS Calc'd for  $\text{C}_{40}\text{H}_{42}\text{O}_4\text{N}_2\text{S}_2\text{Cu}$ : 742.1959. Found: 742.1960; Anal. Calc'd for  $\text{C}_{40}\text{H}_{42}\text{O}_4\text{N}_2\text{S}_2\text{Cu}$ : C, 64.71; H, 5.70; N, 3.77. Found: C, 64.32; H, 5.82; N, 3.79.

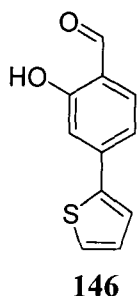
**Data for 143e.** ESI-MS:  $m/z = 564$  ( $[\text{M}+\text{Na}]^+$ ); IR (KBr):  $\nu = 3432, 2923, 1613, 1579, 1518, 1469, 1381, 1174, 1168, 819, 807, 755 \text{ cm}^{-1}$ ; UV-Vis ( $\text{CH}_2\text{Cl}_2$ ):  $\lambda_{\text{max}} = 466, 316$  nm; Mp. = 271-276 °C; High Res. MS Calc'd for  $\text{C}_{28}\text{H}_{19}\text{N}_2\text{O}_2\text{S}_2\text{Cu}$ : 542.0184. Found: 542.0182; Anal. Calc'd for  $\text{C}_{28}\text{H}_{20}\text{O}_3\text{N}_2\text{S}_2\text{Cu}$ : C, 60.04; H, 3.60; N, 5.00. Found: C, 60.08; H, 3.96; N, 4.84.



#### Synthesis of Zn(II) salphen complex 144a –

Dithienylsalphen **140a** (1 equiv.) and zinc(II) acetate dihydrate (2 equiv.) were dissolved in 20 mL of THF. The resulting solution was heated to reflux overnight to obtain a cloudy solution with some yellow precipitate, which was filtered through celite. Methanol was added to precipitate the product, after the volume of solvent was reduced and the resulting solid was collected on a Büchner funnel and washed with methanol and hexanes. Yield: 0.049 g, 0.066 mmol, 42%.

**Data for 144a.**  $^1\text{H}$  NMR (300 MHz, DMSO- $d_6$ )  $\delta$  9.05 (s, 2H, CH=N), 7.73 (d, 2H,  $J$  = 2.6 Hz, aromatic CH), 7.55 (dd, 2H,  $J_1$  = 8.9 Hz,  $J_2$  = 2.6 Hz, aromatic CH), 7.53 (s, 2H, aromatic CH), 7.35 (dd, 2H,  $J_1$  = 5.1 Hz,  $J_2$  = 1.1 Hz, aromatic CH), 7.26 (dd, 2H,  $J_1$  = 3.6 Hz,  $J_2$  = 1.1 Hz, aromatic CH), 7.06 (dd, 2H,  $J_1$  = 5.1 Hz,  $J_2$  = 3.6 Hz, aromatic CH), 6.75 (d, 2H,  $J$  = 8.9 Hz, aromatic CH), 4.17 (t, 2H, OCH<sub>2</sub>), 1.80-0.87 (m, 22H, hexyl chain); ESI-MS:  $m/z$  = 743 ([M+H]<sup>+</sup>).

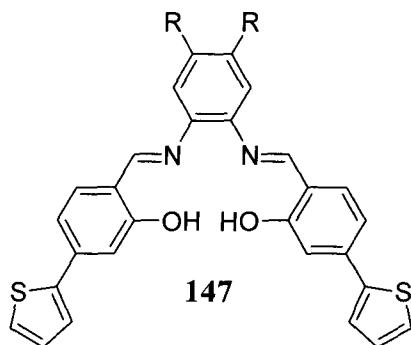


**Synthesis of 4-(2-thienyl)salicylaldehyde (146)** – To a mixture of 4-iodosalicylaldehyde **145** (4.095 g, 16.5 mmol) and trans-dichlorobis(triphenylphosphine) palladium (II) (0.606 g, 0.863 mmol) was added a solution of tributylstannylthiophene (8.0 mL, 25.2 mmol) in DMF (40 mL). After heating for 16 h, the reaction solution was diluted with ether

(100 mL) and washed with aqueous ammonium chloride (3 x 150 mL). The organic layer was filtered through silica and the solvent was removed under vacuum to obtain a beige

solid, which was washed with hexanes and filtered to yield 3.088 g (0.794 mmol, 92%) of product.

**Data for 146.**  $^1\text{H}$  NMR (400 MHz,  $\text{CDCl}_3$ )  $\delta$  11.12 (s, 1H, OH), 9.84 (s, 1H, CHO), 7.53 (d, 1H,  $J = 8.1$  Hz, aromatic CH), 7.45 (d, 1H,  $J = 3.9$  Hz, aromatic CH), 7.40 (d, 1H,  $J = 4.8$  Hz, aromatic CH), 7.25 (dd, 1H,  $J_1 = 8.1$  Hz,  $J_2 = 1.5$  Hz, aromatic CH), 7.21 (s, 1H, aromatic CH), 7.11 (dd, 1H,  $J_1 = 4.8$  Hz,  $J_2 = 3.9$  Hz, aromatic CH);  $^{13}\text{C}$  NMR (75.5 MHz,  $\text{CDCl}_3$ )  $\delta$  195.7, 162.3, 142.7, 142.6, 134.5, 128.7, 127.7, 125.9, 119.8, 117.6, 114.1; ESI-MS:  $m/z = 227$  ( $[\text{M} + \text{Na}]^+$ ); IR (KBr):  $\nu = 3098, 3074, 2834, 2748, 1650, 1625, 1557, 1529, 1492, 1431, 1312, 1235, 1207, 1184, 995, 852, 800, 694$   $\text{cm}^{-1}$ ; UV-Vis ( $\text{CH}_2\text{Cl}_2$ ):  $\lambda_{\text{max}} (\epsilon) = 331 (2.7 \times 10^4)$  nm ( $\text{L mol}^{-1}\text{cm}^{-1}$ ); Mp. = 92-94  $^\circ\text{C}$ ; Anal. Calc'd for  $\text{C}_{11}\text{H}_8\text{O}_2\text{S}$ : C, 64.69, H, 3.95. Found C, 64.30, H, 3.99.



**Synthesis of  $N,N'$ -Phenylenebis(4-(2-thienyl)salicylideneimines (147)** - 1,2-Dihexyloxy-4,5-diaminobenzene **115a** (0.297 g, 0.962 mmol) and 4-thienylsalicylaldehyde (0.486 g, 2.37 mmol) were combined in a 100 mL Schlenk flask under nitrogen.

To this mixture was added 20 mL of dry THF to form an orange solution. The solution was heated to reflux overnight and was cooled to room temperature, after which the volume of solution was reduced. Addition of methanol to the solution caused precipitation of an orange solid, which was collected on a Büchner funnel and washed with additional methanol. Yield: 0.587 g, 0.86 mmol, 89%. Compounds **147e** and **147f**

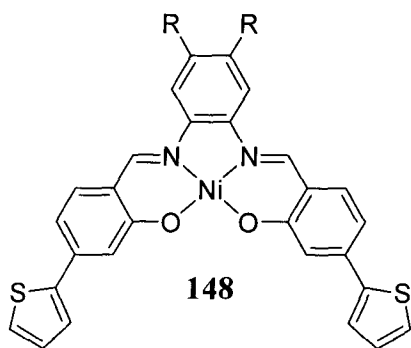
were synthesized in an analogous fashion using **115e** and **115f** with yields of 0.355 g (0.66 mmol, 77%) and 0.525 g (0.61 mmol, 66%), respectively.

**Data for 147a.**  $^1\text{H}$  NMR (300 MHz,  $\text{CDCl}_3$ )  $\delta$  13.34 (s, 2H, OH), 8.56 (s, 2H, HC=N), 7.39 (dd, 2H,  $J_1 = 3.7$  Hz,  $J_2 = 0.9$  Hz, aromatic CH), 7.35 (d, 2H,  $J = 8.0$  Hz, aromatic CH), 7.32 (m, 4H, aromatic CH), 7.16 (dd, 2H,  $J_1 = 8.0$  Hz,  $J_2 = 1.7$  Hz, aromatic CH), 7.08 (dd, 2H,  $J_1 = 5.0$  Hz,  $J_2 = 3.7$  Hz, aromatic CH), 6.79 (s, 2H, aromatic CH), 4.05 (t, 4H,  $\text{OCH}_2$ ), 1.86-0.88 (m, 22H, hexyl chain);  $^{13}\text{C}$  NMR (75.5 MHz,  $\text{CDCl}_3$ )  $\delta$  161.7, 161.1, 149.3, 143.7, 138.7, 135.6, 132.7, 128.4, 126.3, 124.6, 118.8, 116.8, 114.3, 105.0, 70.0, 31.8, 29.5, 25.9, 22.8, 14.2; ESI-MS:  $m/z = 681$  ( $[\text{M} + \text{H}]^+$ ); IR (KBr):  $\nu = 2950, 2928, 2853, 1608, 1510, 1375, 1263, 1189, 850, 804, 695$   $\text{cm}^{-1}$ ; UV-Vis ( $\text{CH}_2\text{Cl}_2$ ):  $\lambda_{\text{max}}$  ( $\epsilon$ ) = 360 ( $5.0 \times 10^4$ ) nm ( $\text{L mol}^{-1}\text{cm}^{-1}$ ); Mp. = 176-178  $^\circ\text{C}$ ; Anal. Calc'd for  $\text{C}_{40}\text{H}_{44}\text{N}_2\text{O}_4\text{S}_2$ : C, 70.56, N, 4.11, H, 6.51. Found C, 70.36, N, 4.43, H, 6.43.

**Data for 147e.**  $^1\text{H}$  NMR (400 MHz,  $\text{CDCl}_3$ )  $\delta$  13.21 (s, 2H, OH), 8.62 (s, 2H, HC=N), 7.39 (dd, 2H,  $J_1 = 3.7$  Hz,  $J_2 = 1.0$  Hz, aromatic CH), 7.36 (d, 2H,  $J = 8.0$  Hz, aromatic CH), 7.35-7.32 (m, 6H, aromatic CH), 7.25 (m, 2H, aromatic CH), 7.17 (dd, 2H,  $J_1 = 8.0$  Hz,  $J_2 = 1.7$  Hz, aromatic CH), 7.08 (dd, 2H,  $J_1 = 5.0$  Hz,  $J_2 = 3.7$  Hz, aromatic CH);  $^{13}\text{C}$  NMR (100.7 MHz,  $\text{CDCl}_3$ )  $\delta$  162.9, 162.0, 143.6, 142.6, 139.3, 133.1, 128.4, 128.0, 126.5, 124.8, 119.8, 118.6, 116.9, 114.5; EI-MS:  $m/z = 480$  ( $\text{M}^+$ ); High Res. MS Calc'd for  $\text{C}_{28}\text{H}_{20}\text{N}_2\text{O}_2\text{S}_2$ : 480.09662. Found: 480.09674.

**Data for 147f.**  $^1\text{H}$  NMR (400 MHz,  $\text{CDCl}_3$ )  $\delta$  13.31 (s, 2H, OH), 8.58 (s, 2H, HC=N), 7.39 (d, 2H,  $J = 3.7$  Hz, aromatic CH), 7.35 (d, 2H,  $J = 8.0$  Hz, aromatic CH), 7.32 (m,

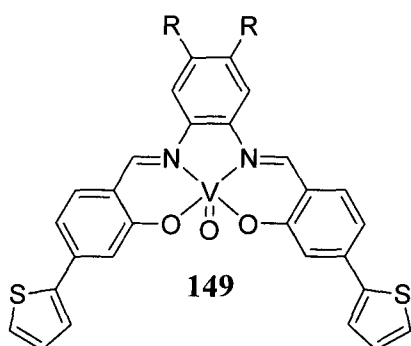
4H, aromatic *CH*), 7.17 (dd, 2H,  $J_1 = 8.0$  Hz,  $J_2 = 1.6$  Hz, aromatic *CH*), 7.08 (dd, 2H,  $J = 5.0$  Hz,  $J = 3.7$  Hz, aromatic *CH*), 6.81 (s, 2H, aromatic *CH*), 4.06 (t, 4H,  $OCH_2$ ), 1.86-0.88 (m, 46H, dodecyl chain);  $^{13}C$  NMR (100.7 MHz,  $CDCl_3$ )  $\delta$  161.7, 161.0, 149.4, 143.6, 139.1, 135.2, 133.0, 128.4, 126.4, 124.7, 118.6, 116.9, 114.4, 105.0, 70.1, 32.2, 29.9, 29.9, 29.7, 29.6, 29.5, 26.3, 22.9, 14.3; EI-MS:  $m/z = 848$  ( $M^+$ ); High Res. MS Calc'd for  $C_{52}H_{68}N_2O_4S_2$ : 848.46205. Found: 848.46226.



**Synthesis of Ni(II) salphen complex (148a)** – To a mixture of **147a** (0.137 g, 0.201 mmol) and nickel(II) acetate tetrahydrate (0.226 g, 0.908 mmol) was added 10 mL of distilled THF. The red solution was heated to reflux for 16 h. After cooling, MeOH was added to precipitate a red solid, which was subsequently filtered and washed with MeOH and petroleum ether. Yield: 0.095 g, 0.13 mmol, 64%.

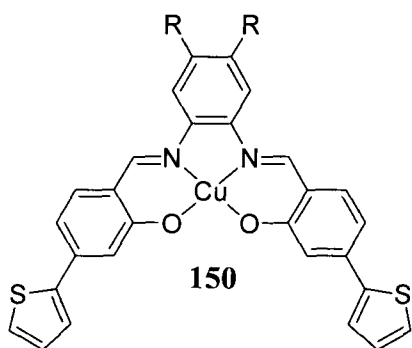
**Data for 148a.**  $^1H$  NMR (400 MHz,  $CDCl_3$ )  $\delta$  7.87 (s, 2H,  $HC=N$ ), 7.43 (s, 2H, aromatic *CH*), 7.39 (d, 2H,  $J = 3.4$  Hz, aromatic *CH*), 7.32 (d, 2H,  $J = 5.0$  Hz, aromatic *CH*), 7.26 (d, 2H,  $J = 8.3$  Hz, aromatic *CH*), 7.07 (m, 2H, aromatic *CH*), 7.02 (s, 2H, aromatic *CH*), 6.88 (d, 2H,  $J = 8.3$  Hz, aromatic *CH*), 3.97 (t, 2H,  $OCH_2$ ), 1.81-0.88 (m, 22H, hexyl chain);  $^{13}C$  NMR (75.5 MHz,  $CDCl_3$ )  $\delta$  165.4, 151.4, 149.7, 144.0, 139.9, 136.3, 133.7, 128.4, 126.4, 124.8, 119.7, 117.9, 114.1, 98.8, 64.2, 31.9, 29.4, 25.9, 22.8, 14.3; ESI-MS:  $m/z = 759$  ( $[M + Na]^+$ ); IR (KBr):  $\nu = 2953, 2930, 2859, 1607, 1584, 1501, 1475, 1438, 1362, 1282, 1188, 699$   $cm^{-1}$ ; UV-Vis ( $CH_2Cl_2$ ):  $\lambda_{max}$  ( $\epsilon$ ) = 361 ( $4.3 \times 10^4$ ), 403 ( $5.6 \times 10^4$ ),

489 ( $2.2 \times 10^4$ ) nm ( $\text{L mol}^{-1}\text{cm}^{-1}$ ); Mp.  $> 300$  °C; Anal. Calc'd for  $\text{C}_{40}\text{H}_{42}\text{N}_2\text{O}_4\text{S}_2\text{Ni}$ : C, 65.13, H, 5.74. Found C, 65.16, H, 5.82.



**Synthesis of vanadyl salphen complex (149a)** - To a mixture of **147a** (0.166 g, 0.244 mmol) and vanadyl acetylacetonate (0.191 g, 0.720 mmol) was added 10 mL of distilled THF. The red solution was heated to reflux for 16 h. After cooling, the volume of the solution was reduced and MeOH was added to precipitate a red-brown solid. The product was subsequently filtered and washed with MeOH and petroleum ether. Yield: 0.136 g, 0.18 mmol, 75%.

**Data for 149a.** ESI-MS:  $m/z = 768$  ( $[\text{M} + \text{Na}]^+$ ); IR (KBr):  $\nu = 2956, 2927, 2857, 1604, 1577, 1509, 1479, 1430, 1377, 1275, 1191, 980, 696$   $\text{cm}^{-1}$ ; UV-Vis ( $\text{CH}_2\text{Cl}_2$ ):  $\lambda_{\text{max}}$  ( $\epsilon$ ) = 364 ( $4.6 \times 10^4$ ), 422 ( $5.0 \times 10^4$ ) nm ( $\text{L mol}^{-1}\text{cm}^{-1}$ ); Mp. = 293 °C (dec.); Anal. Calc'd for  $\text{C}_{40}\text{H}_{44}\text{N}_2\text{O}_6\text{S}_2\text{V}$ : C, 62.89, H, 5.81, N, 3.67. Found C, 63.09, H, 5.87, 3.91.



**Synthesis of Cu(II) salphen complex (150a)** - To a mixture of **147a** (0.158 g, 0.232 mmol) and copper(II) acetylacetonate (0.186 g, 0.710 mmol) was added 20 mL of distilled THF. The brown solution was heated to reflux for 16 h. After cooling, the solution was reduced and MeOH was added to precipitate the product. Subsequent filtration afforded a red

solid which was washed with MeOH and petroleum ether. The product was recrystallized from DCM and MeOH. Yield: 0.118 g, 0.16 mmol, 69%.

**Data for 150a.** MALDI-TOF-MS:  $m/z = 742$  ( $M^+$ ); IR (KBr):  $\nu = 2952, 2925, 2856, 1608, 1587, 1500, 1474, 1374, 1275, 1187, 696$   $\text{cm}^{-1}$ ; UV-Vis ( $\text{CH}_2\text{Cl}_2$ ):  $\lambda_{\text{max}}$  ( $\epsilon$ ) = 356 ( $4.2 \times 10^4$ ), 383 ( $4.0 \times 10^4$ ), 432 ( $4.3 \times 10^4$ ) nm ( $\text{L mol}^{-1}\text{cm}^{-1}$ ); Mp. > 300 °C; Anal. Calc'd for  $\text{C}_{40}\text{H}_{42}\text{N}_2\text{O}_4\text{S}_2\text{Cu}$ : C, 64.71, H, 5.70, N 3.77. Found C, 64.99, H, 5.80, N, 4.00.

**Electrochemistry** - Cyclic voltammetry experiments were conducted using a Pine AFCBP1 bipotentiostat. The working electrode was either a Pt disk, an indium tin oxide (ITO) thin film on glass or Au (1000 Å) deposited on Si using a Cr (50 Å) adhesion layer. The counter electrode was a Pt mesh and the reference electrode a silver wire. An internal reference (decamethylferrocene) was added to correct the measured potentials with respect to saturated calomel electrode (SCE).  $[(n\text{-Bu})_4\text{N}]\text{PF}_6$  was used as a supporting electrolyte and was purified by triple recrystallization from ethanol and dried at 90 °C under vacuum for 3 days. Dichloromethane used for CV was purified by passing the solvent through an activated alumina tower. Polymerizations were carried out in a solution containing 0.1 M electrolyte, and 1 mM monomer (compounds **140a,e** - **143a,e** and **147a** -**150a**). Polymers were grown by cycling a potential between 0 V and the onset of monomer oxidation (= 1.6 V) for a total of 10 cycles.

## 6.4 References

- (1) Marvel, C. S.; Tarköy, N. *J. Am. Chem. Soc.* **1957**, *79*, 6000-6002.
- (2) Marvel, C. S.; Tarköy, N. *J. Am. Chem. Soc.* **1958**, *80*, 832-835.
- (3) Vitalini, D.; Mineo, P.; Di Bella, S.; Frangalà, I.; Maravigna, P.; Scamporrino, E. *Macromolecules* **1996**, *29*, 4478-4485.
- (4) Leung, A. C. W.; Chong, J. H.; Patrick, B. O.; MacLachlan, M. J. *Macromolecules* **2003**, *36*, 5051-5054.
- (5) Leung, A. C. W.; MacLachlan, M. J. *J. Mater. Chem.* **2007**, *17*, 1923-1932.
- (6) Kingsborough, R. P.; Swager, T. M. *Adv. Mater.* **1998**, *10*, 1100-1104.
- (7) Kingsborough, R. P.; Swager, T. M. *J. Am. Chem. Soc.* **1999**, *121*, 8825-8834.
- (8) Reddinger, J. L.; Reynolds, J. R. *Macromolecules* **1997**, *30*, 673-675.
- (9) Reddinger, J. L.; Reynolds, J. R. *Chem. Mater.* **1998**, *10*, 1236-1243.
- (10) Di Bella, S.; Frangalà, I. *Synth. Met.* **2000**, *115*, 191-196.
- (11) Carswell, W. E.; Paley, M. S.; Frazier, D. O. *Polym. Prepr. (Am. Chem. Soc., Div. Polym. Chem.)* **2000**, *41*, 1068-1069.
- (12) Ma, C.; Lo, A.; Abdolmaleki, A.; MacLachlan, M. J. *Org. Lett.* **2004**, *6*, 3841-3844.

## Chapter 7

### Conclusions and Future Directions

#### 7.1 Overview

This thesis has discussed the synthesis and characterization of a variety of new phenanthrene and triphenylene derivatives. Phenanthrene and triphenylene with opposing bromo, iodo and formyl groups were found to be useful precursors for both Schiff base condensation and Sonogashira coupling reactions. Phenanthrene ethynylene groups were incorporated into both [3+3] Schiff base macrocycles and luminescent conjugated polymers. The macrocycles and polymers are sensitive to the presence of dinitrotoluene, and exhibit quenched luminescence in its presence. Self-assembly of both large macrocycles were investigated and was found to occur in the less conjugated of the two macrocycles. While there had been a great deal of research in the area to polycyclic aromatic hydrocarbons to this point, the work in this thesis explored the use of phenanthrene and triphenylene in macrocycles and polymers, where they have been seldom used. Over thirty new phenanthrene precursors were synthesized and could be used to make a variety of new supramolecular structures and materials.

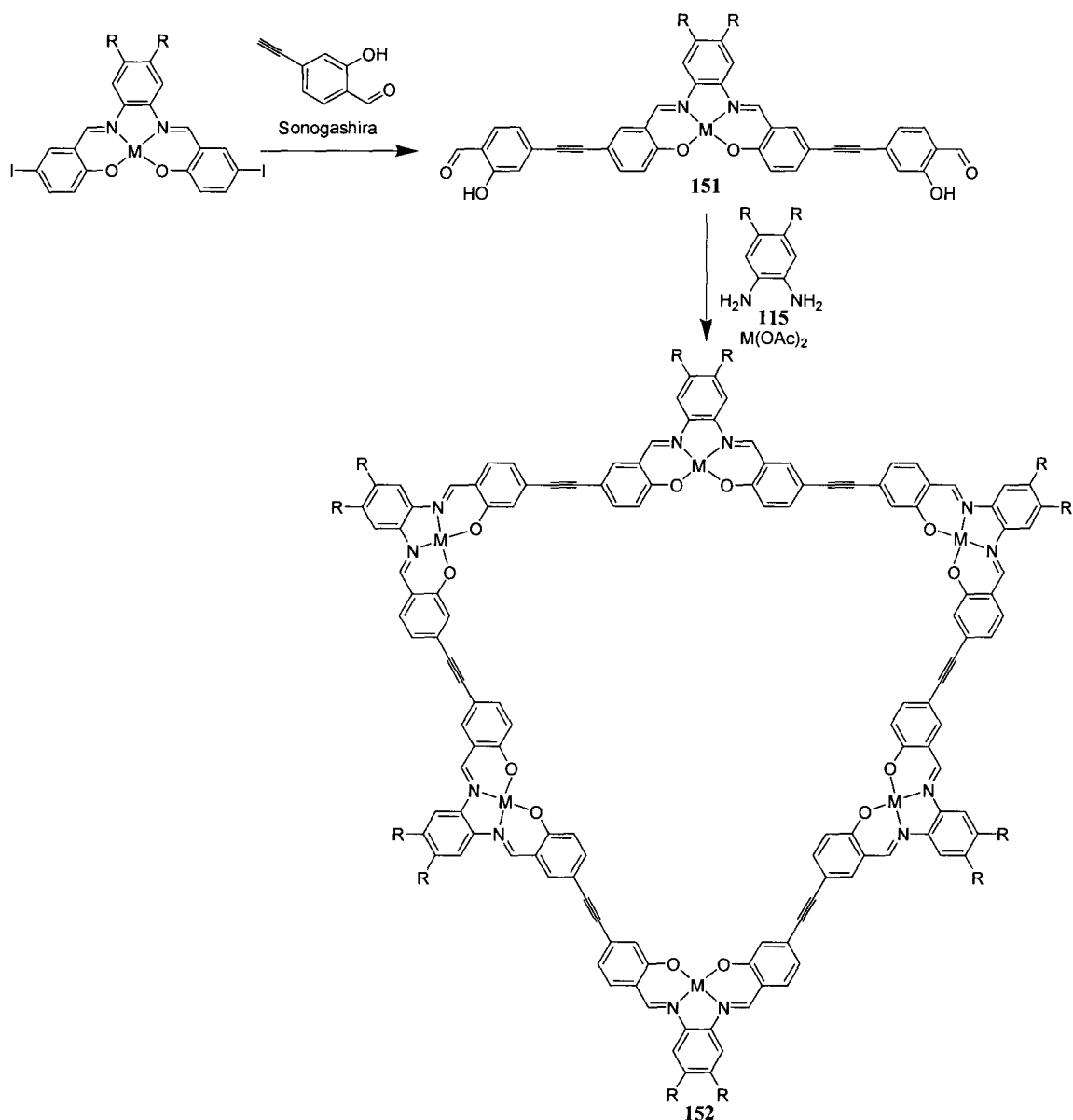
In addition, a variety of new thiophene-containing Schiff base monomers for electropolymerization were prepared. These monomers will be used for polymerization in both gravity and microgravity and any films obtained will be studied for NLO properties.

## 7.2 Future Directions

### 7.2.1 Schiff Base Macrocycles

The MacLachlan group has been working to expand the size and shape of [3+3] Schiff base macrocycles. Although the original goal of creating smaller phenanthrene macrocycles such as **68** was not as successful as anticipated, larger macrocycles **74** and **75** were successfully synthesized. To our knowledge, these are the largest [3+3] Schiff base macrocycles synthesized to date. In theory, even larger macrocycles could be envisioned by adding even more ethynyl or aromatic groups to the diol. Macrocycles **74** and **75** are essentially the same size except the salphen and the phenanthrene groups are in opposite positions. To complete the series, diol **151** would form a macrocycle with salphen in both positions (**152**) (Scheme 7.1). The starting materials needed to make this diol have previously been synthesized in our group and have been shown to be useful precursors for Sonogashira coupling reactions.<sup>1, 2</sup> Macrocycle **152** would present new ways to tune the properties of the macrocycles. First, the presence of two separate salphen groups would allow the possibility of coordination of two different metals into the macrocycle. Second, different alkoxy chains can be used on the phenylenediamine, which will tune the solubility of the macrocycle.

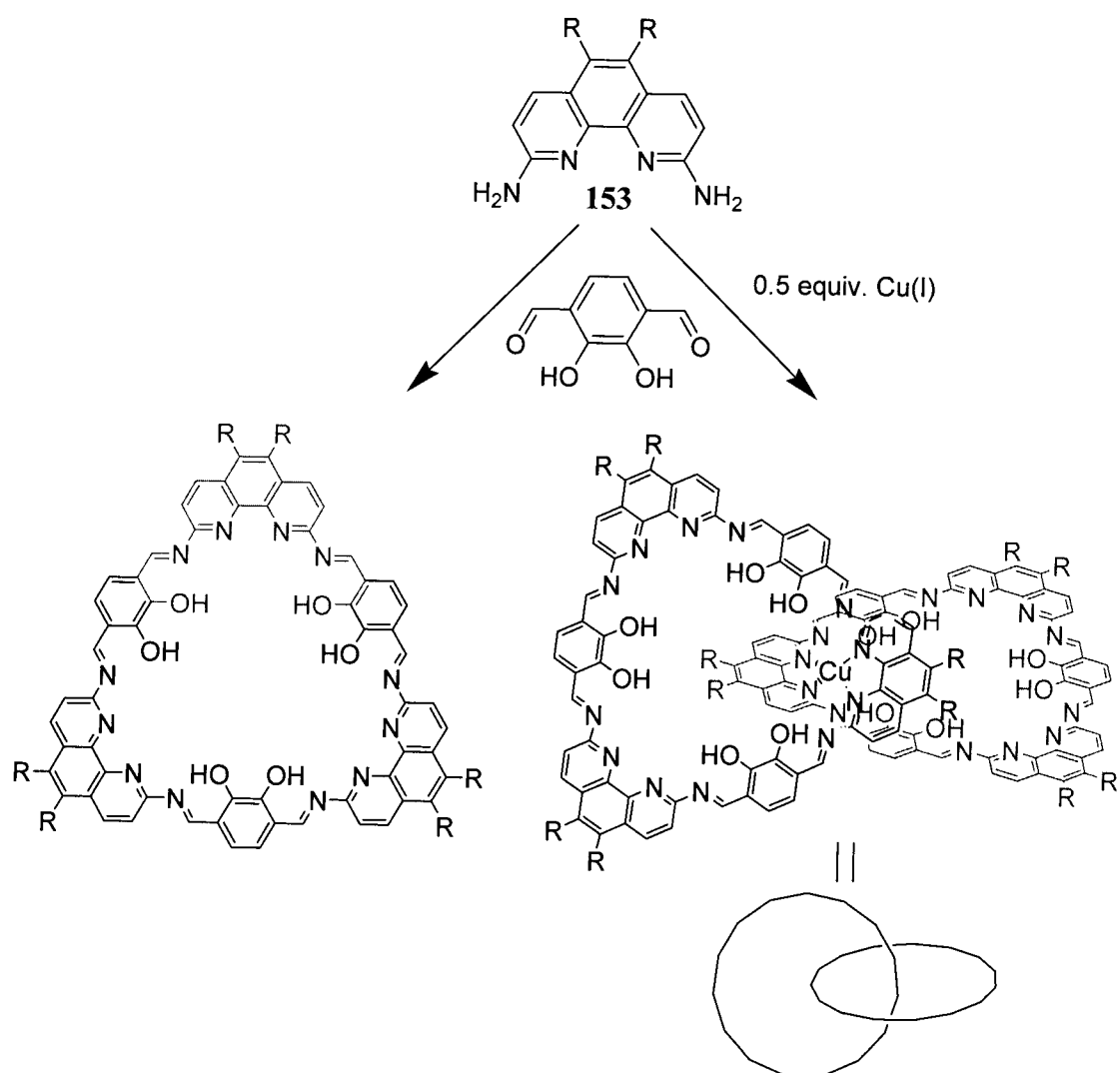
**Scheme 7.1** Proposed synthesis of **151** and **152**.



While the macrocycle has been expanded by increasing the size and shape of the bis(salicylate) spacers, few attempts have been made to expand the macrocycle by using larger diamines. The most intriguing candidate for an expanded diamine would be phenanthrolinediamine **153** (Scheme 7.2). Using this compound in a Schiff base macrocycle would form a coordination pocket that is larger than a typical salphen  $N_2O_2$

site (denoted in red), which would introduce a different geometry of coordination. Secondly, incorporation of phenanthroline would enable two macrocycles to link, forming a catenane, if the condensation reaction was performed in the presence of a Cu(I) template.<sup>3</sup>

**Scheme 7.2** Proposed incorporation of phenanthroline into [3+3] Schiff base macrocycles.



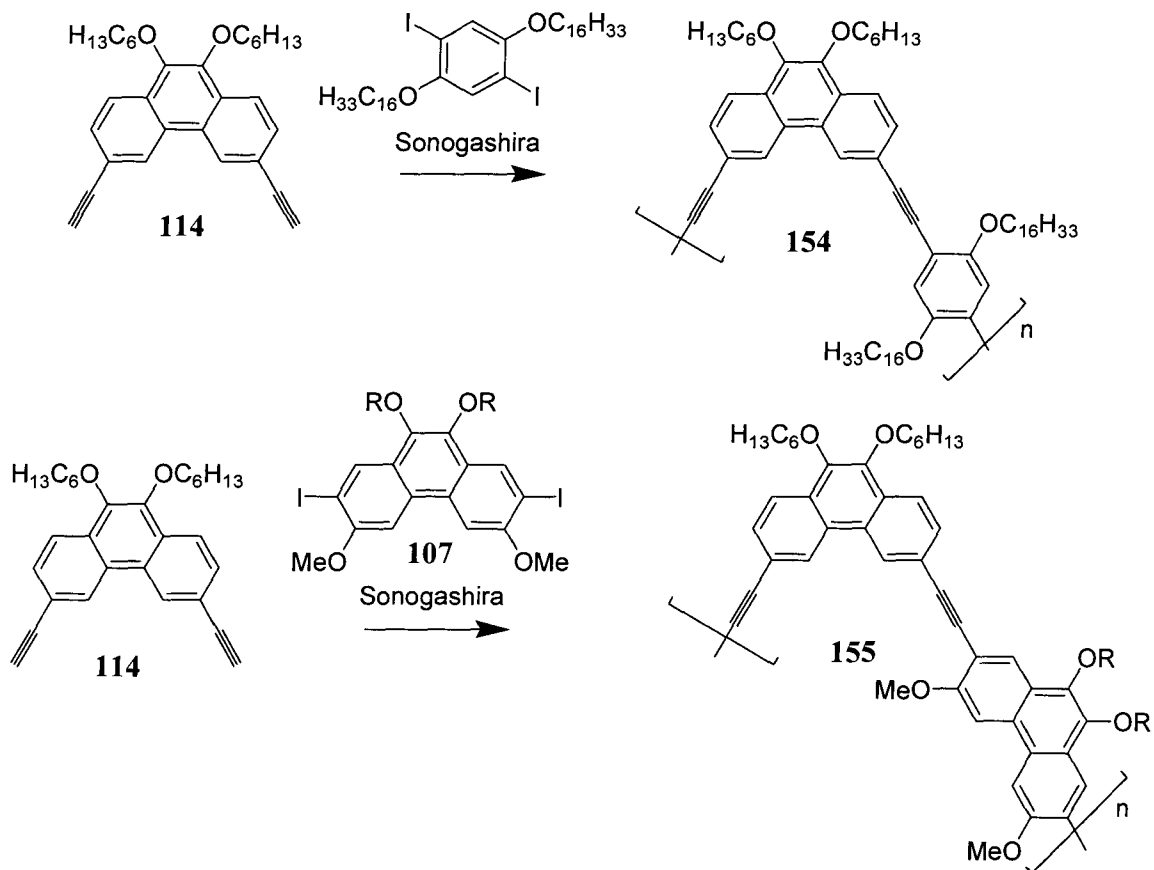
### 7.2.2 Self-Assembly

Macrocyclic **75** was found to aggregate in solution, but **74** does not. Further work in this area would be to explore self-assembly of **75** in different solvents and with different chains on the phenanthrene or phenylenediimine groups. Preliminary experiments demonstrated that **75** also aggregates in toluene- $d_8$  and there is the possibility that this will occur in acetone and THF as well. Phenyleneethynylene macrocycles like **13** have been found to behave differently in a variety of solvents, and the side chain has been found to affect this behaviour as well.<sup>4-6</sup> Another aspect of this work that still needs to be addressed is the structure of the macrocycle in films. Some macrocycles have been found to form nanofibrils,<sup>7</sup> and it would be of interest to see whether **75** self-assembles when cast into films.

### 7.2.3 Phenanthrene-Containing Polymers

Polymers **77** and **128** were synthesized using **107c** as a co-monomer in Sonogashira and Heck couplings, and were found to be luminescent, and potentially useful for solar cells or sensors. Using compounds **107** and **114**, a variety of other phenanthrene-containing conjugated polymers could be synthesized. The helical analogue of **77** (**154**) may be synthesized according to Scheme 7.3. Additionally, an alternating phenanthrene copolymer could be synthesized by reacting **107** and **114** together using a Sonogashira coupling reaction to make polymer **155**. Use of the Stille, Suzuki or Glaser reactions with **86**, **99** or **107** could also lead to a variety of new conjugated polymers.

**Scheme 7.3** Proposed syntheses of helical PPEs **154** and **155**.



#### 7.2.4 Sensing

Solutions of **74**, **75** and **77** were found to exhibit quenched luminescence in the presence of DNT. Macrocycles **74** and **75** are not highly luminescent and decompose in solution, so they are not strong sensors. Luminescence of **77** is almost entirely quenched when DNT is added, which is expected as other PPEs display the same behaviour.<sup>8</sup> However, previous nitroaromatic sensors have been studied as films, and it would be of interest to see whether films of **74**, **75** and **77** are active sensors as well.

### 7.3 References

- (1) Leung, A. C. W.; Chong, J. H.; Patrick, B. O.; MacLachlan, M. J. *Macromolecules* **2003**, *36*, 5051-5054.
- (2) Ma, C.; Lo, A.; Abdolmaleki, A.; MacLachlan, M. J. *Org. Lett.* **2004**, *6*, 3841-3844.
- (3) Cesario, M.; Dietrich-Buchecker, C. O.; Guilhem, J.; Pascard, C.; Sauvage, J. -P. *J. Chem. Soc., Chem. Commun.* **1985**, 244-247.
- (4) Zhao, D.; Moore, J. S. *J. Org. Chem.* **2002**, *67*, 3548-3554.
- (5) Zhang, J.; Moore, J. S. *J. Am. Chem. Soc.* **1992**, *114*, 9701-9702.
- (6) Lahiri, S.; Thompson, J. L.; Moore, J. S. *J. Am. Chem. Soc.* **2000**, *122*, 11315-11319.
- (7) Naddo, T.; Che, Y.; Zhang, W.; Balakrishnan, K.; Yang, X.; Yen, M.; Zhao, J.; Moore, J. S.; Zang, L. *J. Am. Chem. Soc.* **2007**, *129*, 6978-6979.
- (8) Toal, S. J.; Trogler, W. C. *J. Mater. Chem.* **2006**, *16*, 2871-2883.